

**ULTRAFILTRATION AND
NANOFILTRATION HYBRID SYSTEMS
IN WASTEATER TREATMENT AND
REUSE**

By

Hokyong Shon



Submitted in fulfillment for the degree of

Doctor of Philosophy

Faculty of Engineering

University of Technology, Sydney (UTS)

Australia

2005

CERTIFICATE

I certify that this thesis has not already been submitted for any degree and is not being submitted as part of candidature for any other degree.

I also certify that the thesis has been written by me and that any help that I have received in preparing this thesis, and all sources used, have been acknowledged in this thesis.

Signature of Candidate

Production Note:
Signature removed prior to publication.

.....

TABLE OF CONTENTS

Title page	i
Certificate	ii
Table of contents	iii
Nomenclature	xiii
List of the tables	xv
List of the figures	xix
Abstract	xxix

CHAPTER 1

INTRODUCTION 1-1

1.1 Introduction	1-2
1.2 Structure of the Study	1-2
1.3 Objectives	1-5

Chapter 2

LITERATURE REVIEW 2-1

2.1 Introduction	2-2
2.2 Wastewater Reclamation/Reuse in Australia	2-2
2.3 Wastewater Characteristics	2-4
2.4 Typical Processes Used in Wastewater Treatment	2-6
2.5 Effluent Organic Matter (EfOM) in Wastewater	2-7
2.5.1 Overview	2-7
2.5.2 Constituents of EfOM in BTSE	2-8

2.5.3	Characteristics of EfOM from BTSE	2-11
2.5.4	Specific EfOM Components Present in BTSE	2-13
2.5.4.1	Extracellular Polymeric Substances (EPSs) and Soluble Microbial Products (SMPs)	2-15
2.5.4.2	Protein	2-16
2.5.4.3	Carbohydrate	2-17
2.5.4.4	Fat, Oil and Grease	2-19
2.5.4.5	Surfactant	2-20
2.5.4.6	Priority Pollutant	2-22
2.5.4.7	Endocrine disrupting chemicals (EDCs) and pharmaceutical and personal care products (PPCPs)	2-22
2.6	Adverse and Benign Effects of EfOM	2-26
2.7	Typical treatment processes of EfOM	2-27
2.7.1	Introduction	2-27
2.7.2	Removal of EfOM by Flocculation	2-29
2.7.2.1	General	2-29
2.7.2.2	Flocculation for EfOM removal	2-30
2.7.3	Removal of EfOM by Adsorption	2-33
2.7.3.1	General	2-33
2.7.3.2	Adsorption for EfOM removal	2-34
2.7.4	Removal of EfOM by Biofiltration	2-36
2.7.4.1	General	2-36
2.7.4.2	Biofiltration for EfOM removal	2-38
2.7.5	Removal of EfOM by Ion Exchange	2-39
2.7.5.1	General	2-39
2.7.5.2	Removal of EfOM by MIEX [®] Process	2-42
2.7.6	Removal of EfOM by Advanced Oxidation Process (AOP)	2-44
2.7.6.1	General	2-44
2.7.6.2	AOPs for EfOM removal	2-46
2.7.7	Removal of EfOM by Membrane Technology	2-50
2.7.7.1	General	2-50
2.7.7.2	Membrane technology for EfOM removal	2-52
2.8	Comparison of Different Treatment Methods used in EfOM Removal	2-57
2.9	Concluding Remarks	2-61

CHAPTER 3

EXPERIMENTAL INVESTIGATION	3-1
3.1 Introduction	3-2
3.2 Experimental Materials	3-2
3.2.1 Wastewater	3-2
3.2.1.1 Synthetic Wastewater	3-2
3.2.1.2 Real Wastewater	3-3
3.2.2 Membranes	3-5
3.2.3 Activated Carbon	3-7
3.2.4 Photocatalytic powder	3-8
3.3 Experimental Methods	3-9
3.3.1 Flocculation	3-9
3.3.2 PAC Adsorption	3-9
3.3.3 GAC Biofilter	3-10
3.3.4 Photocatalytic Set-up	3-11
3.3.5 Crossflow Filtration Set-up	3-12
3.4 Experimental Analyses	3-13
3.4.1 EfOM Characterization	3-13
3.4.1.1 Dissolved Organic Carbon (DOC) and Specific UV Absorbance (SUVA)	3-13
3.4.1.2 Colloidal Organic Fraction	3-14
3.4.1.3 Fractionation of EfOM	3-15
3.4.1.4 Molecular Weight (MW) Distribution	3-17
3.4.1.5 MW Distribution of BTSE-W/S	3-18
3.4.1.6 MW Distribution of Fractions in BTSE-S	3-19
3.4.1.7 Fluorescence Excitation-Emission Matrix (EEM)	3-20
3.4.1.8 Fluorescence Chromatograms of BTSE-W/S	3-20
3.4.1.9 Fluorescence Chromatograms of Fractions in BTSE-S	3-21
3.4.1.10 Diffusion Coefficient	3-22
3.4.2 Membrane Characterization	3-23
3.4.2.1 Zeta potential	3-23

3.4.2.2 Contact Angle	3-24
3.4.2.3 ATR-FTIR for Functional Groups	3-25
3.4.2.4 Scanning Electron Microscopy (SEM) and Atomic Force Microscope (AFM)	3-26

CHAPTER 4

INFLUENCE OF FLOCCULATION AND ADSORPTION AS PRETREATMENT TO MEMBRANE FILTRATION

	4-1
4.1 Introduction	4-2
4.2 DOC Removal and SUVA with Pretreatment	4-5
4.3 Removal of Colloidal Organics	4-5
4.4 Removal of Fractions with Pretreatment	4-6
4.5 MW Distribution	4-7
4.6 Fluorescence Chromatograms	4-10
4.7 Experiments with Ultrafiltration (UF) Membrane	4-11
4.7.1 DOC Removal	4-11
4.7.2 MW Distribution	4-13
4.8 Experiments with NF Membrane	4-14
4.8.1 DOC Removal	4-14
4.8.2 MW Distribution Analysis of NF Effluent	4-15
4.9 Comparison of UF and NF Performances	4-16
4.10 Membrane Characterization with/without Pretreatment	4-18
4.10.1 Effect of Contact Angle	4-18
4.10.2 Zeta Potential	4-20
4.10.3 ATR-FTIR Spectroscopy Results for Different Pretreatments	4-20
4.10.4 SEM Analysis of Clean and Fouled Membranes	4-23
4.11 Characterization of Foulants on Membrane Surfaces	4-25
4.11.1 DOC Concentration of the Foulant	4-25
4.11.1 Foulant Interpretation	4-26
4.12 Concluding Remarks	4-27

CHAPTER 5

EFFECT OF SEMI FLOCCULATION AND SEMI ADSORPTION AS PRETREATMENT TO ULTRAFILTRATION

	5-1
5.1 Introduction	5-2
5.2 Removal of DOC from Synthetic Wastewater by Different Treatments	5-4
5.3 Effect of Semi Flocculation	5-5
5.3.1 Removal of DOC by Semi FeCl ₃ Flocculation	5-5
5.3.2 Flux Decline of UF with Pretreated Wastewater	5-6
5.3.3 Molecular Weight (MW) Distribution	5-7
5.3.4 Effect of Semi Flocculation Followed by Semi Adsorption (SFSA)	5-11
5.3.4.1 Removal of DOC by SFSA	5-11
5.3.4.2 Flux Decline of UF with Pretreated Wastewater	5-13
5.3.4.3 Molecular Weight (MW) Distribution of Organic Matter	5-15
5.4 Concluding Remarks	5-20

CHAPTER 6

ROLE OF DIFFERENT FRACTIONS IN WASTEWATER ON MEMBRANE FOULING

	6-1
6.1 Introduction	6-2
6.2 Theoretical consideration	6-3
6.2.1 Isotherm Equilibrium	6-3
6.2.1.1 Freundlich Model	6-3
6.2.1.2 Sips Model	6-4
6.2.1.3 Talu Model	6-4
6.2.1.4 Adsorption Batch Kinetics	6-5
6.3 Membrane Filtration	6-6
6.3.1 Performance of UF with Different Fractions of BTSE-S	6-6
6.3.2 Fouling of Different Fractions during UF Membrane at Constant Transmembrane Pressure	6-7

6.3.3	Membrane Characterization of the Fouled Membrane Surface with Different Fractions	6-8
6.3.3.1	Foulant Concentration	6-8
6.3.3.2	Contact Angle	6-9
6.3.3.3	Zeta Potential	6-10
6.3.3.4	ATR-FTIR Spectroscopy Results for Different Pretreatments	6-11
6.4	Effect of Pretreatment for Different Fractions of BTSE-S	6-12
6.4.1	Flocculation as Pretreatment for BTSE-S	6-12
6.4.2	Adsorption as Pretreatment for BTSE-S	6-13
6.4.3	Adsorption Kinetics of BTSE-S	6-15
6.4.4	Adsorption as Pretreatment for Different Fractions of BTSE-S	6-16
6.5	MW Distribution	6-19
6.5.1	MW Distribution of Different Fractions	6-19
6.5.2	After Flocculation of Different Fractions of BTSE-S	6-20
6.5.3	After Adsorption of Different Fractions of BTSE-S	6-21
6.5.4	MW Distribution with HP	6-22
6.5.5	MW Distribution with TP	6-22
6.5.6	MW Distribution with HL	6-23
6.5	Concluding Remarks	6-23

CHAPTER 7

PRODUCTIVITY ENHANCEMENT IN A CROSS-FLOW ULTRAFILTRATION MEMBRANE SYSTEM THROUGH AUTOMATED DE-CLOGGING OPERATIONS

7.1	Introduction	7-2
7.2	Theoretical	7-3
7.2.1	Net Productivity	7-3
7.2.2	Membrane Resistance	7-4
7.2.3	Automated Operation	7-5
7.3	Experimental	7-6

7.3.1	Automation Set-up	7-6
7.4	Results and Discussion	7-10
7.4.1	Effect of Different Pressures	7-10
7.4.2	Effect of Relaxation, Cross-flow and Relaxation and Cross-flow Cleanings	7-12
7.4.3	Effect of Different Cleaning Intervals	7-15
7.4.4	Modeling of Effective Flux Loss	7-17
7.4.5	Effect of Cleaning Time Ratio	7-21
7.4.6	Effect of Different Pressures with Optimum Cleaning Conditions	7-23
7.4.7	Effect of Different Cleaning Intervals	7-15
7.4.8	Effect of Adsorption with Optimum Cleaning Conditions	7-25
7.5	Concluding Remarks	7-27

CHAPTER 8

MATHEMATICAL MODELING OF ULTRAFILTRATION

	ASSOCIATED WITH PRETREATMENT	8-1
8.1	Introduction	8-2
8.2	Theoretical	8-4
8.2.1	Empirical Flux Decline (EFD) Model	8-4
8.2.2	Series Resistance Flux Decline (SRFD) Model	8-7
8.2.3	Modified Series Resistance Flux Decline (MSRFD) Model	8-8
8.2.4	Model Application	8-9
8.3	Results and Discussion	8-9
8.3.1	EFD Model Prediction of Experimental Results with Different Pressures	8-9
8.3.2	EFD Model Prediction of UF Experimental Results with Different Pretreatments	8-10
8.3.3	SRFD Model Prediction of Experimental Results	8-12
8.3.4	MSRFD Model Coefficients Calculated for UF with Different Pretreatments	8-14
8.3.5	MSRFD Model Coefficients Calculated For UF operated at	

	Different Pressures	8-15
8.4	Concluding Remarks	8-16

CHAPTER 9

PHOTOCATALYSIS HYBRID SYSTEM IN THE REMOVAL OF ORGANIC MATTER FOR WASTEWATER REUSE

9.1	Introduction	9-2
9.1.1	Photo-Fenton reaction	9-3
9.1.2	Chloride-based flocculant	9-3
9.1.3	pH Effect	9-4
9.1.4	PAC addition	9-4
9.2	Comparison of Nanofiltration with Flocculation-Microfiltration-Photocatalysis Hybrid system	9-5
9.2.1	Flocculation-Microfiltration-Photocatalysis Hybrid System	9-5
9.2.1.1	DOC Removal	9-5
9.2.1.2	Molecular Weight Distribution	9-6
9.2.1.3	Nanofiltration for SOM Removal	9-8
9.2.2	Chemical Coupling of Photocatalysis with Flocculation and Adsorption in the Removal of Organic Matter	9-10
9.2.2.1	Effect of the Surface Area of UV Lamp on Photocatalytic Reaction	9-10
9.2.2.2	Effect of TiO ₂ Concentration on Photocatalytic Reaction	9-11
9.2.2.2	Effect of PAC Adsorption as a Pretreatment to TiO ₂ Photocatalysis	9-13
9.2.2.4	Performance of Simultaneous Addition of PAC and TiO ₂ in the Photocatalytic System	9-14
9.2.2.5	Effect of FeCl ₃ Flocculation as a Pretreatment to TiO ₂ Photocatalysis	9-15
9.2.2.6	Molecular Weight Distribution	9-15
9.2.2.7	Synergistic Effect of FeCl ₃ Flocculation to Photocatalysis	9-17
9.2.3	Application of Photocatalysis Hybrid System to Biologically	

Treated Sewage Effluent (BTSE)	9-19
9.2.3.1 Effect of UV Light Intensity on Photodegradation	9-19
9.2.3.2 Effect of Fractions in Photodegradation	9-21
9.2.3.3 Effect of Simultaneous FeCl ₃ and TiO ₂ Addition in Photocatalysis	9-22
9.2.3.4 Effect of FeCl ₃ Flocculation Followed by Photocatalysis	9-23
9.2.3.5 Effect of PAC Adsorption as a Pretreatment to TiO ₂ Photocatalysis	9-24
9.3 Concluding Remarks	9-26

CHAPTER 10

CONCLUSIONS AND RECOMMENDATIONS 10-1

10.1 Conclusions	10-2
10.1.1 Characteristics of Wastewater and Membrane	10-2
10.1.2 Flocculation as Pretreatment	10-3
10.1.3 Adsorption as Pretreatment	10-4
10.1.4 Flocculation Followed by Adsorption as Pretreatment	10-5
10.1.5 Biofiltration as Pretreatment	10-7
10.1.6 Photocatalysis Membrane Hybrid System	10-8
10.1.7 Automated Declogging Hybrid System	10-9
10.1.8 Pretreatment of Different Fractions in BTSE	10-10
10.1.9 Flux Decline Model with Pretreatment	10-11
10.2 Recommendations	10-11
10.2.1 Near-Zero Fouling System I	10-12
10.2.2 Near-Zero Fouling System II	10-13
10.2.3 Near-Zero Fouling System III	10-14

References	R-1
Appendix A	
Normalized molecular weight distribution	A-1
Appendix B	
Simple calculations of series resistances	A-5
Appendix C	
Synergistic effect of flocculation and photocatalysis	A-6
Appendix D	
Publications made from the study	A-14

NOMENCLATURE

a''	= modified series resistance flux decline (MSRFD) constant with Langmuir
b''	= MSRFD constant with Langmuir
C	= bulk organic concentration (ML^{-3})
C_b	= bulk concentration (ML^{-3})
C_e	= equilibrium organic concentration (ML^{-3})
C_m	= interfacial membrane concentration (ML^{-3})
C_p	= permeate concentration (ML^{-3})
C_s	= saturation organic concentration (ML^{-3})
d	= flux decline kinetic constant (T^{-1})
D	= organic diffusion coefficient (L^2T^{-1})
d_h	= equivalent hydraulic diameter (L)
D_s	= surface diffusion coefficient of organic (L^2T^{-1})
H	= adsorption constant, function of temperature
J	= permeate flux at a given time of operation (MT^{-1})
J_0	= pure water permeate flux (MT^{-1})
k	= apparent photodegradation rate constant (T^{-1})
K	= Talu reaction constant
k_0	= flux decline potential which is dimensionless
k_1	= rate constant (T^{-1})
k_f	= external film mass transfer coefficient of organic (LT^{-1})
K_F	= Freundlich constant
K_F'	= series resistance flux decline (SRFD) constant with Freundlich constant
K_F''	= MSRFD constant with Freundlich isotherm constant
K_s	= energy of adsorption
K_s''	= MSRFD constants with Sips
k_{SE}	= Boltzmann constant ($ML^2T^{-2} K^{-1}$)
L	= channel length (L)
L_p	= pure water permeability ($MT^{-1}kPa^{-1}$)
M	= weight of the adsorbent (M)
M_i	= i is an incrementing index over all MW present (Da)
M_n	= number-average molecular weight (Da)

M_w	=	weight-average molecular weight (Da)
M_z	=	z-average molecular weight (Da)
N_i	=	number of molecules having a MW
$1/n$	=	Freundlich constant
$1/n'$	=	SRFD constant with Freundlich constant
$1/n''$	=	MSRFD constants with Freundlich isotherm constant
P	=	polydispersivity
q	=	measured amount organic adsorbed (MM^{-1})
q_m	=	sorption capacity (MM^{-1})
q_m''	=	sorption capacity with Sips
R_{as}	=	resistance due to strong adsorption (L^{-1})
R_{aw}	=	resistance due to weak adsorption (L^{-1})
R_{cp}	=	resistance due to concentration polarization (L^{-1})
R_g	=	resistance due to the gel layer (L^{-1})
r_p	=	radius of adsorbent particle (L)
t	=	illumination (operation) time (T)
T	=	absolute temperature (K)
U	=	average velocity of the feed fluid (ML^{-1})
V	=	volume of the solution in batch reactor (L^3)
\bar{q}	=	average adsorbed phase organic concentration (MM^{-1})
T_p	=	duration of permeate production cycle (T)
T_c	=	duration of cleaning cycle (T)
$C_{coefficient}^{baseline}$	=	experimental value of the flux decline
$Flux_{net}$	=	productivity of the cross-flow membrane system operating with periodic cleaning
$C_{coefficient}^{simulated}$	=	simulated flux values for different model coefficients
μ	=	dynamic viscosity ($kPaT^{-1}$)
η	=	viscosity of the organic phase ($L^2N^{-1}T^{-1}$)
ξ	=	zeta potential (mV)
ρ_p	=	particle density of adsorbent (ML^{-1})
Ψ	=	concentration spreading parameter

LIST OF TABLES

- Table 2.1 Annual wastewater reuse from WWTPs in Australia, 2001 (adapted from Radcliffe, 2003)
- Table 2.2 Wastewater reuse in State capital cities expressed as a percentage of sewage effluent treated, 2001 (adapted from Radcliffe, 2003)
- Table 2.3 Physical, chemical and biological characteristics of wastewater and their sources (adapted from Tchobanoglous and Burton, 1991)
- Table 2.4 Percentage composition of EfOM in BTSE (adapted from Painter, 1973)
- Table 2.5 Physical, chemical and biological characteristics of wastewater and their sources (adapted from Tchobanoglous and Burton, 1991)
- Table 2.6 Composition of organic materials in wastewater (adapted from Balmat, 1957; Levine et al., 1985)
- Table 2.7 Global characteristics of EfOM in wastewater and BTSE (adapted from Dignac et al., 2000)
- Table 2.8 Concentrations of specific organic compounds in the influent and BTSE (adapted from Dignac et al., 2000)
- Table 2.9 Comparison of the distributions of amino acids in the influent wastewater and their efficiencies (adapted from Dignac et al., 2000)
- Table 2.10 Comparison of the distributions of monosaccharide in the influent wastewater and their efficiencies (adapted from Dignac et al., 2000)
- Table 2.11 Comparison of the distributions of fatty acids in the influent wastewater and their removal efficiencies (adapted from Dignac et al., 2000)
- Table 2.12 Composition of a soapless washing powder (adapted from Tchobanoglous and Burton, 1991)
- Table 2.13 Concentration and removal of EDC and PPCP in WWTP (adapted from Snyder et al., 2003)
- Table 2.14 Classes of emerging compounds (adapted from Barceló, 2003)
- Table 2.15 EfOM removal by flocculation
- Table 2.16 Removal efficiency (%) of EDC and PPCP with different flocculants (adapted from Snyder and Westerhoff, 2005)
- Table 2.17 Classes of organics adsorbed onto activated carbon (adapted from Montgomery, 1985)

- Table 2.18 EfOM removal from BTSE by adsorption
- Table 2.19 Removal of EDC and PPCP from BTSE by PAC adsorption (adapted from Snyder et al., 2003)
- Table 2.20 Typical biofilter design parameters used in tertiary wastewater and surface water treatment (adopted from Rachwal et al., 1996)
- Table 2.21 Lists of the DOC removal by filtration with BTSE
- Table 2.22 Removal of EDC and PPCP with full scale GAC biofilter in ppt unit (adapted from Snyder and Westerhoff, 2005)
- Table 2.23 Characteristics of resins used in the treatment of BTSE
- Table 2.24 Removal of EDC and PPCP by different concentrations of MIEX[®] (adapted from Snyder and Westerhoff, 2005)
- Table 2.25 Advanced oxidation processes used in water treatment
- Table 2.26 Comparison of DOC removal with different AOP in BTSE
- Table 2.27 Easily oxidized organic compounds by photocatalytic processes (adapted from Pirkanniemi and Sillanpaa, 2002)
- Table 2.28 Removal of EDC and PPCP with chlorination at pH 5.5 (adapted from Snyder and Westerhoff, 2005)
- Table 2.29 Removal of EDC and PPCP with ozone/H₂O₂ (adapted from Snyder and Westerhoff, 2005)
- Table 2.30 Size range of membrane separation process (adapted from Cho, 2005)
- Table 2.31 DOC removal by different membrane processes
- Table 2.32 Removal of EDC and PPCP by UF (adapted from Snyder and Westerhoff, 2005)
- Table 2.33 Removal of EDC and PPCP by NF (adapted from Snyder and Westerhoff, 2005)
- Table 2.34 DOC removal by membrane technology with pretreatment
- Table 2.35 Efficiency of different treatment processes in the removal of different fractions from BTSE
- Table 2.36 Unit processes and operations used for EDC and PPCP removal in WWTP (adapted from Barceló, 2003)
- Table 2.37 Unit processes and operations used for EDC and PPCP removal (adapted from Snyder et al., 2003)
- Table 3.1 Constituents and characteristics of the synthetic wastewater

- Table 3.2 Characteristics of biologically treated sewage effluent during one year (adapted from GCHERI, 2005)
- Table 3.3 Skin-layer functional groups of membranes (adapted from Thanuttamavong, 2002)
- Table 3.4 Specification of membranes obtained by the manufacturer (Nitto Denko Corp., Japan)
- Table 3.5 Values of pure water permeability with membranes used in this study
- Table 3.6 Characteristics of powdered activated carbon (PAC) used (James Cumming & Sons Pty Ltd., Australia)
- Table 3.7 Physical properties of GAC used (Calgon Carbon Corp., USA)
- Table 3.8 Characteristics of P25 Degussa photocatalytic powdered used
- Table 3.9 Comparison of SUVA values by different water sources (adapted from Cho, 1998; Her, 2002)
- Table 3.10 Organic colloidal portion (in DOC) in the BTSE
- Table 3.11 Characteristics of UF and NF membranes used
- Table 3.12 FTIR functional group on the clean membrane
- Table 4.1 DOC removal and SUVA values with different pretreatments.
- Table 4.2 Organic colloidal portion (in DOC) in the secondary effluent with and without a treatment of flocculation and adsorption
- Table 4.3 HP, TP, and HL fractions in BTSE-W (FeCl_3 : 41 mg-Fe/L and PAC: 1 g/L)
- Table 4.4 Removal of HP, TP, and HL fractions in BTSE-S (FeCl_3 : 28 mg-Fe/L and PAC: 1 g/L)
- Table 4.5 The contact angle of the clean and fouled UF membrane surfaces
- Table 4.6 The effect of the contact angle on different membrane surfaces
- Table 4.7 Functional groups obtained by IR spectra (on the fouled membrane surfaces)
- Table 4.8 MW values of foulants on the UF membranes (initial BTSE-S - number-averaged (median value) MW (M_n^*): 759 daltons, weight-averaged MW (M_w^{**}): 1158 daltons and polydispersivity ($P^{***} = M_w/M_n$): 1.53)
- Table 4.9 MW values of foulants on the NF membrane (initial number-averaged (median) MW (M_n^*): 759 daltons, weight-averaged MW (M_w^{**}): 1158 daltons and polydispersivity ($P^{***} = M_w/M_n$): 1.53)
- Table 5.1 Relationship between the size in nm and MW in daltons

- Table 5.2 Weight-averaged MW values of the effluent samples after pretreatment (weight-averaged MW of initial = 29760 daltons)
- Table 5.3 Weight-averaged MW values of organic matter after pretreatment of flocculation and adsorption after post treatment of UF (all units: daltons)
- Table 6.1 FTIR functional group with different fractions
- Table 6.2 FTIR functional group with the HL fraction
- Table 6.3 Isotherm parameter values (PAC with BTSE-S at initial concentration of 6.5 mg/L)
- Table 6.4 Film mass transfer coefficient (k_f) and diffusion coefficient (D_s) of batch experiments at initial PAC concentration of 1 g/L
- Table 6.5 Isotherm parameter values for different fractions
- Table 6.6 Film mass transfer coefficient (k_f) and diffusion coefficient (D_s) of fractions at initial PAC concentration of 1 g/L
- Table 7.1 Status of solenoid valves during varied modes of operation.
- Table 7.2 Membrane cross-flow rate and transmembrane pressure for each operating mode
- Table 7.3 Flux recovered for each varied production interval
- Table 8.1 Effect of the k_0 value for EFD model ($k_1 = 0.201$ and $d = 0.002$)
- Table 8.2 Effect of the k_1 value for EFD model ($k_0 = 0.060$ and $d = 0.002$)
- Table 8.3 Effect of the d value for EFD model ($k_0 = 0.060$ and $k_1 = 0.201$)
- Table 8.4 Sensitivity of K_F' ($1/n' = 0.773$)
- Table 8.5 Sensitivity of $1/n'$ ($K_F' = 1.0E+11$)
- Table 8.6 EFD model coefficients obtained from experimental data with different pressures ($k_1 = 2.15E-02$)
- Table 8.7 Flux decline coefficients by EFD model with pretreatment ($k_1 = 2.15E-02$)
- Table 8.8 Flux decline coefficients by SRFD model (Freundlich) with automation ($1/n' = 7.75E-01$)
- Table 8.9 Flux decline coefficients by SRFD model (Freundlich) with pretreatment ($1/n' = 7.75E-01$)
- Table 8.10 Concentration of organic matter and adsorption resistance
- Table 8.11 Flux decline coefficients by MSRFD model (Freundlich) with different pressures

LIST OF FIGURES

- Figure 1.1 Schematic of research scope conducted in this study
- Figure 2.1 Future recycling commitments (adapted from Kahn, 2004)
- Figure 2.2 Typical organic constituents in BTSE and their size ranges (adapted from Levine et al., 1985)
- Figure 2.3 Different fractions of DOC and their constituents (adapted from Thurman, 1985; Cho, 1998)
- Figure 2.4 Components of a closed water cycle with indirect potable reuse (adapted from Petrović et al., 2003)
- Figure 2.5 Size ranges of the applied treatments in treating EfOM
- Figure 2.6 DOC removal mechanisms by MIEX[®] resin (adapted from Bourke et al., 1999)
- Figure 2.7 DOC removal by different processes (FeCl₃ flocculation, PAC adsorption, IX with MIEX[®], AOP (photocatalysis) with TiO₂, GAC biofiltration, UF (with 17500 daltons MWCO membrane), NF1 (with 700 daltons MWCO membrane) and NF2 (with 200 daltons MWCO membrane)) in biologically treated sewage effluent from a wastewater treatment plant (adapted from Shon et al., 2004 and 2005)
- Figure 2.8 MW distribution of the influent BTSE and effluents from different treatments (flocculation, adsorption, GAC biofiltration, photocatalysis, MIEX[®], UF and NF)
- Figure 3.1 Schematic of treatment processes in Gwangju wastewater treatment plant
- Figure 3.2 Pure water permeability (L_p) of membranes used at 30°C of temperature
- Figure 3.3 Schematic of the batch experimental set-up (speed controller 0-150 rpm, beaker 1 L)
- Figure 3.4 Schematic drawing of the fixed bed GAC biofilter
- Figure 3.5 Comparison of (a) TiO₂ (non-porous media) and (b) PAC (porous media)
- Figure 3.6 Schematic of the photocatalytic reactor
- Figure 3.7 Schematic drawing of cross-flow unit studied
- Figure 3.8 Schematic drawing of colloidal and non-colloidal fractions with Spectra/Por-3 regenerated cellulose dialysis membrane bag (MWCO, 3500 daltons)

- Figure 3.9 Schematic drawing of fractionation for hydrophobic, transphilic and hydrophilic components with XAD-8 and XAD-4 resins
- Figure 3.10 High pressure size exclusion chromatography (HPSEC) to measure MW distribution
- Figure 3.11 MW distribution of (a) BTSE-W and (b) BTSE-S
- Figure 3.12 MW distribution of HP, TP, and HL fractionations
- Figure 3.13 Schematic drawing of HPLC-UVA-fluorescence
- Figure 3.14 Comparison of (a) fluorescence chromatogram and (b) MW distribution of EfOM with BTSE-S (initial DOC concentration = 6.5 mg/L)
- Figure 3.15 Comparison of (a) fluorescence chromatogram and (b) MW distribution of HP, TP and HL fractions with BTSE-S
- Figure 3.16 Schematic drawing of diffusion cell
- Figure 3.17 Zeta potential of clean membrane surfaces as a function of solution pH (background electrolyte concentration = 10 mM NaCl)
- Figure 3.18 FTIR spectra on clean membranes (NTR 7410, NTR 729HF, LES 90 and LF 10)
- Figure 3.19 Top and side views of beam energies on filed FE-SEM images of each membrane (working distance of 12 mm and magnification of 50000 and 5000)
- Figure 3.20 AFM images of each membrane (adapted from Thanuttamavong, 2002)
- Figure 4.1 MW distributions of the BTSE-W with and without pretreatments (a) flocculation, b) PAC adsorption and c) Floc-Ads)
- Figure 4.2 MW distribution of BTSE-S after different treatments (flocculation, adsorption and Floc-Ads)
- Figure 4.3 Fluorescence chromatograms after different treatments with BTSE-S
- Figure 4.4 Effect of different pretreatment methods in terms of DOC removal with BTSE-S (UF membrane used = NTR 7410; MWCO of 17500 daltons, crossflow velocity = 0.5 m/s, transmembrane pressure = 300 kPa, Reynold's number: 735.5, shear stress: 5.33 Pa)
- Figure 4.5 MW distribution of the soluble EfOM after different pretreatments in BTSE-S and in UF; a) UF alone, GAC biofilter, and Floc-Ads and b) after flocculation and PAC adsorption (membrane used = NTR 7410 UF with a MWCO of 17500, crossflow velocity = 0.5 m/s and transmembrane pressure = 300 kPa)

- Figure 4.6 Organic removal by NF with and without pretreatment in BTSE-S (membrane used = LES 90, crossflow velocity = 0.5 m/s, transmembrane pressure = 300 kPa)
- Figure 4.7 MW distribution of the NF effluent with different pretreatments (BTSE-S; LES 90 with a MWCO of 250 daltons; crossflow velocity = 0.5 m/s and transmembrane pressure = 300 kPa)
- Figure 4.8 Temporal variation of filtration flux and DOC ratio with and without pretreatment in BTSE-S (UF NTR 7410, $J_0 = 3.01$ m/d at 300 kPa; crossflow velocity = 0.5 m/s; NF LES 90, $J_0 = 0.77$ m/d at 300 kPa; crossflow velocity = 0.5 m/s; C and C_0 = the effluent and influent DOC values; J_0 = pure water permeate flux)
- Figure 4.9 The effect of pretreatments on the zeta potential of UF membrane
- Figure 4.10 FTIR spectra (a) for clean membrane and for fouled membranes without any pretreatment and after a pretreatment of Floc-Ads (b) for membranes after pretreatments of flocculation, PAC adsorption and GAC biofilter (NTR 7410 membrane with BTSE-S)
- Figure 4.11 FTIR spectra with clean membrane, without any pretreatment, and after Floc-Ads (a) NTR 729HF membrane, (b) LES 90 membrane, and (c) LF 10 membrane with BTSE-S
- Figure 4.12 Cross section of beam energies on filed FE-SEM images of NTR 7410 membrane after 18-hour filtration (working distance of 12 mm and magnification of 20,000)
- Figure 4.13 DOC concentration of adsorbed EfOM on the fouled membrane surfaces after different pretreatments (a) EfOM concentration adsorbed on the UF membrane and b) on the NF membrane)
- Figure 5.1 DOC removal of different membranes with and without pretreatment
- Figure 5.2 DOC removal by semi flocculation followed by UF
- Figure 5.3 Temporal variation of filtration flux of UF after a pretreatment of flocculation at different FeCl_3 doses (NTR 7410 UF membranes, $J_0 = 1.84$ m/d at 300 kPa; crossflow velocity = 0.5 m/s; MWCO of 17,500 daltons; Reynold's number: 735.5; shear stress: 5.33 Pa)
- Figure 5.4 MW distribution of SOM in the synthetic wastewater (a), b): individual components in the wastewater; c) wastewater (with all compounds mixed together)

- Figure 5.5 MW distribution in the flocculated effluent ($J_0 = 1.84$ m/d at 300 kPa; crossflow velocity = 0.5 m/s; MWCO = 17,500 daltons; Reynold's number.: 735.5; shear stress: 5.33 Pa; a) MW distribution of SOM with higher doses of FeCl_3 (17 - 23 mg-Fe/L); b) with FeCl_3 of lower doses (7 - 14 mg-Fe/L flocculation); c) flocculation followed by UF
- Figure 5.6 Correlation between the FeCl_3 concentrations and the corresponding weight-averaged MW values in the flocculated effluent.
- Figure 5.7 DOC removal by PAC adsorption at different doses of PAC
- Figure 5.8 DOC removal of SFSA and UF (UF membrane used = NTR 7410; MWCO of 17500 daltons; crossflow velocity = 0.5 m/s; transmembrane pressure = 300 kPa; Reynold's number: 735.5; shear stress: 5.33 Pa; DOC removal with UF alone: 75.3%)
- Figure 5.9 Temporal variation of filtration flux with UF NTR 7410 after adsorption pretreatment ($J_0 = 1.84$ m.d/L at 300 kPa; crossflow velocity = 0.5 m.s/L; MWCO of 17500 daltons; Reynold's number: 735.5; shear stress: 5.33 Pa)
- Figure 5.10 Temporal variation of filtration flux and DOC ratio with semi flocculation followed by semi adsorption (SFSA) with UF NTR 7410 ($J_0 = 1.84$ m/d at 300 kPa; crossflow velocity = 0.5 m/s; MWCO of 17,500 daltons; Reynold's number: 735.5; shear stress: 5.33 Pa; (a) after 23 mg-Fe/L flocculation; (b) after 17 mg-Fe/L; (c) after 10 mg-Fe/L; (d) after 3 mg-Fe/L)
- Figure 5.11 MW distribution after (a) adsorption with the large doses of PAC, and (b) adsorption with the small doses of PAC
- Figure 5.12 MW distribution of organic matter after semi flocculation followed by semi adsorption
- Figure 5.13 MW distribution after flocculation and adsorption as pretreatment and UF as post treatment ($J_0 = 1.84$ m/d at 300 kPa; crossflow velocity = 0.5 m/s; MWCO of 17500 daltons; Reynold's number: 735.5; shear stress: 5.33 Pa)
- Figure 5.14 Correlation of flocculant and adsorbent concentration vs DOC concentration and averaged-weight MW ($J_0 = 1.84$ m/d at 300 kPa; crossflow velocity = 0.5 m/s; MWCO = 17500 daltons; Reynold's number.: 735.5; shear stress: 5.33 Pa; (a) FeCl_3 concentration vs DOC concentration of semi flocculation followed by semi adsorption; (b) FeCl_3 concentration versus MW of semi flocculation followed by semi adsorption)

- Figure 6.1 DOC removal of different fractions with UF performance (UF membrane used = NTR 7410; MWCO of 17,500 daltons, crossflow velocity = 0.5 m/s, transmembrane pressure = 300 kPa, Reynold's number.: 735.5, shear stress: 5.33 Pa)
- Figure 6.2 Temporal variation of filtration flux with different fractions ($J_0 = 3.01$ m/d (125.4 L/m²·h) at 300 kPa; crossflow velocity = 0.5 m/s)
- Figure 6.3 DOC concentration of adsorbed fractions on the fouled UF membrane surfaces
- Figure 6.4 Contact angle on the fouled UF membrane surfaces
- Figure 6.5 Zeta potential on the fouled UF membrane surfaces
- Figure 6.6 DOC removal efficiency of different fractions by FeCl₃ flocculation
- Figure 6.7 Effect of PAC dose in the DOC removal from BTSE-S (initial DOC = 6.5 mg/L; conductivity = 15 mS/cm)
- Figure 6.8 Adsorption isotherm results (BTSE-S with 15 mS/cm: 6.5 mg/L; Temp.: 25 °C)
- Figure 6.9 Adsorption kinetics of BTSE-S with 1 g/L PAC at 25 °C
- Figure 6.10 DOC removal of different BTSE-S fractions by PAC adsorption (PAC dose: 1 g/L; initial DOC concentration: 6.5 mg/L; mixing speed: 100 rpm; operation: 1 h; pH: 7)
- Figure 6.11 Adsorption isotherm plots (initial DOC concentration: 6.5 mg/L; Temp.: 25 °C)
- Figure 6.12 Adsorption kinetics result by PAC adsorption
- Figure 6.13 MW distribution of HP, TP, and HL fractions in terms of UV response and
- Figure 6.14 MW distribution of (a) BTSE-S and (b) different fractions after flocculation
- Figure 6.15 MW distribution of BTSE-S before and after PAC adsorption (PAC dose: 1 g/L)
- Figure 6.16 MW distribution of a) different PAC concentrations and b) batch kinetics
- Figure 6.17 MW distribution of a) different PAC concentrations and b) batch kinetics
- Figure 6.18 MW distribution of a) different PAC concentrations and b) batch kinetic
- Figure 7.1 Schematic representations of resistances in series

- Figure 7.2 Block diagram for the control system used for periodic cleaning of the cross-flow membrane system
- Figure 7.3 Experimental set-up of the cross-flow membrane system with the inclusion of 4 automated solenoid valves for control of the operating modes
- Figure 7.4 Operating mode popup screen in the SCADA system with Windows application
- Figure 7.5 Results of the flux decline versus time for the three different values of transmembrane pressure (UF membrane used = NTR 7410; MWCO of 17,500 daltons, crossflow velocity = 0.5 m/s, transmembrane pressure = 100, 300 and 500 kPa, Reynold's number: 735.5, shear stress: 5.33 Pa)
- Figure 7.6 Different membrane resistances by fouling and flux decline at different pressures
- Figure 7.7 Results of the flux decline versus time for different cleaning techniques (UF membrane used = NTR 7410; MWCO of 17,500 daltons, crossflow velocity = 0.5 m/s, transmembrane pressure = 300 kPa, Reynold's number: 735.5, shear stress: 5.33 Pa)
- Figure 7.8 Different membrane resistances by fouling and flux decline at different cleaning techniques
- Figure 7.9 Results of the flux decline versus time for different production periods (UF membrane used = NTR 7410; MWCO of 17,500 daltons, crossflow velocity = 0.5 m/s, transmembrane pressure = 300 kPa, Reynold's number: 735.5, shear stress: 5.33 Pa)
- Figure 7.10 Different membrane resistances by fouling at different production periods
- Figure 7.11 Results of the flux recovery versus cleaning time used with the relaxation and the high rate cross flow
- Figure 7.12 Results of the flux decline versus the production time used at a transmembrane pressure of 300 kPa
- Figure 7.13 Results of the net flux loss versus the production time used
- Figure 7.14 Results of the flux decline versus time for the 3 different cleaning ratios (UF membrane used = NTR 7410; MWCO of 17,500 daltons, crossflow velocity = 0.5 m/s, transmembrane pressure = 300 kPa, Reynold's number: 735.5, shear stress: 5.33 Pa)

- Figure 7.15 Different membrane resistances by fouling and flux decline at the 3 different cleaning ratios
- Figure 7.16 Results of the flux decline versus time for the optimal cleaning conditions (UF membrane used = NTR 7410; MWCO of 17,500 daltons, crossflow velocity = 0.5 m/s, transmembrane pressure = 100 and 500 kPa, Reynold's number: 735.5, shear stress: 5.33 Pa)
- Figure 7.17 Results of the flux decline versus time after FeCl_3 flocculation for the optimal cleaning conditions (UF membrane used = NTR 7410; MWCO of 17,500 daltons, crossflow velocity = 0.5 m/s, transmembrane pressure = 300 kPa, Reynold's number: 735.5, shear stress: 5.33 Pa)
- Figure 7.18 Different membrane resistances by fouling and flux decline at different FeCl_3 concentrations
- Figure 7.19 Results of the flux decline versus time after adsorption for the optimal cleaning conditions (UF membrane used = NTR 7410; MWCO of 17,500 daltons, crossflow velocity = 0.5 m/s, transmembrane pressure = 300 kPa, Reynold's number: 735.5, shear stress: 5.33 Pa)
- Figure 7.20 Different membrane resistances by fouling and flux decline at different PAC concentrations
- Figure 8.1 Effect of k_0 , k_1 and d values on flux decline (UF membrane used = NTR 7410; MWCO of 17,500 daltons; crossflow velocity = 0.5 m/s; transmembrane pressure = 300 kPa ($J_0 = 1.84$ m/d); Reynold's number: 735.5; shear stress: 5.33 Pa)
- Figure 8.2 Effect of K_F' and $1/n'$ on flux decline
- Figure 8.3 Experimental and predicted flux decline profiles with different pressures
- Figure 8.4 Experimental and predicted flux decline in UF after a pretreatment (UF membrane of MWCO 17,500 daltons; pressure = 300 kPa)
- Figure 8.5 Comparison of flux-decline coefficients by EFD model
- Figure 8.6 Experimental and predicted flux decline in UF after a) different pressures, b) flocculation and c) PAC adsorption (UF membrane of MWCO 17,500 daltons; pressure = 300 kPa)
- Figure 8.7 Comparison of experimental and predicted adsorption resistance values calculated from MSRFD model
- Figure 8.8 Comparison of flux-decline coefficients by MSRFD model

- Figure 9.1 DOC removal by photocatalysis with and without pretreatment ($T = 25\text{ }^{\circ}\text{C}$; Air = 1.5 VVM; $\text{TiO}_2 = 1\text{ g/L}$ without pretreatment; UV lamp intensity = 8 W; C_0 and C = influent and effluent DOC concentration)
- Figure 9.2 MW size distributions of synthetic wastewater with photocatalysis at different times ($T = 25\text{ }^{\circ}\text{C}$; air = 1.5 VVM; $\text{TiO}_2 = 1\text{ g/L}$ without pretreatment; UV lamp intensity = 8 W)
- Figure 9.3 Molecular size distributions of SOM (after the treatment of flocculation and microfiltration ($T = 25\text{ }^{\circ}\text{C}$; Air = 1.5 VVM; $\text{TiO}_2 = 0.5\text{ g/L}$ with pretreatment, UV lamp intensity = 8 W)
- Figure 9.4 Schematic of Photo-Fenton degradation of SOM (modified from Sarria et al., 2003)
- Figure 9.5 DOC removal and permeate flux with NF unit (NTR 729HF nanofiltration membrane, Nitto Denko Corp., operating pressure 300 kPa, flow rate = 0.5 m/s, $T = 30\text{ }^{\circ}\text{C}$)
- Figure 9.6 MW size distribution of nanofiltration effluent with synthetic wastewater (NTR 729HF nanofiltration membrane, Nitto Denko Corp., operating pressure 300 kPa, flow rate = 0.5 m/s, $T = 30\text{ }^{\circ}\text{C}$, Reynold's no. = 735.5 (laminar flow) and shear stress = 5.33 Pa)
- Figure 9.7 Effect of surface area of UV lamp on photocatalysis ($\text{TiO}_2 = 1\text{ g/L}$; initial DOC of the wastewater = 11.46 mg/L; $T = 25\text{ }^{\circ}\text{C}$; Air = 3.3 VVM; intensity = 8 W UV-C)
- Figure 9.8 Effect of TiO_2 concentration on photocatalysis (initial concentration (C_0) = 11.46 mg/L (in terms of DOC); $T = 25\text{ }^{\circ}\text{C}$; Air = 3.3 VVM; intensity = 8 W with the 3 lamps)
- Figure 9.9 Effect of PAC adsorption followed by photocatalysis (wastewater concentration (DOC) = 11.46 mg/L; $\text{TiO}_2 = 2\text{ g/L}$; $T = 25\text{ }^{\circ}\text{C}$; Air = 3.3 VVM; intensity = 8 W with the 3 lamps)
- Figure 9.10 Performance of coupling of PAC adsorption with TiO_2 photocatalysis system (wastewater concentration (DOC) = 11.46 mg/L; $\text{TiO}_2 = 2\text{ g/L}$; $T = 25\text{ }^{\circ}\text{C}$; Air = 3.3 VVM; intensity = 8 W with the 3 lamps)
- Figure 9.11 Effect of FeCl_3 flocculation followed by photocatalysis (wastewater concentration (DOC) = 11.46 mg/L; $\text{TiO}_2 = 2\text{ g/L}$; $T = 25\text{ }^{\circ}\text{C}$; Air = 3.3 VVM; intensity = 8 W with the 3 UV lamps)

- Figure 9.12 MW distribution after FeCl₃ flocculation (mixing speed: 1 min at 100 rpm and 20 min at 30 rpm) and PAC adsorption (mixing speed: 100 rpm; contact time: 1 h)
- Figure 9.13 MW distribution of PAC adsorption followed by photocatalysis (wastewater concentration (DOC) = 11.46 mg/L; T = 25 °C; Air = 3.3 VVM; each 3 UV lamps intensity = 8 W; TiO₂ concentration = 2 g/L)
- Figure 9.14 MW distribution after FeCl₃ flocculation followed by TiO₂ photocatalysis (wastewater concentration (DOC) = 11.46 mg/L; FeCl₃ dose = 23 mg-Fe/L; T = 25 °C; Air = 3.3 VVM; three lamps with an intensity of each lamp = 8 W; TiO₂ concentration = 2 g/L)
- Figure 9.15 DOC removal by i) TiO₂ adsorption alone, ii) flocculation alone, iii) flocculation followed by TiO₂ adsorption, iv) photocatalysis at pH 4 alone and flocculation followed by photocatalysis at pH 4
- Figure 9.16 (a) DOC variations and (b) reaction rates of different initial concentrations in photocatalysis (T = 30 °C; Air = 0.1 VVM; intensity = 8 W with the 3 lamps)
- Figure 9.17 C/C₀ variation at different UV intensities (initial DOC concentration = 6.5 mg/L; TiO₂ concentration = 2 g/L; air = 25 L/min)
- Figure 9.18 MW distribution of EfOM at different UV intensities (initial DOC concentration = 6.5 mg/L; TiO₂ concentration = 2 g/L; air = 25 L/min)
- Figure 9.19 (a) C/C₀ profile and MW distribution of different fractions of EfOM by photocatalysis with (b) HP, (c) TP, and (d) HL fractions (initial concentration = 6.5 mg/L; TiO₂ concentration = 2 g/L; air = 5 VVM; UV intensity = UV-C 15W)
- Figure 9.20 (a) C/C₀ profile and (b) MW distribution after simultaneous FeCl₃ and TiO₂ additions in photocatalysis (initial concentration = 6.5 mg/L; TiO₂ concentration = 2 g/L; air = 5 VVM; UV intensity = UV-C 15W; Figure (b) corresponds to 56 mg-Fe/L addition)
- Figure 9.21 (a) C/C₀ variation and (b) MW distribution with FeCl₃ flocculation (69 mg-Fe/L) followed by photocatalysis (initial DOC concentration = 6.5 mg/L; TiO₂ concentration = 2 g/L; air = 5 VVM)
- Figure 9.22 C/C₀ variation of (a) simultaneous PAC addition and (b) PAC adsorption followed by photocatalysis (initial concentration = 6.5 mg/L; TiO₂ concentration = 2 g/L; air = 5 VVM)

Figure 9.23 MW distribution of EfOM with PAC adsorption followed by photocatalysis (initial concentration = 6.5 mg/L; TiO₂ concentration = 2 g/L; 5 VVM)

Figure 10.1 Schematic of near-zero fouling system I

Figure 10.2 Schematic of near-zero fouling system II

Figure 10.3 Schematic of near-zero fouling system III

ABSTRACT

Wastewater reuse is increasingly seen as an essential strategy for making better use of limited freshwater resources, and as a means of preventing deterioration of the aquatic environment from wastewater disposal. Membrane processes are now being successfully used to obtain water of recyclable quality. However, membrane fouling is a critical limitation on the application of membranes to wastewater reuse. Pretreatment of biologically treated sewage effluent (BTSE) prior to membrane processes will reduce organic deposition and subsequent biogrowth on membranes due to dissolved organic matter. Pretreatment also reduces the need for frequent chemical cleaning, which is a major factor that impacts on membrane life. From these perspectives, pretreatment offers significant potential for improving the efficiency of membrane processes.

The main objectives in this study are i) to evaluate different pretreatment methods of removing effluent organic matter (EfOM) from BTSE and in reducing membrane fouling, ii) to investigate the variation in the ultrafiltration (UF) and nanofiltration (NF) membrane foulant characteristics in terms of molecular weight (MW) distribution of foulants and the characteristics of fouled membrane, iii) to examine the effect of semi flocculation and semi adsorption (with partial doses of flocculants and adsorbents, respectively) on the membrane filtration, iv) to study the phenomena of membrane filtration and pretreatment using different fractions (hydrophobic (HP), transphilic (TP) and hydrophilic (HL)) of BTSE, v) to assess the effect of hybrid hydrodynamic cleaning with high rate crossflow and relaxation modes in comparison with pretreatment to membrane, vi) to evaluate the merits/demerits photocatalysis hybrid system in comparison with NF and UF with pretreatment and vii) to develop different flux decline models to quantitatively compare different pretreatments.

The highest removal of organic matter was observed when flocculation followed by adsorption was used as pretreatment. The flocculation and adsorption removed 68.5% and 71.4% of hydrophobic organic matter. After the flocculation pretreatment, the majority of large MW EfOM was removed. The pretreatment of the flocculation followed by adsorption led to very high removal of both small and large organic matter. Further, this pretreatment led to practically no filtration flux decline. The weight averaged MW (M_w) of the organics in the foulant on the membrane surface was 510

daltons (UF) and 190 (NF) without pretreatment and 350 (UF) and 180 (NF) after pretreatment with flocculation followed by adsorption, respectively. The flux decline with the HP fraction was high compared with the TP and HL fractions. It was observed that a particular amount of flocculant and adsorbent to UF was necessary below which the UF membrane became heavily fouled. The detailed analysis of M_w indicated that the M_w values of organic matter in the synthetic wastewater and in the flocculated effluent were 29800 daltons (initial), > 25000 (after flocculation with 40 mg/L $FeCl_3$ or less) and < 1000 (after flocculation with 50 mg/L $FeCl_3$ or more). The M_w values suggested the reason why the permeate flux was decreased with 40 mg/L $FeCl_3$ semi flocculation followed by semi adsorption due to the remaining large M_w .

A detailed investigation of the utilisation of two automated cleaning techniques to reduce fouling problems was explored. The two cleaning techniques studied were periodic membrane relaxation and a periodic high rate cross-flow. The study found that an optimised usage of these two de-clogging techniques, with a 1 hour production period followed by a 1 minute relaxation period and then a 1 minute high cross-flow rate period resulted in a net productivity increase of 14.8%. Three different semi-empirical mathematical models were investigated to partially quantify the effects of different pressures and pretreatments. The three different models used were i) empirical flux decline (EFD) model, ii) series resistance flux decline (SRFD) model and iii) modified series resistance flux decline (MSRFD) model. The flux decline coefficient values determined from the EFD and SRFD models can be used as an index to assess flux decline and compare different operating conditions and pretreatments. With the MSRFD model, when flocculation of 21 mg-Fe/L was used as a pretreatment at a pressure of 300 kPa, the values of the bulk concentration (C_b), the concentration on the membrane surface (C_m) and adsorption resistance (R_a) significantly decreased by 4.4, 3.1 and 12.9 times, respectively. After 0.1 g/L adsorption as a pretreatment, the values decreased by 2.2, 2.0 and 1.8 times, respectively. Thus, pretreatment can significantly decrease membrane fouling.

Although pretreatment reduces flux decline caused by membrane fouling, it cannot completely prevent membrane fouling. Further, as time proceeds, membrane fouling by organic matter is converted into biofouling and the concentration from the retentate

constantly increases. To resolve these problems, this study recommends three near-zero fouling systems with an integrated photocatalysis membrane hybrid system.

CHAPTER 1



University of Technology, Sydney
Faculty of Engineering

INTRODUCTION

1.1 Introduction

The need for wastewater reuse is becoming increasingly important as the population of the world grows and industrialization increases around the world. Reuse of wastewater will help maintain environmental quality, help relieve the unrelenting pressure on natural freshwater resources. Although the effluent from the secondary and tertiary wastewater treatment can be discharged into waterways, it cannot be reused for domestic or industrial purposes without further treatment. An advanced treatment technology is therefore required to remove various effluent organic matters (EfOMs), pathogenic microorganisms and persistent organic pollutants (POPs) from wastewater.

Membrane technology, namely reverse osmosis (RO), nanofiltration (NF) and ultrafiltration (UF) can remove the majority of the pollutants including dissolved EfOM. However, their operating costs are high because of high energy requirements. These membranes are also easily fouled by EfOM present in biologically treated sewage effluent (BTSE), and thus require an appropriate pretreatment prior to membrane filtration.

To investigate performance of different pretreatments to alleviate or reduce membrane fouling, a number of pretreatment systems have to be studied in terms of their capability to remove a specific range of organic matter. A detailed characterization of EfOM and membrane foulant layer is essential in optimizing the pretreatment and the operating conditions associated with the membrane process. An alternative to pretreatment is hydrodynamic membrane cleaning. A rational hydrodynamic cleaning can prolong the operational life of membranes through reducing the formation of irreversible foulant layer.

1.2 Structure of the Study

Figure 1.1 presents an outline of the scope for this study. To minimize membrane fouling, different pretreatments, such as flocculation, adsorption, photocatalysis, biofiltration and flocculation followed by adsorption, were employed. The

characteristics of EfOM with different pretreatments and membrane filtration were investigated in terms of molecular weight (MW) distribution, fraction (hydrophobic (HP), transphilic (TP) and hydrophilic (HL) compounds), colloidal organic portion, dissolved organic carbon (DOC) and specific UV absorbance (SUVA). Interaction between pretreatment and membrane filtration was also identified by characterizing clean and fouled membranes. They were studied in terms of contact angle, zeta potential, functional group, organic fouling concentration and foulant layer thickness using scanning electron microscopy. An alternative to pretreatment is cleaning. Using an innovative combination of hydrodynamic cleaning methods was also investigated. The performance of UF and NF in treating BTSE was also evaluated.

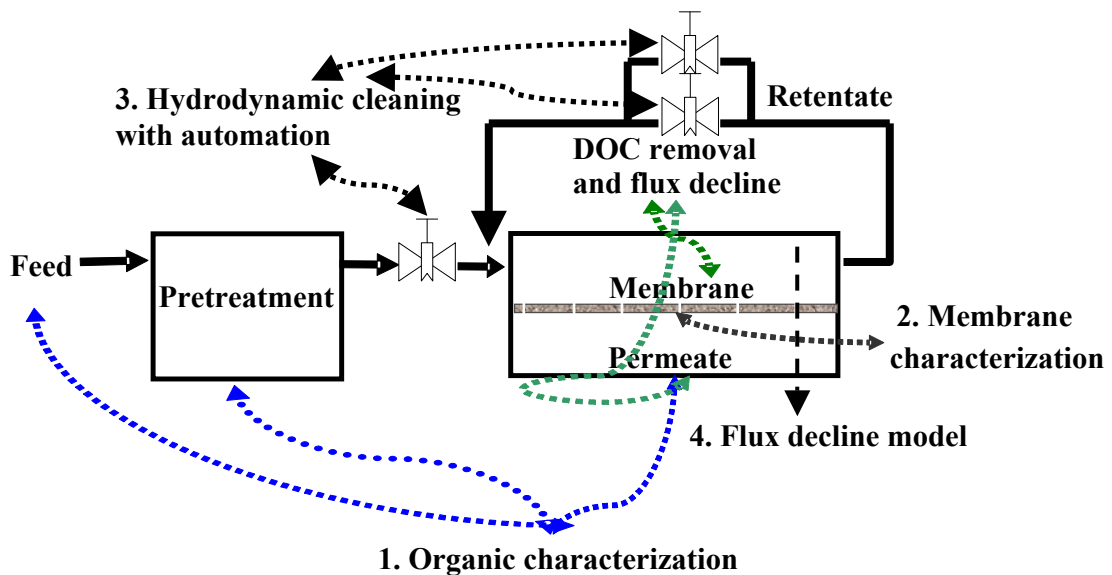


Figure 1.1 Schematic of research scope conducted in this study

Chapter 2 (literature review) presents i) a detailed review of the constituents of EfOM in BTSE, iii) concepts of different pretreatments and iv) their application in water reuse.

The experimental investigation presented in Chapter 3 describes i) materials and methods of pretreatment and membrane filtration, ii) experimental methodology associated with organic characterization and iii) experimental procedures used to characterize the clean and fouled membranes.

Chapter 4 presents the influence of different pretreatments on UF and NF. The experimental results presented in this chapter provide detailed information on EfOM removal. The characteristics of clean and fouled membranes are also discussed in terms of efficiency of different pretreatment methods.

The use of a large quantity of adsorbents and flocculants are not cost effective and also lead to large sludge production. Thus, Chapter 5 discusses organic removal by UF using semi flocculation (partial dose of flocculants) and semi adsorption (partial dose of adsorbents).

It is important to identify the specific fraction mainly contributing to the fouling to select the appropriate pretreatment method. Chapter 6 presents details on the effect of different fractions (HP, TP and HL) on membrane fouling.

An appropriate hydrodynamic cleaning using a crossflow system is also expected to reduce the reversible fouling caused by reversible foulants. Chapter 7 discusses the effects of automated hydrodynamic cleaning consisting of a high rate crossflow and relaxation mode in improving the membrane flux.

A simple flux decline model (SFDM) is believed to be useful in optimising pretreatment requirements, and compare different pretreatment methods in a quantitative manner. Chapter 8 presents three simple flux decline models namely, i) empirical flux decline, ii) series resistance flux decline and iii) modified series resistance flux decline. The sensitivity of different coefficients in the models is discussed in detail together with their capability of predicting the experimental data trends

Photocatalysis is an efficient way to degrade the effluent organic matter. Chapter 9 presents the effect of photocatalysis in a membrane hybrid system on organic removal.

Chapter 10 presents the conclusions from the study with recommendations for future work. A near-zero fouling system is proposed, which combines photocatalysis and

membrane systems that efficiently removes EfOM from biologically treated sewage effluents.

1.3 Objectives

The main objectives in this study are to:

- i) Evaluate EfOM removal by different pretreatments and their roles in reducing membrane fouling (Chapter 4).
- ii) Investigate the membrane (UF and NF) foulant characteristics after the BTSE has undergone different pretreatments (Chapter 4).
- iii) Examine the effect of semi flocculation and semi adsorption on the membrane filtration in terms of MW distribution (Chapter 5).
- iv) Study the effect of pretreatment to membrane filtration using different EfOM fractions (HP, TP and HL) in BTSE to identify those that cause membrane fouling (Chapter 6).
- v) Assess the effect of a hybrid hydrodynamic cleaning that has high rate crossflow and relaxation modes as this procedure is an alternative to pretreatment so as to reduce reversible fouling and to increase membrane flux (Chapter 7).
- vi) Evaluate the capacity of different flux decline models in predicting the flux decline over time and to quantitatively compare different pretreatment methods (Chapter 8).
- vii) Study the efficacy of a photocatalysis hybrid system in comparison with different pretreatments and nanofiltration (Chapter 9).

CHAPTER 2



University of Technology, Sydney
Faculty of Engineering

LITERATURE REVIEW

2.1 Introduction

Wastewater treatment is envisaged as an action to protect the quality of limited freshwater resources and therefore make it available for beneficial purposes. However, achieving this objective remains elusive as the total discharge of biologically treated sewage effluent (BTSE) is continually on the rise due to increasing population and urbanization. Wastewater reclamation has been recognized as one of the most effective ways of increasing the availability of limited freshwater resources. Wastewater discharges can be diverted from polluting the water sources and at the same time, the use of reclaimed water can reduce the demand for freshwater. Consequently, there is a suitable motto about wastewater reuse, which is “*My water today is your water tomorrow*”. For the purpose of wastewater reclamation/reuse, it is imperative to study in detail the characteristics of effluent organic matter (EfOM) in the BTSE in order to design effective treatment methods.

2.2 Wastewater Reclamation/Reuse in Australia

Reuse of wastewater from wastewater treatment plants (WWTPs) has been widely used in Australia. Almost 10% of Australia’s BTSE is being recycled in one form or another (Table 2.1). During 2000, 109 WWTPs in New South Wales used some of their effluent for recycling, and 56 of these recycled more than half of their total effluent flow (Water Directorate, 2000). The most significant uses of reclaimed water from the New South Wales WWTPs are on golf courses and for pasture production. However, within the major capital cities, there has only been limited recycling of water beyond that needed for operation of the plants (Table 2.2). By 2010, most of the States of Australia will increase their wastewater reuse rate by up to 20%. Some of the future activities are highlighted in Figure 2.1.

Table 2.1 Annual wastewater reuse from WWTPs in Australia, 2001 (adapted from Radcliffe, 2003)

Region	Effluent, GL/yr	Reuse, GL/yr	%
Queensland	339	38	11.2
New South Wales	694	61.5	8.9
Australian Capital Territory	30	1.7	5.6
Victoria	448	30.1	6.7
Tasmania	65	6.2	9.5
South Australia	101	15.2	15.1
Western Australia	126	12.7	10.0
Northern Territory	21	1.1	5.2
Australia (total)	1824	166.5	9.1

Table 2.2 Wastewater reuse in State capital cities expressed as a percentage of sewage effluent treated, 2001 (adapted from Radcliffe, 2003)

State Capital	% recycled water use	State Capital	% recycled water use
Sydney	2.3	Adelaide	11.1
Melbourne	2.0	Perth	3.3
Brisbane	6.0	Hobart	0.1

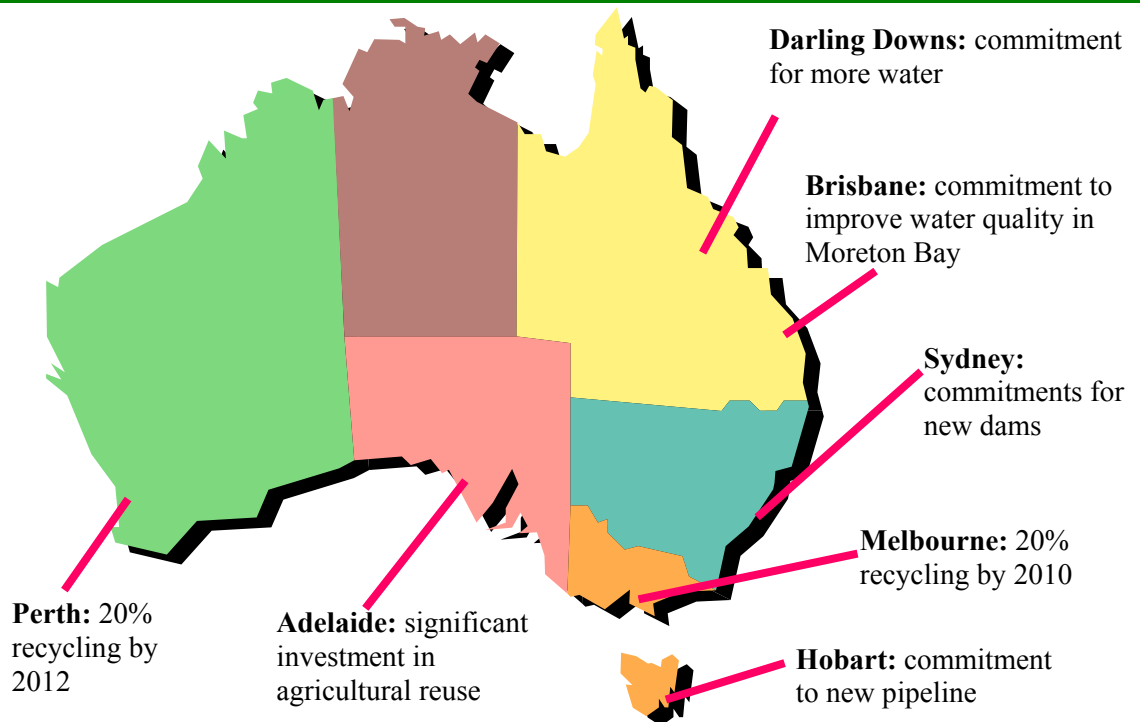


Figure 2.1 Future recycling commitments (adapted from Kahn, 2004)

2.3 Wastewater Characteristics

An understanding of the chemical composition of wastewater is important since this allows an understanding of their reactions and interactions with the organic and inorganic compounds (Roila et al., 1996). The organic chemistry and microbiology of wastewater is a reflection of the reactions during water usage (such as industrial, domestic and agricultural activities). Wastewater is treated, discharged to a receiving water body, and withdrawn for reuse by a downstream population. Consequently, the chemical and bacteriological composition must be monitored to ensure public health. In addition, the oxygen consuming material in the wastewater must be minimized to protect the receiving stream from low dissolved oxygen concentrations that can be harmful to desirable aquatic species.

Nutrients, such as nitrogen and phosphorus, should be removed to prevent eutrophication and subsequent siltation. Microbiological contaminants and other pollutants should also be removed to protect downstream users. The organic composition of wastewater is nearly 50 percent proteins, 40 percent carbohydrates, 10 percent fats and oils, and trace amounts of priority pollutants and surfactants. The microbiological composition of domestic wastewater includes 10^5 - 10^8 colony forming unit (CFU)/mL of coliform organisms, 10^3 - 10^4 CFU/mL fecal streptococci, 10^1 - 10^3 protozoan cysts, and 10^1 - 10^2 virus particles. To protect public health adequately, the safety of wastewater discharged to a receiving stream must be ensured (Ellis, 2004).

Fundamental information on specific organic matter is important in the optimization of treatment processes used in WWTP. The chemical composition of the sediments, organic macromolecules, or sewage sludge has been identified in many studies (Del Rio et al., 1998; Réveillé et al., 2003).

Wastewater qualities can be classified into 3 groups: i) physical, ii) chemical and iii) biological characteristics. The principal physical, chemical and biological characteristics of wastewater and their sources are shown in Table 2.3. It should be noted that many of the parameters listed are interrelated. Tchobanoglous and Burton (1991) observed that temperature, a physical property, affects both the biological activity in the wastewater and the amounts of gases dissolved in the wastewater.

Table 2.3 Physical, chemical and biological characteristics of wastewater and their sources (adapted from Tchobanoglous and Burton, 1991)

	Characteristic	Sources
Physical properties	Color	Domestic and industrial wastes, natural decay of organic materials
	Odor	Decomposing wastewater, industrial wastes
	Solids	Domestic water supply, domestic and industrial wastes, soil erosion, inflow/infiltration
	Temperature	Domestic and industrial wastes
Chemical properties	Carbohydrates, fats, oils and grease	Domestic, commercial and industrial wastes
	Pesticides	Agricultural wastes
	Phenols	Industrial wastes
	Proteins, Surfactants and volatile organic matter	Domestic, commercial, and industrial wastes
	Alkalinity and chlorides	Domestic wastes, domestic water supply, groundwater, infiltration
	Heavy metals	Industrial wastes
	Nitrogen	Domestic and agricultural wastes
	Phosphorus	Domestic, commercial, and agricultural wastes; natural runoff
	Sulfur	Domestic water supply; domestic, commercial, and industrial wastes
	Hydrogen sulfide and methane	Decomposition of domestic wastes
	Oxygen	Domestic water supply, surface-water infiltration
Biological properties	Animals and plants	Open watercourses and treatment plants
	Eubacteria and archaeobacteria	Domestic wastes, surface-water infiltration, treatment plants
	Viruses	Domestic wastes

The harmful contaminants in wastewater affect the aquatic environment and groundwater. Suspended solid (SS) can lead to developing sludge deposits and anaerobic conditions when untreated wastewater is discharged into on aquatic environment. In addition, their biological stabilization can lead to depletion of oxygen and to the increase of septic conditions. Nutrients, both nitrogen and phosphorus along with carbon, are essential nutrients for bacterial growth. When discharged into the aquatic environment, these nutrients can lead to the growth of undesirable aquatic life.

When discharged in excessive amounts on land, they can lead to the pollution of groundwater.

Many of the priority pollutants including pesticides, EDCs, and PPCPs are found in BTSE. The problem is that they cannot be treated by conventional methods of wastewater treatment. Typical examples include surfactants, phenols and agricultural pesticides.

2.4 Typical Processes Used in Wastewater Treatment

Wastewater collected from municipalities, communities and industries contains a wide range of pollutants from suspended, colloidal to dissolved solids. The treatment normally adopted includes physical, chemical, and biological methods. WWTP is divided into 4 groups: i) preliminary, ii) primary, iii) secondary, and iv) tertiary treatment. Conventional sewage treatment includes primary treatment to remove the majority of suspended solids, secondary biological treatment to degrade the biodegradable dissolved organic matter and nitrogen, and, tertiary treatment to remove most of the remaining organic and inorganic solids and pathogenic microorganisms.

The primary process is called preliminary treatment in WWTP. The preliminary treatment of wastewater is carried out to remove coarse and readily settleable inorganic solids with the size range of more than 0.01 mm, such as sand and grit particles. Their removal is carried out using screens and grit chambers, respectively. After coarse and floating solids in preliminary treatment are removed, the primary treatment endeavors to remove suspended solids in wastewater, which is carried out in sedimentation tanks or clarifiers. In sedimentation, the contaminant of the size from 0.1 mm to 35 μm including organic and inorganic matters is removed. Out of the 70-90 percent of suspended solids, removed by sedimentation, 30-40 percent reduction is oxygen-demanding suspended solids (Tchobanoglous and Burton, 1991).

Secondary treatment is employed to remove oxygen-demanding organic pollutants which are present mostly dissolved form in wastewater. This process utilizes biological degradation mechanisms of microorganisms to remove the dissolved pollutants of all the

ranges. At the same time, they produce SMPs and extracellular polymeric substances (EPSs), which cause toxic compounds and inhibition to nitrification. Finally, the purpose of tertiary treatment is to remove part of the remaining organic pollutants, and to reduce the bacterial count. This is mainly adopted to avoid inferior-treated effluent quality and to protect the receiving water. For example, chlorination is used as the final tertiary treatment step to reduce the level of pathogenic organisms in wastewater.

2.5 Effluent Organic Matter (EfOM) in Wastewater

2.5.1 Overview

The systematic treatment of wastewater was started in the late 1800s and early 1900s (Tchobanoglous and Burton, 1991). For the last two centuries, wastewater treatment has continually been developed to meet strict disposal standards. Recently, wastewater for reuse is being increasingly emphasized as a strategy for rational use of limited freshwater resources and as a means of safeguarding the quality of aquatic environments from deterioration caused by wastewater disposal.

Although many previous researchers have worked extensively on natural organic matter (NOM) in surface waters, there have been few studies related to EfOM in wastewater. This is probably due to the diverse characteristics of wastewater which vary from place to place and season to season. However, as concern of wastewater in the community increases, an interest in characterizing the EfOM has become more important.

The characteristics of EfOM are the combination of those of NOM and soluble microbial products (SMPs). Most of the NOMs come from tap water into wastewater, while SMPs come from biological treatment and non-biodegradable organic matter (persistent organic pollutants (POPs)). The trace harmful chemicals are also becoming a major concern. Wastewater reuse may cause an adverse effect on human health if compounds such as disinfection by-products (DBP), *N*-nitrosodimethylamines (NDMA), pesticides, herbicides, and endocrine disrupting chemicals (EDCs) are

present in recycled water. It may also cause ecological risks due to the presence of hormone and pharmaceutical and personal care products (PPCPs).

2.5.2 Constituents of EfOM in BTSE

The presence of organic pollutant in wastewater has been the cause of public concern in recent decades due to their potential health hazards. EfOM in wastewater consists of both particulates and dissolved substances. EfOM can be summarized into three different classes based on their origins:

- i) refractory natural organic matter (NOM) derived from drinking water sources,
- ii) synthetic organic compounds (SOC) produced during domestic use and disinfection by-products (DBP) generated during disinfection processes of water and wastewater treatment and
- iii) soluble microbial products derived during biological processes of wastewater treatment (Drewes and Fox, 1999).

The constituents that are found in BTSE are shown in Figure 2.2. The fraction of particulate organic material measured as suspended solids (SS) includes protozoa, algae, bacterial floc and single cell, waste product and other miscellaneous debris. Dissolved organic matter (smaller than 0.45 μm) are typically cell fragments, viruses, and macromolecules. Thus, EfOM can be classified into two main groups by size:

- i) particulate organic carbon (POC) above 0.45 μm and
- ii) dissolved organic carbon (DOC) below that limit. Both groups include a wide variety of constituents (Figure 2.2).

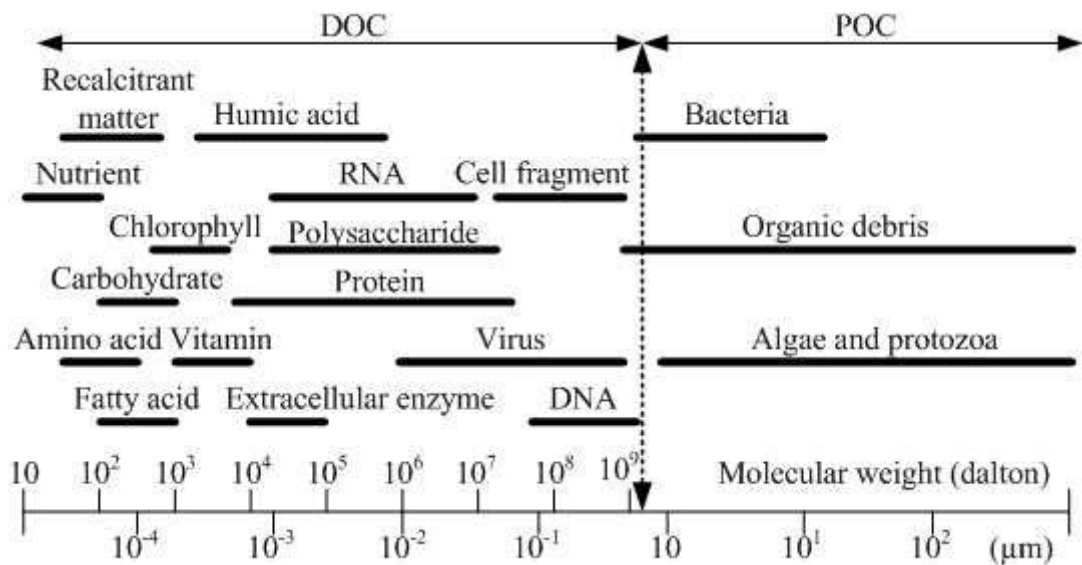


Figure 2.2 Typical organic constituents in BTSE and their size ranges (adapted from Levine et al., 1985)

Painter (1973) and Levine et al. (1985) showed that contaminants of interest in wastewater range in size from less than 0.001 μm to well over 100 μm (Table 2.4). The major macromolecules in BTSE are the polysaccharides, proteins, lipids and nucleic acids. EfOM in the range from 1,000 to 1,000,000 daltons include humic acid and fulvic acids present in drinking water. Wastewater compounds smaller than 10³ daltons include carbohydrates, amino acids (AA), vitamins, and chlorophyll. Persistent chemical compounds such as dichloro-diphenyl-trichloroethane (DDT), polychlorinated biphenyl (PCB) and other toxic substances of public health significance are also low molecular weight (MW) compounds (Stull et al, 1996; Pempkowiak and Obarska-Pempkowiak, 2002). To remove these compounds, it is important to examine the interrelationship between contaminant size ranges and wastewater treatment operations and processes.

Table 2.4 Percentage composition of EfOM in BTSE (adapted from Painter, 1973)

Composition	Dialysable (MW<10 kDa)	Non-dialysable (i.e. MW>10 kDa)
Ether extractables	-	-
Proteins	-	1.7
Amino acids	4.6	-
Charbohydrates and polysaccharides	0.2	4
Tannins and lignins	5.1	-
Alkyl benzene sulphonate (ABS)	-	-
Anionic detergents	3.2	-
Non-ionic detergents	1.6	-
Humic, fulvic, and humathomelanic acids	-	-
Volatile acids	5.4	-
Non-volatile acids	11.8	-
Neutral volatile compounds	3.1	-
Steroids	0.8	-
Optical brighteners	0.5	-
Organo-chlorine compounds	<0.001	-
Unidentified	3.7	54.3
Also identified in low (50 µg/L) concentrations	-	Glucose, fructose, sucrose, mannose, allulose, xylose, raffinose, formic acid, acetic acid, propionic acid, butyric acid, iso-butyric acid, iso-valeric acid, caproic acid, uric acid, pyrene, perylene, benzpyrenes, DDT, BHC, dieldrin, coprostanol and cholesterol

The POC includes zooplankton, algae, bacteria, and debris organic matter from soil and plants. It can easily be removed by solid-liquid separation processes. However, the DOC impart many adverse effects on water quality and therefore it remains a focus of research in wastewater treatment. Figure 2.3 shows the most significant DOC components in water in terms of different fractions.

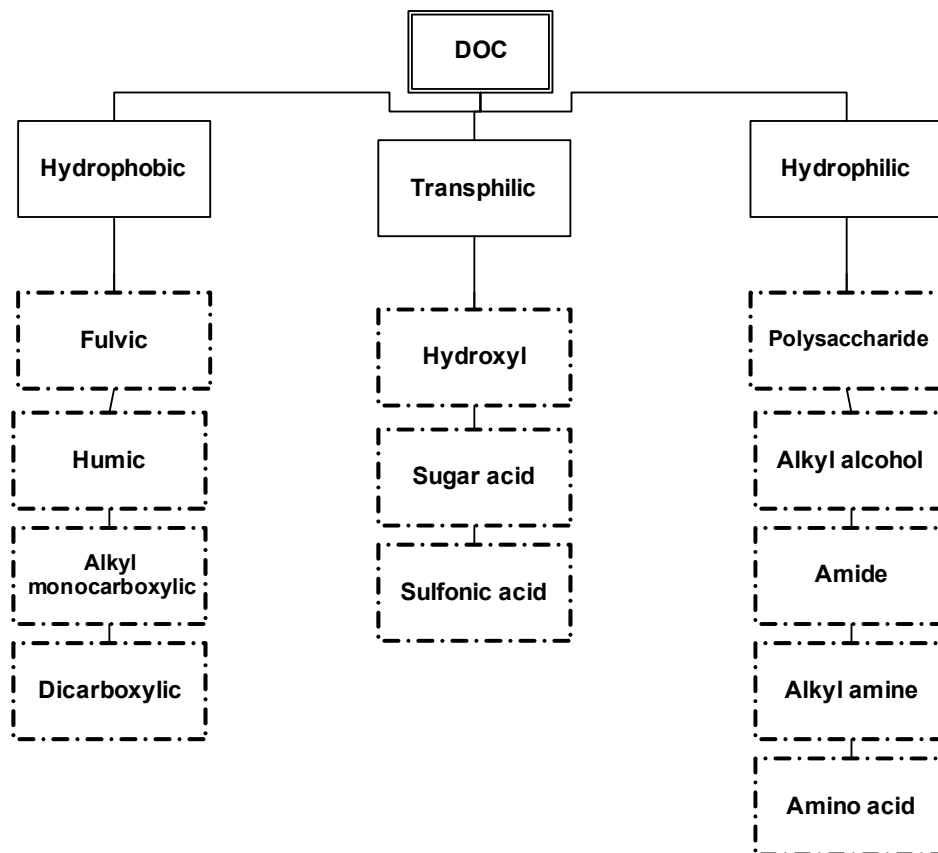


Figure 2.3 Different fractions of DOC and their constituents (adapted from Thurman, 1985; Cho, 1998)

2.5.3 Characteristics of EfOM from BTSE

EfOM includes many mixtures from NOMs, synthetic organic matters (SOMs) and soluble microbial pollutants (SMPs). Most of NOM is from tap water (about 1.5 – 5 mg/L of DOC) and SOM and SMP (range from 4 – 10 mg/L of DOC) come from industries and municipal wastewater treatment. The SMP is due to biological treatment processes involved in removing nutrients (especially N and P) and organic matters from wastewater.

Wastewater qualities can be classified into 3 groups: i) physical, ii) chemical and iii) biological characteristics. The principal physical, chemical and biological characteristics of wastewater and their sources are shown in Table 2.5. It should be noted that many of the parameters listed are interrelated. Tchobanoglous and Burton

(1991) observed that temperature, a physical property, affects both the biological activity in the wastewater and the amounts of gases dissolved in wastewater.

Table 2.5 Physical, chemical and biological characteristics of wastewater and their sources (adapted from Tchobanoglous and Burton, 1991)

	Characteristic	Sources
Physical properties	Color	Domestic and industrial wastes, natural decay of organic materials
	Odor	Decomposing wastewater, industrial wastes
	Solids	Domestic water supply, domestic and industrial wastes, soil erosion, inflow/infiltration
Chemical properties	Temperature	Domestic and industrial wastes
	Carbohydrates, fats, oils and grease	Domestic, commercial and industrial wastes
	Pesticides	Agricultural wastes
	Phenols	Industrial wastes
	Proteins, Surfactants and volatile organic matter	Domestic, commercial, and industrial wastes
	Alkalinity and chlorides	Domestic wastes, domestic water supply, groundwater, infiltration
	Heavy metals	Industrial wastes
	Nitrogen	Domestic and agricultural wastes
	Phosphorus	Domestic, commercial, and agricultural wastes; natural runoff
	Sulfur	Domestic water supply; domestic, commercial, and industrial wastes
Biological properties	Hydrogen sulfide and methane	Decomposition of domestic wastes
	Oxygen	Domestic water supply, surface-water infiltration
	Animals and plants	Open watercourses and treatment plants
	Eubacteria and archaeobacteria	Domestic wastes, surface-water infiltration, treatment plants
	Viruses	Domestic wastes

The harmful contaminants in wastewater affect the aquatic and groundwater environments. Suspended solid (SS) can lead to developing sludge deposits and anaerobic conditions when untreated wastewater is discharged into an aquatic environment. In addition, their biological stabilization can lead to the depletion of oxygen and to an increase in septic conditions. Nutrients, both nitrogen and phosphorus along with carbon, are essential nutrients for bacterial growth. When discharged to the aquatic environment, these nutrients can lead to the growth of undesirable aquatic life.

When discharged in excessive amounts on land, they can ultimately lead to the pollution of groundwater.

Many of the priority pollutants including pesticides, EDCs, and PPCPs are found in BTSE. The problem is that they cannot be removed by conventional methods of wastewater treatment. Typical examples include surfactants, phenols and agricultural pesticides.

2.5.4 Specific EfOM Components Present in BTSE

The contaminants in BTSE can be separated into four size fractions by successive sedimentation, centrifugation and filtration (Ricket and Hunter, 1971). The four fractions are classified by size range as settleable, supracolloidal, colloidal, or soluble. The size range and the organic content of each fraction are summarized in Table 2.6. An important conclusion from the early studies is that particles smaller than 1.0 μm can be degraded biochemically at a much more rapid rate than particles larger than 1.0 μm .

Table 2.6 Composition of organic materials in wastewater (adapted from Balmat, 1957; Levine et al., 1985)

	Classification			
	Soluble	Colloidal	Supracolloidal	Settleable
Size range (μm)	< 0.08	0.08 – 1.0	1 - 100	> 100
COD (% of total)	25	15	26	34
TOC (% of total)	31	14	24	31
Organic constituents (% of total solids)				
Grease	12	51	24	19
Protein	4	25	45	25
Carbohydrates	58	7	11	24
Biochemical oxidation rate, k , d^{-1} (base 10)	0.39	0.22	0.09	0.08

The global characterization of EfOM and its apparent removal efficiency are also presented in Table 2.7. Most of the EfOM of the treated water is found in the soluble fraction (86% of the COD). The global elimination of EfOM by the biological treatment is 90% for the soluble fraction and 96% for the bulk EfOM.

Table 2.7 Global characteristics of EfOM in wastewater and BTSE (adapted from Dignac et al., 2000)

		TOC (mg/L)	COD (mg/L)
Wastewater (influent)	Total	318	967
	Soluble	82	299
	Soluble (%)	26	31
BTSE	Total		35
	Soluble		30
	Soluble (%)		86

In a wastewater, about 75 percent of the suspended solids and 40 percent of the filterable solids are organic in nature. These solids are derived from both animals and plants as well as human activities. Organic compounds are normally comprised of a combination of carbon, hydrogen and oxygen with nitrogen in some cases. Other important elements, such as sulphur, phosphorus and iron, may also be present. The principal groups of organic substances found in wastewater are proteins (40 – 60%), carbohydrates (25 – 50%), and fats, oils, and grease (10%). Urea, the chief constituent of urine, is another important organic compound found in wastewater.

The concentration of simple molecules measured in BTSE after hydrolysis is low (Table 2.8). In wastewater, individually measured amino acids, carbohydrates, greases and phenolic compounds together account for 46% of the organic carbon (Dignac et al., 2000).

Table 2.8 Concentrations of specific organic compounds in the influent and BTSE (adapted from Dignac et al., 2000)

		Sugar	Protein	FA*	Sterol	Phenol
Wastewater (influent)	Total	138	143	32	2	1.2
	Soluble	24	46	5	0.6	0.3
BTSE	Soluble	2.10	2.80	0.06	0.01	0.01
Removal	Soluble	91%	95%	99%	99%	95%

* FA: fatty acid; all units: mg/L

Along with protein, carbohydrate, fat, oil, grease and urea, wastewater also contains small quantities of a large number of different synthetic organic molecules. Typical examples include surfactants, organic priority pollutants, volatile organic compounds, and agricultural pesticides. The number of such compounds is growing as organic molecules are continually being synthesized. The presence of these substances has complicated wastewater treatment because many of them either cannot be or are slowly decomposed biologically.

2.5.4.1 Extracellular Polymeric Substances (EPSs) and Soluble Microbial Products (SMPs)

During biological wastewater treatment, biomass not only consumes organic material present in the wastewater, but also produces SMP and EPS (Parkin and McCarty, 1981; Namkung and Rittmann, 1986; Noguera et al., 1994; Barker and Stuckey, 2001). EPS and SMP appear to be cellular components that are released during cell lysis, compounds that diffuse through the cell membrane and are lost during synthesis, or compounds that are excreted for some other purpose (Rittmann and McCarty, 2001). They are all important because they are always formed during biological treatment and they constitute the majority of the effluent COD.

Most bacteria produce EPS of biological origin that takes part in forming microbial aggregates. They grow in suspended cultures or in biofilms. The microbial biofilm includes bacterial cells enveloped by a matrix of large polymeric molecules. By definition, EPS are located at or outside the cell surface. Their composition may be controlled by different processes, such as active secretion, shedding of cell surface material, cell lysis and adsorption from the environment (Wingender et al., 1999).

SMP can be subdivided into two categories:

- i) substrate-utilization-associated products that are produced directly during substrate metabolism, and;

- ii) biomass-associated products that are formed from biomass, presumably as part of decay (Namkung and Rittmann, 1986).

Toxicity of SMP is of increasing concern. In other words, SMP may actually be more toxic than the original organic compounds present in BTSE. Mutagenic response is more in BTSE than in the primary effluent. Some SMPs have also been found to be inhibitory to nitrification (Chudoba, 1985). More details on EPS and SMP can be found in Rittmann et al., 1987 and Barker and Stuckey, 2001.

2.5.4.2 Protein

Proteins are the major constituents of animal organisms. Some SMPs also consist of proteins and amino acids. Proteins are complex in chemical structure and unstable, being subject to many forms of decomposition. Some are in soluble form in BTSE; others are in insoluble form. All proteins contain carbon as well as hydrogen and oxygen. They also contain a high and constant proportion of nitrogen (about 16 percent). In many cases, sulphur, phosphorus and iron are also constituents. Urea and proteins are the chief sources of nitrogen in BTSE. When proteins are present in wastewater, extremely foul odors are produced during their decomposition (Tchobanoglous and Burton, 1991).

Table 2.9 shows the distribution of proteins in influent wastewater. Serine, glycine, arginine, alanine, proline and tyrosine are relatively enriched in the BTSE compared to influent wastewater. Their removal efficiencies range from 89% to 100%. The amino acids that are preferentially lost during the biological treatment are the aspartic acid, histidine, cysteine and valine, with removal efficiencies between 96% and 100%.

Table 2.9 Comparison of the distributions of amino acids in the influent wastewater and their efficiencies (adapted from Dignac et al., 2000)

Amino acids	Total amino acids of the influent (%)	Removal efficiency (%)
Aspartic acid	6	96
Serine	3	90
Glutamic acid	9	95
Glycine	5	89
Histidine	3	97
Arginine	4	88
Threonine	3	94
Alanine	5	89
Proline	17	86
Cysteine	15	97
Tyrosine	5	89
Methionine	5	92
Valine	1	100
Lysine	7	95
Isoleucine	3	92
Leucine	5	94
Phenylalanine	4	93

Amino acids and proteins are potential carbon and nitrogen sources for heterotrophs and these have received significant attention because of their importance to protein synthesis, bacterial metabolism and algal/bacterial interactions. Organic nitrogen results in forming nitrogenous DBPs, which are of health and regulatory concern and these are also known to cause membrane fouling.

2.5.4.3 Carbohydrate

Carbohydrates include sugars, starches, cellulose and wood fiber. All of these are often found in wastewater. Carbohydrates contain carbon, hydrogen and oxygen. The common carbohydrates contain six or a multiple of six carbon atoms in a molecule, and hydrogen and oxygen in the proportions in which these elements are found in water.

Some carbohydrates, notably the sugars, are soluble in water; others, i.e. the starches, are insoluble. Sugars tend to decompose; the enzymes of certain bacteria and yeasts set up fermentation thus producing alcohol and carbon dioxide. Starches, on the other hand, are more stable but are converted into sugars by microbial activity as well as by dilute mineral acids. From the standpoint of bulk and resistance to decomposition, cellulose is the most important carbohydrate observed in wastewater due to its particular decomposition. Wastewaters containing high-carbohydrate are often from industries such as food processing and fermentation. These wastewaters can cause serious pollution if released into the natural environment without proper treatment or disposal. Kumar et al. (1998) and Pawar et al. (1998) discussed the treatment of high-carbohydrate wastewater in detail.

Table 2.10 shows the distribution of different sugars in influent wastewater. Mannose is the carbohydrate that is less affected by the biological treatment and this could either be due to its protection or to the bacterial release of mannose during treatment. Fucose is only decreased by 46% during the treatment. Rhamnose, ribose and glucose are also relatively concentrated in the hydrolysate of the BTSE. The presence of N-acetylamino carbohydrates is revealed in the wastewater (total and soluble fraction) and BTSE. These compounds could contribute to the uncharacterized fraction of the EfOM and nitrogen. DNA, another nitrogen-containing compound, is present in influent wastewater and in activated sludge, but is not detected in the soluble fractions of influent wastewater and BTSE. The EfOM percentage of monosaccharides follows the order of glucose > mannose > xylose > rhamnose.

Table 2.10 Comparison of the distributions of monosaccharide in the influent wastewater and their efficiencies (adapted from Dignac et al., 2000)

Monosaccharides	Total amino acids of the influent (%)	Removal efficiency (%)
Rhamnose	6	80
Fucose	3	50
Ribose	5	83
Arabinose	26	96
Xylose	42	96
Mannose	3	3
Galactose	7	93
Glucose	8	82

The carbohydrates of the EfOMs lead to operational problems in the biological treatment of activated sludge such as sludge bulking. Although some polysaccharides such as lignin are difficult to degrade, in general carbohydrates provide a carbon source to micro and macroorganisms. As such, they also have an important role in biological treatment processes. Carbohydrates do not interfere significantly with traditional treatment technologies but are recognized as major foulants in membrane separation processes (Cho, 1998; Jarusutthirak, 2002; Shon et al., 2004).

2.5.4.4 Fat, Oil and Grease (FOG)

FOGs are the third most abundant component in BTSE. FOGs are in domestic wastewater through materials such as butter, lard, margarine and vegetable FOGs. In addition, some mineral oil can also enter the wastewater treatment plant. FOGs can be measured after hydrolysis as fatty acids (FA).

Table 2.11 summarizes the percentage of different FAs in wastewater. Practically, all FAs are eliminated during the biological treatment (98% to 100%) except for the 20:4 ω 6, which is removed to a lesser degree (93%). This FA is not found in bacteria, and more likely originates from non-degraded lipids of the wastewater. The profiles of FAs in the influent wastewater and BTSE are not significantly different.

Table 2.11 Comparison of the distributions of fatty acids in the influent wastewater and their removal efficiencies (adapted from Dignac et al., 2000)

Fatty acids	Total amino acids of the influent (%)	Removal efficiency (%)
12:0	6	98
14:0	4	98
115:0	1	100
a15:0	1	100
15:0	2	100
16:0	20	98
16:1	3	97
18:0	8	98
18:1 ω 9	30	98
18:1 ω 7	3	100
18:2	19	98
18:3 ω 3c	1	97
20:0	0.5	100
20:4 ω 6	0.5	92
22:0	0.5	96
24:0	0.5	97

FOGs in wastewater can cause many problems in both sewer pipes and WWTPs. If FOGs are not removed before the discharge of the waste, it can interfere with the ecology of the surface waters and create unsightly appearance due to floating matter and films.

2.5.4.5 Surfactant

The term surfactant is an abbreviation for surface active agent. Surfactants lower the surface tension of a liquid, allowing easier spreading. Surfactants are usually made of organic compounds that consist of both hydrophobic and hydrophilic groups, which are semi-soluble in both organic and aqueous solvents. Thus, they prefer neither to be in water or in an organic phase. They are placed at the boundary between the organic and water phases. In some cases, they will congregate together and form micelles. Both

detergents and soaps are considered as surfactants. Surfactants that are not soaps are considered as detergents. Detergents are also commonly known as cleaning mixtures containing surfactants. Ionic detergents include sodium deoxycholate and sodium dodecyl sulfate. Detergents are used in cleaning, such as dishwashing in our daily life. Surfactants are an important source of pollution and are often transferred to waterways by industrial and domestic effluents. Most household products such as toothpastes, shampoos, shaving foams and bubble baths contribute to surfactants in wastewater.

Before 1965, the type of surfactant present in synthetic detergents, called alkylbenzene-sulfonate (ABS), was especially troublesome because it resisted biodegradation (White et al., 1994). As a result of legislation, ABS in detergents has been replaced by linear-alkyl-sulfonate (LAS), which is biodegradable. Surfactant has always been used even though there is still a potential danger. For instance, degradation products from the widely used alkylphenol polyethoxylate (APE) surfactants, which are contaminants in BTSE, have been shown to be estrogenic and bioaccumulative. Table 2.12 summarizes the composition of general surfactants found in wastewater.

Table 2.12 Composition of a soapless washing powder (adapted from Tchobanoglous and Burton, 1991)

Function	Characteristic	Classification
Surfactant detergent	Cleaning	Sodium alkyl benzene sulphonate
Builder	Softening water, floating a pollutant	Sodium tripolyphosphate
Conditioner	Maintaining alkalinity and protecting machine	Anhydrous sodium silicate
Filler	Breaking a particle	Anhydrous sodium silicate
Bleaching agent	Removing stain and contaminant	Sodium perborate
Bleach precursor	Possible bleaching at lower temperature	Tetra acetyl ethylene diamine (TAED)
Anti-redeposition agent	Floating a pollutant	Sodium carboxy methyl cellulose
Foam stabilizer	Improving foaming	Ethanolamide
Fluorescing agent	Improving whitening	
Perfumes and dyes	Improving smell and color	
Enzymes	Removing protein-like substance	

The impacts caused by detergents in the water are,

- i) propagation of algae due to phosphate; it inhibits carbon dioxide gas from leaving the water and at the same time inhibits oxygen from dissolving in the water (not favorable for biodegradation),
- ii) selection of microorganisms (anaerobic prevalence), and,
- iii) foam formation and aquatic toxicity.

2.5.4.6 Priority Pollutant

As the use of SOC increases, more and more contaminants have been found in BTSE. Pesticides and herbicides widely used to control weeds and insects in urban environments are classified as priority pollutants. Industrial wastewater also discharges these compounds to wastewater treatment plants. The U.S. Environmental Protection Agency has identified approximately 129 priority pollutants even as early as 1981 as persistently harmful compounds to aquatic environment.

Priority pollutants (both inorganic and organic) are selected on the basis of their known or suspected carcinogenicity, mutagenicity, teratogenicity or high acute toxicity. Most priority pollutants affect liver and kidney and raise the risk of cancer. Details of each compound can be found on the website of USEPA. The majority of these compounds are volatile organic compounds (VOCs). VOCs are of great concern since;

- i) once such compounds are in the vapor state they are much more mobile and, therefore, more likely to be released to the environment; and;
- ii) the presence of some of these compounds in the atmosphere may pose a significant public health risk.

2.5.4.7 Endocrine disrupting chemicals (EDCs) and pharmaceutical and personal care products (PPCPs)

Until the beginning of the 1990s, nonpolar hazardous compounds (i.e. persistent organic pollutants (POPs) and heavy metals) were the focus of interest as priority pollutants. Nowadays, these compounds are less troublesome in the industrialized

countries, since a dramatic reduction of emissions has been achieved through the adoption of suitable measures and the elimination of the dominant sources of pollution. However, in recent years, the presence of trace concentrations (below $\mu\text{g/L}$) of various compounds in wastewater has become a concern due to their potential to disrupt the endocrine system of humans and animals.

This class of chemicals is referred to as endocrine disrupting chemicals (EDCs), pharmaceutical and personal care products (PPCPs), polyaromatic hydrocarbons, plasticizers, hormones (e.g. estrogen) and pesticides. Metabolites of all of these may also act as endocrine disruptors. Naturally occurring compounds, such as phytoestrogens and their metabolites, may also contribute to this effect. The EDC and PPCP are toxic to most life-forms. These chemicals are not common constituents of domestic wastewater but result mostly from surface runoff from agricultural, vacant, parklands, etc. The detailed molecular structure of these compounds can be found in Vanderford et al. (2003).

It is generally accepted that there are the three major classes of endocrine endpoints:

- i) estrogenic (compounds that mimic or block natural estrogens),
- ii) androgenic (compounds that mimic or block natural testosterone) and
- iii) thyroidal (compounds with direct or indirect impacts to the thyroid).

Most research has focused only on estrogenic compounds; however, disruption of androgen and thyroid function may be of greater or equal importance biologically.

More recently, PPCPs have been discovered in WWTPs, some of which have been linked to ecological impacts at trace concentrations. Most of the EDCs and PPCPs are more polar than traditional contaminants and the majority of them have acidic or basic functional groups. These properties, coupled with occurrence at trace levels (i.e. $< 1 \mu\text{g/L}$), create unique challenges for both analytical detection and removal processes (Snyder et al., 2003). Table 2.13 presents the removal of EDCs and PPCP in WWTP.

Table 2.13 Concentration and removal of EDC and PPCP in WWTP (adapted from Snyder et al., 2003)

Compound	Influent (ng/L)	Effluent (ng/L)	Removal (%)
Nicotine	7560	274	96.4
Caffeine	58400	393	99.3
Carbamazepine	3230	471	85.4
DEET	2540	357	85.9
Phenacetin	3850	ND	>99
Oxybenzone	3460	253	93
BPA	1730	511	70.5
Estrone	108	38.5	64.4
Coprastanol	46400	155	99.7
Acetaminophen	17700	ND	>99
Diphenhydramine	3860	855	77.8
Cocaine	1230	ND	>91
Codeine	1710	447	73.9
Octylphenol	1390	15	99
Nonylphenol	78000	1060	98
Nonylphenol- monoethoxylate	28900	1790	94
Nonylphenol-diethoxylate	13400	2410	82
Monobutyltin	1153	ND	>96
Dibutyltin	950	7	99
Tributyltin	94	4	96
Tetrabutyltin	ND	ND	

Daughton and Ternes (1999) reviewed the occurrence of over 50 individual PPCP (metabolites from more than 10 broad classes of therapeutic agents or personal care products in environmental samples) in BTS. Acidic drugs are comprised of the major group of PPCP detected in municipal WWTP and, among them, bezafibrate, naproxen and ibuprofen are most plentiful (concentrations up to 4.6 µg/L in municipal WWTP). Tixier et al. (2003) also found that carbamazepine presented the highest daily load from WWTP into Lake Greifensee (Switzerland), followed by diclofenac and naproxen. Their elimination during their passage through WWTP was usually found to be quite low in the range 35–90%. Carbamazepine showed an extremely low removal (only 7%). Thus, through WWTP effluent discharge, PPCPs can enter receiving surface waters and thus present a risk to drinking water obtained from these surface waters. For example, clofibric acid, a metabolite of three lipid regulating agents (clofibrate, etofibrate and fenofibrate), has been identified in river and groundwater and even in drinking water at concentrations of up to 165 ng/L.

Reports of EDC and PPCP in water have raised significant concern among the public and regulatory agencies; however, little is known about the fate of these compounds during wastewater treatment. Many studies have shown that conventional WWTP cannot completely remove most of the EDCs and PPCPs (Ternes, 1998; Ternes et al., 1999a and b; Snyder et al., 2003). Thus, it is important to study the fate of these compounds, especially when wastewater is recycled.

One of the major limitations in the analysis of emerging contaminants remains the lack of methods for quantification of low concentrations. The prerequisite for proper risk assessment and monitoring of the quality of waste, surface and drinking waters is the availability of multi-residual methods that permit measurement at the low ng/L level (or even below that). So far, however these compounds have received little attention because they are not on regulatory lists as environmental pollutants. Analytical methodology for different groups of emerging contaminants is being developed and an increasing number of methods are reported in the literature. The analysis of this group of contaminants still requires further improvement in terms of sensitivity and selectivity, especially for complex matrices, such as wastewater.

Presence of these chemicals can result in fish kills and can cause problems in water supplies. Many of these chemicals are classified as priority pollutants. Evidence of the increased prevalence of endocrine disruptors in the environment includes physiological changes in human and animal populations, for example, increased birth defects, alterations in sexual development and functioning (such as decreased sperm counts, diminished sexual organs, and hypospadias), and other neurological effects. While drinking water is only a minor contributor to the total exposure to endocrine disrupting compounds, their prevalence and persistence in the environment is a concern (Ellis, 2004).

As synthetic compounds in household and industry increase, many synthetic compounds are emerging in WWTP. Table 2.14 presents classes of emerging compounds. Emerging contaminants correspond mostly to unregulated contaminants, which may be candidates for future regulation depending on research on their potential

health effects and monitoring data regarding their occurrence. The characteristic of these groups of contaminants is that they do not need to persist in the environment to cause negative effects since their high transformation/removal rates can be compensated for by their continuous introduction into environment (Barceló, 2003). For most of these emerging contaminants, occurrence, risk assessment and ecotoxicological data are not available and it is therefore difficult to predict their health effects.

Table 2.14 Classes of emerging compounds (adapted from Barceló, 2003)

Compound class	Examples
	Pharmaceuticals
Veterinary and human antibiotics	Trimethoprim, erythromycin, lincomycin, suffamethoxazole
Analgesics and anti-inflammatory drugs	Codein, ibuprofen, acetaminophen, acetylsalicylic acid, diclofenac, fenoprofen
Psychiatric drug	Diazepam
Lipid regulators	Bezafibrate, clofibrac acid, fenofibrac acid
B-blockers	Metoprolol, propranolol, timolol
X-ray contrast media	Lopromide, iopamidol, diatrizoate
Steroids and hormones (contraceptives)	Estradiol, estrone, estriol, diethylstilbestrol
	Personal care products
Fragrances	Nitro, polycyclic and macrocyclic musks
Sun-screen agents	Benzophenone, methylbenzylidene camphor
Insect repellents	N,N-dimethyltoluamide
Antiseptics	Triclosan, chlorophene
Surfactants and surfactant metabolites	Alkylphenol ethoxylates, alkylphenols (nonylphenol and octylphenol), alkylphenol carboxylates
Flame retardants	Polybrominated diphenyl ethers (PBDEs), Tetrabromo bisphenol A, Tris(2-chloroethyl)phosphate
Industrial additives and agents	Chelating agents (EDTA), aromatic sulfonates
Gasoline additives	Dialkyl ethers, methyl-4-butyl ether (MTBE)
Disinfection by-products	Iodo-THMs, bromoacids, bromoacetonitriles, bromoaldehydes, cyanoformaldehyde, bromate, NDMA

2.6 Adverse and Benign Effects of EfOM

EfOM affects essentially all chemicals and biological processes in aquatic environments. It has a stabilizing effect, opposite to that of metal ions. The EfOM in WWTP:

- i) produces precursor for disinfection-by-products (DBPs) formation,
- ii) exerts higher coagulant and oxidant demands,
- iii) fouls adsorbents and membranes,
- iv) causes aesthetic and corrosion problems, and
- v) supplies substrate for biomass growth in water distribution networks.

The presence of EfOM in BTSE can also be helpful in some instances, for example, EfOM substances can react with metals and many compounds to reduce toxicity. Some treatment processes implicitly benefit from the physico-chemical effects of EfOM on colloids. Humic acids can be used as direct means to extract pollutants (Yates and Von Wandruszka, 1999).

2.7 Typical treatment processes of EfOM

2.7.1 Introduction

Treatment processes for EfOM were initially developed in response to the concern for public health and the adverse conditions caused by the discharge of organic matter. From about 1900 to the early 1970s, treatment objectives were only concerned with i) the removal of suspended and floating material and ii) the elimination of pathogenic organisms (Tchobanoglous and Burton, 1991). However, as the use of various chemicals has increased, the pollutants of EfOM have become more numerous, such as complex organic compounds, EDC including pesticides and PPCP.

One of the main sources of emerging contaminants is untreated urban wastewaters and WWTP effluents (Figure 2.4). Most current WWTPs are not designed to treat these types of substances and a high portion of emerging compounds and their metabolites escape elimination in WWTP and enter the aquatic environment via sewage effluents.

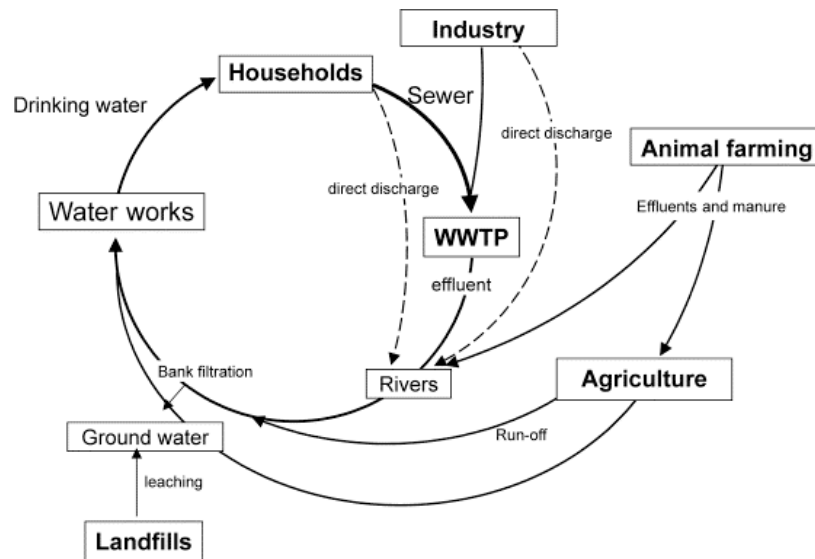


Figure 2.4 Components of a closed water cycle with indirect potable reuse (adapted from Petrović et al., 2003)

In sewage treatment processes, EfOM in BTSE is removed by physical, chemical, and biological means. Treatment methods where the application of physical force predominates are known as physical unit operations. Physical treatments consist of flocculation and filtration. Chemical treatments mean that the removal or conversion of contaminants is brought about by the addition of chemicals or by other chemical reactions. Flocculation, precipitation, ion exchange (IX), adsorption, and disinfection are the most common chemical treatment methods. Biological treatment involves with the biodegradation of organic matter using microbes. It is therefore important to select an appropriate treatment to remove different compounds found in EfOM. In order to treat these compounds, it is necessary to understand the roles and mechanisms of different treatment methods with respect to EfOM removal.

In this review, treatments such as flocculation, adsorption, biofiltration, ion exchange (IX), advanced oxidation process (AOP) and membrane process are discussed. The efficiency of different treatment processes is evaluated in terms of TOC/DOC removal, EDC/PPCP removal and MW distribution because:

- i) TOC indicates the general information for removal by treatments used,

- ii) EDC and PPCP represent removal of the small MW compounds (about 150 – 500 daltons) which cannot be removed using a conventional treatment process and
- iii) MW distribution gives information on the removal in terms of different MW ranges.

The effectiveness of specific processes in treating EfOM is strongly influenced by the size (or MW) of EfOM. The main treatment methods used are: i) flocculation, ii) adsorption, iii) IX, iv) AOP, v) filtration and vi) membrane technology. The size ranges of EfOM removed by different treatment methods are shown in Figure 2.5.

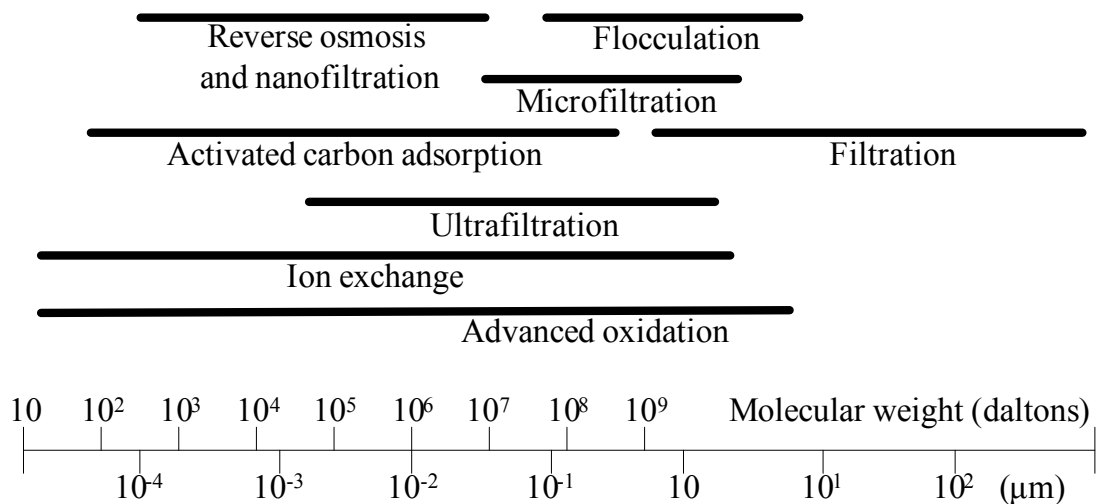


Figure 2.5 Size ranges of the applied treatments in treating EfOM

2.7.2 Removal of EfOM by Flocculation

2.7.2.1 General

Since about 1970, the need to provide more complete removal of the organic compounds and nutrients (nitrogen and phosphorus) contained in wastewater has brought about renewed interest in chemical flocculation (Tchobanoglous and Burton, 1991). Most colloids in wastewater carry a negative charge, but a colloidal dispersion does not have a net electrical charge. The primary charges on the particles are counterbalanced by charges in the aqueous phase, resulting in an electrical double layer at every interface between the solid and water. The forces of diffusion and electrostatic

attraction spread the charge around each particle in a diffuse layer. Repulsive electrical forces and attractive van der Waals forces interact between the particles in the solution, producing a potential barrier that prevents aggregation. The process of overcoming the repulsive barrier and allowing aggregation to occur is called coagulation (DeWolfe et al., 2003).

Coagulation consists of four distinct mechanisms: i) compression of the diffuse layer (van der Waals interaction), ii) adsorption to produce charge neutralization (destabilization), iii) enmeshment in a precipitate (sweep coagulation) and iv) adsorption to permit interparticle bridging (complex between particle and polymer with synthetic organic coagulant). Rapid mixing leads to the charge neutralization of colloids/particles through uniform and immediate disposal of chemicals with water. Flocculation which follows the rapid mixing results in the aggregation of particles. Flocculation can occur through three major mechanisms: i) Brownian movement of fluid molecules (perikinetic flocculation), ii) velocity gradient in the fluid (orthokinetic flocculation) and iii) differential settling of different sizes of particles in the water (Vigneswaran and Visvanathan, 1995).

Coagulants are classified into three groups in practical applications: i) aluminium sulfate (alum), ii) ferric salts, and iii) polyaluminum chlorides (PACl). Alum sulfate is the most common coagulant. The use of ferric chloride and PACl for water treatment has been increasing over the last few decades.

2.7.2.2 Flocculation for EfOM removal

It is possible to obtain a clear effluent, substantially free from suspended and colloidal solids by flocculation. FeCl_3 flocculation can remove 80 to 90% of the total suspended solids, 40 to 70% of BOD, 30 to 60% of COD, and 80 to 90% of the bacteria. However, the organic matter (DOC) removal depends on the characteristics of BTSE (Table 2.15).

Table 2.15 EfOM removal by flocculation

Researcher	Flocculant	Removal	Wastewater
Adin et al., 1998	FeCl ₃	99% (TPC)	Dan region BTSE, Tel Aviv, Jerusalem
Abdessemed and Nezzal, 2002	FeCl ₃ (Jar test)	77% (COD)	Staoueli BTSE, Algeria
Chapman et al., 2002	FeCl ₃ (Floating medium flocculator)	45%	Olympic park BTSE, Australia
Choo and Kang, 2003	FeCl ₃ followed by PAC adsorption	88% (COD)	Gyeongsan BTSE, Korea
Shon et al., 2004	FeCl ₃	57.6%	Gwangju BTSE, Korea
	FeCl ₃ followed by PAC adsorption	91%	

Table 2.16 presents the removal of EDC and PPCP by flocculation (Snyder and Westerhoff, 2005). The concentrations of ferric chloride and alum used in this study were 30 mg/L and 28 mg/L. The water was stirred at 100 rpm for 2 min and at 30 rpm for 20 min. Then, it was settled for 1 hr. The compounds which consist of aromatic ring such as benzo[a]pyrene, benzo[g,h,l]perylene, benzo[k]fluoranthene, mirex, benzo[b]fluranthene, and benzo[a]anthracene showed a high removal of more than 85%. However, the compounds such as diazepam, diclofenac, and meprobamate, indicated the lowest removal (less than 10%). Alum as a coagulant resulted in better removal compared to ferric chloride coagulants. EDCs or PPCPs are removed by partially adsorbing on particles in water and metal hydroxide particles formed during flocculation (Snyder et al., 2003).

Table 2.16 Removal efficiency (%) of EDC and PPCP with different flocculants (adapted from Snyder and Westerhoff, 2005)

EDC/PPCP	Ferric chloride	Alum	EDC/PPCP	Ferric chloride	Alum
Acetaminophen	0	0	a-BHC	5	16
Androstenedione	0	17	Acenaphthene	0	7
Atrazine	0	0	Acenaphthylene	0	11
Caffeine	0	3	a-Chlordane	28	30
Carbamzepine	0	7	Aldrin	50	51
DEET	0	6	Anthracene	0	0
Diazepam	0	5	b-BHC	12	27
Diclofenac	0	0	Benz[a]anthracene	26	29
Dilantin	0	0	Benzo[a]pyrene	66	67
Erythromycin-H2O	0	2	Benzo[b]fluoranthene	59	61
Estrodiol	0	12	Benzo[k]fluoranthene	62	64
Estriol	0	4	Chrysene	28	32
Estrons	0	9	d-BHC	8	22
Ethinylestradiol	0	16	DDD	24	26
Fluoxetine	0	20	DDE	57	57
Genfibrozil	2	20	DDT	45	46
Hydrocodone	0	6	Dieldrin	3	0
Ibuprofen	0	0	Endrin	0	0
Iopromide	0	12	Fluoranthene	3	12
Meprobamate	0	0	Fluorene	3	8
Naproxen	0	0	Galaxolide	15	18
Oxybenzone	0	0	g-BHC	5	22
Pentoxifylline	0	2	g-Chlordane	38	37
Progesterone-APCI	0	20	Heptachlor	30	30
Progesterone-ESI	0	6	Heptachlor epoxide	7	13
Sulfamethoxazole	0	0	Methoxychlor	29	32
TCEP	0	0	Metolachlor	9	26
Testosterone	0	16	Mirex	62	65
Triclosan	0	13	Musk keton	0	18
Trimethoprim	0	3	Naphthalene	20	29
Phenanthrene	0	4			

Flocculation can remove moderate amounts of HP organic contaminants that have a strong affinity for adsorbed EfOM. Most of these compounds are relatively polar (log Kow values less than 3) and as a result, only a few EDC and PPCP (e.g., nonylphenol, fluoroanthene, pyrene) are removed during this treatment. Adams et al., (2002) also

demonstrated that flocculation with alum and iron salts or excess lime/soda ash did not result in significant removal of antibiotics (i.e., carbadox, sulfachlorpyridazine, sulfadimethoxine, sulfamerazine, sulfamethazine, sulfathiazole, and trimethoprim). Sacher et al., (2000) found that ferric chloride flocculation did not remove several pharmaceuticals (diclofenac, carbamazepine, bezafibrate, and clofibrac acid). Certain pesticides were not effectively removed by flocculation and approximately 50% of the PAHs, pyrene, fluoranthene, and anthracene were removed through hydrophobic interactions (Rebhun et al., 1998). In summary, EDCs and PPCPs that are associated with colloidal or particulate material are removed by flocculation

2.7.3 Removal of EfOM by Adsorption

2.7.3.1 General

Adsorption is a physical and surface phenomenon by which molecules of organics (adsorbates) are attracted to the surface of adsorbent by intermolecular forces of attraction. Physical adsorption is mainly caused by van der Waals forces and electrostatic forces between adsorbate and adsorbent molecules. In principle, any porous solid can be an adsorbent, however for an efficient and economical adsorption process, the adsorbent must have a large surface, long life, and a well-defined microcrystalline structure to possess high adsorption selectivity and capacity.

Adsorption is the process of collecting soluble substances that are in solution on a suitable interface. As EfOM in BTSE mainly constitutes of organic matter from about 250 to 3500 daltons, they can be successfully removed by adsorption.

The main factors that affect the adsorption of EfOM are:

- i) the characteristics of adsorbent: surface area, particle size, and pore structure,
- ii) the characteristics of adsorbate: solubility, molecular structure, ionic or neutral nature and
- iii) the characteristics of the solution: pH, temperature, presence of competing organic and inorganic substances.

Other factors affecting adsorption of organics are related to specific chemical affinities between functional groups on the adsorbate and on the adsorbent. Table 2.17 shows the classes of organic compounds that are easily or poorly removed by activated carbon in general. The compounds that are poorly removed are highly soluble (hydrophilic) and have low MW. In the case of organic acids and bases, adsorption is strongly dependent on pH because of the preference for removal of neutral species from aqueous solution.

Table 2.17 Classes of organics adsorbed onto activated carbon (adapted from Montgomery, 1985)

	Classes	Compounds
Readily adsorbed	Aromatic solvents	Benzene, toluene, nitrobenzenes, etc.
	Chlorinated aromatics	PCB, chlorobenzenes, chloronaphthalene
	Phenol and chlorophenols	
	Polynuclear aromatics	Acenaphthene
	Pesticides	DDT, Aldrin, chlordane, BHCs, heptachlor, etc.
Poorly adsorbed	Chlorinated nonaromatics	Carbon tetrachloride, chloroalkyl ethers, hexachlorobutadiene, etc.
	Large MW hydrocarbons	Dyes, gasoline, amines, humics
	Alcohols	Low MW ketones, acids, and aldehydes
	Sugars and starches	
	Very-high-MW	Colloids
	Low-MW aliphatics	

2.7.3.2 Adsorption for EfOM removal

Previous studies have shown that activated carbon can adsorb EfOM in significant quantities and produce high quality effluent (Summers and Roberts, 1984; Najm et al., 1990). Since BTSE contains different types of organic and inorganic substances, it is possible that physical and chemical adsorption takes place when it comes in contact with activated carbon. However, for simplicity reasons, only physical adsorption is considered since most of the adsorption-separations are due to physical adsorption.

The adsorption process is competitive in nature. The extent of competition depends on the strength of adsorption of the competing molecules, the concentration of these molecules and the characteristics of the adsorbent (activated carbon). In a competitive adsorption environment, desorption of a compound may take place by displacement by other compounds, as the adsorption process is reversible in nature. It results in an effluent concentration of EfOM greater than the influent concentration in some cases (Snoeyink, 1990). Past experimental results on EfOM removal by adsorption is summarized in Table 2.18.

Table 2.18 EfOM removal from BTSE by adsorption

Researcher	Process	Removal	Wastewater
Arana et al., 2002	PAC adsorption	53% (DOC)	BTSE from Universidad de Las Palmas de Gran Canaria, Spain
Abdessemed and Nezzal, 2002	PAC adsorption	71% (COD)	Staoueli BTSE, Algeria
Shon et al., 2004	PAC adsorption	60 - 71.4% (DOC)	Gwangju BTSE, Korea

Table 2.19 presents the removal of EDC and PPCP by adsorption. Compared to flocculation, adsorption removes EDC/PPCP in significant quantities. PAC which has hydrophobic characteristics interacts with nonpolar organic compounds of EDC/PPCP. Snyder et al. (2003) suggested that PAC adsorption is effective in removing nonylphenol, nonylphenol ethoxylates, triclosan, dilatin, bisphenol A, and octylphenol (about 60 - 80% removal).

Table 2.19 Removal of EDC and PPCP from BTSE by PAC adsorption (adapted from Snyder et al., 2003)

EDC/PPCP	Removal (%)	EDC/PPCP	Removal (%)	EDC/PPCP	Removal (%)
Acetaminophen	87	a-BHC	0	Fluorene	96
Androstenedione	58	Acenephtene	90	Galaxolide	63
Atrazine	54	Acenapththylene	95	g-BHC	67
Caffeine	19	a-Chlordane	82	g-Chlordane	0
Carbamzepine	55	Aldrin	92	Heptachlor	88
DEET	0	Anthracene	77	Heptachlor epoxide	35
Diazepam	53	b-BHC	77	Methoxychlor	0
Diclofenac	64	Benz[a]anthracene	91	Metolachlor	57
Dilantin	0	Benzo[a]pyrene	94	Mirex	90
Erythromycin-H ₂ O	44	Benzo[b]fluoranthene	90	Musk keton	73
Estrodiol	2	Benzo[k]fluoranthene	91	Naphtalene	96
Estriol	54	Chrysene	93	Phenanthrene	94
Estrons	79	d-BHC	23	Meprobamate	0
Ethynylestradiol	67	DDD	52	Naproxen	87
Fluoxetine	92	DDE	93	Oxybenzone	93
Genfibrozil	0	DDT	80	Pentoxifylline	65
Hydrocodone	72	Diedrin	52	Progesterone-APCI	45
Ibuprofen	48	Endrin	14	Progesterone-ESI	91
Iopromide	33	Fluoranthene	91	Sulfamethoxazole	43
Testosterone	35	Trimethoprim	40	TCEP	71
Triclosan	93	Pyrene	85		

2.7.4 Removal of EfOM by Biofiltration

2.7.4.1 General

Any type of filter with attached biomass on the filter-media is called a biofilter. It can be a trickling filter used in a wastewater treatment plant, a horizontal rock filter used in a polluted stream, granular activated carbon (GAC) or slow sand filter used in a water treatment plant.

Biofilter has been successfully used to treat organic pollutants from air, water and wastewater. The biofilter (in the form of trickling filter) was first introduced in England

in 1893 (Metcalf and Eddy, 1991), and since then, it has been successfully used for the treatment of domestic and industrial wastewater. Originally, this biofilter was developed using rock or slag as filter media, however at present, several types and shapes of plastic media are used. There are a number of small package treatment systems with different brand names that are currently available in the market where different shaped plastic materials are packed as filter media.

In a biofiltration system, the pollutants are removed by biological degradation rather than physical straining as is the case in normal filter. With the progression of the filtration process, microorganisms (aerobic, anaerobic and facultative bacteria; fungi; algae; and protozoa) are gradually developed on the surface of the filter media and form a biological film or slime layer known as biofilm. The development of biofilm may take few days or months depending on the influent organic concentration. The crucial point for the successful operation of a biofilter is to control and maintain a healthy biomass on the surface of the filter. Since the performance of the biofilter entirely depends on the microbial activities, a constant source of substrates (organic substance and nutrients) is required for its consistent and effective operation. There are three main biological processes that can occur in a biofilter: i) attachment of microorganism, ii) growth of microorganism and iii) decay and detachment of microorganisms. As the success of a biofilter depends on the growth and maintenance of microorganisms (biomass) on the surface of filter media, it is necessary to understand the mechanisms of attachment, growth and detachment on the surface of the filter media.

The parameters that can affect the performance of a biofilter are the characteristics of filter media, hydraulic and organic loading rate, and filter backwash techniques. Other factors that can influence the performance of a biofilter are temperature and the presence of oxidants, i.e. O_3 , H_2O_2 , Cl_2 , and NH_4Cl etc. in the influent (Urfer et al., 1997, Goel et al., 1995). These factors should be carefully studied when designing a biofiltration system. Typical design values of biofilter for water and wastewater treatment are presented in Table 2.20.

Table 2.20 Typical biofilter design parameters used in tertiary wastewater and surface water treatment (adopted from Rachwal et al., 1996)

Parameter	Slow sand filter	Sand or multi-media Rapid filter	Granular activated carbon Rapid filter
Filtration rate (m/h)	0.1 - 0.3	5 - 30	5 - 15
Media effective size (mm)	0.2 - 0.4	0.5 - 2	0.5 - 1
Media depth (m)	0.3 - 1.5	0.6 - 2.5	0.6 - 3.5
Media contact time (h)	1 - 15	0.07 - 0.2	0.1 - 0.5
Specific Media surface area (m ² /m ³)	10,000*	4400*	4600*, 5 x 10 ⁸ #

* based on assumed spherical media, # based on manufacturers quoted molecular scale adsorption surface area

2.7.4.2 Biofiltration for EfOM removal

A biofilter can be employed either as a primary treatment unit or as secondary unit in the wastewater treatment system. In advanced wastewater treatment, biofilter can be used along with conventional physico-chemical processes such as coagulation-flocculation, filtration and sedimentation. The conventional filter and the biofilter units can be combined depending on the suspended solid concentration. Since the main purpose of the biofilter is to remove the dissolved organics, the suspended particles are removed in conventional filter before the entry of the wastewater to the biofiltration system.

Adsorption of organics and biological degradation of the organic matter adsorbed onto the activated carbon are two major mechanisms for the consistent removal of organics in the GAC biofiltration system. A summary of past research on DOC and EDC/PPCP removal by biofiltration is presented in Tables 2.21 and 2.22.

Table 2.21 Lists of the DOC removal by filtration with BTSE

Researcher	Process	Removal	Wastewater
Kim et al., 2002	- Dual media + GAC biofilter	64%	BTSE, Singapore
	- Dual media + GAC biofilter with a flocculant	75%	
Shon et al., 2003	- GAC biofilter	60%	Gwangju BTSE, Korea

Table 2.22 Removal of EDC and PPCP with full scale GAC biofilter in ppt unit (adapted from Snyder and Westerhoff, 2005)

Compounds	Raw water	After coagulation	GAC influent	GAC effluent	GAC Removal (%)
Caffeine	7.1	2.7	17	3.1	81.8
Erythromycin-H ₂ O	1.4	1.9	1.8	<1.0	<44.4
Sulfamethoxazole	1.2	1.6	6.0	<1.0	83.3
Meprobamate	2.0	2.0	1.2	<1.0	<16.7
Dilantin	1.4	2.2	1.8	<1.0	<44.4
TCEP	2.0	1.7	2.0	1.3	35
Carbamazepine	2.5	2.4	2.2	<1.0	<54.5
DEET	4.0	3.6	1.8	<1.0	<44.4
Atrazine	571	571	650	6.1	99.1
Iopromide	2.2	2.4	3.3	<1.0	<69.7
Ibuprofen	2.4	2.9	1.1	<1.0	<9.1
Gemfibrozil	4.8	4.5	1.2	<1.0	<16.7
Metolachlor	122	121	122	<1.0	<99.2

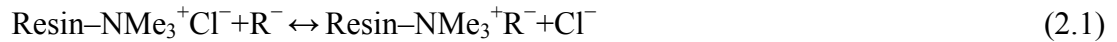
2.7.5 Removal of EfOM by Ion Exchange

2.7.5.1 General

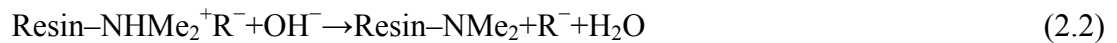
Wastewaters containing low MW EfOM are difficult to be treated by coagulation/flocculation processes, as this process is less effectively in removing the smaller MW species. Ion exchange (IX) is claimed to be more economical than activated carbon, carbonaceous resins or metal oxides in removing EfOM if on-site regeneration of ion exchanger can be performed. The charged impurities in water and wastewater can be easily removed by IX. Since EfOM has a negative charge at neutral pH, basic anion exchange resins are commonly used in wastewater applications. The IX

in treating EfOM from BTSE can be divided into two groups: i) strongly basic anion exchange and ii) weakly basic anion exchange.

The quaternary ammonium resins are generally used as strongly basic anion exchange in the chloride form. The following reaction occurs with charged DOC (which is represented by R^- and anion exchange resins):



The resins used in treating EfOM can be regenerated with an excess of brine or caustic brine. A strongly basic resin requires salt and alkali well in excess of the stoichiometric amounts. On the other hand, weakly basic resin requires lower amount of chemicals. The chemicals used in latter case are lime and mineral acid at only slightly above equivalent levels:



Thus, weakly basic resins have cost advantages in terms of regenerated usage. The calcium salts of humic and fulvic acids are obtained in the regenerated liquid. Regeneration can be achieved without salt, which can simplify the disposal of the waste (Bolto et al., 2004). The properties of resins that are used in the removal of EfOM are listed in Table 2.23.

Table 2.23 Characteristics of resins used in the treatment of BTSE

Researcher	Remarks
Brattebo et al., (1987)	- Strongly basic resins in the chloride form remove EfOM better than their hydroxide forms.
Meyers (1995)	- Resins with a smaller particle size are more efficient.
Symons et al., (1995) and Gottlieb, (1996)	- Better EfOM removal with an IX of polyacrylic skeleton than styrenic resin. - More flexible acrylic skeleton enables resins to adsorb more water and swell, making them less prone to fouling. - The acrylic skeleton facilitates the removal of HL organic acids in addition to more abundant HP acids (humics).
Kunin and Yarnell, (1997)	- Macroporous resins with a moderate to high porosity are more suited to stresses in a continuous process compared to gel resins. - Macroporous resins are more physically stable than gel resins under aggressive conditions including hydraulic pressures and presence of chlorine.
Frederick, (1997)	- The smaller average particle diffusion distances within the smaller resin beads result in an improvement to regeneration (and loading) kinetics. - The same property also results in reductions of rinse times required to remove regenerant from the beads.

In water and wastewater applications, magnetic ion exchange resin (MIEX[®]) is increasingly being used. The MIEX[®] resin was originally developed in Australia (Orica Watercare Ltd.) for the removal of DOC. The DOC removal from water minimizes the formation of DBP in drinking water supplies. The name MIEX[®] comes from magnetic ion exchange, because the adsorption is achieved by means of IX and the resin particles contain a magnetized component within their structures (Figure 2.6). MIEX[®] has been developed to enable the adsorption of dissolved organic matter. This process occurs in a stirred contactor, similar to a flash mixer in a conventional water treatment plant. The negatively charged DOC is removed by exchanging with a chloride ion on active sites on the resin surface.

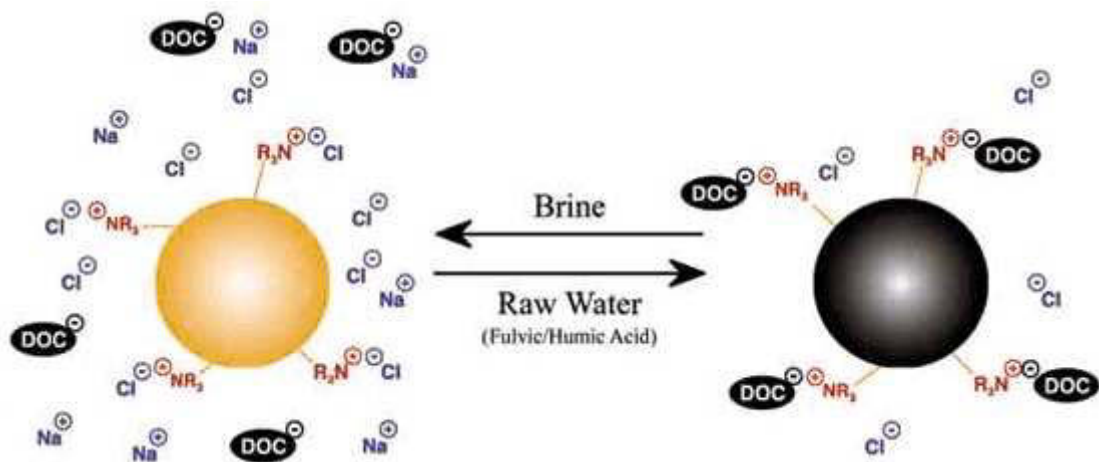


Figure 2.6 DOC removal mechanisms by MIEX[®] resin (adapted from Bourke et al., 1999)

Several bench-scale and pilot-scale studies have proved its capability in removing negatively charged EfOM (Bourke et al., 1999). Preliminary experiments indicate that MIEX[®] and enhanced coagulation can effectively remove small MW organic matter and large MW organic matter, respectively. The process was developed on the following recognized premises (Fearing et al., 2004)

- i) resins with quaternary ammonia functional groups are more effective,
- ii) resins with a polyacrylic skeleton are the best for EfOM removal,
- iii) macroporous resins are more suited to continuous processes than gel resins,
- iv) resins need a high specific IX capacity and
- v) smaller sized resin particles are more efficient.

2.7.5.2 Removal of EfOM by MIEX[®] Process

In the MIEX[®] process, the removal of EfOM is achieved by IX. On average, 70-80 % of the EfOM are weak organic acids that are found in ionized form in the pH range of 6 to 8. These polydispersed anions have a carboxyl content of 11 to 15 meq/g TOC which makes them good candidates for IX (Symons et al., 1995).

In terms of MW of organic matter, smaller EfOM (MW 1000-10000 daltons) are exchanged rapidly both during resin loading and regeneration. On the other hand, large EfOM (MW > 10000 daltons) have been found to have slower exchange kinetics but form stronger ionic bonds with the resin. As a result of this, they are harder to extract during resin regeneration and have potential to foul the resin. The smallest EfOM (MW < 1000) is neutral, and thus not removed by resin. In addition, the effectiveness of EfOM removal by IX varies from one source water to another depending not only on the composition of EfOM but also on pH, temperature and presence of other anions, especially sulphate. Efficiency of the EfOM removal in an IX process can be improved by optimizing resin characteristics and/or process conditions. Both of above factors have been utilized in the MIEX[®] DOC process (Slunjski et al., 1999).

A pilot plant study treating raw water received from a water treatment plant revealed the following: MIEX[®] resin reduced the raw water THM formation potential (THMFP) by 69.5% (from 167 g/L to 51 g/L) and the HAA formation potential (HAAFP) by 61% (from 94 g/L to 37 g/L) (AWWA, 2004). MIEX[®] treatment reduced the raw water DOC by an average of 71% (from 11.8 mg/L to 3.4 mg/L), which allows compliance with the EPA DBP standards. Table 2.24 presents the removal of EDC and PPCP by MIEX[®] treatment. Some EDCs/PPCPs (triclosan and diclofenac are effectively removed, while most EDCs/PPCPs cannot be removed this this treatment. The DOC removal by MIEX[®] was 60 to 70% in BTSE. Zhang et al. (2005) reported that MIEX[®] resin can easily be regenerated and even after several regenerations with a similar removal with Gwangju BTSE, Korea.

Table 2.24 Removal of EDC and PPCP by different concentrations of MIEX[®] (adapted from Snyder and Westerhoff, 2005)

EDC/PPCP	(5 mL of MIEX)/(L of water)	10 mL/L	15 mL/L	20 mL/L
Triclosan	84	90	93	94
Sulfamethoxazole	0	0	0	4
Oxybenzone	4	24	36	40
Naproxen	18	20	44	53
Ibuprofen	0	2	16	20
Gemfibrozil	0	0	13	20
Ethinylestradiol	0	0	20	20
Estradiol	0	0	3	3
Dilantin	0	0	21	22
Diclofenac	68	81	88	90

2.7.6 Removal of EfOM by Advanced Oxidation Process (AOP)

2.7.6.1 General

Although the number of refractory substances found in BTSE is increasing, it is not possible to achieve a complete removal of EfOM by the conventional treatment processes. Photocatalytic oxidation is relatively a new technology that can be used to mineralize the refractory EfOM. During the past 10 years, there has been considerable research and commercial interest in the use of AOP for the treatment of organic contaminants in wastewater.

AOP is typically characterized by the generation of the highly reactive hydroxyl radical ($\cdot\text{OH}$) that can mineralize dissolved organic pollutants into CO_2 and H_2O . They are: i) ozonolysis, ii) UV/ozone, iii) UV/ H_2O_2 iv) irradiation with electrons and v) combinations of the above methods. This process has shown considerable potential in the treatment of a number of recalcitrant organic pollutants such as humic substances, EDC, PPCP, textile dye waste and sewage sludge. In addition, this process has been tested with alternative disinfectants to disinfect protozoa such as *Cryptosporidium*. In the recent years, this technique has also been coupled with membrane systems to obtain better results (Molinari et al., 2001; Tang and Chen, 2001).

Oxidative hydroxyl radical (HO•) is generated by photochemical and non-photochemical pathways (Table 2.24). The oxidative potential (OP) of species indicates the power of an oxidant, with a higher value indicating higher reactivity. For example, the OP for OH• is +2.8 volts, compared to ozone at 2.07 volts. The hydroxyl radical is a strong and non-specific oxidant and therefore able to rapidly oxidize a large number of recalcitrant molecules. Many of the AOPs utilize the chemical hydrogen peroxide as oxidant. The oxidizing strength of hydrogen peroxide alone is relatively weak (OP +1.76 volts), but the addition of UV light enhances the rate and strength of oxidation through production of increased amounts of hydroxyl radicals. Hydrogen peroxide (even in low concentrations) will enhance other AOPs, as the molecule easily splits into two hydroxyl radicals. Fenton's reagent has been proven to be very effective in the treatment of organic molecules. However, this is expensive as a complicated sludge matrix is produced that requires disposal. It requires continuous supply of feed chemicals.

Table 2.25 Advanced oxidation processes used in water treatment

Reagents Used	Main Chemical Reactions
Fenton's reagent/hydrogen peroxide	$\text{Fe}^{2+} + \text{H}_2\text{O}_2 \rightarrow \text{Fe}^{3+} + \text{OH}^- + \text{HO}\bullet$ (wavelengths < 580 nm) $\text{Fe}^{3+} + \text{H}_2\text{O}_2 \rightarrow \text{Fe}^{2+} + \text{H}^+ + \text{HOO}\bullet$
Ozone/hydrogen peroxide or hydroxide	$2\text{O}_3 + \text{H}_2\text{O}_2 \rightarrow 2\text{HO}\bullet + 3\text{O}_2$
Ozone/UV	$\text{O}_3 + \text{UV} + \text{H}_2\text{O} \rightarrow 2\text{HO}\bullet + \text{O}_2$
Hydrogen peroxide/UV	$\text{H}_2\text{O}_2 + \text{UV} \rightarrow 2\text{HO}\bullet$ $\text{HO}\bullet + \text{H}_2\text{O}_2 \rightarrow \text{HO}_2\bullet + \text{H}_2\text{O}$ $\text{HO}_2\bullet + \text{HO}_2\bullet \rightarrow \text{H}_2\text{O}_2 + \text{O}_2$
TiO ₂ /UV photocatalysis	$\text{TiO}_2 + h\nu \rightarrow \text{TiO}_2(e^- + h^+)$ (wavelengths < 390 nm) $h^+ + \text{OH}^- \rightarrow \text{HO}\bullet$ $e^- + \text{O}_2 \rightarrow \bullet\text{O}_2$ (h ⁺ ... holes = valence band electron vacancies e ⁻ ... conduction band electrons)

The TiO₂/UV photocatalytic process is also one of the attractive AOPs as its reactive species is the HO• radical as in all other AOPs. Degradation of waste compound proceeds via oxidative (electrophilic) attack of HO• and leads to complete

mineralization to yield innocuous CO₂ and mineral acids, taking advantage of the extremely high redox potential (2.8 volts) of the HO•. This process is based on the electronic excitation of a molecule or solid caused by light absorption e.g. UV light that drastically alters its ability to lose or gain electrons and promote decomposition of pollutants to harmless by-products (Molinari et al., 2002). Photoinduced electrons (e⁻) and positive holes (h⁺) are produced from TiO₂ with UV light. These charged species can further generate free radicals. The highly oxidizing positive hole (h⁺) is considered to be the dominant oxidizing species contributing to the mineralization process resulting from the TiO₂ photocatalysis (Chu and Wong, 2004). The principal advantages of the TiO₂/UV process compared to other AOPs are:

- i) suitable in wastewater treatment without the addition of large amounts of chemicals,
- ii) no follow-up treatments (filtration, etc.) are necessary and
- iii) applicability over a wide range of pH values.

There are also some limitations of UV/oxidation (Gogate and Pandit, 2004).

(i) The aqueous stream being treated must allow good transmission of UV light (high turbidity causes interference on the passage of UV light). Free radical scavengers can inhibit contaminant destruction efficiency. Excessive dosages of chemical oxidizers may act as a scavenger.

(ii) The aqueous stream to be treated by UV/oxidation should be relatively free of heavy metal ions (less than 10 mg/L) and insoluble oil or grease to minimize the potential of fouling of the quartz sleeves.

(iii) When UV/O₃ is used on volatile organics, the contaminants may be volatilized (e.g., stripped) rather than getting destroyed. They would then have to be removed from the off-gas by activated carbon adsorption or catalytic oxidation.

(iv) Costs may be higher than competing technologies because of energy requirements. Pretreatment of the aqueous stream may be required to minimize ongoing cleaning and maintenance of UV reactor and quartz sleeves.

(v) Handling and storage of oxidizers require special safety precautions.

2.7.6.2 AOPs for EfOM removal

Typical AOPs use ozone, hydrogen peroxide and UV radiation to generate the hydroxyl radicals in treating EfOM in BTSE. One of the more recent and more practical methods of producing hydroxyl radicals is the use of UV along with a suspended TiO₂ catalyst. This method is believed to have the advantage of better control in terms of producing the hydroxyl radicals while avoiding or minimizing the formation of the potentially toxic DBP (Al-Bastaki, 2003).

Table 2.26 presents removal of EfOM from BTSE by different AOPs. The use of O₃/H₂O₂/UV results in a shorter reaction time and requires less oxidant than the other AOPs (Ito et al., 1998). When photocatalysis was combined with FeCl₃, the removal of DOC increased by up to 90%. This may be due to the decrease of organic loading and/or increase of Fenton reaction (Shon et al., 2005).

Table 2.26 Comparison of DOC removal with different AOP in BTSE

Researcher	Condition	Processes	DOC Removal (%)
Ito et al., 1998 (Hiroshima BTSE, Japan)	O ₃ dosage: 2.86 mg O ₃ min ⁻¹ ,	O ₃ /H ₂ O ₂ /UV	55
	H ₂ O ₂ : less than 200 mg/L, UV	O ₃ /H ₂ O ₂	20
	intensity (253.7 nm): 2.6*10 ⁻⁶ Einstein s ⁻¹ , air: 100 mL/min	H ₂ O ₂ /UV	45
Shon et al., 2005 (Gwangju BTSE, Korea)	EfOM initial concentration = 6.65 mg/L; TiO ₂ concentration = 2 g/L; air = 25 L/min, PAC = 1 g/L, FeCl ₃ = 1 mM, H ₂ O ₂ = 1 mM, O ₃ = 0.1 L/min	TiO ₂ /UV	50
		O ₃ /TiO ₂ /UV	75
		H ₂ O ₂ /TiO ₂ /UV	80
		FeCl ₃ /TiO ₂ /UV	90
		PAC/TiO ₂ /UV	80

Practically any organic contaminants that are reactive with the hydroxyl radical can potentially be treated. A wide variety of organic and explosive contaminants are susceptible to destruction by UV/oxidation, including petroleum hydrocarbons; chlorinated hydrocarbons that are used as industrial solvents and cleaners. In many cases, chlorinated hydrocarbons that are resistant to biodegradation may be effectively treated by UV/oxidation. Typically, easily oxidized organic compounds, such as those with double bonds (e.g., trichloroethylene and vinyl chloride), as well as simple

aromatic compounds (e.g., toluene, benzene, xylene, and phenol), are rapidly destroyed in UV/oxidation processes (Table 2.27). More details can be found elsewhere (Gogate and Pandit, 2004; Pirkanniemi and Silanpää, 2002).

Table 2.27 Easily oxidized organic compounds by photocatalytic processes (adapted from Pirkanniemi and Sillanpää, 2002)

	Compounds	Catalyst	Spectral range and oxidant
Chlorinated organics and phenolic compounds	4-chlorophenol	- TiO ₂ on SiO ₂	UV and H ₂ O ₂
	Tetrachloroethene, trichloroethene, cis-dichloroethene, (and toluene, ethylbenzene, xylene),	- Pt-TiO ₂ on ambersorb	UV
	2,4-Dichlorophenol	- Fenton on Nafion membrane	Visible light and H ₂ O ₂
	Pentachlorophenol	- TiO ₂ (sol-gel)	UV
	4-Chlorophenol	- TiO ₂ on silica fiber glass	UV
	Phenol and ortho-substituted phenolic compounds: 2-chlorophenol, guaiacol, catecol	- TiO ₂	UV
Others	Salicylic acid (formic acid)	- TiO ₂	UV and sonolysis
	Nitrotoluenes	- TiO ₂	UV and O ₂
	Formic acid	- Fe on TiO ₂	UV
	Benzamide	- TiO ₂ on fiberglass	UV
	Dithiocarbamate	- TiO ₂ on fiberglass	UV

Tables 2.28 and 2.29 present the removal of EDC/PPCP by different AOPs. The processes between conventional oxidation (chlorination) and AOP (ozone and ozone-H₂O₂) are compared in terms of individual removal. Chlorination removes the EDC/PPCP compounds such as 17 β -estradiol, oxybenzone, sulfamethoxazole, triclosan and benzo[a]anthracene by up to 90%, whereas the removal of the EDC/PPCP compounds such as androstenedione, DDT, progesterone and mirex is less than 40%. The breaking point of each molecule is different by chlorination. Single aromatic bond is broken from double bond by chlorination. The removal of DOC by ozonation shows better results compared to chlorination. The details on the removal of EDCs and PPCPs by chlorination, chlorine dioxide, ozonation, and UV irradiation can be found in Snyder et al., 2003.

Table 2.28 Removal of EDC and PPCP with chlorination at pH 5.5 (adapted from Snyder and Westerhoff, 2005)

EDC/PPCP	Removal (%)	EDC/PPCP	Removal (%)	EDC/PPCP	Removal (%)
Acetaminophen	96	a-BHC	26	g-BHC	21
Androstenedione	40	Acenaphthene	92	g-Chlordane	30
Atrazine	15	Acenaphthylene	92	Heptachlor	39
Caffeine	58	a-Chlordane	28	Heptachlor epoxide	21
Carbamzepine	98	Aldrin	50	Methoxychlor	43
DEET	16	Anthracene	91	Metolachlor	32
Diazepam	71	b-BHC	16	Mirex	8
Diclofenac	96	Benz[a]anthracene	91	Musk keton	25
Dilantin	32	Benzo[a]pyrene	71	Naphtalene	46
Erythromycin-H2O	95	Benzo[b]fluoranthene	71	Phenanthrene	68
Estrodiol	98	Benzo[k]fluoranthene	86	Oxybenzone	96
Estriol	98	Chrysene	89	Pentoxifylline	86
Estrons	98	d-BHC	21	Progesterone-APCI	50
Ethinylestradiol	98	DDD	24	Progesterone-ESI	50
Fluoxetine	20	DDE	34	Sulfamethoxazole	97
Gemfibrozil	98	DDT	25	TCEP	4
Hydrocodone	98	Dieldrin	28	Testosterone	52
Ibuprofen	44	Endrin	22	Triclosan	97
Iopromide	7	Fluoranthene	94	Trimethoprim	98
Meprobamate	16	Fluorene	30	Pyrene	53
Naproxen	93	Galaxolide	39		

Table 2.29 Removal of EDC and PPCP with ozone/H₂O₂ (adapted from Snyder and Westerhoff, 2005)

EDC/PPCP	Removal (%)	EDC/PPCP	Removal (%)	EDC/PPCP	Removal (%)
Acetaminophen	96	a-BHC	16	g-BHC	13
Androstenedione	98	Acenaphthene	89	g-Chlordane	0
Atrazine	52	Acenaphthylene	92	Heptachlor	54
Caffeine	98	a-Chlordane	0	Heptachlor epoxide	8
Carbamzepine	98	Aldrin	50	Methoxychlor	91
DEET	83	Anthracene	91	Metolachlor	86
Diazepam	85	b-BHC	0	Mirex	23
Diclofenac	96	Benz[a]anthracene	88	Musk keton	33
Dilantin	88	Benzo[a]pyrene	71	Naphthalene	88
Erythromycin-H ₂ O	96	Benzo[b]fluoranthene	89	Phenanthrene	94
Estrodiol	98	Benzo[k]fluoranthene	87	Pyrene	93
Estriol	98	Chrysene	92	Oxybenzone	96
Estrons	98	d-BHC	9	Pentoxifylline	98
Ethinylestradiol	98	DDD	75	Progesterone-APCI	98
Fluoxetine	98	DDE	62	Progesterone-ESI	98
Gemfibrozil	98	DDT	61	Sulfamethoxazole	97
Hydrocodone	98	Dieldrin	0	TCEP	15
Ibuprofen	88	Endrin	93	Testosterone	98
Iopromide	60	Fluoranthene	93	Triclosan	82
Meprobamate	61	Fluorene	93	Trimethoprim	98
Naproxen	93	Galaxolide	89		

2.7.7 Removal of EfOM by Membrane Technology

2.7.7.1 General

Membrane technology has been found to be a successful technology in wastewater reuse. Microfiltration (MF) and ultrafiltration (UF) membrane systems have already proven their advantages in terms of superior water quality and economics. Nanofiltration (NF) and reverse osmosis (RO) membranes are used in wastewater reclamation. NF membranes can reject smaller size molecules that cannot be removed by MF and UF membranes. However, it requires much higher energy consumption

during the operation. Therefore, low-pressure driven type of NF has been investigated for the removal of organic matter (Thanuttamavong et al., 2002; Shon et al., 2004).

There are many references regarding on the boundary of applications of different membranes (Vigneswaran et al., 1991; Mulder, 1996; Fane, 1996; Schafer, 2001). However, since the boundary of each membrane is uncertain, many researchers have used different definitions for the choice of membranes. Hence, it is necessary to put forward a detailed and clear definition for the pore size of the membrane. Table 2.30 presents the classification of different membranes, and this would avoid overlapping of the definition of pore sizes for different membranes in terms of the tight and loose membranes.

Table 2.30 Size range of membrane separation process (adapted from Cho, 2005)

Membrane Process	RO	NF		UF		MF	
		Tight	Loose	Tight	Loose	Tight	Loose
Molecular Weight Cutoff (daltons)	<150	150 to 300	300 to 1000	1000 to 10000	10000 to 100000	100000 to 0.01 μm	0.01 μm to 0.05 μm

MF is the membrane process with the largest pores. It can be used to filter suspended particulates, large colloids and bacteria. The MF is also used as a pretreatment for NF and RO processes. Since the pore size of the MF is relatively large, air backflush or permeate backwash can be used to clean the deposits from the pores and the surface of the membrane. Physical sieving is the major rejection mechanism in MF. The deposit or cake on the membrane also acts as a self-rejecting layer, and thus MF can retain even smaller particles or solutes than its pore size (Chaudhary, 2003).

UF should be able to remove virus and this results in the partial removal of color. It enables the concentration, purification and fractionation of macromolecules such as proteins, dyes and other polymeric materials. It is widely used in the industrial wastewater treatment where recycling of raw materials, products and by-products are of primary concern. For example, it can be used to recover paints in the electrophoretic painting industries, lignin and liginosulforates from black liquor in the pulp and paper industry. UF is also used as a pretreatment to NF and RO processes (Schafer, 2001).

NF is a membrane process located between UF and RO. Simpson et al. (1987) has defined NF as charged UF. Sometimes it is referred to as a low pressure RO. The NF can remove 60-80% of hardness, more than 90% of color causing substances and almost all turbidity. The NF has the advantage of low operating pressure compared to RO and has a high rejection of organics compared to UF. Both charge and size are important in NF rejection. At a neutral pH, most NF membranes are negatively charged, whereas at lower pH are positively charged (Zhu and Elimelech, 1997). Physical sieving is another dominant mechanism in removing colloids and large molecules. However, for the removal of ions and lower MW organics, chemical interactions between the solutes and membrane play an important role.

RO was the first membrane process to be widely commercialized. Reverse osmosis is the reversal of the natural process of osmosis in which water from a dilute solution passes through a semi-permeable membrane into a more concentrated solution due to osmotic pressure. In reverse osmosis, an external pressure greater than osmotic pressure is applied so that the water from concentrated solution passes into the diluted solution. Thus it can be used to separate salts and low MW pollutants from water and wastewater (Chaudhary, 2003). RO is used as the polishing treatment in water reclamation projects.

2.7.7.2 Membrane technology for EfOM removal

EfOM represents a complex matrix of organics with different sizes, structure and functional groups. Important characteristics that control the interactions with membrane include MW distribution, hydrophobic (aromatic) and hydrophilic (aliphatic) nature of EfOM, and (acidic) functional groups of EfOM. Similarly, molecular weight cutoff (MWCO), hydrophobicity and surface charge are important properties of membrane that can affect the interaction with EfOM. Three types of possible interactions between EfOM and membrane have been reported in the literature: i) adsorption (fouling), ii) electrostatic exclusion (rejection) and iii) steric exclusion (rejection) (Mulder, 1996). A number of researchers reported that for the negatively charged UF and NF, the characteristics of EfOM contributing to rejection include high MW and negative charge density. The other factors that can affect the EfOM rejection and membrane fouling are pH, ionic strength and calcium content in the solution (Amy and Cho, 1999).

The EfOM removal by different membranes is shown in Table 2.31. In general, UF removes EfOM up to 40 – 60% and NF removes more than 80%. Tables 2.31 and 2.32 also show the removal of EDC and PPCP by UF and NF. The UF used in this study had 8000 daltons cutoff and -32.2 mV zeta potential (from Desal/Osmonics (GM membrane)). The pore size and the zeta potential of NF were 200 daltons and -11.1 mV (from Hydranautics (ESNA)). Since, the compounds of EDCs and PPCPs consist of the smallest MW from 150 to 500 daltons, MF and UF could not remove these compounds. However, NF and RO can remove more than 90% (Huang and Sedlak, 2001). Snyder et al. (2003) found that when polar and charged compounds were combined with other organic and inorganic compounds, these compounds led to better removal compared to less polar or neutral compounds. For instance, the removal of low MW increased at higher pH due to electrostatic repulsion and the removal of neutral compounds improved linearly with MW. Table 2.34 presents the removal of organic matter (in terms of DOC) by membrane processes with different pretreatments prior to membrane applications.

Table 2.31 DOC removal by different membrane processes

Researcher	Process	DOC removal	Wastewater
Duin et al., 2000	UF NF (spiral wound)	10% (COD) 75-80% (COD)	Driebergen BTSE, The Netherlands
Jarusutthirak and Amy, 2001	UF (NTR 7410, 20000 Da) UF (PM10, 10000 Da) UF (GM, 8000 Da) NF (ESNA, 200 Da)	40% 25% 30% 92%	Boulder BTSE, USA
Lee et al., 2003	UF (T-8000, 8000 Da) UF (GM, 8000 Da) NF (T-1000, 1000 Da) NF (ESNA, 250)	38% 58% 40% 95%	Gwangju BTSE, Korea
Ernst et al., 2000	NF (DK5, 200) NF (MP 35, 1000) NF (NF-PES10, 1000) NF (C5F, 5000)	96% 73% 67% 42%	Ruhleben BTSE, Germany
Kishino et al., 1996	SMBR (with activated sludge)	98% (BOD, from activated sludge)	Shinyodogawa BTSE, Japan
Ahn and Song, 1999	MBR with hollow fiber membrane (0.1 μm , with activated sludge)	92.8% (COD)	KIST dormitory BTSE, Korea
Gander et al., 2000	SMBR* (0.3-0.1 μm with activated sludge) Side stream (0.1 μm) Side stream (50000 Da)	86-97% (COD) 98.7% (COD) 88-94.5% (COD)	Porlock, UK
Shon et al., 2003	UF (NTR 7410, 17500 Da) NF (NTR 729HF, 700 Da) NF (LES 90, 250 Da) NF (LF 10, 200 Da)	44% 79% 91% 91%	Gwangju BTSE, Korea

* SMBR: submerged membrane bioreactor

Table 2.32 Removal of EDC and PPCP by UF (adapted from Snyder and Westerhoff, 2005)

EDC/PPCP	Removal (%)	EDC/PPCP	Removal (%)
Acetaminophen	63	Genfibrozil	0
Androstenedione	0	Hydrocodone	20
Atrazine	6	Ibuprofen	30
Caffeine	0	Iopromide	37
Carbamzepine	0	Meprobamate	0
DEET	0	Naproxen	72
Diazepam	7	Oxybenzone	83
Diclofenac	50	Pentoxifylline	0
Dilantin	0	Progesterone-APCI	0
Erythromycin-H2O	0	Progesterone-ESI	77
Estrodiol	0	Sulfamethoxazole	23
Estriol	0	TCEP	32
Estrons	14	Testosterone	0
Ethinylestradiol	98	Triclosan	93
Fluoxetine	0	Trimethoprim	0

Table 2.33 Removal of EDC and PPCP by NF (adapted from Snyder and Westerhoff, 2005)

EDC/PPCP	Removal (%)	EDC/PPCP	Removal (%)
Acetaminophen	82	Genfibrozil	15
Androstenedione	65	Hydrocodone	82
Atrazine	66	Ibuprofen	78
Caffeine	32	Iopromide	92
Carbamzepine	61	Meprobamate	32
DEET	58	Naproxen	89
Diazepam	75	Oxybenzone	97
Diclofenac	74	Pentoxifylline	66
Dilantin	19	Progesterone-APCI	62
Erythromycin-H2O	80	Progesterone-ESI	93
Estrodiol	0	Sulfamethoxazole	72
Estriol	63	TCEP	82
Estrons	65	Testosterone	50
Ethinylestradiol	77	Triclosan	97
Fluoxetine	92	Trimethoprim	43

Table 2.34 DOC removal by membrane technology with pretreatment

Researcher	Process	DOC removal	Wastewater
Jarusutthirak et al., 2002	MF + UF (GM, 8000 Da) MF + NF (ESNA, 200 Da)	75% 92%	St. Julien l'Ars and Naintre BTSE, France
Abdessemed and Nezzal, 2002	Flocculation + adsorption + UF (15000 Da)	96% (COD)	Staoueli BTSE, Algeria
Lopez-Ramirez et al., 2003	Flocculation + sand filter + UV ray + RO (4040-MSY-CAB2, Hydranautics)	88% (COD)	La Barrosa, Chiclana de la Frontera BTSE, Spain
Kim et al., 2002	UF + RO (spiral wound, Fluid systems, USA) Dual media + GAC + RO Dual media + GAC with a coagulant + RO	79% 76% 64%	Local BTSE, Singapore
Alonso et al., 2001	MF (0.2 µm) + UF (50000 Da)	50% (COD)	Seville BTSE, Spain
Tchobanoglous et al., 1998	Media filter + Hollow fiber UF (100000 Da)	79% (COD)	Davis BTSE, USA
Chapman et al., 2002	Floating medium flocculator + MF (0.2 µm, CFMF*)	50%	Olympic park BTSE, Australia
Shon et al., 2005	Flocculation + UF (NTR 7410, 17500 Da) Adsorption + UF (NTR 7410, 17500 Da) GAC biofiltration + UF (NTR 7410, 17500 Da) Flocculation + adsorption + UF (NTR 7410, 17500 Da) Flocculation + adsorption + NF (LES 90, 250 Da)	72% 78% 84% 90% 92%	Gwangju BTSE, Korea

* CFMF: crossflow microfiltration

2.8 Comparison of Different Treatment Methods used in EfOM Removal

The removal of EfOM from BTSE depends significantly on the treatment processes used (Figure 2.7). The organic matter was considered in terms of DOC. The DOC was measured after filtration of the sample through 0.45 μm mixed cellulose ester membrane. A Sievers-820 analyzer (Sievers-820, Sievers, Co., USA) was used to measure the DOC of the filtered sample. Ammonium persulfate was used as a chemical oxidizer. PAC adsorption, GAC biofiltration, NF1 (700 daltons) and NF2 (200 daltons) relatively resulted in high DOC removal of EfOM compared to that of flocculation, IX, AOP and UF. This suggests that EfOM consists mainly of small MW organic matter in the BTSE used.

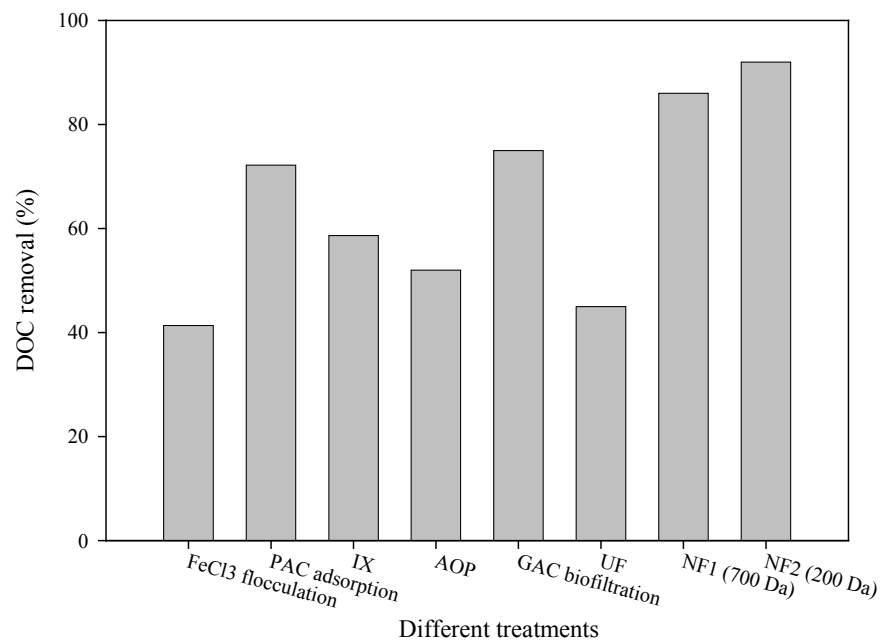


Figure 2.7 DOC removal by different processes (FeCl₃ flocculation, PAC adsorption, IX with MIEX[®], AOP (photocatalysis) with TiO₂, GAC biofiltration, UF (with 17500 daltons MWCO membrane), NF1 (with 700 daltons MWCO membrane) and NF2 (with 200 daltons MWCO membrane)) in biologically treated sewage effluent from a wastewater treatment plant (adapted from Shon et al., 2004 and 2005)

Removals of different fractions are helpful to determine the efficiency of different treatments in removing HP, TP and HL fractions. The XAD-8 and XAD-4 resins were used for fractionating EfOM into hydrophobic (HP) EfOM (XAD-8 adsorbable; mostly hydrophobic acids with some hydrophobic neutrals; humic and fulvic acids), transphilic (TP) EfOM (XAD-4 adsorbable; hydrophilic (HL) bases and neutrals) components. The remaining fraction escaping the XAD-4 was the hydrophilic component.

Table 2.35 shows the removal of HP, TP and HL fractions with different treatments. PAC adsorption removed a large amount of the HP compounds. FeCl₃ flocculation removed higher amount of HL fraction. This is probably due to the ionic effects of EfOM. The flocculation removes the HL fraction when the pollutants are more negative charged. In general, flocculation and adsorption are used mainly to remove HP of large and small MW organics. The removal of HL by flocculation (in this case) may be due to the large dose of FeCl₃ used (through sweep flocculation mechanism). The removal of HL by adsorption could be attributed to the physical affinity between HL organic molecules and PAC (through Vander Waals, electro static forces and chemisorption). Ion exchange with MIEX[®] also exhibited very high removal rates of hydrophilic compounds.

Table 2.35 Efficiency of different treatment processes in the removal of different fractions from BTSE

	Initial (mg/L)	MIEX [®] (mg/L)	PAC adsorption (mg/L)	Flocculation (mg/L)	Photocatalysis (mg/L)
HP	1.645	0.715 (56.5%)	0.460 (72.0%)	0.999 (39.3%)	0.802 (51.2%)
TP	1.034	0.705 (31.8%)	0.282 (72.7%)	0.802 (22.4%)	0.703 (32.0%)
HL	3.822	1.180 (69.1%)	1.258 (67.1%)	1.540 (59.7%)	2.810 (26.5%)

MW distribution of EfOM is very important in the understanding of the removal of different size ranges of pollutants by different treatment methods. The MW distribution was measured using high pressure size exclusion chromatography (HPSEC, Shimadzu Corp., Japan) with a SEC column (Protein-pak 125, Waters Milford, USA). The separation ranges are from 1000 to about 50000 daltons. The effluent was made of pure water with phosphate (pH 6.8) and NaCl (0.1 M). The detection limit of UV was 0.001 per cm. Standards of MW of various polystyrene sulfonates (PSS: 210, 1800, 4600, 8000, and 18000 daltons) were used to calibrate the equipment. The details of these experiments are given elsewhere (Her, 2002)

Figure 2.8 presents the MW distribution of EfOM after different treatments. The MW distribution of EfOM in the BTSE used is comprised of small (263 daltons, 580 and 865) and large (43110 daltons) MW compounds. Flocculation removed mainly the large MW compounds and did not remove the majority of small MW (263 daltons, 330 and 580). Adsorption mainly removed the small MW compounds, however, NF removed practically all MW ranges of EfOM.

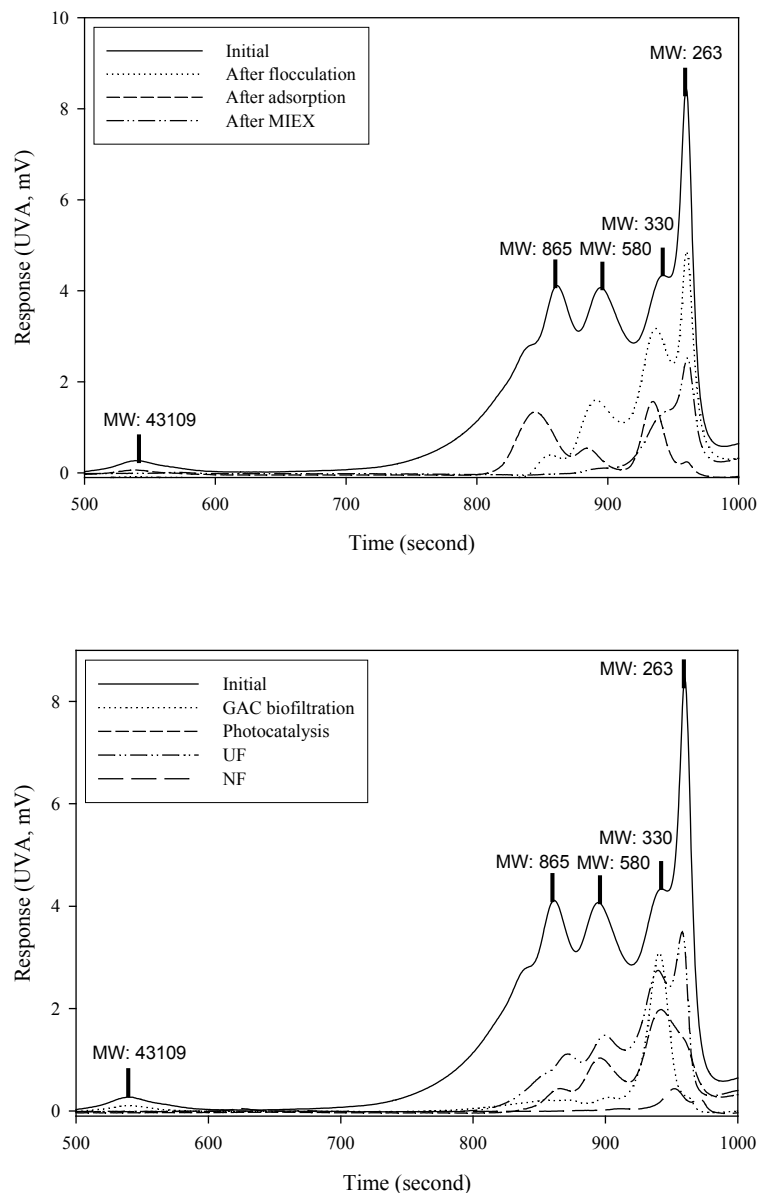


Figure 2.8 MW distribution of the influent BTSE and effluents from different treatments (flocculation, adsorption, GAC biofiltration, photocatalysis, MIEX[®], UF and NF)

It is difficult to remove EDCs and PPCPs in EfOM within the range from 100 to 500 daltons. Removal of EDCs and PPCPs thus is considered as the decisive parameter in determining the suitability of a particular treatment. With the treatments of flocculation, adsorption and oxidation, the removal of these compounds showed different trends (Table 2.36). Some of them are removed by up to 90%, while the others can only be partially removed. This suggests that removal of the emerging contaminants requires the careful selection of treatment methods depending on the individual EDC and PPCP compounds.

Table 2.36 Unit processes and operations used for EDC and PPCP removal in WWTP (adapted from Barceló, 2003)

Treatments	Compounds
Flocculation	>50% removal of: benzo[a]pyrene, benzo[g,h,l]perylene, benzo[k]fluoranthene, mirex, benzo[b]fluoranthene, benzo[a]anthracene <10% removal of: diazepam, diclofenac, meprobamate, sulfamethoxazole, trimethoprim
Adsorption	>90% removal of: triclosan, fluoxetine, oxybenzone, mirex, DDT <50% removal: meprobamate, sulfamethoxazole, iopromide, trimethoprim, gemfibrozil
Chlorination	>90% removal of: 17 β -estradiol, oxybenzone, triclosan, sulfamethoxazole, benzo[a]anthracene <40% removal of: androstenedione, progesterone, DDT, tri(2-chloroethyl) phosphate, mirex
Ozonation	>90% removal of: 17 β -estradiol, fluoxetine, carbamazepine, progesterone, trimethoprim <50% removal of: lindane, musk ketone, iopromide, TCEP, meprobamate

Table 2.37 presents the performance of different unit processes in removing specific classes of EDC and PPCP. The RO and NF membranes remove the majority of the EDC and PPCP. However, the removal of these compounds by different treatment methods depends on the characteristics of each compound.

Table 2.37 Unit processes and operations used for EDC and PPCP removal (adapted from Snyder et al., 2003)

Group	Classification	AC	O ₃ /AOP	Cl ₂ /ClO ₂	Flocculation	NF	RO
EDC	Pesticides	E	L-E	P-E	P	G	E
	Industrial chemicals	E	F-G	P	P-L	E	E
	Steroids	E	E	E	P	G	E
	Metals	G	P	P	F-G	G	E
	Inorganics	P-L	P	P	P	G	E
	Organometallics	G-E	L-E	P-F	P-L	G-E	E
PPCP	Antibiotics	F-G	L-E	P-G	P-L	E	E
	Antidepressants	G-E	L-E	P-F	P-L	G-E	E
	Anti-inflammatory	E	E	P-F	P	G-E	E
	Sunscreens	G-E	L-E	P-F	P-L	G-E	E
	Antimicrobials	G-E	L-E	P-F	P-L	G-E	E
	Surfactants/detergents	E	F-G	P	P-L	E	E

AC, activated carbon; E, excellent (>90%); G, good (70-90%); F, fair (40-70%); L, low (20-40%); P, poor (<20%)

2.9 Concluding Remarks

Although a number of previous studies have dealt with characteristics of natural organic matter (NOM) in surface waters, there have not been many studies of effluent organic matter (EfOM) in biologically treated sewage effluent (BTSE) having diverse characteristics of EfOM. EfOMs consist of NOMs, soluble microbial products (SMPs), persistent organic matters (POPs) and emerging pollutants such as endocrine disrupting chemicals (EDCs) and pharmaceuticals and personal care products (PPCPs). Most of NOMs come from tap water into wastewater and SMPs are a by-product of biological treatment. In addition, POPs, EDCs and PPCPs are from the use of synthetic organic matter (SOM) in our daily life.

Extracellular polymeric substances (EPSs) and SMPs obtained after biological treatment are important because they constitute the majority of EfOMs. Toxicity of

SMP is of increasing concern due to a lack of information. Priority pollutants should be also considered due to their known or suspected carcinogenicity, mutagenicity, teratogenicity or high acute toxicity. Proteins, carbohydrates, fat, oil and grease are also the major constituents of EfOM which are often found in wastewater. These compounds lead to disinfection by-products (DBPs) upon disinfection, membrane fouling, sludge bulking in activated sludge (biological treatment), clogging of sewer pipes, floating matter and films in waterways.

The efficiency of different treatments (flocculation, adsorption, biofiltration, ion exchange (IX), advanced oxidation process (AOP) and membrane technology) has been investigated in terms of dissolved organic matter (DOC) removal, fraction removal (preferential removal of hydrophobicity), EDC/PPCP removal (representation of smallest MW compounds) and MW distribution (different MW sizes). PAC adsorption, GAC biofiltration, NF with 700 daltons MWCO and NF with 200 daltons MWCO resulted in high DOC removal of EfOM compared to that of flocculation, IX, AOP and UF. This suggests that EfOM consists mainly of small MW organic matter in the BTSE used. In terms of hydrophobic (HP), transphilic (TP) and hydrophilic (HL) fraction, FeCl₃ flocculation removed relatively high amounts of the HL fraction. PAC adsorption preferentially removed HP fraction.

It is difficult to remove EDCs and PPCPs in EfOM in the range from 100 to 500 daltons with conventional treatments. The removal of these compounds with the treatments of flocculation, adsorption and oxidation shows different trends. Some of them were removed by up to 90%, while the others showed minor removal. The RO and NF membranes removed the majority of the EDC and PPCP. The removal of these compounds by different treatment methods also depended on the characteristics of individual compound. This proposes that the removal of the emerging contaminants requires the careful selection of treatment methods and this depends on the individual EDC and PPCP compounds in BTSE.

MW distribution of EfOM was investigated before and after different treatments. Flocculation mainly removed the large MW compounds and did not remove the majority of small MW (263 daltons, 330 and 580). Adsorption essentially removed the small MW compounds. However, NF removed practically all MW ranges of EfOM.

Thus, MW distribution can give useful information in the selection of appropriate treatment methods.

Harmful trace chemicals such as POPs, EDCs and PPCPs are becoming a major concern. Nonetheless, the efficiency of removing the majority of these compounds by different treatment processes is still unknown due to the lack of sensitive analytical methods. In addition, the investigation of the toxicity of these compounds is becoming an important and urgent issue and therefore, this review recommends the development of sensitive analysis of specific compounds and their toxicity.

CHAPTER 3



University of Technology, Sydney
Faculty of Engineering

EXPERIMENTAL INVESTIGATION

3.1 Introduction

In this chapter, the experimental materials and methods used in this study are introduced in detail. Furthermore, fundamental information on EfOMs and membranes is characterized in terms of various experimental methods.

3.2 Experimental materials

3.2.1 Wastewater

In this study, two kinds of wastewaters were used; in the majority of theoretical experiments, synthetic wastewater was used and the real wastewater (biologically treated sewage effluent (BTSE)) from domestic wastewater treatment plant was used in the other experiments. The following details of the wastewaters used in the study are presented.

3.2.1.1 Synthetic Wastewater

The majority of experiments using synthetic wastewater were conducted in the laboratories of the University of Technology, Sydney (UTS), Australia. The composition of the synthetic wastewater used in this study is presented in Table 3.1. This synthetic wastewater represents effluent organic matter (EfOM) generally found in the biologically treated sewage effluent (BTSE) (Seo et al., 1997). Tannic acid, sodium lignin sulfonate, sodium lauryl sulfate, peptone and arabic acid contributed to the large molecular weight (MW) size organic matter, while the natural organic matter (NOM) from tap water, peptone, beef extract and humic acid consisted of the small MW organic matters. The MW of the mixed synthetic wastewater ranged from 290 to about 34100 daltons with the highest fraction at 940 – 1200 daltons. The weight-averaged MW of the wastewater was approximately 29500 daltons.

Table 3.1 Constituents and characteristics of the synthetic wastewater

Compounds	Concentration (mg/L)	Main molecular weight (dalton)	Fraction by DOC
Beef extract	1.8	298, 145, 65	0.065
Peptone	2.7	34265, 128, 80	0.138
Humic acid	4.2	1543, 298	0.082
Tannic acid	4.2	6343	0.237
Sodium lignin sulfonate	2.4	12120	0.067
Sodium lauryle sulfate	0.94	34265	0.042
Arabic gum powder	4.7	925, 256	0.213
Arabic acid (polysaccharide)	5.0	38935	0.156
(NH ₄) ₂ SO ₄	7.1	-	-
K ₂ HPO ₄	7.0	-	-
NH ₄ HCO ₃	19.8	-	-
MgSO ₄ •7H ₂ O	0.71	-	-

3.2.1.2 Real Wastewater

Real wastewater was drawn from Gwangju domestic wastewater treatment plant, South Korea (Figure 3.1). A number of experiments were conducted with BTSE in Gwangju Institute of Science and Technology (GIST), South Korea. The wastewater treatment facility is a medium size activated sludge unit (25000 m³/d). The characteristics of the BTSE used are presented in Table 3.2. The hydraulic retention time (HRT) and the sludge age were 6 hours and approximately 8 days, respectively. The MW of the BTSE ranged from 250 to about 30000 daltons with a large fraction ranging from 250 to 520 daltons. In general, the MW distribution of this BTSE ranged from 200 to 50,000 daltons in winter season and from 200 to 3000 daltons in summer. This also varies from place to place, with the characteristics of the sewage and with the operational conditions of the sewage treatment plant. For example, the range of MW of the BTSE was 300 to 40000 daltons (with a peak between 300 and 3,000 daltons) in Gwangju (Shon et al., 2004a), whereas it was 100 – 50000 daltons in Hawaii (USA) with a peak between 900 and 20,500 daltons (Her, 2002).

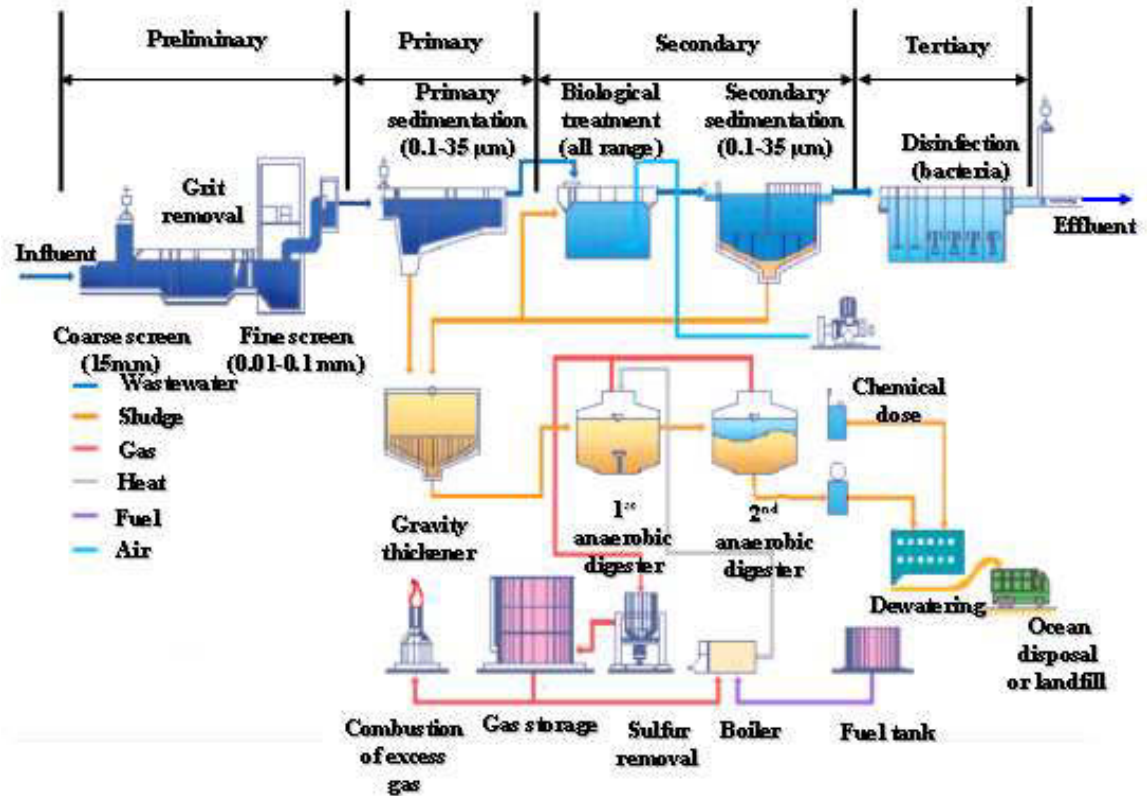


Figure 3.1 Schematic of treatment processes in Gwangju wastewater treatment plant

Table 3.2 Characteristics of biologically treated sewage effluent during one year (adapted from GCHERI, 2005)

	Jan	Feb	Mar	Apr	May	Jun	Jul	Aug	Sep	Oct	Nov	Dec	Ave.
BOD	14.9	10.9	6.6	4.8	7.1	1.6	4.8	2.3	1.2	5.6	7.4	2.3	5.8
SS	8.5	3.8	5.0	3.6	8.5	9.6	2.5	3.3	0.7	2.4	4.5	0.5	4.4
Colority	36	29	30	30	29	16	17	14	13	22	20	14	22.5
Turbidity	2.3	1.4	1.1	1.3	1.2	0.32	0.41	0.64	0.45	0.56	1.13	0.61	0.95
Residual Chlorine	0	0	0	0.1	0.1	0.1	0.1	0.3	0.4	0.4	0.4	0.7	0.2
T-N	23	25	17	11	23	16	8	11	11	20	14	8	16
T-P	1.0	0.8	1.5	1.2	1.0	1.1	1.4	0.7	1.0	1.6	0.9	0.8	1.1
Mn	0.08	0.05	0.01	0.03	0.03	0.03	0.03	0.01	0	0.09	0.02	0.01	0.03
Fe	0	0	0	0.1	0.1	0	0	0	0	0	0	0	0.1
Hardness	85	77	72	76	78	85	80	72	75	95	75	34	
Cl ⁻	92	82	78	75	76	52	60	28	25	80	69	58	65
Temp.	8.9	9.7	12.3	15.9	21	23.4	24.3	23.6	23.7	23.8	17.0	16.0	18.3
pH	7.1	6.9	7.1	7.1	7.1	6.9	6.4	6.3	6.6	6.8	6.8	7.4	6.9
Cond.	174	424	363	696	680	520	550	337	429	678	508	784	512
E-Coli	2,000	1,200	44	0	0	0	0	0	0	0	0	0	270

3.2.2 Membranes

The membranes used in this study were NTR 7410 (UF), NTR 729HF (NF), LES 90 (NF), and LF 10 (NF) (Nitto Denko Corp., Japan). The detailed characteristics provided by the manufacturer are given in Tables 3.3 and 3.4. All the membranes used in this study were made from polymer.

Table 3.3 Skin-layer functional groups of membranes (adapted from Thanuttamavong, 2002)

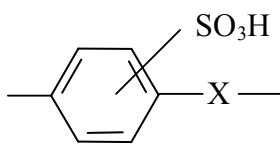
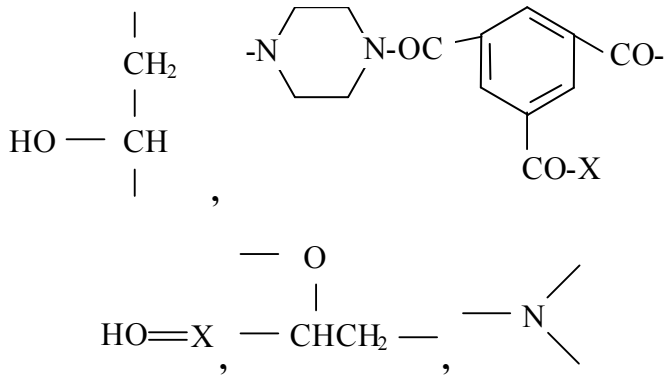
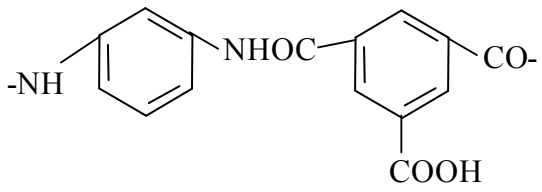
Code	Material	Skin-layer materials
NTR 7410	Sulfonated polysulfones	 $\text{X} = \text{SO}_2, \text{O}$
NTR 729HF	Polyvinylalcohol/ polyamides	
LES 90	Aromatic polyamides	
LF 10	Polyvinylalcohol + aromatic polyamides	

Table 3.4 Specification of membranes obtained by the manufacturer (Nitto Denko Corp., Japan)

Membrane	NTR 7410	NTR 729HF	LES 90	LF 10	
NaCl rejection	5	92	95	99	
Condition	Conc. (%)	0.2	0.15	0.05	0.15
	Pressure (MPa)	0.5	1.0	0.5	1.5
	Temp. (°C)	25	25	25	25
	Recovery (%)	50	10-20	10-25	10-25
	pH	6.5	6.5	7	7
Range	Maximum Temp.	90	40	40	40
	pH	2-11	2-8	2-10	2-10
	Maximum pressure	4.9	2.9	2	4.1
	Chlorine (mg/L)	<100	<1	-	-

Figure 3.2 presents the effect of transmembrane pressure with a constant temperature. When osmotic pressure was neglected, pure water permeability (L_p) of different membranes was investigated in terms of the transmembrane pressure and the water flux. When both functions were plotted, the pure water permeability was calculated by the slope of the straight line. The values of the membranes used in this study are provided in Table 3.5.

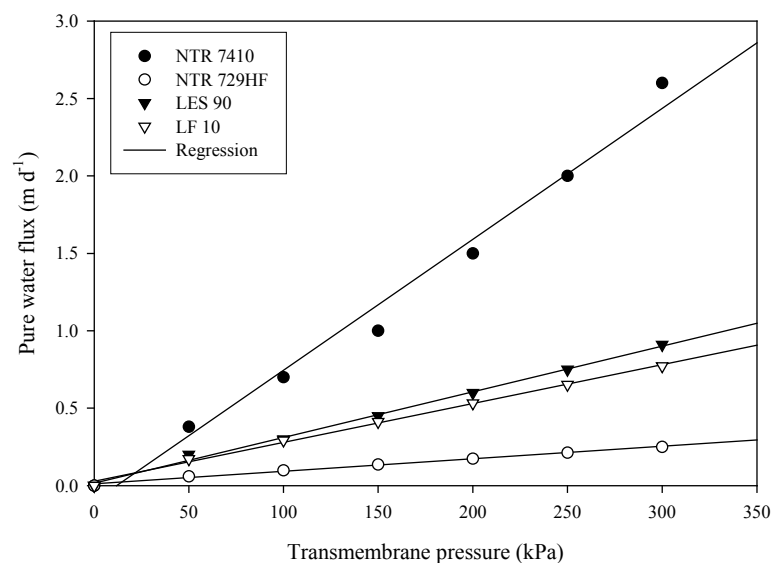


Figure 3.2 Pure water permeability (L_p) of membranes used at 30°C of temperature

Table 3.5 Values of pure water permeability with membranes used in this study

Membranes	Pure water permeability (L_p , m/d kPa)	R^2
NTR 7410	8.457×10^{-3}	0.9845
NTR 729HF	8.071×10^{-4}	0.9943
LES 90	2.954×10^{-3}	0.9969
LF 10	2.511×10^{-3}	0.9967

3.2.3 Activated Carbon

The characteristics of the PAC and GAC used in the study are presented in Tables 3.6 and 3.7.

Table 3.6 Characteristics of powdered activated carbon (PAC) used (James Cumming & Sons Pty Ltd., Australia)

Specification	PAC-WB
Iodine number (mg/g min)	900
Ash content (%)	6 max.
Moisture content (%)	5 max.
Bulk density (kg m^{-3})	290-390
Surface area (m^2/g)	882
Nominal size	80% min finer than 75 micron
Type	Wood based
Mean pore diameter (Å)	30.61
Micropore volumn (cm^3/g)	0.34
Mean diameter (μm)	19.71
Product code	MD3545WB powder

Table 3.7 Physical properties of GAC used (Calgon Carbon Corp., USA)

Specification of the GAC	Estimated Value
Iodine number, mg/(g·min)	800
Maximum Ash content	5 %
Maximum Moisture content	5 %
Bulk density, kg/m ³	748
BET surface area, m ² /g	1112
Nominal size, m	3 x 10 ⁻⁴
Average pore diameter, Å	26.14

3.2.4 Photocatalytic powder

The characteristics of P25 Degussa photocatalytic powdered used as catalyst in the photocatalytic experiments are shown in Table 3.8.

Table 3.8 Characteristics of P25 Degussa photocatalytic powdered used

Specification	P25 Degussa TiO ₂
Structure	Non-porous
Components	65% anatase, 25% rutile, 0.2% SiO ₂ , 0.3% Al ₂ O ₃ , 0.3% HCl, 0.01% Fe ₂ O ₃
Average aggregate particle diameter	Non-porous
Primary crystal size	3 µm
Mean pore diameter	6.9 nm
Band gap	3.03 (from 500 to 300 nm) with UV-Vis
Apparent density	130 kg/m ³
Surface area	42.32±0.18 m ² /g
Type	Powdered
Product code	Degussa P25, Frankfurt am Main, Germany

3.3. Experimental Methods

3.3.1 Flocculation

Flocculation was carried out using the optimum dose of ferric chloride (FeCl_3) predetermined by standard jar tests (Figure 3.3). Ferric chloride was chosen in these experiments as it is capable of removing colloidal organic matter. The BTSE was placed in a 1-liter container and an optimum dose of ferric chloride was added. The sample was stirred rapidly for 1 minute at 100 rpm, followed by 20 minutes of slow mixing at 30 rpm and 30 minutes of settling.

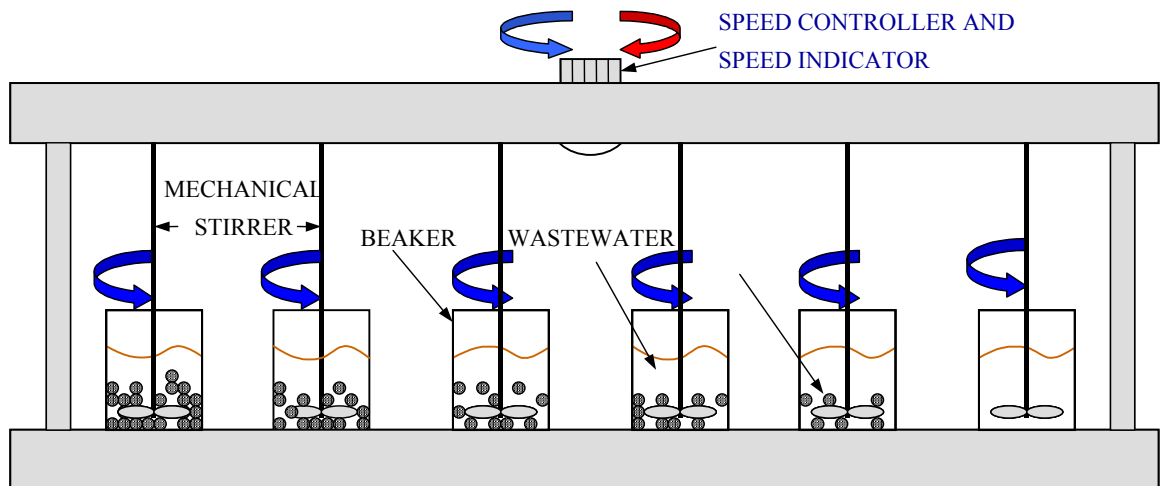


Figure 3.3 Schematic of the batch experimental set-up (speed controller 0-150 rpm, beaker 1 L)

3.3.2 PAC Adsorption

The PAC used in the experiments was washed with distilled water and dried in the oven at $103.5\text{ }^{\circ}\text{C}$ for 24 hours. It was kept in a desiccator before use in the adsorption experiments. For the adsorption experiments, one gram of PAC was added to 1 L of BTSE and stirred with a mechanical stirrer at 100 rpm for one hour. For studying the pretreatment of flocculation followed by adsorption (Floc-Ads), the experimental conditions were similar to flocculation and adsorption alone, respectively. Flocculation took place first and the adsorbent was added to the supernatant obtained after

flocculation and settling. During the PAC adsorption experiment, the contact time was too short (1 hour) for any biogrowth to occur so the treatment of adsorption can be considered to be physical adsorption only.

3.3.3 GAC Biofilter

A GAC biofilter column was used for the long-term bioadsorption experiments. The filter column had ports for influent feeding, effluent collection and backwashing. The column was packed with 20 g (bed depth of 7 cm) of GAC (Figure 3.4). A shallow bed depth was chosen to attain quick biofilm formation and acclimatization. The GAC bed was acclimatized at a constant filtration rate of 1 m/h. The filter was backwashed (to attain up to 30% bed expansion) for approximately 5 minutes every 24 hour of filtration run. The backwashing was done to remove the removal of suspended solids. Only negligible amounts of biofilm were washed out during this operation. After 45 days of operation of the biofilter, four liters of the effluent were collected from the biofilter and used as a feed to filtration. Here, the main mechanism of GAC biofilter is considered as biosorption.

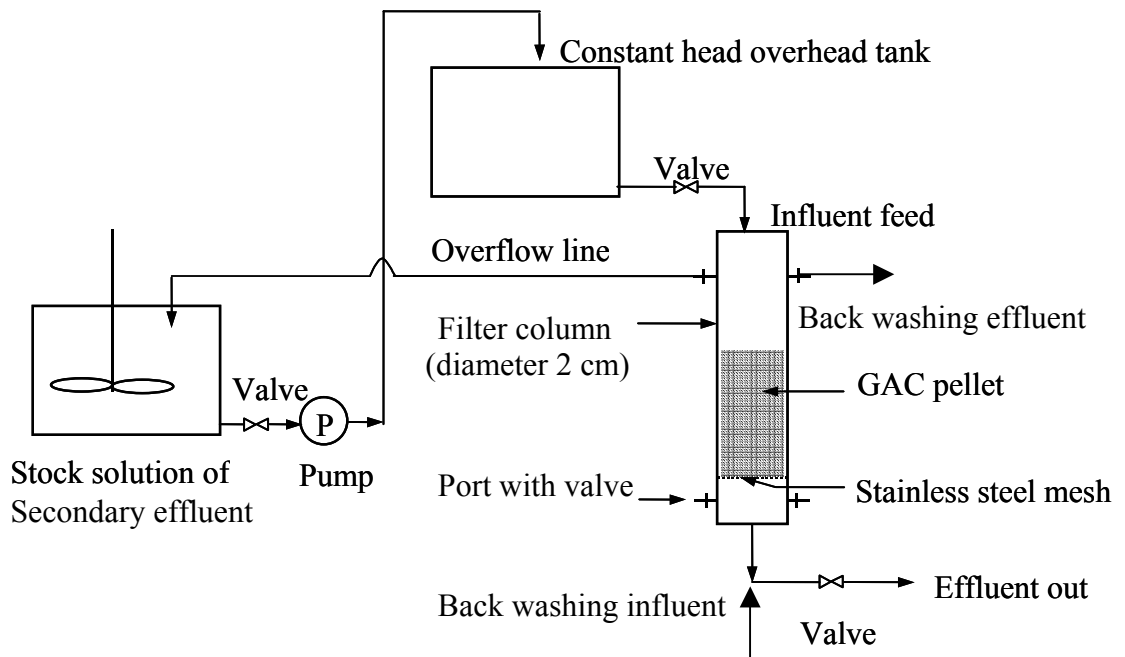


Figure 3.4 Schematic drawing of the fixed bed GAC biofilter

3.3.4 Photocatalytic Set-up

Photocatalysis experiments were conducted with powdered P25 Degussa TiO₂ particle as a catalyst (Kleine et al., 2002; Molinari et al., 2001; Al-Rasheed and Cardin, 2003). Figure 3.5 presents the nonporous structures of TiO₂. However, PAC particles include porous structures. Photoreactor used for the degradation runs consisted of a batch reactor with three 8 W UV lamps, air blower and magnetic bar (Figure 3.6). The total surface area of all three UV lamps was 537 cm². The total volume of the reactor was 2 L. Air sparging was provided to supply oxygen into the reactor (3.3 VVM-(air volume)/(solution volume·minute)). The circulation of tap water around the reactor maintained the temperature at 25 °C.

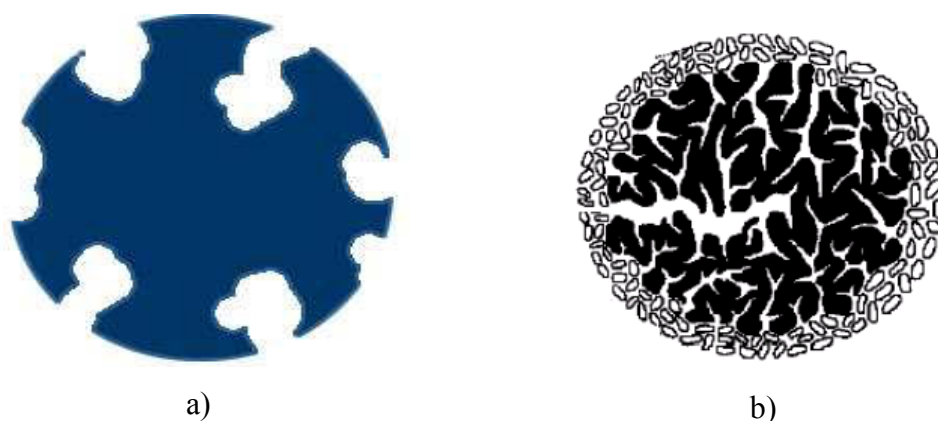


Figure 3.5 Comparison of (a) TiO₂ (non-porous media) and (b) PAC (porous media)

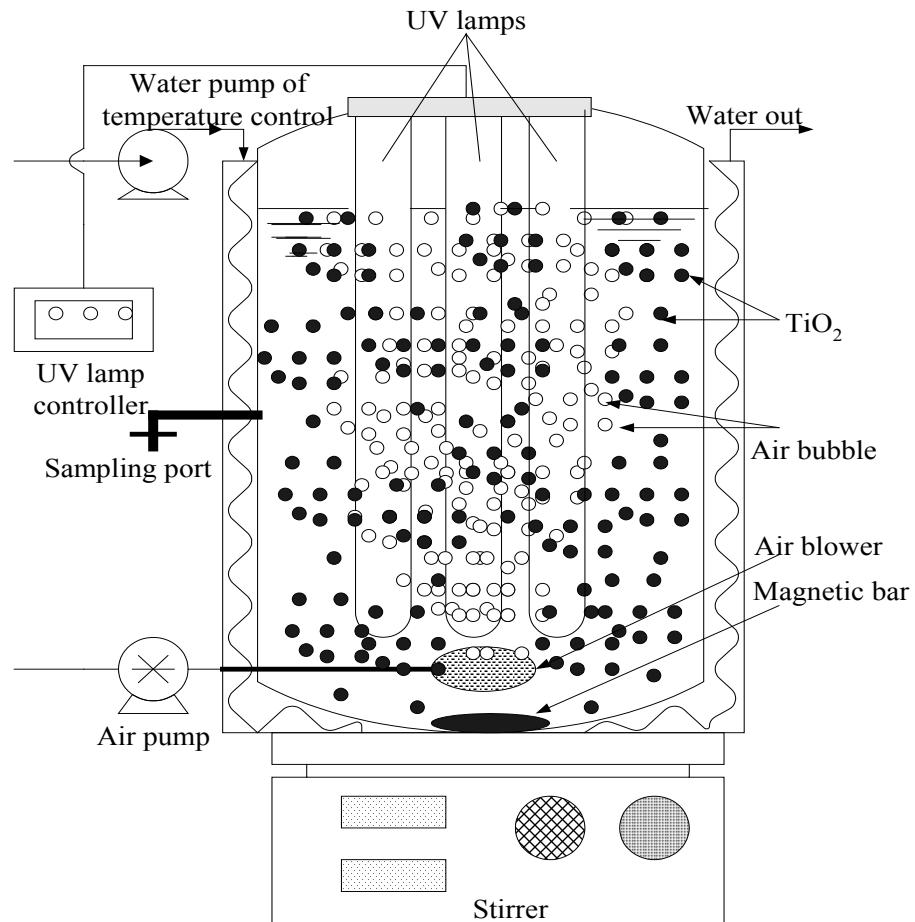


Figure 3.6 Schematic of the photocatalytic reactor

3.3.5 Crossflow Filtration Set-up

A crossflow membrane filtration unit (Nitto Denko Corp., Japan) was used to study the effect of pretreatment on the membrane performance. The schematic diagram of crossflow ultra- and nano-filter experimental setup is illustrated in Figure 3.7. Both the permeate and the retentate were recycled back to the feed tank except for the sample withdrawn for DOC measurements. New membranes were used in each experiment to avoid the effect of residual fouling and to compare the results obtained under different conditions. Wastewater, with and without pretreatment, was pumped into a flat sheet membrane module (effective membrane area of 0.006 m²). The operating transmembrane pressure and cross-flow velocity were controlled at 300 kPa and 0.5

m/s by means of by-pass and regulating valves. The Reynold's number and shear stress at the wall were 735.5 (laminar flow) and 5.33 Pa, respectively.

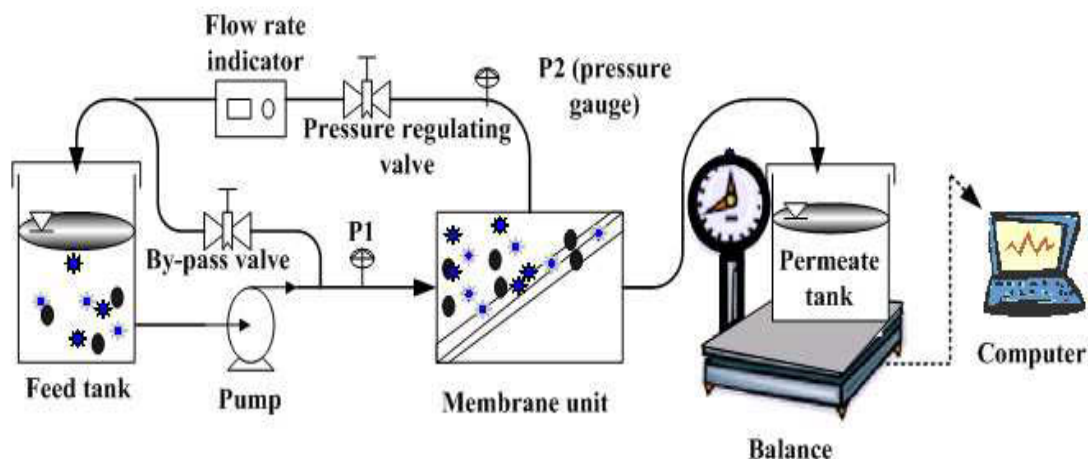


Figure 3.7 Schematic drawing of cross-flow unit studied

3.4 Experimental Analyses

3.4.1 EfOM Characterization

3.4.1.1 Dissolved Organic Carbon (DOC) and Specific UV Absorbance (SUVA)

All samples underwent a 0.45 μm mixed cellulose ester microfiltration as a prefilter. A Sievers-820 analyzer (Sievers-820, Sievers, Co., USA) was performed to measure the DOC with an auto sampler (Sievers-820A, Sievers, Co., USA). Ammonium persulfate was used as a chemical oxidizer. UV radiation converted the EfOM into carbon dioxide and water. The carbon dioxide produced was then detected using a sensitive membrane-based conduct-metric technique.

The SUVA is defined as the ratio of UV absorbance and DOC (e.g., $\text{UVA}_{254}/\text{DOC}$). The UVA was measured at 254 nm using a UV-1601 UV/Visible spectrophotometer (Shimadzu, Japan) with a 10 mm quartz cell. The SUVA value generally represents an index of aromaticity or hydrophobicity of EfOM.

The study was conducted with BTSE drawn from a sewage treatment plant in Gwangju, South Korea. Table 3.9 shows SUVA values of BTSE. The SUVA values of BTSE are smaller than those of different water sources (groundwater and surface water), suggesting that EfOM from BTSE includes more aliphatic compounds. On the other hand, groundwater has the highest aromaticity among the three water sources.

Table 3.9 Comparison of SUVA values by different water sources (adapted from Cho, 1998; Her, 2002)

Water source	Area	UVA254 (1/cm)	DOC (mg/L)	SUVA (L/m mg)
BTSE	Gwangju, Korea	0.114	9.55	1.19
	Hawaii, USA	0.29	12.9	2.25
Ground water	Irvine Ranch, USA	0.79	11.9	6.6
	Orange county, USA	0.387	6.81	5.7
Surface water	Horsetooth reservoir, USA	0.092	3.12	2.9
	Baseflow silver lake, USA	0.048	2.0	2.4

3.4.1.2 Colloidal Organic Fraction

The dialysis was performed with a Spectra/Por-3 regenerated cellulose dialysis membrane bag (MWCO 3500 daltons) (Figure 3.8). The dialysis membrane was washed by soaking it in 4 liters of pure water for 24 hours. The wastewater sample was acidified with HCl to pH 1 and placed in the pre-washed dialysis membrane bag. It was dialyzed for 8 hours (each time) against three 4 L portions of 0.1 N HCl (to remove salts and low MW of EfOM). It was then dialyzed until the silica gel precipitate was dissolved against 4 liter of 0.2 N HF. Finally, it was dialyzed for 12 hours (each time) against two 4 L portions of pure water. This was to remove residual HF and fluosilicic acid. Finally, the sample was taken out of the dialysis membrane from the last 4 L of dialysate of deionized water and measured for its TOC content. This represents the EfOM colloidal matter (with MW range from 3,500 daltons to 0.45 μm). In wastewater engineering practice, organic matter of 3500 daltons is conventionally too small to be called organic colloidal matter.

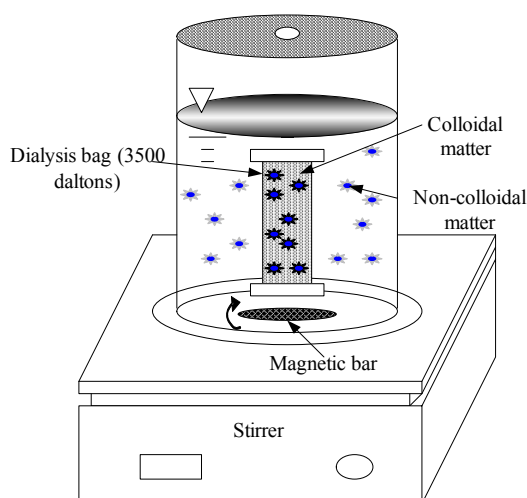


Figure 3.8 Schematic drawing of colloidal and non-colloidal fractions with Spectra/Por-3 regenerated cellulose dialysis membrane bag (MWCO, 3500 daltons)

The organic colloidal portion in the BTSE was determined and is presented in Table 3.10. The organic colloidal matter is defined as the one having a size between 3,500 daltons to 0.45 μm (a standard method to measure the colloidal portion in NOM or EfOM). The compounds consisted of approximately 38.4% of DOC in this study. This suggests that EfOM in BTSE includes the majority of small MW (< 3500 daltons). The SUVA value of the colloidal fraction showed a lower level compared with that of the influent. This may be due to the HL compounds such as polysaccharides and proteins.

Table 3.10 Organic colloidal portion (in DOC) in the BTSE

	Initial concentration (SUVA)	Colloidal portion of EfOM (SUVA)
BTSE (mg/L)	10.53 (2.053)	4.04 (1.287)

3.4.1.3 Fractionation of EfOM

Figure 3.9 shows the fractionation using XAD-8 (a nonionic adsorbent from acrylic ester polymer with nominal pore size 23.5 nm, Rohm and Haas, PA) and XAD-4 (a nonionic adsorbent from polystyrene with nominal pore size 5 nm, Supelco, PA) resins. A resin column (Spectra/Chrom, Spectrum Chromatography: 1.5 cm diameter x 30 cm

length) was used. The resins were used for fractionating EfOM into hydrophobic (HP) EfOM (XAD-8 adsorbable; mostly hydrophobic acids with some hydrophobic neutrals; humic and fulvic acids), transphilic (TP) EfOM (XAD-4 adsorbable; hydrophilic (HL) bases and neutrals) components. The remaining fraction escaping the XAD-4 was the hydrophilic component.

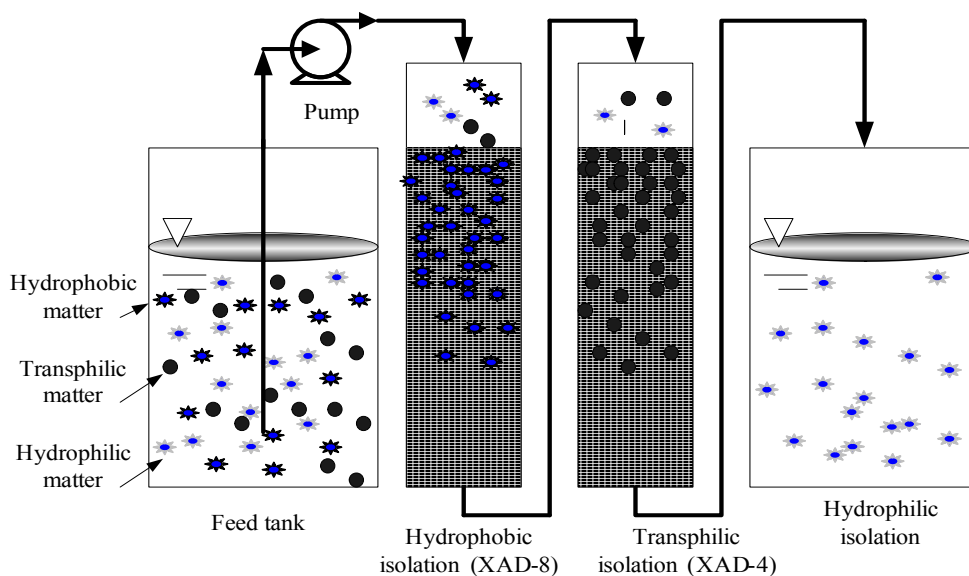


Figure 3.9 Schematic drawing of fractionation for hydrophobic, transphilic and hydrophilic components with XAD-8 and XAD-4 resins

To investigate the effects of different fractions, the isolated fractions were concentrated using a freeze dryer (ilShin Lab Co. Ltd., South Korea). The initial concentration of each fraction was adjusted to approximately 6.5 mg/L, which was equivalent to that of BTSE. The conductivity of the isolated fractions was also adjusted to 15 mS/cm with NaCl because the NaOH and HCl solutions used to isolate the fractions increased the ionic strength. Thus, all the fractions used in membrane filtration experiments had the same conductivity of 15 mS/cm.

The resin in the column was washed in order of pure water, 0.1 N NaOH, pure water, 0.1 N HCl and pure water. After filtering all the samples, they were then acidified to pH 2 due to reduction of HP interaction between EfOMs and resins. The acidified samples passed through the resins with low velocity (2 ml/min). The effluents which underwent the XAD-8/4 resins were decided as the HL fraction (Figure 3.9). The adsorbed HP and TP fractions on the XAD-8/4 were eluted with 0.1 N NaOH. The DOC was measured with the eluted effluents. The content percentage of each fraction

was calculated by mass balance. The resins used were regenerated in methanol followed by acetonitrile with a Soxhlet extraction for 48 hours. The general mass loss reported during the isolation of each EfOM fraction was about 5 – 15% (Lee, 2004).

3.4.1.4 Molecular Weight (MW) Distribution

High pressure size exclusion chromatography (HPSEC, Shimadzu Corp., Japan) with a SEC column (Protein-pak 125, Waters Milford, USA) was used to determine the MW distributions of EfOM (Figure 10). The separation ranges are between 1000 and 30000 daltons. The effluent was made of pure water with phosphate (pH 6.8) and NaCl (0.1 M). The detection limit of UV was 0.001 per cm. Standards of MW of various polystyrene sulfonates (PSS: 210, 1800, 4600, 8000, and 18000 daltons) were used to calibrate the equipment. The MW calculation can be classified into three groups: i) number-average MW, ii) weight-average MW and iii) z-average MW. The number-average MW called “median” can be calculated as follows:

$$M_n = \frac{\sum_{i=1}^n (N_i M_i)}{\sum_{i=1}^n (N_i)} \quad (3.1)$$

The weight-average MW which is commonly used can be calculated from the following equation:

$$M_w = \frac{\sum_{i=1}^n (N_i M_i^2)}{\sum_{i=1}^n (N_i M_i)} \quad (3.2)$$

where N_i is the number of molecules having a MW M_i and i is an incrementing index over all MW present.

The MW distribution was represented by a UV response (mV intensity) with time. The MW distribution was also presented as normalized fraction percentage. It was obtained by dividing each incremental height of the chromatogram with a sum of the heights when the chromatogram was divided into incremental mass intervals (Cho et al., 2000; Lee et al., 2002). Both representations were similar to that of normalized fraction percentages, making it easier to visualize the reduction of a peak of organic matter by different treatments, such as flocculation and adsorption. Most of figures were drawn in terms of UV response with time in this study. The representation with the normalized fraction percentage can be found in Appendix A.

In general, UV absorbance at 254 nm detects limited components (mostly π -bonded molecules) of organic matter so this method is mainly applied to the MW estimations of humic and fulvic acids as well as hydrophobic (aromatic) organic matter. The UV detector used in this study had a limitation in detecting low UV-absorptivity components, such as proteins and polysaccharides. Thus, a relative intensity of UV response was employed to interpret the results (Cho et al., 2000; Lee et al., 2002).



Figure 3.10 High pressure size exclusion chromatography (HPSEC) to measure MW distribution

3.4.1.5 MW Distribution of BTSE-W/S

MW distribution of EfOM is an influential factor to understand and estimate EfOM size. It is necessary to comprehend the range of MW of EfOM. This will help in identifying the characteristics of the majority of EfOMs and in the selection of suitable processes and mechanisms for a given application. HPSEC is used to measure MW distribution. HPSEC measurements have been used to analyze MW distribution and weight-averaged MW values using a modified silica column (Chin et al., 1994). Many researchers have applied the technique to measure MW distribution of EfOM.

As mentioned above, typical MW distribution of BTSE is different from season to season. MW distribution of EfOM during winter (BTSE-W) and summer (BTSE-S)

seasons illustrates in Figure 3.11. The MW range of EfOM shows from 50,000 to 200 daltons in BTSE-W. On the other hand, the MW distributed from 3000 to 200 daltons with the highest response in BTSE-S.

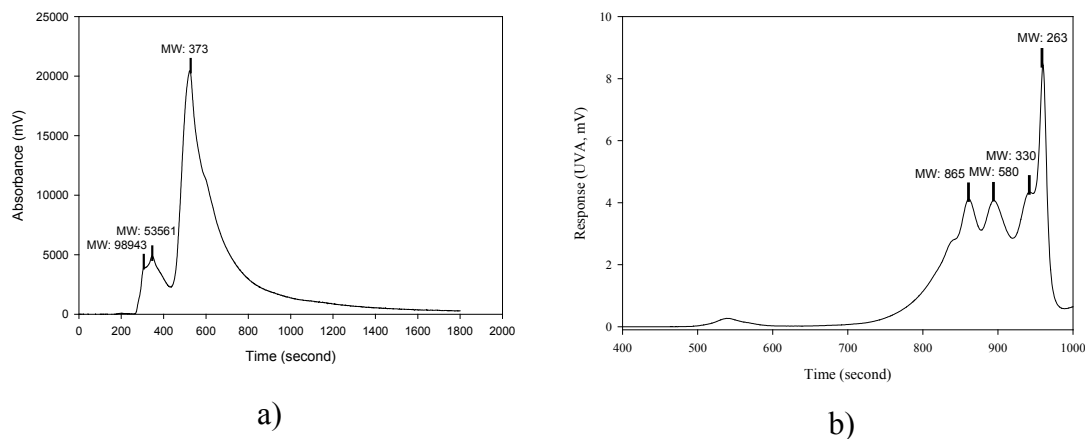


Figure 3.11 MW distribution of (a) BTSE-W and (b) BTSE-S

3.4.1.6 MW Distribution of Fractions in BTSE-S

The BTSE-S was fractionated into HP, TP and HL using XAD-4/8 resins. The MW distribution of the HP, TP and HL fractions was investigated in Figure 3.12. The HP fraction included 580, 865, and 43109 daltons; TP (580 and 865 daltons); and HL (from 263 to 580 daltons). The results were an agreement with those of previous study (Huber, 1998; Jarusutthirak, 2002).

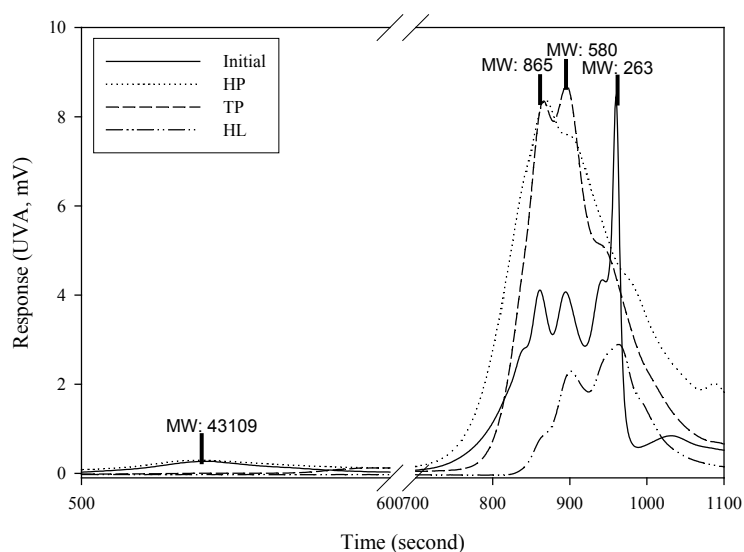


Figure 3.12 MW distribution of HP, TP, and HL fractionations

3.4.1.7 Fluorescence Excitation-Emission Matrix (EEM)

A fluorescence detector was also used to identify protein-like substances at excitation (279 nm) and emission (353 nm). The analysis set-up is presented in Figure 3.13. Standards of polystyrene sulfonates with different MW (PSS: 210, 1800, 4600, 8000, and 18000 daltons) at lower concentration were used to calibrate the equipment. Details on the measurement methodology are given elsewhere (Her, 2002).

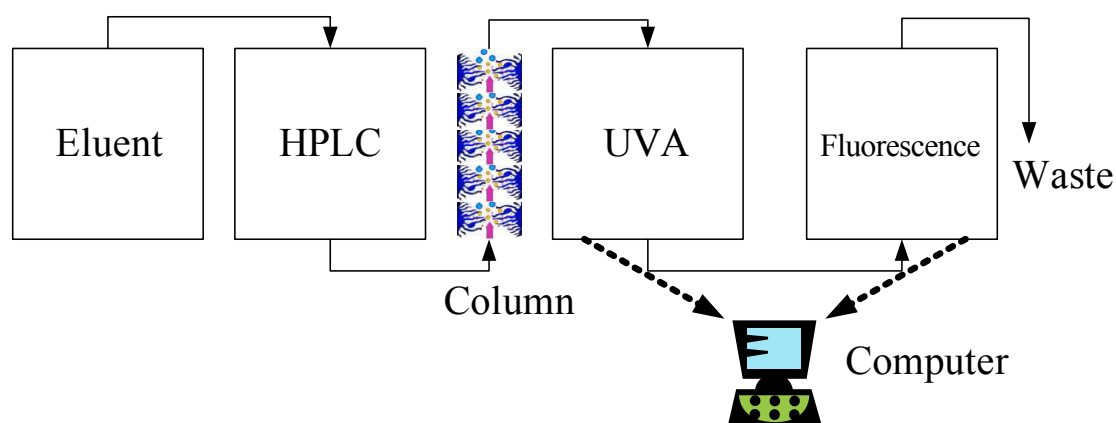


Figure 3.13 Schematic drawing of HPLC-UVA-fluorescence

3.4.1.8 Fluorescence Chromatograms of BTSE-W/S

The EfOM of protein-like substances in BTSE-S shows the high response at 44944 and 235 daltons in BTSE (Figure 3.14 (a)). However, the MW of 376 and 748 daltons indicates the low intensity, suggesting that these peaks may be due to humic substances including humic and fulvic acids compared to MW distribution (Figure 3.14 (b)).

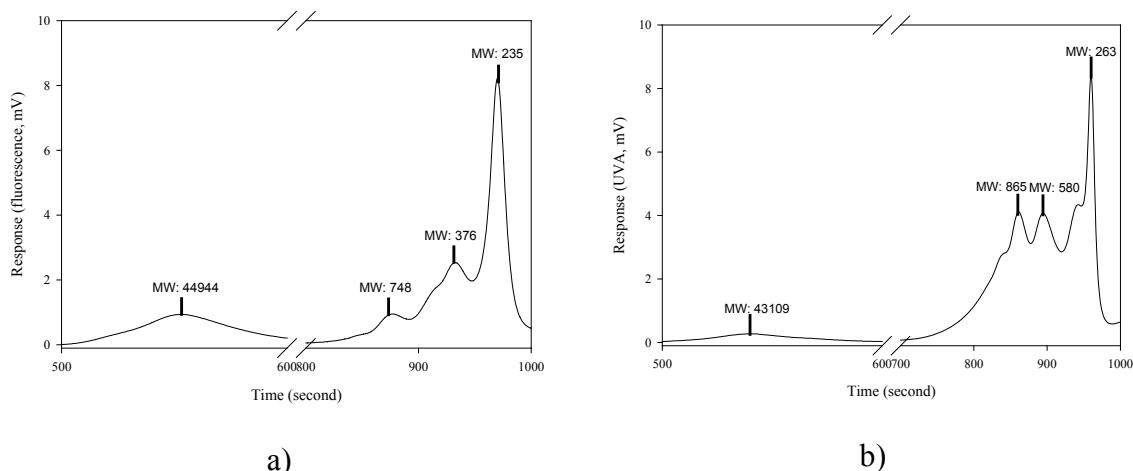


Figure 3.14 Comparison of (a) fluorescence chromatogram and (b) MW distribution of EfOM with BTSE-S (initial DOC concentration = 6.5 mg/L)

3.4.1.9 Fluorescence Chromatograms of Fractions in BTSE-S

The protein-like substances were also detected with fluorescence chromatograms in terms of different fractions (Figure 3.15). The majority of the protein-like substances were found at 235, 23440, and 44944 daltons in HP, 235 and 44944 daltons in TP and 235 daltons in HL. In principle, a typical BTSE includes the majority of HL fractions (polysaccharides and extracellular enzymes) as a large MW (Her, 2002; Jarusutthirak, 2002). However, in this study, the HP and TP compounds involved the same response of the protein-like substances, while in the HL fraction only the smallest MW (236 daltons) protein-like substances could be identified.

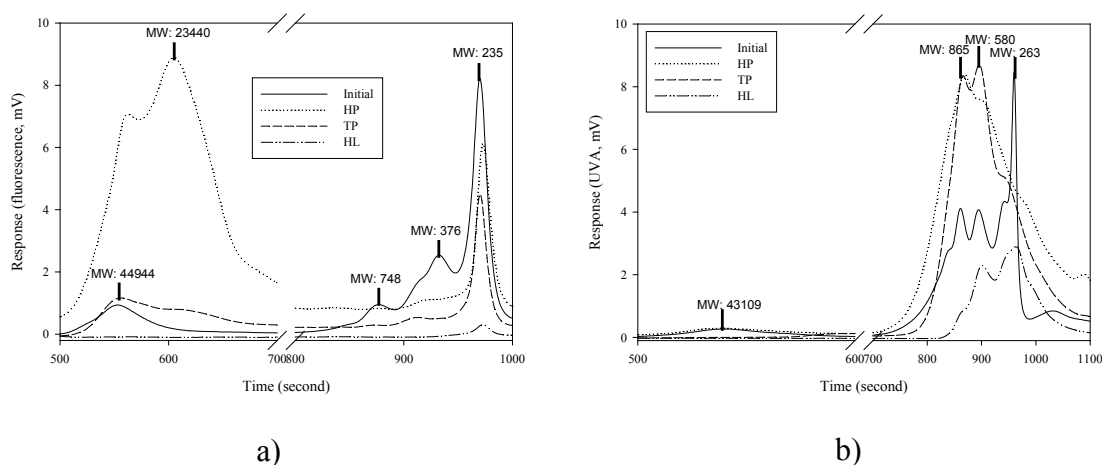


Figure 3.15 Comparison of (a) fluorescence chromatogram and (b) MW distribution of HP, TP and HL fractions with BTSE-S

3.4.1.10 Diffusion Coefficient

The transport of organic matter near the membrane and within the pores is related to its diffusivity. Thus, diffusion coefficient is an important mass transfer parameter. Uncertainties in diffusivity data can lead to serious errors in predicting the flux, especially in laminar flow situations where the mass transfer coefficient is highly dependent on diffusivity (Wang et al., 2001; Cheryan, 1998).

There are a few different ways to obtain diffusion coefficients. When an organic MW is known, the Brownian diffusivity of a particle of radius (r) is given by the Stokes-Einstein relationship:

$$D = \frac{k_{SE}T}{6\pi\eta r} \quad (3.3)$$

Where k_{SE} ($= 1.38 \times 10^{-16} \text{ g cm}^2 \text{ s}^{-2} / ^\circ\text{K}$) is the Boltzmann constant, T is the absolute temperature and η is the viscosity of the organic phase.

The diffusion coefficient can also be obtained by a simple experimental cell. The diffusion cell is shown in Figure 3.16. The device had two chamber cells with a membrane (regenerated cellulose 12000 – 14000 MWCO) separating the left and right cells. The left chamber in the cell was filled with BTSE, while the right chamber was filled with the same volume of Milli-Q water. Temperature was controlled by immersing the cell in a water bath. The solutions in both chambers were vigorously stirred by two magnetic stirrers positioned under the bath and cell. The stirring speed was fixed at 400 rpm. UV absorbance at 254 nm of organic matter with BTSE was measured with time. The diffusion coefficients of synthetic wastewater and BTSE-W used in this study were 5.696×10^{-10} and $4.3758 \times 10^{-10} \text{ m}^2/\text{s}$, respectively. The detailed methods employed can be found elsewhere (Wang et al., 2001).

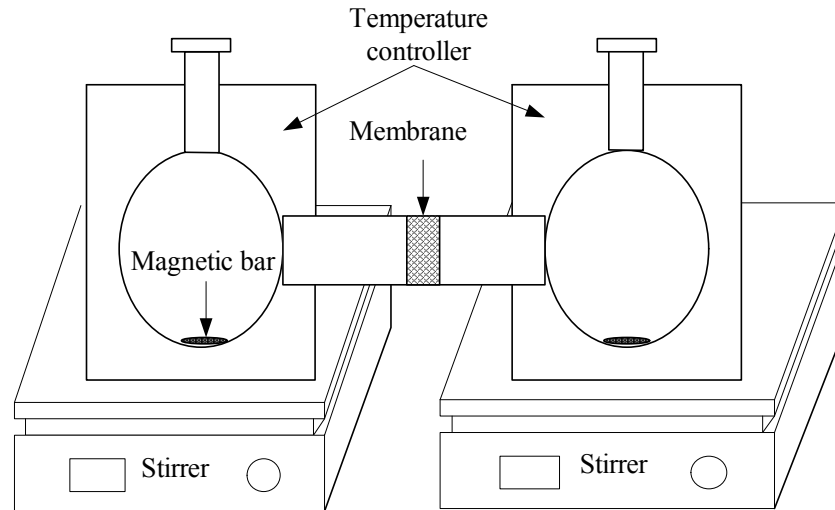


Figure 3.16 Schematic drawing of diffusion cell

3.4.2 Membrane Characterization

3.4.2.1 Zeta potential

Zeta potential on the different membrane surfaces was measured by an electrophoresis method (ELS-8000, Otsuka Electronics Co., Ltd., Japan) using polylatex (520 nm) in 10 mM NaCl solution as a standard particle (Levine et al., 1985; Chun et al., 2002; Weis et al., 2003). The pH of solution was adjusted with 0.1 N HCl and NaOH.

The potential for electrostatic interactions along the membrane surface can be investigated by zeta potential using an electrophoresis method. Figure 3.17 shows the variation in zeta potential of clean membranes as a function of pH. The results imply that an operation at pH 6 – 10 is the most appropriate to repulse the negative EfOM. The isoelectro points (IEP) of NTR 7410, NTR 729HF, LES 90 and LF 10 are pH 2.6, pH 3.3, pH 3.4 and pH 3.4, respectively. The higher negative zeta potential values of NTR 7410 and NTR 729HF are probably due to its larger pore sizes compared with other membranes (Thanuttamavong, 2002).

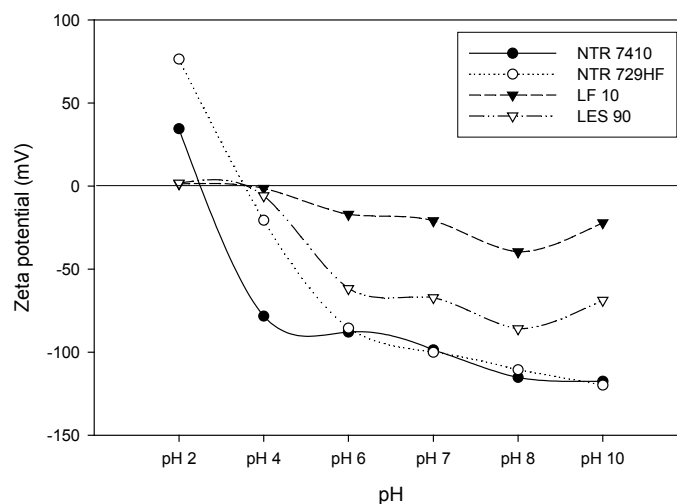


Figure 3.17 Zeta potential of clean membrane surfaces as a function of solution pH (background electrolyte concentration = 10 mM NaCl)

3.4.2.2 Contact Angle

Contact angle measurements using the sessile drop method with a contact angle meter (Contact angle meter, Tantec, Co., USA) were used to determine an index of membrane hydrophobicity. 20 μ L of Milli-Q water was dropped onto the dried membrane surface and the contact angle was measured within approximately 10 seconds (Cuperus and Smolers, 1991; Cho, 1998).

Contact angle represents a hydrophobicity of membrane's nature. Lee et al. (2004) reported that the contact angle of more than 50° is representative of a hydrophobic surface, on which an HP fraction can better be retained. The membranes used in this study were NTR 7410 (UF), NTR 729HF (NF), LES 90 (NF) and LF 10 (NF) (Nitto Denko Corp., Japan). The detailed characteristics of the contact angle with the sessile drop method are given in Table 3.11. The majority of membranes consist of a hydrophobic character except the NTR 729HF membrane. Cho (1998) observed that the contact angle of cellulose membranes is from 5° to 27.2° , cellulose acetate (46° - 53.3°), polysulfone membrane (44.7° - 69.7°) and polyamide membrane (32.2° - 60.3°).

Table 3.11 Characteristics of UF and NF membranes used

Membrane	MWCO* (dalton)	Contact angle(°)
NTR 7410	17,500	69
NTR 729HF	700	28
LES 90	250	54
LF 10	200	50

3.4.2.3 ATR-FTIR for Functional Groups

The clean and fouled membrane surfaces were analyzed for functional groups using attenuated total reflection-Fourier transform infrared spectroscopy (ATR-FTIR). The prepared membranes were examined by FTIR (460 plus, Jasco, Japan) equipped with an ATR accessory and the IR peak was analyzed with Bio-rad laboratories software.

Attenuated total reflection-Fourier transform infrared spectroscopy (ATR-FTIR) was conducted to analyze a functional group on the clean membrane surfaces (Figure 3.18). Although four membranes consisted of different sub-layer materials (polyamide, polyvinyl alcohol and polysulfone), the FTIR spectra indicated a similar spectral trend. The functional groups of main spectra are given in Table 3.12 (Skoog and Leary, 1992; Bellamy, 1975).

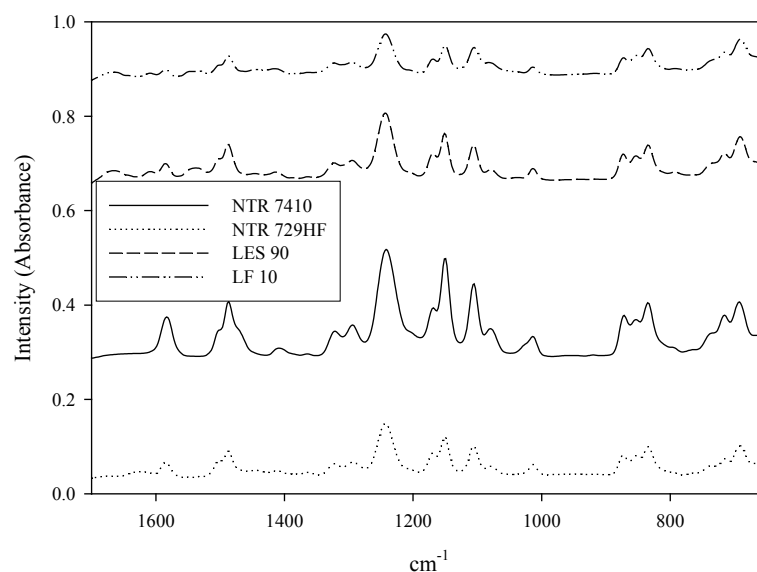


Figure 3.18 FTIR spectra on clean membranes (NTR 7410, NTR 729HF, LES 90 and LF 10)

Table 3.12 FTIR functional group on the clean membrane

	1050 – 1250 1/cm	1250 1/cm	1500 – 1600 1/cm
Functional group	C-O bonds of ethers or carbonxylyic acids	Carboxylic groups	Aromatic double bonds

3.4.2.4 Scanning Electron Microscopy (SEM) and Atomic Force Microscope (AFM)

Scanning electron microscopy (SEM) is a useful tool for investigating membrane structure during membrane fouling (Kim and Fane, 1994). SEM images of the membranes were carried out using the SEM (FE-SEM S-4700, Hitachi Corp., Japan). The voltage was 5 kV and the working distance was 12 mm. The magnification was 20000 times. The top and side views of the membranes were analyzed.

Figure 3.19 shows the SEM images of top view (left) and side view with each clean membrane. The surfaces of four membranes indicated different roughnesses as caused by structures and shapes. The detailed surface morphologies can be determined by atomic force microscope (AFM). The AFM gives a topographical image by scanning a sharp tip, situated at the end of a microscopic cantilever.

Thanuttamavong (2002) took the AFM images of the membranes used in this study (Figure 3.20) and the average roughness ranged from high value to low value as 85.9 nm (LES 90) > 75.2 nm (NTR 729HF) > 64.7 nm (LF 10) > 10.1 nm (NTR 7410). Here, the average roughness represents the arithmetic average of all height values obtained from the AFM images.

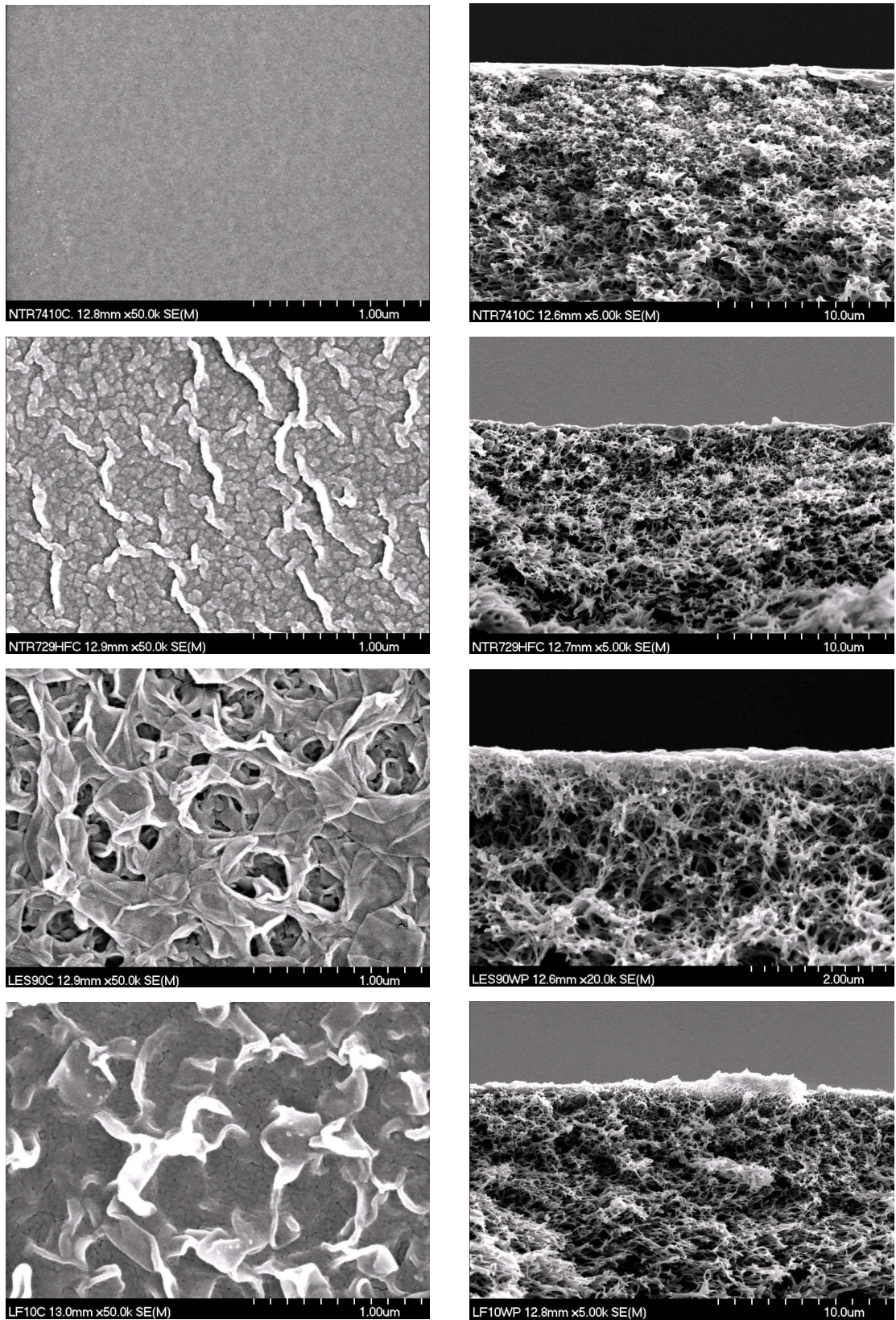


Figure 3.19 Top and side views of beam energies on filed FE-SEM images of each membrane (working distance of 12 mm and magnification of 50000 and 5000)

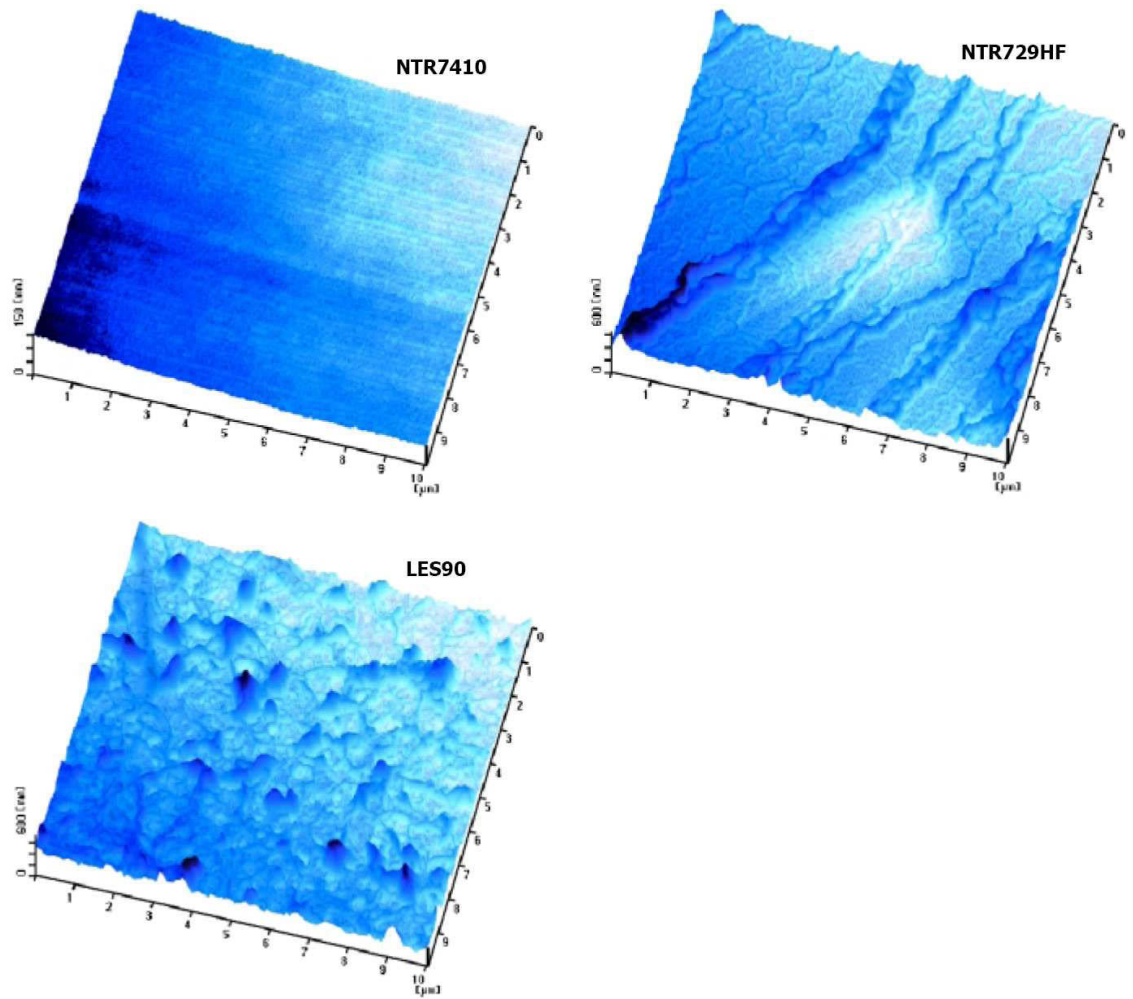


Figure 3.20 AFM images of each membrane (adapted from Thanuttamavong, 2002)

CHAPTER 4



University of Technology, Sydney
Faculty of Engineering

INFLUENCE OF FLOCCULATION AND ADSORPTION AS PRETREATMENT TO MEMBRANE FILTRATION

4.1 Introduction

Membrane processes are now being successfully used to obtain water of recyclable quality from wastewater. Even though membrane processes can effectively remove a variety of contaminants from biologically treated sewage effluent (BTSE), membrane foulants (i.e., sparingly soluble inorganic compounds, colloidal or particulate matter, dissolved organics, chemical reactants and microorganisms) can reduce the water flux through a membrane by as much as 90% (Speth et al., 1998). Pretreatment of BTSE prior to its application to membrane processes will reduce cell deposition and subsequent biogrowth due to dissolved organic matter (Redondo and Lomax, 2001; Tanninen et al., 2003). Pretreatment also reduces the need for frequent chemical cleaning, which is a major factor impacting on membrane life. Pretreatment offers considerable potential for improving the efficiency of membrane processes.

Flocculation, powdered activated carbon (PAC) adsorption, and granular activated carbon (GAC) biofiltration can remove most of the solutes and organic colloids present in BTSE; and hence, they can be used as successful pretreatment processes. Pretreatment such as flocculation can remove 80 – 90% of the total suspended matter, 40 – 70% of the BOD₅, 30 – 60% of the COD, and 80 – 90% of the bacteria (Tchobanoglous and Burton, 1991). Adsorption can remove organics which are not removed by conventional chemical and biological treatment methods. Al-Malack and Anderson (1996), Chapman et al. (2002) and Abdessemed et al. (2000) have studied the effect of flocculation and adsorption as pretreatment on the performance of cross-flow MF and UF of domestic wastewater and BTSE. Al-Malack and Anderson (1996) from their experiments with BTSE found that flux values improved with the addition of alum at an optimal dose of 80 mg/L. This flux improvement was attributed to the agglomeration of particles which could then be easily removed by shearing action. Chapman et al. (2002) indicated that the floating medium flocculator (a static flocculator) with ferric chloride addition produced filterable flocs of about 20 µm sizes, resulting in the removal of 45% of suspended solids, 97% of phosphorus and 45% of the organics from the BTSE. A recent study conducted with flocculation and adsorption as pretreatment to crossflow microfiltration (CFMF) also showed a significant improvement of flux decline of microfiltration with time (Guo et al., 2003).

Abdessemed et al. (2000) have shown that adsorption is efficient in removing the EfOM, while flocculation allows UF as well as MF membranes to perform higher permeate flux. A detailed experimental study was also conducted on a number of pretreatment methods to RO in treating BTSE (Kim et al., 2002). Among the pretreatment methods used, UF was the best pretreatment to RO. Another long-term study conducted with a submerged membrane-adsorption process indicated that PAC adsorption significantly reduced membrane fouling (Vigneswaran et al., 2003). This study indicated that membrane operation could be prolonged by several weeks by PAC addition. Here, PAC functioned as a biosorption system, eliminating the need for frequent removal of PAC. The organics initially adsorbed onto PAC were biologically degraded thereafter. Granular activated carbon (GAC) bioadsorption as a pretreatment is used extensively for achieving superior removal of particulate organic matter and dissolved solids from wastewater effluents by biological and adsorption processes (Shon et al., 2004).

The characterization of membrane fouling is important when choosing the correct design parameters of membranes and pretreatment methods. To identify the fouling on the UF membrane surface, the scanning electron microscopy (SEM), zeta potential, pyrolysis-GC/MS, attenuated total reflection-Fourier transform infrared spectroscopy (ATR-FTIR), etc. are used (Speth et al., 1998; Zhang et al., 2003; Ridgway and Flemming, 1996). The zeta potential is used as the electrokinetic value associating a realistic magnitude of surface charge (Chun et al., 2002; Weis et al., 2003). Chun et al. (2002) found that changes in membrane zeta potential could be used to examine the behavior of cake deposition and fouling during the filtration. The identification of fouling can be investigated both by extraction of organics and by ATR-FTIR analysis of deposits at the surface and in the substructure (Weis et al., 2003). With ATR-FTIR, it is possible to confirm a detailed screen of molecular functional groups contributing to membrane fouling. SEM has been a useful instrument to identify membrane fouling as well as itself being membrane structure (Kim and Fane, 1994). Kim and Fane (1994) and Shon et al. (2004) reported that the thickness of adsorbed protein could be measured in the cake layer of UF using SEM images. Hydrophobicity is suggested to be a very important parameter in membrane fouling as more hydrophobic surface will exhibit a higher degree of fouling. A number of researchers have tried to find a way to express hydrophobicity in a quantitative way (Cuperus and Smolders, 1991; Cho, 1998). Contact angle measurements are routinely used for dense and flat surfaces due to their simple operations but these

values cannot be extended to membranes which have a rough surface and have significant pores.

Yuan and Zydney (2000) have shown that organic matter usually associated with colour (e.g., humic and fulvic acids) is a major foulant during UF. Carbohydrates, proteins and polyhydroxyaromatics are also found to cause membrane fouling in water applications (Speth et al., 1998). This viscous film layer – which has to be removed by physical cleaning - was responsible for most of the flux decline. The viscous foulant material remaining has been related to biological fouling. The characteristics of the foulant matter are thus dominated by biological growth (cells themselves and extracellular materials) (Speth et al., 1998). A number of studies have shown that the colloidal fouling rate increases with increase in ionic strength of the solution, feed colloidal concentration and permeate water flux through the membrane surfaces (Zhu and Elimelech, 1997; Lee et al., 2004; Potts et al., 1981).

None of the above studies attempted to characterize the EfOM in terms of MW distribution. Information on MW distribution has a number of advantages:

- i) a more fundamental understanding of the complex interactions that occur in unit operations and treatment processes,
- ii) process selection and evaluation to develop improved techniques, and,
- iii) determination of applied membrane MW cut-off (MWCO) for targeted pollutants.

The main objective of this chapter is to i) evaluate pretreatment capabilities in removing EfOM and their role in reducing membrane fouling and ii) investigate the variation in the membrane (UF and NF) foulant characteristics (in terms of MW and membrane characterization) after the BTSE has undergone different pretreatments. The pretreatments used prior to the application of the UF and NF were: (i) flocculation with FeCl_3 , (ii) adsorption with PAC, (iii) flocculation followed by adsorption (Floc-Ads) and (iv) GAC biofilter. All the effluents after pretreatments and membrane filtration were characterized in terms of MW distribution. The main role of pretreatment is the simultaneous enhancement of removal efficiency and the reduction in fouling potential of membranes. However, optimizing the pretreatment is also an economic necessity. MW distribution can be used as an index in the optimization of pretreatment.

Membranes were used to filter BTSE and then were characterized in terms of contact angle, zeta potential, ATR-FTIR and SEM.

4.2 DOC Removal and SUVA with Pretreatment

The EfOM removal by the different pretreatment methods was first measured in terms of DOC and SUVA. As can be seen in the Table 4.1, flocculation followed by adsorption (Floc-Ads) led to the highest DOC removal. The SUVA values in the BTSE were relatively lower than in surface water, suggesting that aromaticity of EfOM is less compared with raw water. Her (2002) reported that SUVA value of Silver lake surface water was around 4.5 L/ m·mg.

Table 4.1 DOC removal and SUVA values with different pretreatments.

	Quality of biologically treated effluent	Flocculation alone (rejection, %)	PAC adsorption alone (rejection, %)	Flocculation + adsorption (rejection, %)
DOC (mg/L)	6.60	2.80 (57.6)	2.28 (65.4%)	0.70 (89.4%)
UVA ₂₅₄ (1/cm)	0.110	0.040	0.010	0.005
SUVA (L/m·mg)	1.661	1.429	0.438	0.641

4.3 Removal of Colloidal Organics

The organic colloidal portion in the secondary effluent with and without pretreatment of flocculation and adsorption was determined (Table 4.2). More than 65% of organic colloidal matter was removed by flocculation. Here, the organic colloidal matter is defined as the one having a size between 3500 daltons to 0.45 μm (a standard method to measure the colloidal portion in NOM or EfOM). On the other hand, adsorption removed only 30% of colloidal organic matter. Adsorption works on the principle of adhesion in proportion to porous adsorbing material and surface area (Murray, 1995). The mean pore diameter of PAC is 3 nm which is very small but it removes the majority of colloidal organic matter.

Table 4.2 Organic colloidal portion (in DOC) in the secondary effluent with and without a treatment of flocculation and adsorption

	Colloidal portion of EfOM (DOC)	SUVA (L/m mg)
Secondary effluent	4.04	1.287
After flocculation with 41 mg-Fe/L of FeCl ₃	1.36	0.294
After adsorption with 1 g/L of PAC	3.18	0.440

4.4 Removal of Fractions with Pretreatment

The HP and the HL organic fractions were determined in the BTSE-W (wastewater for the BTSE conducted during winter) before and after the treatment of flocculation and adsorption (Table 4.3). Table 4.3 shows that Floc-Ads resulted in high removal of both HP and HL organic matters. In principle, the flocculation and adsorption are used mainly to remove HP portions of large and small MW organics, respectively. The removal of the HL portion of organics by flocculation may be due to large dose of FeCl₃ used (through sweep flocculation mechanism). The removal of the HL portion of organics by adsorption could be attributed to the physical affinity between hydrophilic organic molecules and PAC (through van der Waals, electro static forces and chemisorption) (Benefield et al., 1982).

Table 4.4 also presents the removal of different fractions by different pretreatments with BTSE-S (wastewater for the BTSE conducted during summer). PAC adsorption removed the large amount of the HP compounds for BTSE samples collected during both seasons. This may be due to the HP characteristics of PAC so that PAC adsorption is favorable to remove HP. However, FeCl₃ flocculation removed HP and HL with different trends. During winter season, HP was removed up to 68.5%, whereas during summer season, HL was removed up to 59.8%. This is probably due to the ion effects. The flocculation removes the fractions which are more negative charged.

Table 4.3 HP, TP, and HL fractions in BTSE-W (FeCl₃: 41 mg-Fe/L and PAC: 1 g/L)

Fraction	DOC of Secondary Effluent (ppm)	DOC of the effluent after flocculation (rejection, %)	DOC of the effluent after adsorption (rejection, %)	DOC of the effluent after Floc-Ads (rejection, %)
HP	4.98	1.57 (68.5)	1.42 (71.4)	0.85 (82.9)
TP	1.68	0.81 (62.9)	0.56 (66.9)	0.79 (53.0)
HL	3.19	1.22 (61.8)	1.36 (57.4)	0.58 (81.8)

Table 4.4 Removal of HP, TP, and HL fractions in BTSE-S (FeCl₃: 28 mg-Fe/L and PAC: 1 g/L)

Fraction	Initial (mg/L)	Floc. (mg/L)	Ads. (mg/L)	Floc-Ads. (mg/L)
HP	1.645	0.999 (39.3%)	0.460 (72.0%)	0.283 (82.8%)
TP	1.034	0.802 (22.4%)	0.282 (72.7%)	0.123 (88.1%)
HL	3.822	1.540 (59.7%)	1.258 (67.1%)	0.545 (85.7%)

4.5 MW Distribution

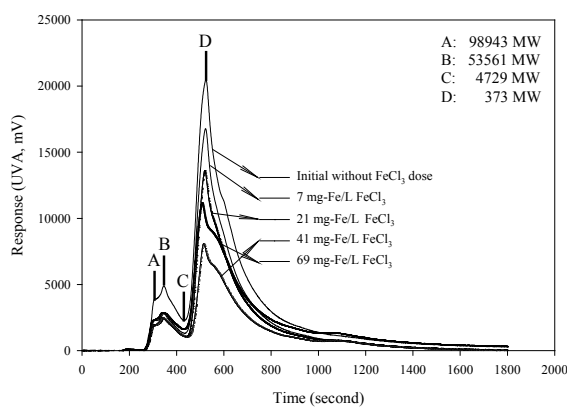
MW distribution of EfOM in BTSE-W was analyzed by using response (mV) data of HPSEC with elapsed time. The MW of the EfOM ranged from 300 daltons to about 98940 with the highest fraction of 300 – 5000 daltons. The points of inflection for the wastewater studied were found at the MW of 98940, 53560, 4730 and 373 (Figure 4.1). They are denoted by A, B, C and D. It should be noted that the wastewater characteristics and the MW distribution of the organic matter vary from season to season and from geographic place to place. For example, the secondary effluent of a wastewater treatment plant in Hawaii showed that the MW size distribution was from approximately 50000 daltons to 100 with the highest fraction of 20500 – 900 daltons (Her, 2002).

The response versus elapsed time graph was drawn for both flocculated and non-flocculated samples (Figure 4.1 (a)). Comparing the flocculation results at different doses of FeCl₃, the flocculation with optimum dose of FeCl₃ (41 mg-Fe/L) produced to the highest removal of organics. In addition to the removal of large MW organics, it also removed a significant quantity of small MW organics. The mechanism of small MW

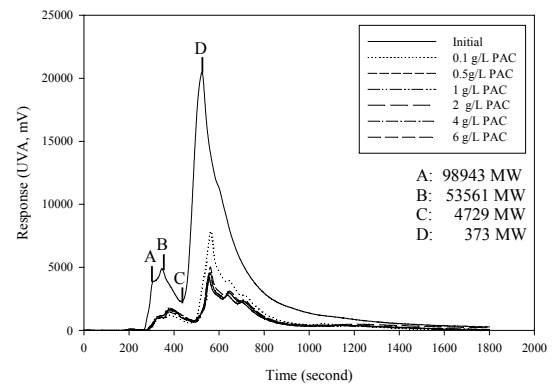
organic matter removal by flocculation with FeCl_3 is mainly through complexation of Fe for wide range of pH (5.5 – 7.5) (Vilge-Ritter et al., 1999). In the present experiment, the pH was between 6.0 and 7.5. Adsorption of small organic molecules on to Fe hydroxide also occurs at a neutral pH (Dempsey et al., 1984).

The MW distribution was also experimentally measured in the BTSE-W after the treatment of adsorption by PAC (Figure 4.1 (b)). As expected, PAC removed the majority of small MW organics. The PAC used had a pore radius from 1 to 5 nm with mean radius of 1.8 nm. The removal of large MW organics by PAC can be explained as adsorption onto the larger pores of PAC and in addition, some of the larger MW organics may have been retained on the outer surface of PAC.

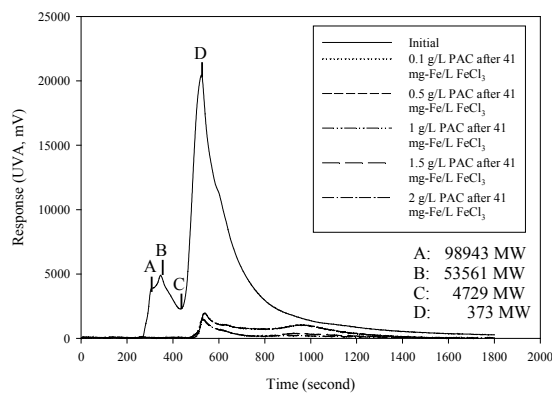
Figure 4.1 (c) also shows the MW distribution of EfOM in the effluent without and with Floc-Ads treatment. This figure indicates that the treatment of Floc-Ads led to a high removal of both small and large organic matters, for example, all of MW from 5000 to 98940 could be removed by this pretreatment.



a)



b)



c)

Figure 4.1 MW distributions of the BTSE-W with and without pretreatments (a) flocculation, b) PAC adsorption and c) Floc-Ads)

The detailed MW distribution for different treatments was also investigated in BTSE-S (Figure 4.2). The MW distribution of the BTSE-S comprised small (260 daltons, 580 and 870) and large (43110 daltons) MW. The peaks with 260 daltons indicated the highest response in BTSE-S. Ferric chloride (FeCl_3) flocculation, PAC adsorption and Floc-Ads with the optimum doses were used as treatment methods. As can be seen in Figure 4.2, the Floc-Ads removed the majority of the organic matter except 330 daltons. However, flocculation alone could not remove the majority of small MW (260 daltons, 330 and 580); and adsorption alone could not remove the large MW compounds (330 daltons, 870 and 43110).

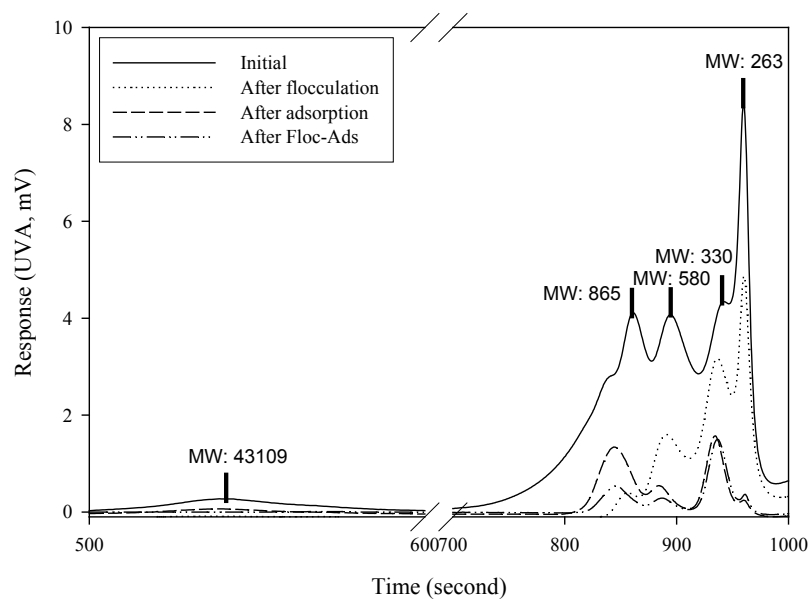


Figure 4.2 MW distribution of BTSE-S after different treatments (flocculation, adsorption and Floc-Ads)

4.6 Fluorescence Chromatograms

The protein-like substances were detected with fluorescence for different treatments (i.e., flocculation, adsorption and Floc-Ads) with BTSE-S (Figure 4.3). The Floc-Ads removed the majority of the protein-like substances, however, PAC adsorption could not remove the MW of 44940 daltons and flocculation 380 and 240 daltons. Proteins found in the range of 13% to 20% in BTSE-S, can significantly be removed by Floc-Ads.

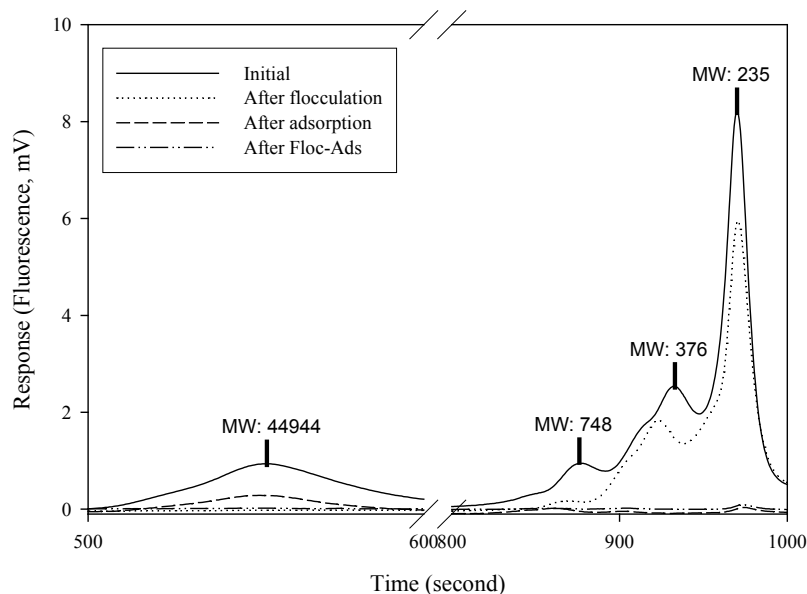


Figure 4.3 Fluorescence chromatograms after different treatments with BTSE-S

4.7 Experiments with Ultrafiltration (UF) Membrane

4.7.1 DOC Removal

The EfOM removal was first measured in terms of DOC in BTSE-S. As can be seen in Figure 4.4, DOC removal by the NTR 7410 UF membrane was only 43.6%, suggesting that a significant portion of EfOM in the BTSE-S consists of low MW compounds much smaller than 17500 daltons. On the other hand, the DOC removal is significant considering that MWCO of the membrane is larger than the weight-averaged MW of the EfOM in the BTSE-S. This may be due to the influence of a number of parameters such as pore size distribution, surface charge effect of the membrane, physicochemical affinity of organic pollutants towards the membrane (hydrophobicity of membrane, solute-solute and solute membrane interactions) and hydrodynamic characteristics of the membrane system (such as crossflow velocity). Similar results were obtained with the same membrane in a previous study (Cho, 1998). Cho (1998) observed a DOC removal of 30% to 60% although the weight-averaged MW in the water was only approximately 1300 daltons. Adsorption (by either PAC or GAC biofilter) was found to be more efficient in removing DOC than flocculation as a pretreatment to UF.

With PAC adsorption as a pretreatment, the MW distribution in the effluent ranged from 3000 to 200 daltons. However, in the effluent of GAC biofilter, some large MW organics (35000 daltons) did remain (Figure 4.5): they are probably the extracellular polymer substances (EPS) like polysaccharides and proteins present in the BTSE-S (which were produced by microorganisms in the biofilter). These molecules may have been responsible for the permeate flux decline in the UF observed after biofiltration. Even though the DOC removal by GAC is greater than that with PAC adsorption, the flux decline of GAC biofilter is higher than that of PAC adsorption. Pretreatment of the Floc-Ads led to a DOC removal as high as 90.1%. In this case, the additional removal by the post treatment of UF was negligible (Figure 4.4).

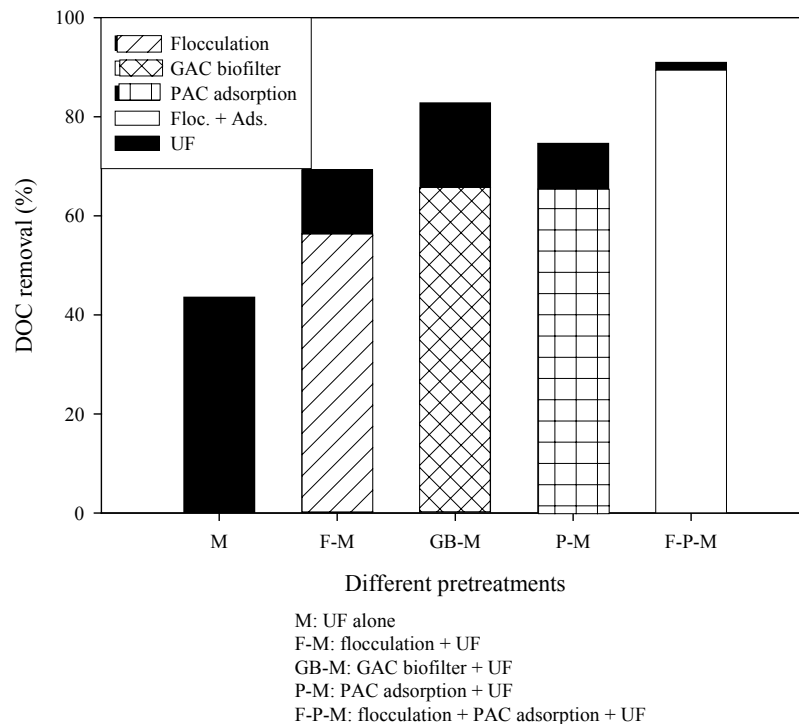


Figure 4.4 Effect of different pretreatment methods in terms of DOC removal with BTSE-S (UF membrane used = NTR 7410; MWCO of 17500 daltons, crossflow velocity = 0.5 m/s, transmembrane pressure = 300 kPa, Reynold's number: 735.5, shear stress: 5.33 Pa)

4.7.2 MW Distribution

MW distribution of the soluble organic matter was measured after each pretreatment and in the UF effluent (Figure 4.5). The efficiency of UF was lower for smaller MW components. When a pretreatment was provided, the additional organic matter removed by UF as post-treatment was not significant (around 1.6% - 17.1%). Figures 4.5 (a) and 4.5 (b) confirm that adsorption (both GAC biofilter and PAC adsorption) removes the majority of organics except the fraction corresponding to MW 330 daltons: this might correspond to non humic substances and hydrophilic components. Figure 4.5 (a) shows that the pretreatment of Floc-Ads is very efficient (except for this fraction) and makes the additional removal by post-treatment of UF negligible. A previous study of the MW distribution of biologically treated effluent related to different organic compounds and the MW range: a fraction of large MW (about 30000 daltons) corresponds to polysaccharides, proteins, and amino-sugars originating from cell components during biological processes and a fraction of small MW (about 250 daltons to 3000) includes humic (3000 daltons to about 800), building blocks (around 500 daltons), acids (about 200 daltons) and amphiphilic compounds (less than 200 daltons) (Huber et al., 1998). In that study, the building blocks refer to humic substance - hydrolysates (350-500 daltons) which are more acidic than fulvic acids and are intermediates in the degradation process of fulvic acids such as low MW organic acids.

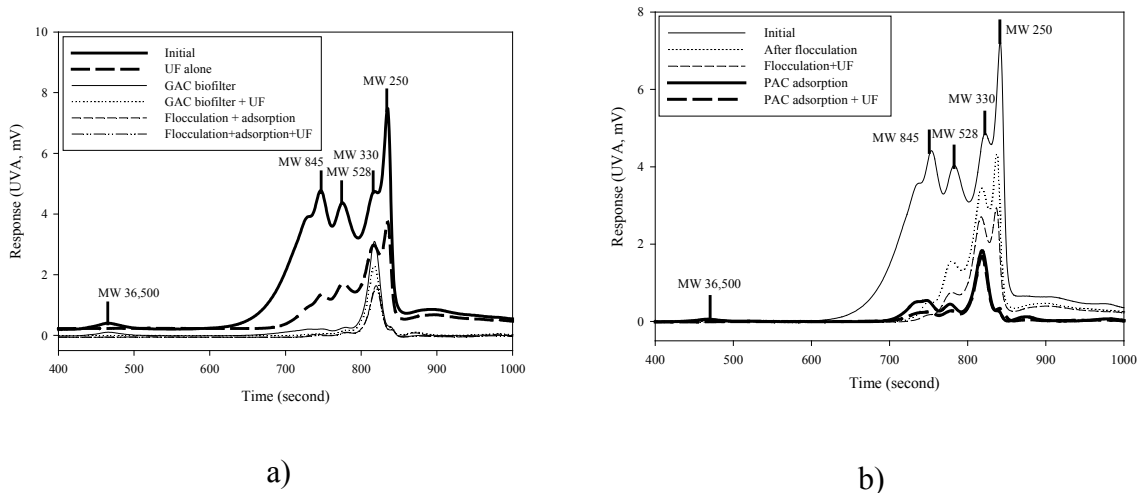


Figure 4.5 MW distribution of the soluble EfOM after different pretreatments in BTSE-S and in UF; a) UF alone, GAC biofilter, and Floc-Ads and b) after flocculation and PAC adsorption (membrane used = NTR 7410 UF with a MWCO of 17500, crossflow velocity = 0.5 m/s and transmembrane pressure = 300 kPa)

4.8 Experiments with NF Membrane

4.8.1 DOC Removal

NF alone and Floc-Ads had nearly the same efficiency in terms of DOC removal (Figure 4.6). The removal efficiency of NF is only slightly improved by a pretreatment of flocculation and adsorption.

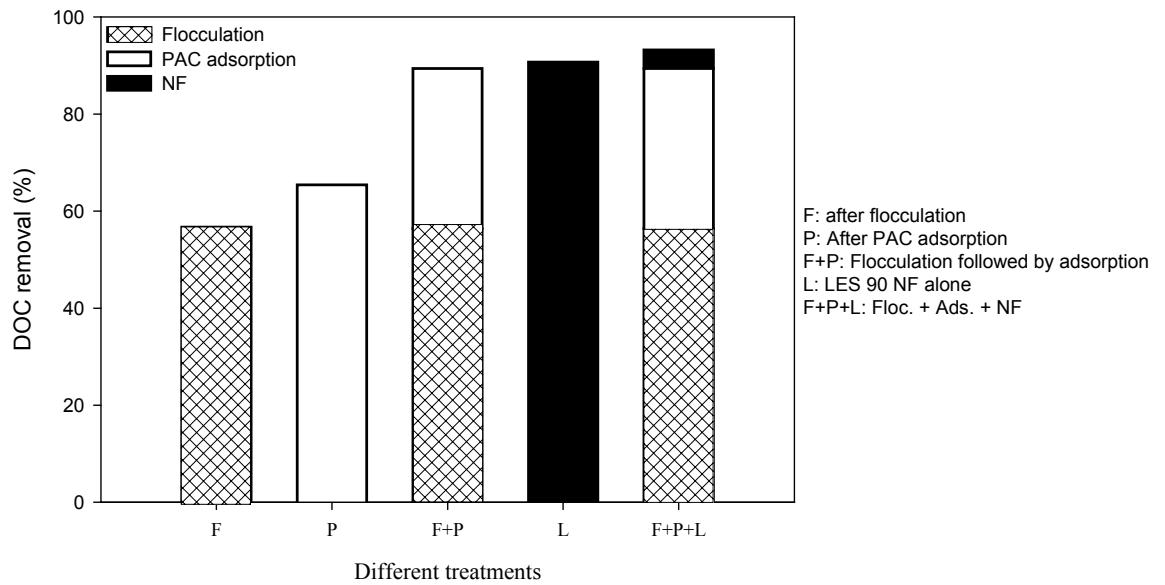


Figure 4.6 Organic removal by NF with and without pretreatment in BTSE-S (membrane used = LES 90, crossflow velocity = 0.5 m/s, transmembrane pressure = 300 kPa)

4.8.2 MW Distribution Analysis of NF Effluent

The results obtained (Figure 4.7) confirm that the NF membrane alone and with the pretreatment of flocculation/adsorption removed all the MW fractions except the soluble organic matter around 330 daltons, which is only partially removed.

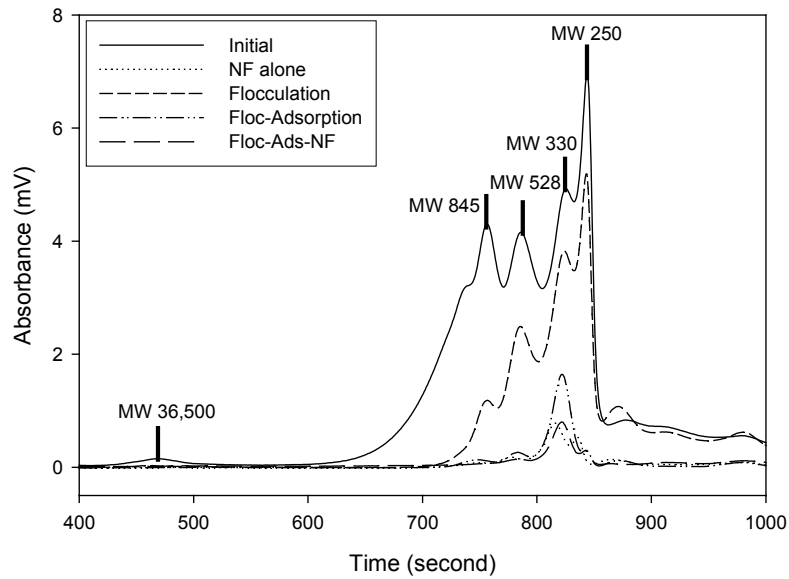


Figure 4.7 MW distribution of the NF effluent with different pretreatments (BTSE-S; LES 90 with a MWCO of 250 daltons; crossflow velocity = 0.5 m/s and transmembrane pressure = 300 kPa)

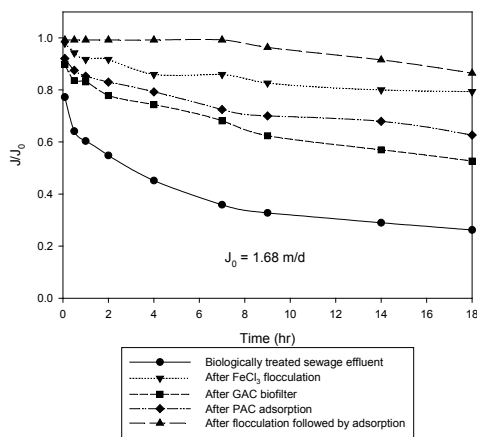
4.9 Comparison of UF and NF Performances

UF and NF performances in BTSE-S were compared in terms of organic removal efficiency (DOC) and normalized permeate flux (J/J_0). The flux decline is due to membrane fouling which depends on the composition of the feed and hydrodynamic conditions. In the present experiments, the hydrodynamic conditions were fixed to a pre-determined value and thus the flux decline is mainly related to the feed composition. The feed composition is influenced by the pretreatment. A fast decline of the permeate flux with time necessitates more frequent backwashing and chemical cleaning which decreases the membrane life and increases the cost of operation (Bruggen et al., 2003).

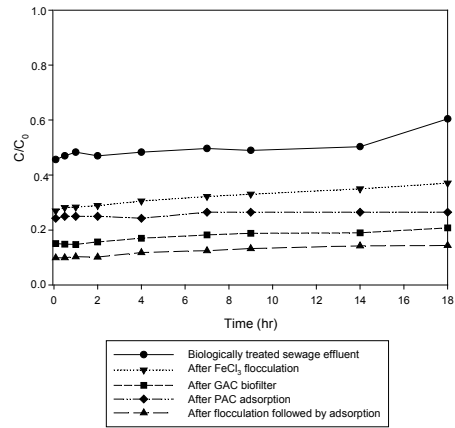
The operation of UF membranes improved with the pretreatment (Figure 4.8 (a)). For example, Floc-Ads as pretreatment resulted in an increase of the initial permeate flux from 32.9 L/m²·h without pretreatment to 108.4 L/m²·h. The UF NTR 7410 filtration without pretreatment resulted in rapid filtration flux decline with time. When large MW was removed by flocculation and Floc-Ads, the rate of flux decline was minimized. The PAC adsorption or GAC biofilter alone as pretreatment also significantly reduced the permeate flux decline to the extent of above pretreatments. This may be due to the MW

distribution of the feed to membranes after the pretreatment. The pretreatment of Floc-Ads led to practically no filtration flux decline and superior DOC removal (Figure 4.8 (b)).

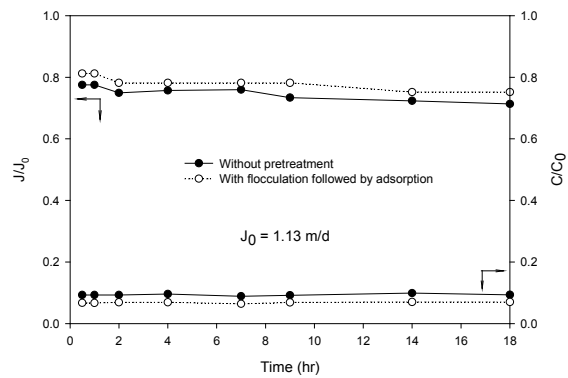
On the other hand, the direct application of NF without any pretreatment showed a similar filtration flux compared with that with pretreatment (Figure 4.8 (c)). The flux ratio (J/J_0) was only marginally higher with pretreatment. J_0 is the pure water permeate flux. The removal efficiency was also similar with and without pretreatment (Figure 4.8 (c)). From this result it can therefore be concluded that in the case of BTSE, NF membranes may be employed for polishing BTSE without any pretreatment. However, the permeate flux of NF is relatively small compared with UF (permeate flux = 22.9 L/m²·h with a transmembrane pressure of 300 kPa).



a) UF NTR 7410 permeate flux



b) UF NTR 7410 DOC ratio



c) NF LES 90

Figure 4.8 Temporal variation of filtration flux and DOC ratio with and without pretreatment in BTSE-S (UF NTR 7410, $J_0 = 3.01$ m/d at 300 kPa; crossflow velocity = 0.5 m/s; NF LES 90, $J_0 = 0.77$ m/d at 300 kPa; crossflow velocity = 0.5 m/s; C and C_0 = the effluent and influent DOC values; J_0 = pure water permeate flux)

4.10 Membrane Characterization with/without Pretreatment

4.10.1 Effect of Contact Angle

A higher contact angle indicates a higher hydrophobicity of the membrane surface (Chun et al., 20002; Weis et al., 2003; Levine et al., 1985). After the membrane operation with different pretreatments, the contact angle of the UF surface was measured. The following order was observed: without any pretreatment < flocculation as pretreatment < PAC adsorption as pretreatment < GAC biofilter as pretreatment <

Floc-Ads as pretreatment (Table 4.5). The contact angle of the UF membrane after undergoing filtration of BTSE-S decreased from 69° (clean membrane) to 30° (for membrane operated without pretreatment). The contact angle of the membrane with pretreated BTSE (flocculation followed by adsorption) was 64°, which is almost the same as that of the clean membrane. This illustrates that the pretreatment with Floc-Ads can preserve the nature of membrane hydrophobicity on the membrane surface. The fouled membrane (by BTSE without any pretreatment) had a lower contact angle because the foulants constitute of HL organic matter such as polysaccharides, urea, etc., which are the extracellular enzyme of microorganisms in BTSE-S.

The clean NF membranes exhibited different contact angles as compared with the UF membrane. This difference may be due to the material of the membrane. The contact angles between clean and fouled membranes were almost similar, suggesting that foulants are essentially HL EfOM such as polysaccharides in the BTSE-S.

Table 4.5 The contact angle of the clean and fouled UF membrane surfaces

	Clean membrane (°)	Membrane without pretreatment (°)	Flocculation + membrane (°)	GAC biofilter + membrane (°)	PAC adsorption + membrane (°)	Floc-Ads + membrane (°)
Contact angle	69	30	39	54	50	64

Table 4.6 The effect of the contact angle on different membrane surfaces

	Clean membrane (°)	Without pre- treatment (°)	After Floc-Ads (°)
NTR 729HF	28	27	26
LES 90	54	49	49
LF 10	50	50	44

4.10.2 Zeta Potential

The zeta potential was also measured for the UF membranes after different pretreatments (Figure 4.9). The zeta potential on the membrane surfaces (with different pretreatments) was higher than that on the clean membrane. The zeta potential increased up to -18 mV after the pretreatment of flocculation. Chun et al. (2002) reported that the growth of the cake layer had been developed with increase in the feed concentration. This weakened the electrokinetic flow owing to a lower permeate flux, thus leading to a decrease in the membrane zeta potential. During FeCl_3 flocculation, the ferric ion may have been adsorbed on the membrane surface. This would have caused increase in zeta potential. These results show a similar effect with Peeters's observation (Peeters et al., 1999). As the concentrations of CaCl_2 and NaCl increased, the zeta potential showed higher values on the nanofilter membranes. Soffer et al. (2002) also found that the zeta potential values of all the fouled membranes were less negative. In the present study this trend was also observed.

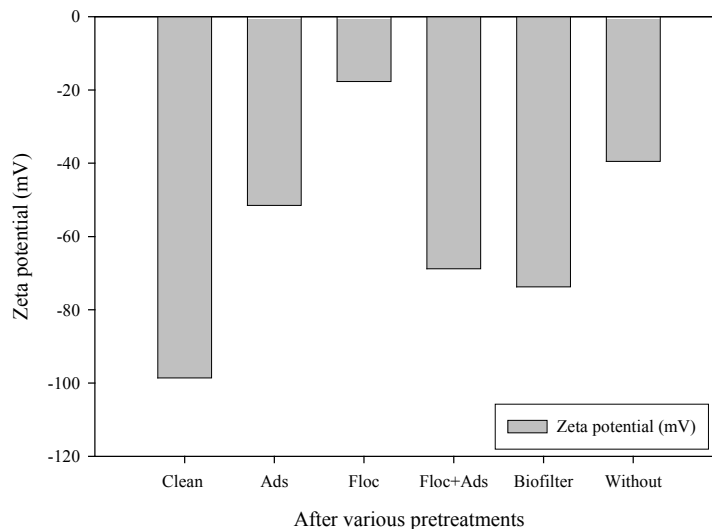


Figure 4.9 The effect of pretreatments on the zeta potential of UF membrane

4.10.3 ATR-FTIR Spectroscopy Results for Different Pretreatments

The clean and fouled membrane surfaces were analyzed for functional groups using attenuated total reflection-Fourier transform infrared spectroscopy (ATR-FTIR) (Figure 4.10). A difference in IR spectra between clean and fouled membranes was observed due to the adsorption phenomena of the organic foulants onto the membrane surfaces (Cho, 1998). The peaks observed at wave numbers of 1540 1/cm and 1640 1/cm are

obtained to be due to the functional group of aromatic carbons (Levine et al., 1985). The peaks between 1040 1/cm and 1240 1/cm show the presence of C-O bonds of ethers, carboxylic acids, and polysaccharides. Cho (1998) identified that possible foulants on the membranes during the operation with BTSE at 1040, 1540, and 1640 1/cm were humic fraction and polysaccharides. In this study, the functional groups on the clean NTR 7410 membrane surface were investigated. The main groups observed were: i) 1625 - 1590 1/cm: aromatic group (ring bond), ii) 1525 - 1470 1/cm: aromatic (ring bond), iii) 1465 - 1430 1/cm: aromatic (ring bond), iv) 1415 - 1390 1/cm: sulfur (CO-SO₂-OC), v) 1375 - 1335 1/cm: sulfur (C-SO₂-OC), vi) 1340 - 1290 1/cm: sulfur (C-SO₂-C), vii) 1300 - 1230 1/cm: sulfur (N=S=O), viii) 1200 - 1050 1/cm: sulfur (C-SO₂-C), ix) 1165 - 1120 1/cm: sulfur (C-SO₂-C), x) 1125 - 1090 1/cm: ether (C-O-C), xi) 1075 - 1000 1/cm: alcohol (R-CH₂-OH), and xii) 950 - 815 1/cm: ether (C-O-C). As can be seen in Figure 4.10, the FTIR absorbance intensity without any pretreatment was very low with a lot of noise. The peaks with very low absorbance intensity on the surface are too difficult to be analyzed for functional groups (Table 4.7). The peaks obtained for membrane surface with different pretreatments were compared with the clean membrane surface. After a pretreatment of PAC adsorption, a peak at 850 - 775 1/cm (ether: C-O-C) was observed. After GAC biofilter pretreatment, there were many overlapped peaks observed with strong intensity. The common feature with these pretreatments was a peak at 1721 - 1626 (not defined) and 1585 - 1535 1/cm (urea: R-NH-CO-NH-R). On the other hand, the peaks observed for the membranes with Floc-Ads as pretreatment were similar to the clean one.

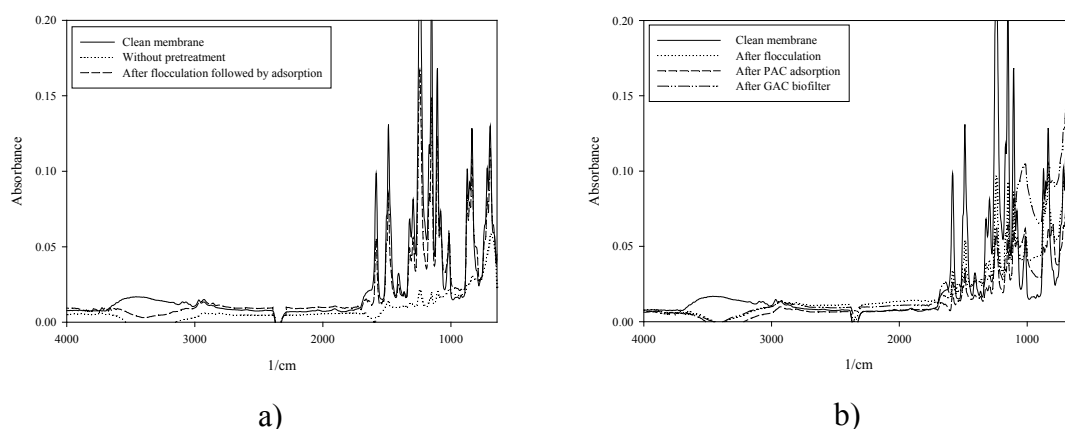


Figure 4.10 FTIR spectra (a) for clean membrane and for fouled membranes without any pretreatment and after a pretreatment of Floc-Ads (b) for membranes after pretreatments of flocculation, PAC adsorption and GAC biofilter (NTR 7410 membrane with BTSE-S)

Table 4.7 Functional groups obtained by IR spectra (on the fouled membrane surfaces)

Pretreatment	Wave number (1/cm)	Functional groups
Without pretreatment		ND*
PAC adsorption	850 – 775	Ether (C-O-C)
GAC biofilter	1721 – 1626	Not defined
	1585 – 1535	Urea (R-NH-CO-NH-R)
Flocculation		ND*
Floc-Ads		ND*

* ND: not detected.

Figure 4.11 shows the functional groups on the fouled membrane surfaces. For the NTR 729HF membrane, only one peak at 790 to 840 1/cm was found on the surface of the fouled membranes (without any pre-treatment). This may be due to the functional group of alkene. For the LES 90 membrane, peaks from 1547 to 1590 1/cm were observed (without any pretreatment). These peaks correspond to urea functional group. LF 10 membrane showed peaks at 1664 – 1670 1/cm (ketone functional group). The common point without any pretreatment was the small intensity of absorbance. The clean and fouled membranes with pretreated wastewater effluent showed similar peaks

at similar intensity. This indicates that most of the organic substances responsible for membrane fouling can successfully removed by pretreatment.

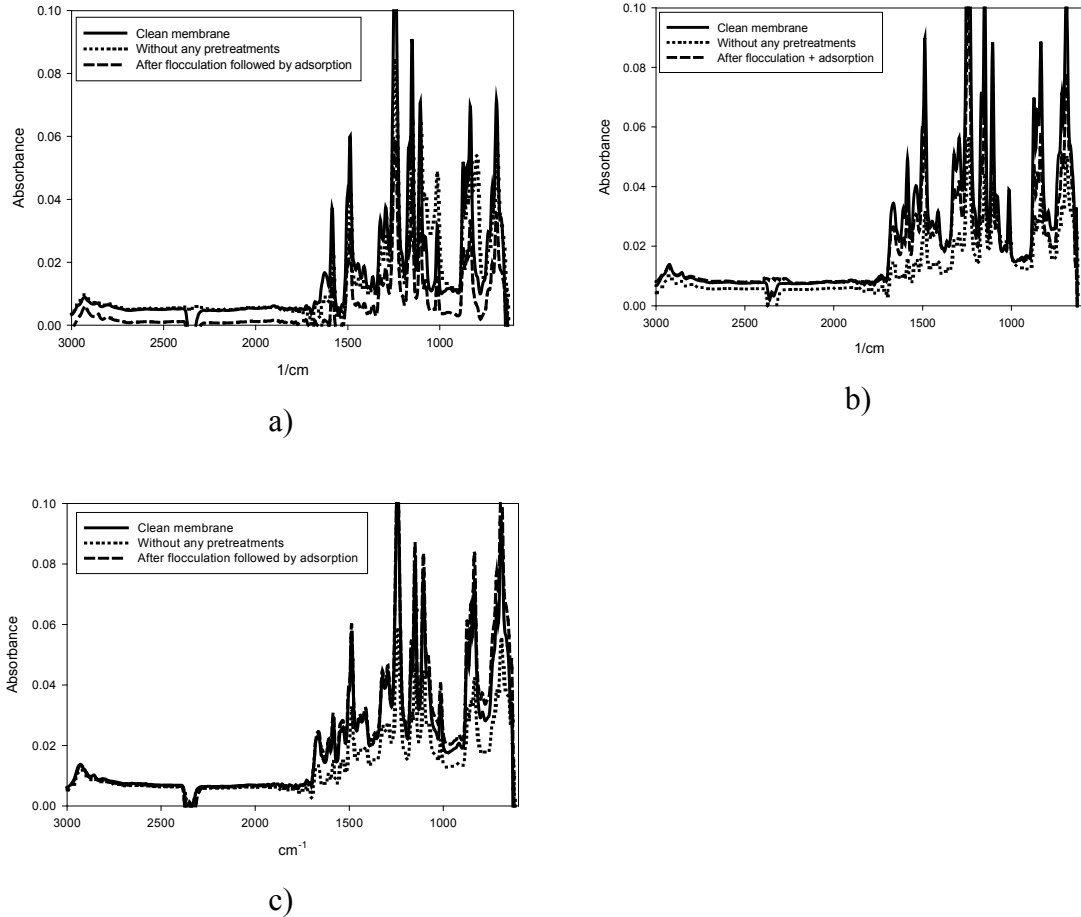


Figure 4.11 FTIR spectra with clean membrane, without any pretreatment, and after Floc-Ads (a) NTR 729HF membrane, (b) LES 90 membrane, and (c) LF 10 membrane with BTSE-S

4.10.4 SEM Analysis of Clean and Fouled Membranes

Figure 4.12 shows the SEM images of the fouled membranes after 18-hour filtration. The membrane experienced a severe fouling when BTSE-S was filtered directly through the membrane without any pretreatment. The SEM image of the membrane cross-section for this case showed a fouling thickness of 4.3 μm (Figure 4.12 (a)). When a pretreatment of flocculation was used prior to the membrane filtration, the thickness of fouling layer was found to be much less (0.13 μm) (Figure 4.12 (b)). The fouling layer thickness from the membrane surface was 0.26 μm after the pretreatment of PAC adsorption (Figure 4.12 (c)). After the pretreatment by GAC biofilter, the

fouling thickness was higher $0.52\ \mu\text{m}$ (Figure 4.12 (d)). On the other hand, a membrane with the pretreatment of Floc-Ads showed almost similar images as that of the clean membrane with a negligible fouling layer.

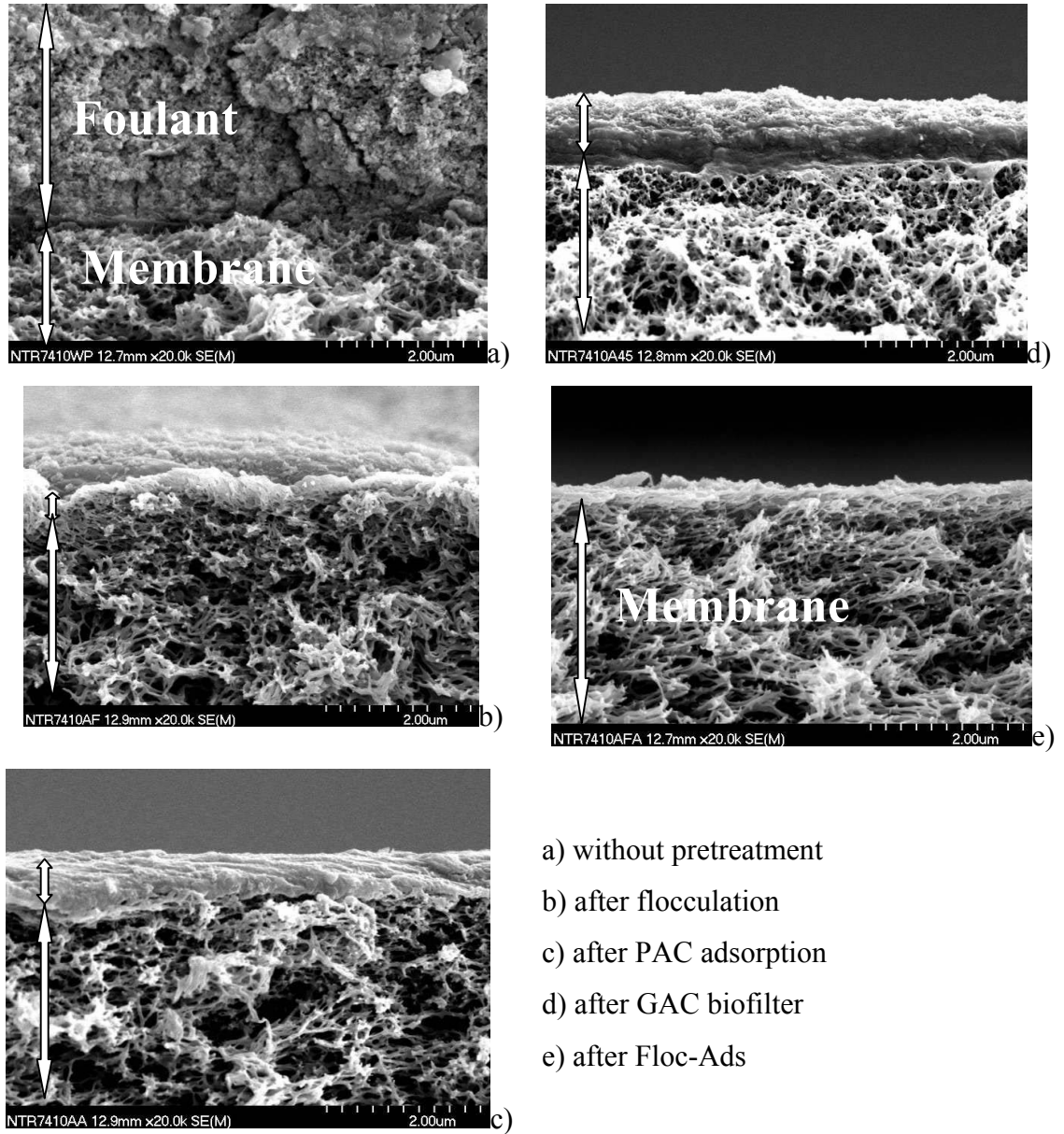


Figure 4.12 Cross section of beam energies on filed FE-SEM images of NTR 7410 membrane after 18-hour filtration (working distance of 12 mm and magnification of 20,000)

4.11 Characterization of Foulants on Membrane Surfaces

4.11.1 DOC Concentration of the Foulant

The adsorbed EfOM foulants of the fouled membrane surfaces were analyzed after washing the membranes with 0.1 N NaOH solution. After the pretreatment of Floc-Ads, the UF gave low foulant concentration (Figure 4.13 (a)). The trend of foulant concentration was strongly proportional to the flux decline on the UF membrane. On the other hand, the foulant concentration on the NF surface was much lower than that of UF (Figure 4.13 (b)).

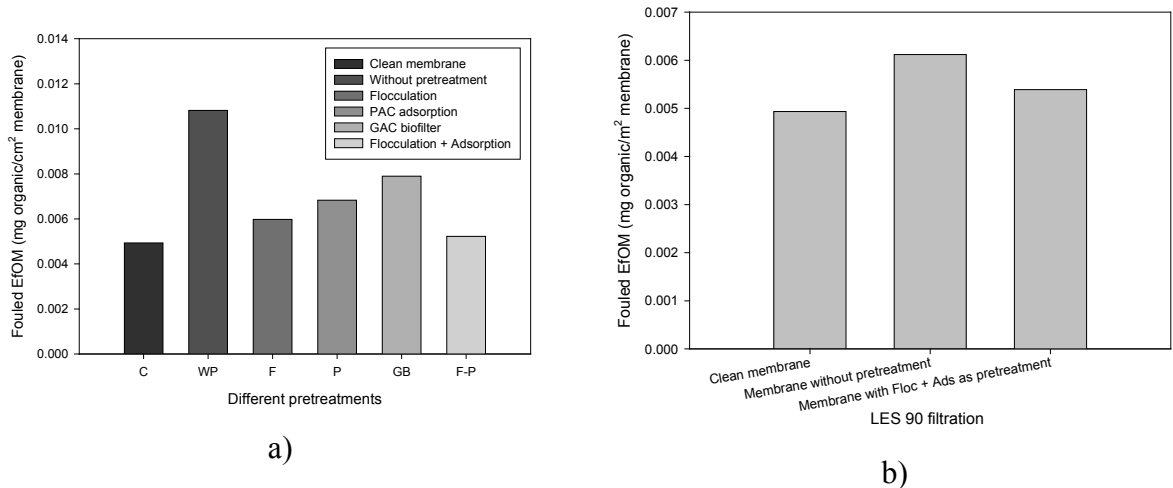


Figure 4.13 DOC concentration of adsorbed EfOM on the fouled membrane surfaces after different pretreatments (a) EfOM concentration adsorbed on the UF membrane and b) on the NF membrane)

Tables 4.8 and 4.9 show the number-averaged and weight-averaged MW values of the foulants on different membranes, with and without pretreatment. The pretreatment of flocculation and/or adsorption reduced not only the amount of foulants on the membrane but also the MW of the foulants. The weight-averaged MW of foulants shifted from 675 daltons (without pretreatment) down to 400 – 300 (with pretreatment).

Table 4.8 MW values of foulants on the UF membranes (initial BTSE-S - number-averaged (median value) MW (M_n^*): 759 daltons, weight-averaged MW (M_w^{**}): 1158 daltons and polydispersivity ($P^{***} = M_w/M_n$): 1.53)

UF	Permeate (daltons)			Foulants (daltons)		
	M_n^*	M_w^{**}	P^{***}	M_n^*	M_w^{**}	P^{***}
UF alone	495	675	1.36	415	513	1.24
Flocculation + UF	355	404	1.14	403	415	1.03
PAC adsorption + UF	330	379	1.15	384	399	1.04
GAC biofilter + UF	324	327	1.01	375	387	1.03
Floc-Ads + UF	301	314	1.04	348	351	1.01

Table 4.9 MW values of foulants on the NF membrane (initial number-averaged (median) MW (M_n^*): 759 daltons, weight-averaged MW (M_w^{**}): 1158 daltons and polydispersivity ($P^{***} = M_w/M_n$): 1.53)

NF	Permeate (daltons)			Foulants (daltons)		
	M_n^*	M_w^{**}	P^{***}	M_n^*	M_w^{**}	P^{***}
NF alone	392	478	1.22	189	192	1.01
Floc. + Ads. + NF	302	310	1.03	182	183	1.01

4.11.2 Foulant Interpretation

The main groups of macromolecules in wastewater are polysaccharides, proteins, lipids and nucleic acids (Kameya et al., 1995). EfOM smaller than 10^3 daltons includes carbohydrates, amino acids, vitamins and chlorophylls. Persistent chemical compounds found in BTSE such as dichloro-diphenyl-trichloroethane (DDT), polychlorinated biphenyl (PCB) and other toxic substances of public health significance are also low molecular weight compounds (Stull et al., 1996; Pempkowiak and Obarska-Pempkowiak, 2002). Thus, as the foulants on the UF and NF membrane surfaces have been found to be in the range of 183-513 daltons, these fouling processes may be assumed to be due to adsorption of recalcitrant matter, carbohydrates, amino acids and fatty acids (Levine et al., 1985). Although the MWCO of UF is large (17500 MWCO), the foulants are small in size (386 daltons). This may be due to the interaction between EfOM and membrane pores. The foulant MW (d_p) to membrane MWCO (d_m) corresponds to a ratio of only

4.3 (where d_p : particle diameter and d_m : membrane pore diameter) because a 17500 MWCO of UF corresponds to a pore size of about 1.3 nm and 386 daltons MW corresponds to 0.3 nm. With such a ratio, strong interaction with the walls of the pores can be expected (Causserand et al., 2004). In this study, the samples were filtered by 0.45 μm membranes before DOC measurement, whereas the studies claiming that the main foulants during UF and NF are humic and fulvic acids (4700 – 30400 daltons) did not use prefiltration with 0.45 μm membranes (Perminova et al., 2003).

4.12 Concluding Remarks

In this chapter, a detailed EfOM and membrane characterization with UF and NF membranes has been undertaken with and without pretreatment. The influence of different pretreatments has been investigated in terms of MW distribution, contact angle, zeta potential, ATR-FTIR, SEM, flux decline, and DOC removal. The foulants were then interpreted with weight-averaged MW. The results led to the following conclusions:

1. The organic colloidal portion in the biologically treated sewage effluent was removed up to 65% through the pretreatment of flocculation. PAC adsorption removed a relatively small amount of organic colloids (less than 30%).
2. A significant amount of HP and HL fractions of organic matter can be removed by incorporating flocculation and adsorption pretreatments. The flocculation and adsorption in BTSE-W removed 51.6% and 58.7% of HL and 68.5% and 71.4% of HP organic fractions, respectively.
3. After the flocculation pretreatment, the removal of both large and small MW organic matter was observed. After the PAC adsorption pretreatment, the majority of small MW organics was removed.
4. The Floc-Ads pretreatment resulted in the highest flux improvement with a DOC removal of more than 90%.

5. The contact angle on the fouled membrane was lower than that for the clean membrane. This could be due to the fact that the foulants may consist of hydrophilic organic matter such as polysaccharides and urea which may be from the extracellular enzyme of microorganisms in BTSE.

6. The zeta potential decreased from -98 mV up to -18 mV after the flocculation pretreatment. It may be due to the adsorption of ferric ion on the membrane surface.

7. The peaks observed on the fouled UF membrane are ether (C-O-C) and urea (R-NH-CO-NH-R). The detected functional groups in the deposit on the NF membrane without any pretreatment were alkene (NTR 729HF), urea (LES 90), keton functional groups (LF 10). The functional groups responsible for membrane fouling were removed by the various pretreatments used.

8. The highest EfOM concentration on the fouled membranes was observed to be 0.011 mg EfOM/cm² membrane surface on the UF membrane. This was with a membrane with no pretreatment. The flocculation pretreatment followed by adsorption led to the lowest fouling concentration (0.0052 mg EfOM/cm² membrane surface). This 0.0052 mg is similar to that for clean membranes. The concentration of organic matter on the membranes decreased from $6.372 * 10^{-3}$ (NTR 729HF) and $4.979 * 10^{-3}$ (LF 10) mg EfOM/cm² on the membrane with the pretreatment to $5.671 * 10^{-3}$ (NTR 729HF) and $4.940 * 10^{-3}$ (LF 10) mg EfOM/cm² of membrane.

9. The foulants on the UF and NF membrane surfaces have been found to be in the range of 183-513 daltons. The observed fouling assumedly is due to the adsorption of recalcitrant matter, carbohydrates, amino acids and fatty acids.

CHAPTER 5



University of Technology, Sydney
Faculty of Engineering

EFFECT OF SEMI FLOCCULATION AND SEMI ADSORPTION AS PRETREATMENT TO ULTRAFILTRATION

5.1 Introduction

UF is an effective process for the removal of colloidal matter, macromolecules, pathogens, etc., however, it removes only a part of dissolved organic matter. Further, membrane fouling is the major obstacle in UF that causes flux decline. Howe and Clark (2003) reported that particulate matter (larger than 0.45 μm) was relatively unimportant in fouling compared with dissolved matter in UF. Dissolved organic matter ranging from 3 - 20 nm in diameter, appears to be important membrane foulants (Zhang and Song, 2000).

The presence of organic pollutant in water and wastewater has been the cause of public concerns in past decades due to their potential health hazard (Wang et al., 2001; Imai et al., 2002). Effluent organic matter (EfOM) in the biologically treated wastewater consists of mixed particulates and soluble substance, which is combined with natural organic matter (NOM) from drinking water and soluble microbial product (SMP) from biological treatment. EfOM can thus be broadly classified into three different groups by their origins:

- (i) refractory NOM derived from drinking water sources,
- (ii) synthetic organic compounds produced during domestic use and disinfection by-products (DBPs) generated during disinfection processes of water and wastewater treatment and
- (iii) SMP derived during biological processes of wastewater treatment (Drewes and Fox, 1999).

Many researchers suggest that flocculation is one of the most effective pretreatment methods to remove EfOM (Abdessemed and Nezzal, 2002; Abdessemed et al., 2002; Shon et al., 2004; Kim et al., 2002). Shon et al. (2004) showed that FeCl_3 flocculation removed 68% of EfOM (in terms of DOC) from the biologically treated wastewater. The majority of organics removed were those with large MW. Al-Malack and Anderson (1996) determined the optimum coagulation conditions for wastewater, 69 mg-Fe/L FeCl_3 at a pH of 9. The COD removal with this optimum dose of FeCl_3 was 99.3%. According to the results of Aguiar et al. (1996), the optimum dose of coagulant was 2.1 ± 0.2 mg Fe per mg of total organic carbon (TOC).

PAC adsorption has been widely studied as a pretreatment to UF. The PAC adsorption was found to remove 60 – 75% of DOC from BTSE (Arana et al., 2002;

Shon et al., 2004). Lin et al. (1999) studied the use of PAC adsorption at a dose up to 400 mg/L as pretreatment to remove humic substances of 20 mg/L in concentration. In their study, the PAC was ineffective in removing the MW fractions of less than 300 or greater than 17,000 daltons. The flux decline in UF for the PAC-treated streams was worse than that without pre-adsorption.

Many researchers have concluded that FeCl_3 flocculation followed by PAC adsorption (Floc-Ads) is a very effective pretreatment to membrane filtration (Mameri et al., 1996). Shon et al. (2004) also observed that Floc-Ads removed 89% of DOC from BTSE. The FeCl_3 flocculation process can be used to aggregate colloids and suspended solids in the size range of 0.1 – 10 μm . A small portion of small MW organic matter in the wastewater effluent can also be removed by complexation with ferric hydroxides. PAC adsorption can successfully remove the majority of small MW organic matter such as refractory organic matter, hydrophobic organic matter in the range of 200 – 3500 daltons and a small portion of the large MW organic matter. The pretreatment of Floc-Ads can therefore remove the majority of dissolved organic matter in the wastewater.

Even though the effectiveness of different pretreatments is helpful, it may not be economic to use large doses of flocculants and adsorbents. Larger chemical doses will also lead to larger quantity of chemical sludge. Thus, it is advisable to use as small doses of flocculants and adsorbents as possible to achieve significant organic removal that can minimize membrane fouling in the post treatment of membrane filtration.

In this chapter, a pretreatment of flocculation with reduced doses of FeCl_3 and adsorption with reduced doses of PAC was investigated in terms of flux decline of UF (used as post treatment) in synthetic wastewater. The characteristics of the synthetic wastewater are presented in Table 3.1 of Chapter 3. Different MW ranges of organic matter removed by different treatments have also been studied. An attempt was made to optimize the pretreatment requirement based on the results of organic matter removal and effective MW.

5.2 Removal of DOC from Synthetic Wastewater by Different Treatments

The removal efficiency of synthetic organic matter (SOM) by the different treatment methods such as powdered activated carbon (PAC) adsorption, ferric chloride (FeCl_3) flocculation and Floc-Ads was first measured in terms of DOC. As can be seen in Figure 5.1, the DOC removal from synthetic wastewater by the pretreatments of adsorption, flocculation and Floc-Ads was 57.1%, 78.6% and 92%, respectively. The DOC removal by adsorption and flocculation showed removal of different trends with synthetic and real wastewater and this may be due to the difference of MW size distribution. When a membrane alone was used, the removal was 71.2% (NTR 7410), 95.8% (NTR 729HF), 95.9% (LES 90), 95.9% (LF 10), suggesting that the removal depends on the molecular weight cut-off (MWCO) of the membranes. As the filtration was combined with different pretreatments, the pretreatment of Floc-Ads resulted in best results. UF (NTR 7410) increased the removal from 71.2% without pretreatment to 91.8% with pretreatment, whereas NF (NTR 729HF, LES90 and LF 10) increased only by 2-3%. This implies that UF is more efficient with pretreatment than NF in terms of DOC removal. The pore of NF is too small to improve further the DOC removal by pretreatment.

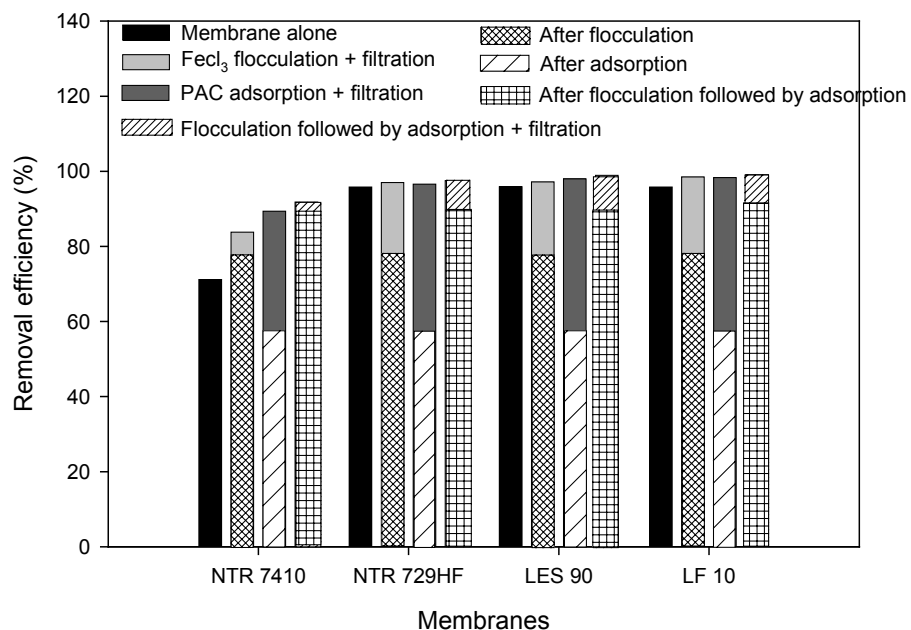


Figure 5.1 DOC removal of different membranes with and without pretreatment

5.3 Effect of Semi Flocculation

5.3.1 Removal of DOC by Semi FeCl₃ Flocculation

The removal of synthetic organic matter (SOM) from the synthetic wastewater by ferric chloride (FeCl₃) flocculation and by the post treatment of UF was investigated in terms of DOC removal (Figure 5.2). DOC removal was highest (78.2%) with the FeCl₃ flocculation at a dose of 23 mg-Fe/L. The optimum FeCl₃ dose was found to be 23 mg-Fe/L from the Jar test experiments. The experiments were also conducted with reduced concentrations of FeCl₃ (semi optimum doses) followed by UF in order to study the effect of semi flocculation on DOC removal. For example, the DOC removal from wastewater was 87.8% with pre-flocculation (23 mg-Fe/L of FeCl₃) and post UF application. The removal efficiency decreased with smaller FeCl₃ doses. Although the semi flocculation (with reduced FeCl₃ doses) led to less pretreatment removal efficiency, the post treatment of UF compensated the total net removal i.e. 82.8% (with 14 mg-Fe /L of FeCl₃) and 82.2% (with 7 mg-Fe/L of FeCl₃). In other words, the post treatment of UF after 23 mg-Fe/L FeCl₃ flocculation removed only 9.6% of additional DOC, whereas that after 7 mg-Fe/L FeCl₃ flocculation removed 48.2% of additional DOC. The semi flocculation as a pretreatment is therefore responsible for the majority of organic removal to UF.

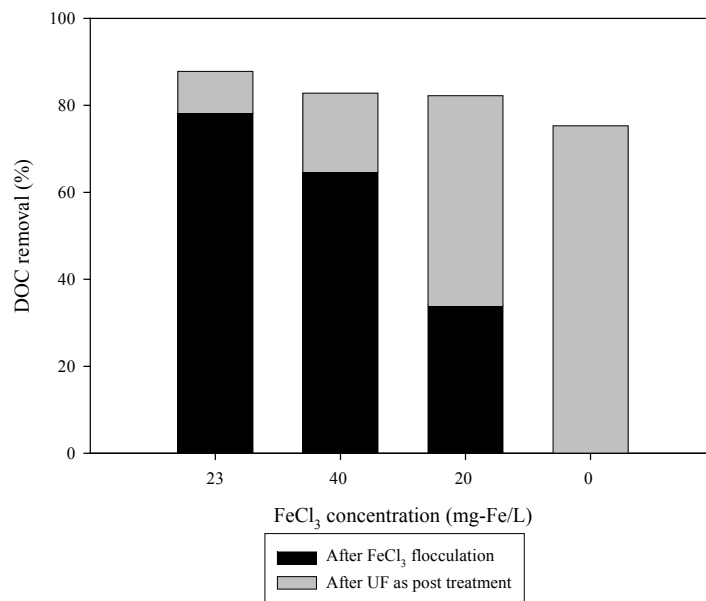


Figure 5.2 DOC removal by semi flocculation followed by UF

5.3.2 Flux Decline of UF with Pretreated Wastewater

The flux decline of UF in treating synthetic wastewater was studied in terms of normalized permeate flux (J/J_0). It was considered both with and without pretreatment of FeCl_3 flocculation at different doses (Figure 5.3). The flux decline (J/J_0) with no pretreatment was 38% after 6 hours of UF operation. After the pretreatment of flocculation with an optimum dose of FeCl_3 (23 mg-Fe/L), the UF did not experience any flux decline. This may be due to the removal of the majority of SOM by flocculation and complexation (Shon et al., 2004a). However, the pre-flocculation with a semi optimum dose of FeCl_3 led to significant flux decline, for example, a pre-flocculation with 7 mg-Fe/L of FeCl_3 led to a flux decline (J/J_0) in the post treatment of UF of 35% in 6 hours. This indicates that the flocculant dose should be sufficient to avoid or minimize the flux decline.

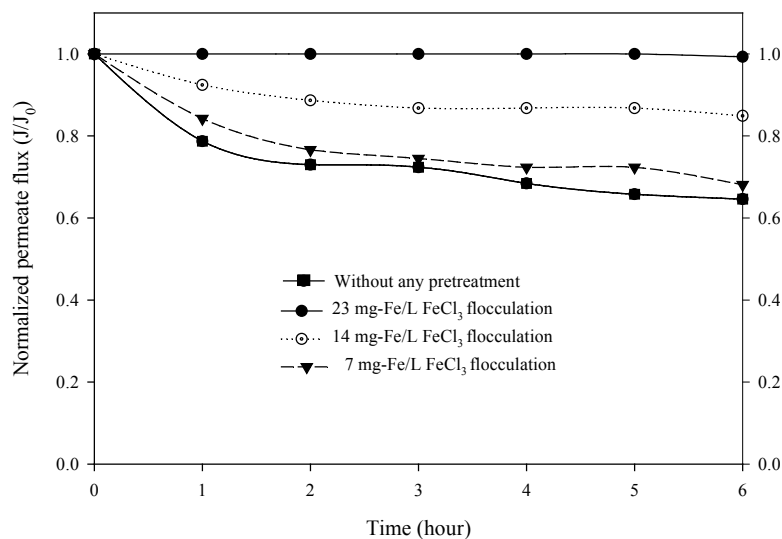


Figure 5.3 Temporal variation of filtration flux of UF after a pretreatment of flocculation at different FeCl_3 doses (NTR 7410 UF membranes, $J_0 = 1.84$ m/d at 300 kPa; crossflow velocity = 0.5 m/s; MWCO of 17,500 daltons; Reynold's number: 735.5; shear stress: 5.33 Pa)

5.3.3 Molecular Weight (MW) Distribution

Synthetic wastewater has a number of known compounds at a known concentration and hence, the MW distribution of each component in the synthetic wastewater was first analyzed (Figure 5.4). The MW of the mixed synthetic wastewater ranged from 290 daltons to about 34120 with the highest fraction between 940 – 1200 daltons. Although sodium lignin sulfonate and tannic acid showed peaks at 12120 and 6340 daltons respectively, the corresponding peaks were not found in the mixed synthetic wastewater (Figure 5.4 (c)). This may be due to aggregation between SOM and inorganic and/or organic compounds in the synthetic wastewater.

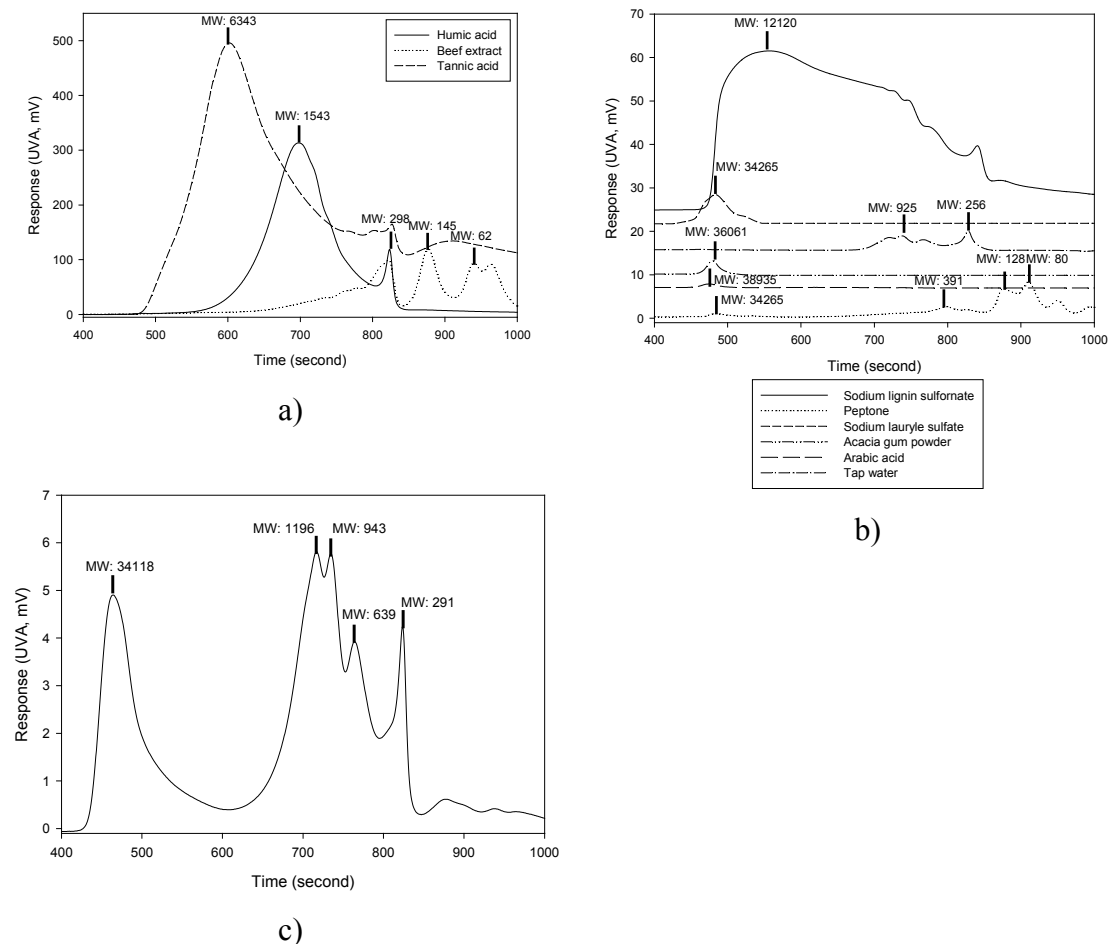
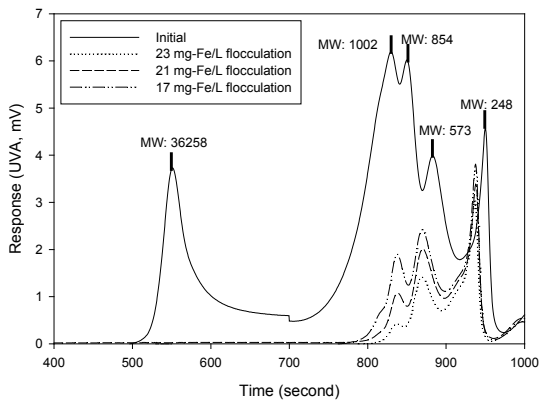


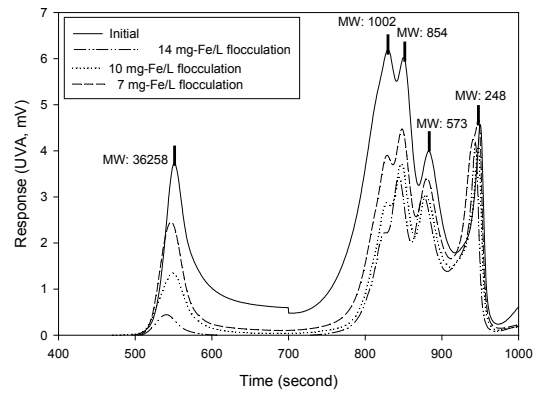
Figure 5.4 MW distribution of SOM in the synthetic wastewater (a), b): individual components in the wastewater; c) wastewater (with all compounds mixed together)

Figure 5.5 describes the MW distribution of UF effluent without any pretreatment and with pre-flocculation (using FeCl_3). It should be noted that the settled flocs were

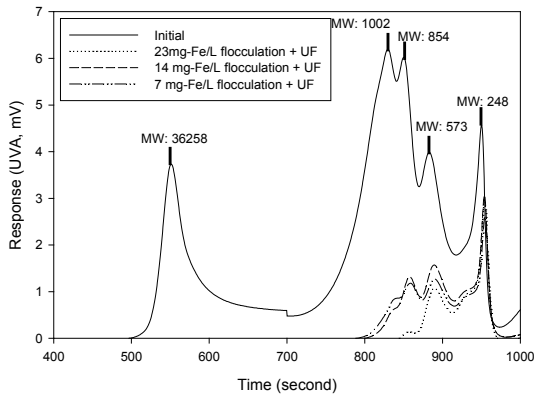
removed after FeCl_3 flocculation and only the supernatant underwent UF. Flocculation with larger doses (75% - 100% of the optimum dose) from 17 mg-Fe/L to 23 mg-Fe/L FeCl_3 removed practically all the large MW SOM such as tannic acid, sodium lignin sulfonate, sodium lauryle sulfate and arabic acid. A FeCl_3 dose of 14 mg-Fe/L removed the majority of large MW SOM, but not all of them. Further, this pre-flocculation was also helpful in removing some of the small MW compounds (573 - 1002 daltons) such as peptone, beef extract and humic acid. However, the smallest MW range of compounds in the range of 248 daltons could not be removed by flocculation. A FeCl_3 dose of 14 mg-Fe/L or less did not remove both the large MW compounds and the majority of small MW compounds. The post treatment of UF with the pretreatment of flocculation removed practically all the organic compounds of more than 1000 daltons. Thus, the large MW SOM remaining in the synthetic wastewater may have been responsible for the flux decline. Zhang and Song (2000) found that the fouling by large nano-size particles was more severe than that with small particles. The indicative relationship between particle size and MW is presented in Table 5.1. Perminova et al. (2003) observed that large molecules (humic and fulvic acids) in the range of 4700-30000 daltons were responsible for the fouling of membranes by organic matter. Howe and Clark (2003) found that the dissolved organic matter, which was smaller than about 3 nm, caused only minimum fouling.



a)



b)



c)

Figure 5.5 MW distribution in the flocculated effluent ($J_0 = 1.84$ m/d at 300 kPa; crossflow velocity = 0.5 m/s; MWCO = 17,500 daltons; Reynold's number.: 735.5; shear stress: 5.33 Pa; a) MW distribution of SOM with higher doses of FeCl_3 (17 - 23 mg-Fe/L); b) with FeCl_3 of lower doses (7 - 14 mg-Fe/L flocculation); c) flocculation followed by UF

Table 5.1 Relationship between the size in nm and MW in daltons

Size (daltons)	Size (nm)
500*	0.394
1,000*	0.496
5,000*	0.846
7,000*	0.946
10,000*	1.065
20,000*	1.341
100,000 [#]	10.0
500,000 [#]	50.0

* The equation used to compute the size is: $Size(\mu m) = \frac{0.0001 * (MW)^{0.3321}}{2}$

[#] Adapted from Mulder (1996)

Table 5.2 presents the weight-averaged MW of the compounds in the supernatant after different FeCl₃ doses. The weight-averaged MW value of the influent was 29760 daltons, which is similar to the effluent after flocculation with 7 mg-Fe/L (around 29590 daltons).

Table 5.2 Weight-averaged MW values of the effluent samples after pretreatment (weight-averaged MW of initial = 29760 daltons)

	FeCl ₃ concentration (mg-Fe/L)					
	23	21	17	14	10	7
MW	520	580	690	26230	29320	29590

All units: daltons

A correlation between the amount of FeCl₃ dose and the weight-averaged MW is presented in Figure 5.6. The deviant crease circle shows that the pretreatment of flocculation with reduced FeCl₃ dose (less than the optimum dose) is possible as an adequate pretreatment to minimize the flux decline and to obtain high DOC removal. In the present study, a dose of 17 mg-Fe/L of FeCl₃ was sufficient to run the UF with no (or minimum) flux decline and high DOC removal. It should be noted that the above finding and the quantitative values are applicable only for the synthetic wastewater

used, since wastewater characteristics differ from geographic area to area and from season to season. Experiments need to be conducted with particular wastewater at the time of operation to determine a suitable dose of FeCl_3 .

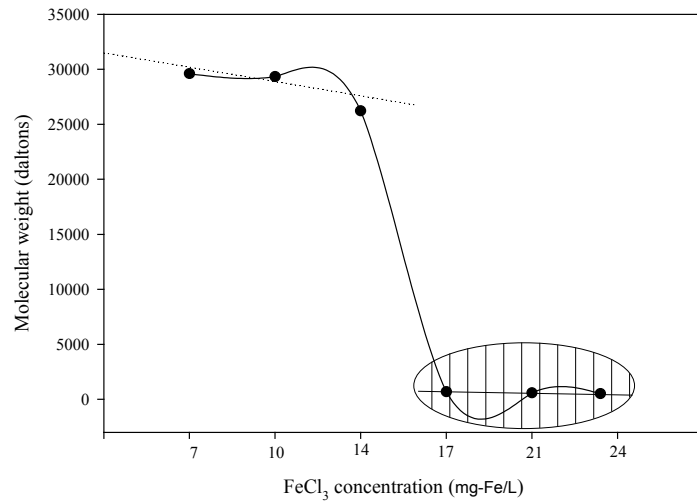


Figure 5.6 Correlation between the FeCl_3 concentrations and the corresponding weight-averaged MW values in the flocculated effluent.

5.3.4 Effect of Semi Flocculation Followed by Semi Adsorption (SFSA)

5.3.4.1 Removal of DOC by SFSA

The efficiency of PAC adsorption was investigated in terms of DOC removal from synthetic wastewater (Figures 5.7). As can be seen in Figure 5.7, PAC was found to remove the DOC from 57.1% to 66.6 % when PAC with a dose of 1 to 2 g/L. For the synthetic wastewater used in this study, the DOC removal was more effective with flocculation than with adsorption, suggesting that the majority of SOM in the synthetic wastewater is constituted of large MW compounds.

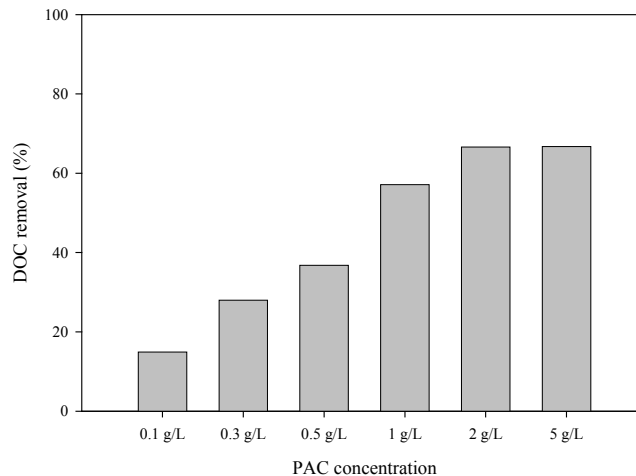


Figure 5.7 DOC removal by PAC adsorption at different doses of PAC

Experiments have also been conducted to study the addition of partial optimum concentration of FeCl_3 and PAC in order to understand the effect of reduced doses of chemicals in DOC removal. The removal efficiency of SOM by flocculation and adsorption at different doses and by post treatment of UF is presented in Figure 5.8. For example, with the addition of an optimum dose of FeCl_3 and reduced doses of PAC (0.05 to 0.5 g/L), the DOC removal from the synthetic wastewater was observed as follows: 82.6%, 89.5%, 89.8%, and 92.2% for PAC doses of 0.05, 0.1, 0.3, and 0.5 g/L PAC, respectively. The above results indicate that the PAC adsorption after flocculation with an optimum dose of FeCl_3 increased the DOC removal. An increase of 15% was observed when a PAC dose of 0.5 g/L. In the same manner, experiments were conducted with reduced doses of FeCl_3 and PAC. When the doses of FeCl_3 and PAC were kept at 10 mg-Fe/L and 0.5 g/L respectively, the DOC removal was still high up to 76%.

The post treatment of UF had the significant effect in the removal of DOC for pretreated waters with lower FeCl_3 and PAC doses. The post treatment of UF led to additional DOC removal of 40% for the pretreated water with 3 mg-Fe/L FeCl_3 and 0.5 g/L of PAC. The pretreatment resulted in approximately 50% DOC removal while the pretreatment followed by UF led to 90% removal. On the other hand, the pretreatment alone with 23 mg-Fe/L of FeCl_3 and 0.5 g/L of PAC led to more than 90% DOC removal, which allowed the post treatment of UF to remove less than 4 % additional DOC.

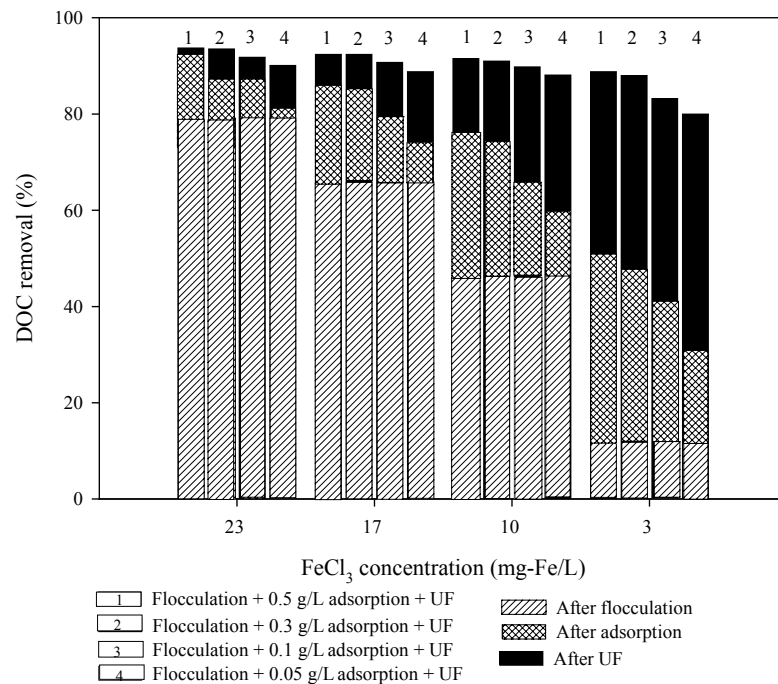


Figure 5.8 DOC removal of SFSA and UF (UF membrane used = NTR 7410; MWCO of 17500 daltons; crossflow velocity = 0.5 m/s; transmembrane pressure = 300 kPa; Reynold's number: 735.5; shear stress: 5.33 Pa; DOC removal with UF alone: 75.3%)

5.3.4.2 Flux Decline of UF with Pretreated Wastewater

The performance of UF was also studied in terms of normalized permeate flux (J/J_0) with and without adsorption pretreatment (Figure 5.9). The pretreatment of PAC adsorption helped in the reduction of flux decline. The flux decline in the UF after a pretreatment of PAC adsorption (with 1 g/L) was 29% after 6 hours of operation. The decline with no pretreatment was 38%.

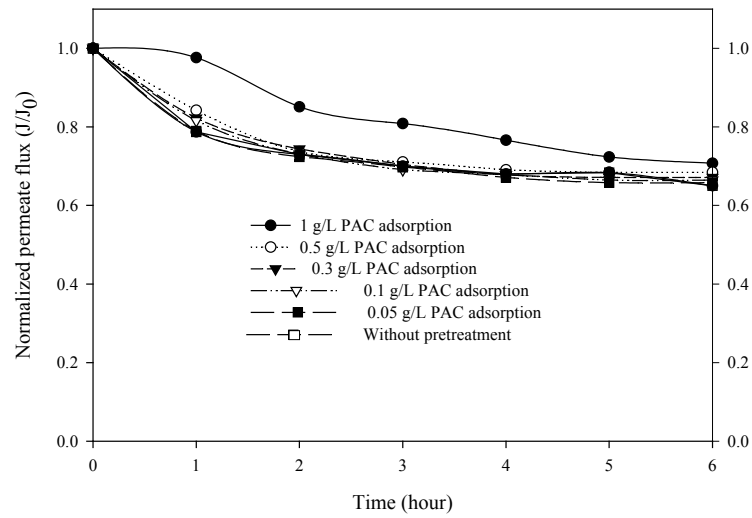


Figure 5.9 Temporal variation of filtration flux with UF NTR 7410 after adsorption pretreatment ($J_0 = 1.84$ m.d/L at 300 kPa; crossflow velocity = 0.5 m.s/L; MWCO of 17500 daltons; Reynold's number: 735.5; shear stress: 5.33 Pa)

Figure 5.10 presents the permeate flux of UF with the wastewater which has undergone flocculation with 23 mg-Fe/L, 17 mg-Fe/L, 10 mg-Fe/L and 3 mg-Fe/L of FeCl_3 followed by PAC adsorption of known concentration of PAC. The flux decline was minimal especially for pre-flocculated waters with FeCl_3 of 17 mg-Fe/L or more.

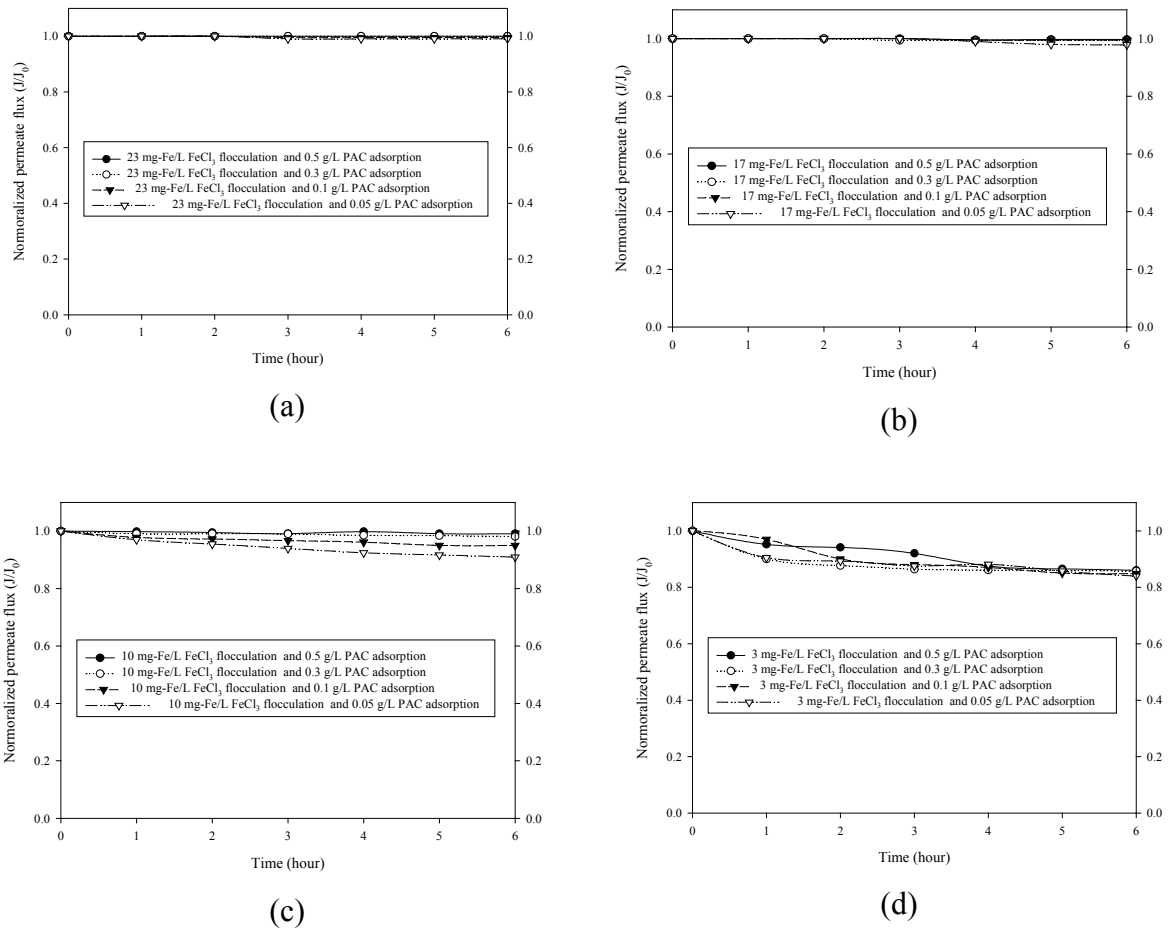


Figure 5.10 Temporal variation of filtration flux and DOC ratio with semi flocculation followed by semi adsorption (SFSA) with UF NTR 7410 ($J_0 = 1.84$ m/d at 300 kPa; crossflow velocity = 0.5 m/s; MWCO of 17,500 daltons; Reynold's number: 735.5; shear stress: 5.33 Pa; (a) after 23 mg-Fe/L flocculation; (b) after 17 mg-Fe/L; (c) after 10 mg-Fe/L; (d) after 3 mg-Fe/L)

5.3.4.3 Molecular Weight (MW) Distribution of Organic Matter

Figures 5.11 (a) and (b) present the MW distribution of pretreated water with PAC. PAC adsorption with larger doses of PAC (0.3 to 0.5 g/L) removed the majority of the small MW of SOM (250 daltons to 570) (Figure 5 (a)). On the other hand, the majority of larger MW SOM was not removed by adsorption alone. The MW distribution results are consistent with a flux decline trend.

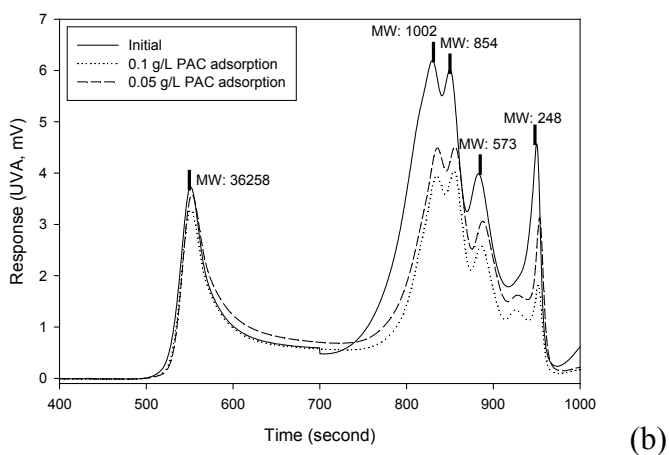
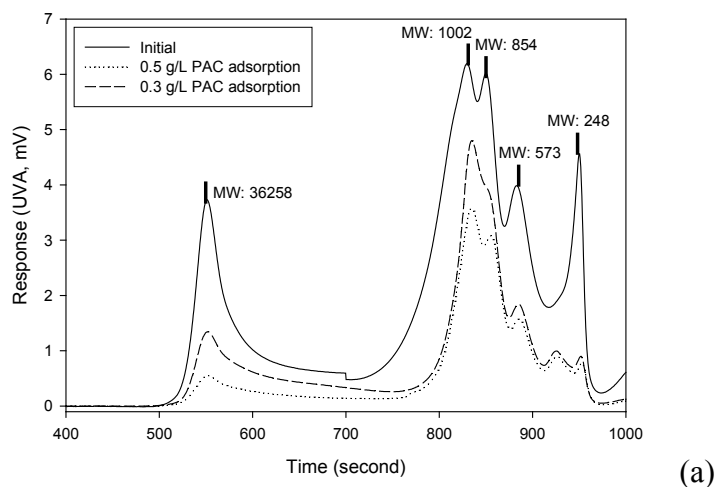
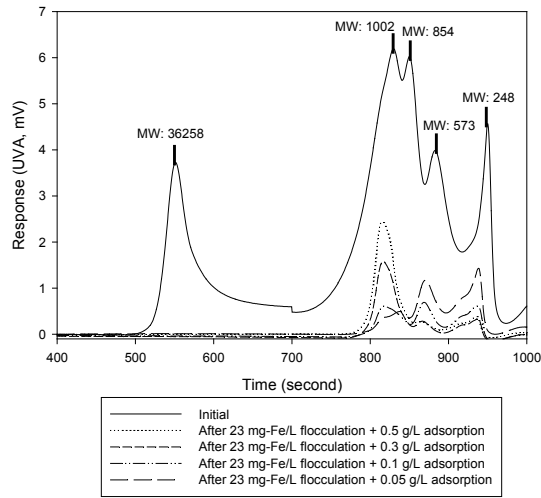
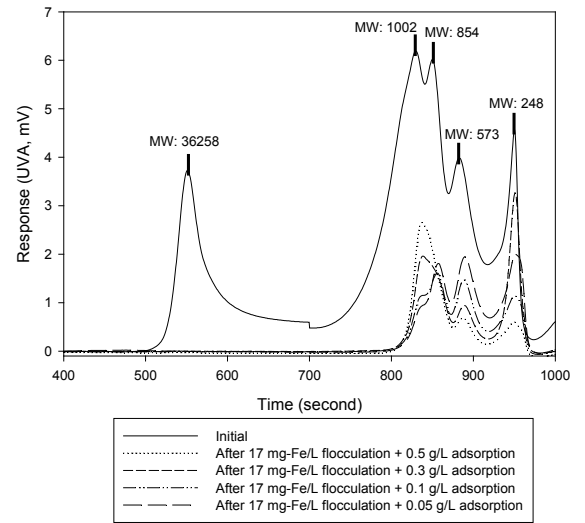


Figure 5.11 MW distribution after (a) adsorption with the large doses of PAC, and (b) adsorption with the small doses of PAC

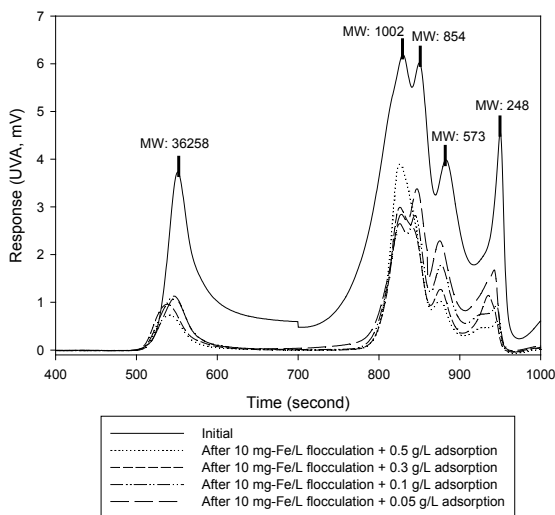
Figure 5.12 shows the MW distribution results after a semi flocculation with a FeCl_3 dose of 10, 17, and 23 mg-Fe/L and by semi adsorption. PAC adsorption removed the majority of smaller MW of 854, 573 and 248 from the pre-flocculated water with more than 17 mg-Fe/L FeCl_3 (Figure 5.11 (a)). However, the peak corresponding to 1002 daltons remained at high intensity. This could be due to the difficulty in removing humic acid, tannic acid and arabic gum powder (which has the peak at 1002 daltons) by flocculation and adsorption compared to the other compounds. A similar trend was observed with FeCl_3 flocculation (17 mg-Fe/L) followed by PAC adsorption (Figure 5.12 (b)). However, flocculation with less than 10 mg-Fe/L FeCl_3 was not sufficient to remove the large MW SOM even after a post adsorption (Figure 5.12 (c)).



(a)



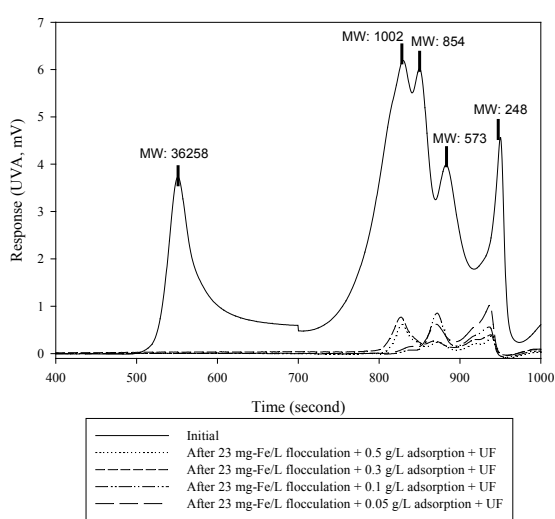
(b)



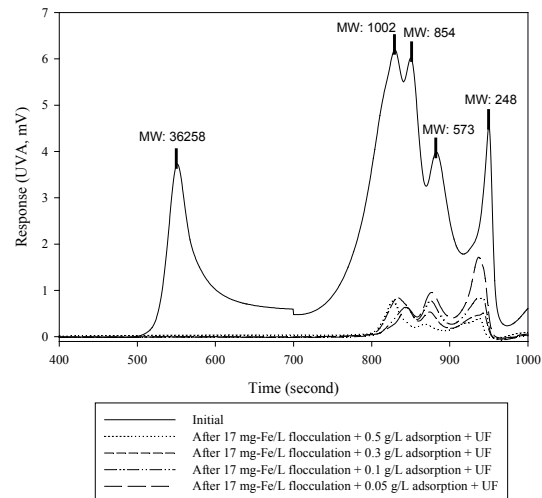
(c)

Figure 5.12 MW distribution of organic matter after semi flocculation followed by semi adsorption

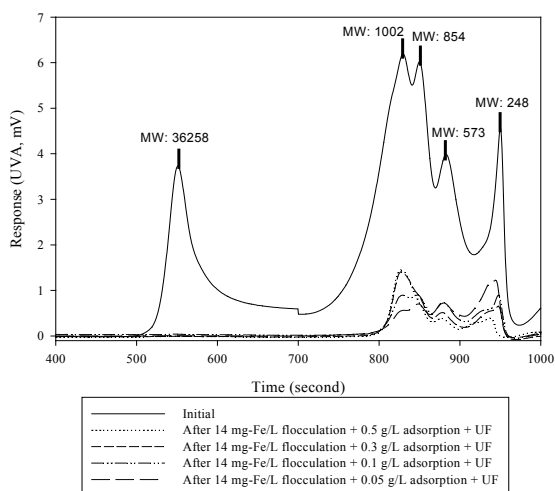
Figure 5.13 presents the MW distribution data after SFSA as pretreatment and UF NTR 7410 filtration as post treatment. All the SOM at the peak corresponding to 36260 daltons have been removed by UF. The flocculation with a reduced dose of FeCl_3 of 3 and 14 mg-Fe/L followed by adsorption did not remove the majority of large MW SOM. This resulted in relatively rapid flux decline in UF. The intensity of the peak corresponding to 1000 daltons increased with the decrease in the FeCl_3 dose used in the pretreatment.



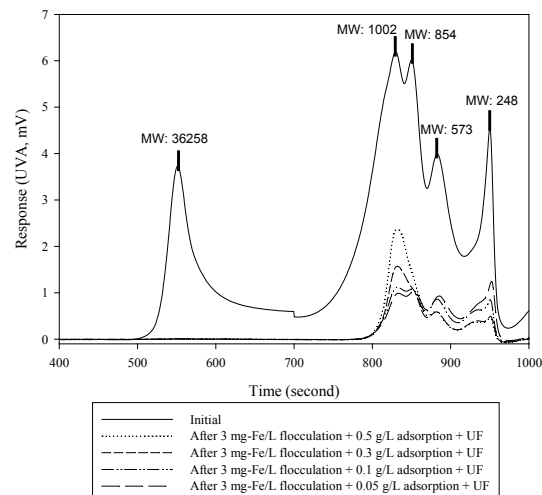
(a)



(b)



(c)



(d)

Figure 5.13 MW distribution after flocculation and adsorption as pretreatment and UF as post treatment ($J_0 = 1.84$ m/d at 300 kPa; crossflow velocity = 0.5 m/s; MWCO of 17500 daltons; Reynold's number: 735.5; shear stress: 5.33 Pa)

Table 5.3 presents the weight-averaged MW (M_w) values of SOM in the pretreated effluent and in the UF effluent. The M_w values of SOM in the wastewater and in the flocculated effluent were 29760 daltons (initial), < 990 (after flocculation with 17 mg-Fe/L FeCl_3 or more), and > 25050 (after flocculation with 14 mg-Fe/L FeCl_3 or less). Thus, a flocculation with more than 17 mg-Fe/L FeCl_3 and PAC adsorption is essential

in removing large and small MW SOM for the synthetic wastewater in this study. The UF as post treatment could not remove smaller MW SOM in a noticeable manner.

When the FeCl₃ concentration was decreased from 17 mg-Fe/L to 14 mg-Fe/L, the increase of M_w was significant. As the FeCl₃ concentration was further decreased from 14 mg-Fe/L to 7 mg-Fe/L, the increase of M_w values of SOM was not significant. The same trend was observed with the PAC adsorption of the flocculated effluent (with FeCl₃ dose of 3 to 14 mg-Fe/L). This phenomenon could be due to following two reasons: i) the FeCl₃ dose of 14 mg-Fe/L or less was not sufficient to remove the large MW SOM, and ii) the PAC adsorbed only smaller MW organic matter. When lower doses of FeCl₃ and PAC were used in the pretreatment, there was a significant difference in the M_w of the pretreated effluent and UF effluent. For example, when a FeCl₃ dose of 14 mg-Fe/L and a PAC dose of 0.5 g/L were used, the effluent from pretreatment had an M_w of 25050 daltons. When this effluent was filtered through UF, the M_w decreased to 913 daltons. This clearly shows that pre-flocculation with insufficient doses of flocculants delegates (or passes) the removal of large MW organic matter to the post treatment of UF. This, in turn, results in severe flux decline of membrane because the UF membrane fouling is mainly caused by large nano-sized MW organic matter.

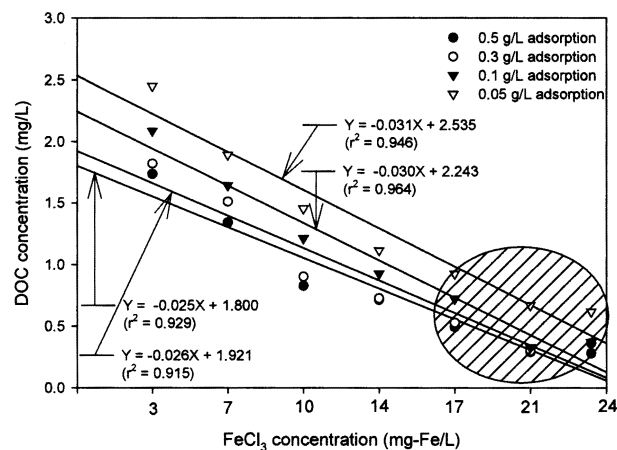
Table 5.3 Weight-averaged MW values of organic matter after pretreatment of flocculation and adsorption after post treatment of UF (all units: daltons)

FeCl ₃ (mg- Fe/L)	PAC concentration							
	0.5 g/L		0.3 g/L		0.1 g/L		0.05 g/L	
	SF**+SA**	Effluent	SF+SA	Effluent	SF+SA	Effluent	SF+SA	Effluent
23	1086	884	1031	862	841	526	675	516
21	1052	867	1011	841	850	681	747	609
17	987	849	948	821	832	680	753	594
14	25046	913	28338	896	29574	820	31924	742
10	31134	912	31196	896	31247	833	31303	752
7	31720	923	32271	897	32311	838	32354	809
3	32041	934	32333	898	32451	840	32493	830

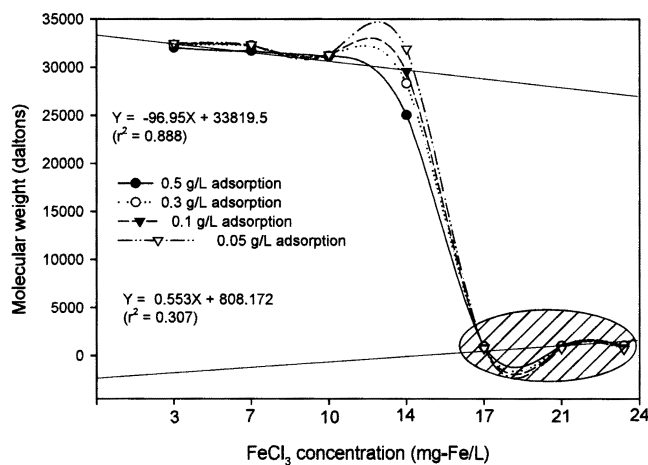
* SF: semi flocculation

**SA: semi adsorption

A correlation between the amount of SFSA and the M_w value is presented in Figure 5.14. The deviant crease circles show the range of flocculant (FeCl_3) and adsorbent (PAC) conditions necessary to reduce the membrane fouling and to obtain superior DOC removal. To obtain high DOC removal for the wastewater used in this study with minimum flux decline, the minimum concentration of flocculant (FeCl_3) and adsorbent (PAC) was 17 mg-Fe/L and 0.05 g/L respectively.



(a)



(b)

Figure 5.14 Correlation of flocculant and adsorbent concentration vs DOC concentration and averaged-weight MW ($J_0 = 1.84$ m/d at 300 kPa; crossflow velocity = 0.5 m/s; MWCO = 17500 daltons; Reynold's number.: 735.5; shear stress: 5.33 Pa; (a) FeCl_3 concentration vs DOC concentration of semi flocculation followed by semi adsorption; (b) FeCl_3 concentration versus MW of semi flocculation followed by semi adsorption)

5.4 Concluding Remarks

In this chapter, the adequateness of semi flocculation and semi adsorption (with reduced doses of ferric chloride (FeCl_3) and PAC) as pretreatment to UF was investigated for synthetic wastewater. The effectiveness of pretreatment was evaluated in terms of the decline of permeate flux and the removal of organic matter of different molecular weights. The findings can be summarized as follows:

1. Pretreatment of flocculation with FeCl_3 dose of 23 mg-Fe/L removed 75% of DOC, which led to only 9.6% of additional DOC removal by the UF used as post treatment. Conversely, a partial FeCl_3 dose of 7 mg-Fe/L removed only 34% of DOC and the post treatment of UF removed another 48%.
2. The flux decline (in terms of J/J_0 in the UF after 6 hours of operation) with no pretreatment was 38%. The UF with the pre-flocculation with the optimum dose of 23 mg-Fe/L FeCl_3 did not experience any flux decline during the 6 hours operation. The preflocculation with sub-optimal doses of FeCl_3 of 7 – 10 mg-Fe/L led to a significant flux decline, whereas a dose of 14 – 17 mg-Fe/L of FeCl_3 showed only a minimum flux decline.
3. The peaks corresponding to larger MW (36258 daltons) were not observed in the flocculated effluent with a FeCl_3 dose of 17 mg-Fe/L and above. The effluent after flocculation with FeCl_3 of less than 14 mg-Fe/L showed peaks corresponding to large MW.
4. PAC adsorption removed the majority of smaller MW of 850, 570 and 250 daltons from the pre-flocculated water with FeCl_3 dose of 17 mg-Fe/L or more.
5. The weight-averaged MW values in the effluent after flocculation with more than 17 mg-Fe/L FeCl_3 was much lower (less than 700 daltons) as compared with those with less than 14 mg-Fe/L FeCl_3 (around 29000 daltons which is in the similar range of the influent).

6. A 17 mg-Fe/L of FeCl₃ and 0.5 g/L of PAC removed a majority of DOC (88%), thus reducing the organic loading to UF used as post treatment. Although flocculation with lower doses of FeCl₃ (3 mg-Fe/L) followed by PAC adsorption of 0.5 g/L and UF removed the same amount of organic matter, the majority of the DOC removal was achieved by the post treatment of UF rather than by pretreatment. This resulted in significant flux decline in UF.

7. When the FeCl₃ concentration was decreased from 17 mg-Fe/L to 14 mg-Fe/L, the increase of M_w was significant. As the FeCl₃ concentration was further decreased from 14 mg-Fe/L to 7 mg-Fe/L, the increase of M_w values of SOM was not significant. The same trend was observed even with the PAC adsorption of the flocculated effluent (with FeCl₃ dose of 3 to 14 mg-Fe/L). This phenomenon could be due to the following two reasons: i) the FeCl₃ dose of 14 mg-Fe/L or less was not sufficient to remove the large MW SOM, and ii) the PAC adsorbed only smaller MW organic matter. The flux decline was proportional to the large M_w . This suggests that flocculation is more important than adsorption (for the particular wastewater used) to increase a permeate flux because flocculation removes the majority of large MW.

CHAPTER 6



University of Technology, Sydney
Faculty of Engineering

ROLE OF DIFFERENT FRACTIONS IN WASTEWATER ON MEMBRANE FOULING

6.1 Introduction

Organic fractions in BTSE can be categorized into three groups, namely hydrophobic (HP), transphilic (TP) and hydrophilic (HL) fractions (Cho et al., 1998). The HL fraction is the most abundant fraction in majority of the BTSE. This fraction consists of 32 – 74% of total organic carbon (TOC) and 17 – 28% of hydrophobic acids.

The specific foulants that cause membrane fouling and the understanding of the related processes are controversial. Some have suggested that the humic substances (HP fraction) are the major foulant which control the rate and extent of fouling (Yuan and Zydney, 2000). Recent studies have however reported that hydrophilic (non-humic) organic matter is mainly responsible for membrane fouling. For example, Gray and Bolto (2003) report that HL and HP base components of organic matter lead to continuous flux decline during membrane operation. Fan et al. (2001) report the fouling potential in the following order: HL neutrals > HP acids > TP acids. Jarusutthirak et al. (2002) found that the colloidal fraction of BTSE that mainly consists of large MW of HL compounds and is the main contributor to membrane fouling. The adsorption tendency of polysaccharides on the membranes was approximately three times of that of humics. Thus, the fractions alone are not sufficient to quantify the membrane fouling. It is also important to investigate the compounds and the MW distribution present in each fraction to estimate the extent of fouling.

Flocculation and adsorption as pretreatments to membrane filtration have been useful in significantly reducing the membrane fouling. It was shown in Chapter 4 that flocculation removes the majority of large MW organic compounds. Adsorption was also found to be an appropriate pretreatment in removing small MW organic matter. A significant amount of HP and HL fractions of organic matter can be removed by incorporating the pretreatment of flocculation and adsorption. The flocculation and adsorption in BTSE removed 51.6% and 58.7% of HL and 68.5% and 71.4% of HP organic fractions, respectively. However, there have not been any results reported in the literature on the effect of pretreatment of the different fractions of BTSE.

In order to optimize the performance of the membrane filtration of BTSE, it is essential to identify the membrane fouling and pretreatment effects of the different fractions of BTSE.

A detailed characterization of membrane fouled with different fractions will help to select a suitable membrane, pretreatment and the optimum range of operating parameters. In this chapter, the results of the phenomena of membrane filtration and pretreatment with different fractions of BTSE are reported and discussed.

6.2 Theoretical consideration

In this study, Freundlich, Sips and Talu type models are used to interpret PAC equilibriums. Homogeneous surface diffusion mode (HSDM) was applied to investigate the intra particle diffusion mechanism and organic uptake rate by the adsorbent.

6.2.1 Isotherm Equilibrium

6.2.1.1 Freundlich Model

The Freundlich isotherm has been widely used as an empirical equation for qualitative purposes in both single component and multicomponent adsorption systems. The isotherm is based on the assumption that there is no association or dissociation of the molecules after they are adsorbed on the surface and chemisorption is completely absent. The adsorbed amount increases infinitely with the increase in concentration, which is unrealistic. Consequently, the Freundlich isotherm is not very successful in describing the isotherm results over a wide range of concentrations:

$$q = K_F C_e^{\frac{1}{n}} \quad (6.1)$$

where: C_e = equilibrium organic concentration, mg/L, K_F = Freundlich constant, $1/n$ = Freundlich constant, q = measured amount organic adsorbed, mg/g.

6.2.1.2 Sips Model

The Sips model is another empirical model for representing equilibrium adsorption data. It is a combination of the Langmuir and Freundlich isotherm type models. The Sips model takes the following form for single solute equilibrium data:

$$q = \frac{q_m C_e^{\frac{1}{n}}}{1 + K_s C_e^{\frac{1}{n}}} \quad (6.2)$$

Unlike other mentioned adsorption isotherm models, this model contains three parameters; q_m (sorption capacity), $1/n$ and K_s (energy of adsorption) which can be evaluated by fitting the experimental data to this model (Al-Asheh et al., 2000).

6.2.1.3 Talu Model

Most of the previous studies on a multicomponent system are based on ideal adsorbed solution theory (IAST) and the Freundlich isotherm. However, the theory of association proposed by Talu and Meunier (1996) in this study was utilized to express the overall isotherm. The association theory takes into account chemical equilibriums, equation of state (EOS) and phase equilibriums of the system, and will be termed as Talu theory hereafter. After simplifying the equations of chemical equilibriums, EOS and phase equilibriums, the Talu model yields the following isotherm equations:

$$C_e = \frac{H\psi \cdot \exp\left(\frac{\psi}{q_m}\right)}{(1 + K\psi)} \quad (6.3)$$

$$\psi = \left(\frac{-1 + (1 + 4K\zeta)^{0.5}}{2K}\right) \quad (6.4)$$

$$\zeta = \frac{q_m q}{q_m - q} \quad (6.5)$$

Where: C_e = equilibrium organic concentration, mg/L, H = adsorption constant, function of temperature, K = Talu reaction constant, q_m = saturation amount of organic

adsorbed, mg/g, ψ = concentration spreading parameter and q = measured amount organic adsorbed, mg/g.

6.2.1.4 Adsorption Batch Kinetics

Adsorption kinetics is the measure of rate of adsorption, and it describes the adsorbate transport mechanism from bulk solution to the adsorption site on an adsorbent surface. Several mathematical models have been developed to describe the adsorption process and predict the process rate using different modes of intraparticle diffusion. The HSDM has been used to investigate the PAC adsorption kinetics. HSDM consists of a three-step process as follows:

- (i) the adsorbate diffuses through a stagnant liquid film layer surrounding the carbon particle,
- (ii) the adsorbate adsorbs from the liquid phase onto the outer surface of the carbon particle, and
- (iii) the adsorbate diffuses along the inner surface of the carbon particles until it reaches its adsorption site.

The overall mass balance in the batch reactor is given by the following equation.

$$V \frac{dC}{dt} + M \frac{d\bar{q}}{dt} = 0 \quad (6.6)$$

The average adsorbed phase concentration is:

$$\bar{q} = \frac{3}{r_p^3} \int_0^{r_p} r^2 q dr \quad (6.7)$$

The mass balance inside a spherical porous adsorbent is:

$$\frac{\partial q}{\partial t} = D_s \left(\frac{\partial^2 q}{\partial r^2} + \frac{2}{r} \frac{\partial q}{\partial r} \right) \quad (6.8)$$

$$t = 0 ; q = 0 \quad (6.9)$$

$$r = 0 ; \frac{\partial q}{\partial r} = 0 \quad (6.10)$$

$$r = r_p ; D_s \rho_p \frac{\partial q}{\partial r} = k_f (C - C_s) \quad (6.11)$$

where: V = volume of the solution in batch reactor (L), M = weight of the adsorbent (g), C = bulk organic concentration (mg/L), \bar{q} = average adsorbed phase organic concentration (mg/g), r_p = radius of adsorbent particle (m), D_s = surface diffusion coefficient of organic (m^2/s), ρ_p = particle density of adsorbent (kg/m^3), k_f = external film mass transfer coefficient of organic (m/s) and C_s = saturation organic concentration (mg/L).

6.3 Membrane Filtration

6.3.1 Performance of UF with Different Fractions of BTSE-S

HP, TP and HL fractions were isolated from BTSE-S and concentrated to examine the effect of different fractions in the fouling of ultrafilter membranes. Here, BTSE-S represents the BTSE collected during summer months (June, July, and August of 2004). The initial concentrations of each fraction were adjusted to a DOC value of approximately 6.5 mg/L which was similar to the DOC of BTSE-S. Figure 6.1 shows the DOC removal efficiency. The DOC removal of HL fraction is very low compared to HP and TP fractions. It can be explained in terms of MW distribution. The HP fraction contains large MW organic compounds so a higher removal of DOC compared to other fractions was observed. In addition, this higher retention of the HP fraction may also be due to the interaction between the HP fraction and membrane surface. The contact angle of 69° of membrane is representative of a hydrophobic surface (Lee et al., 2004), on which the HP compound is likely to be preferentially retained.

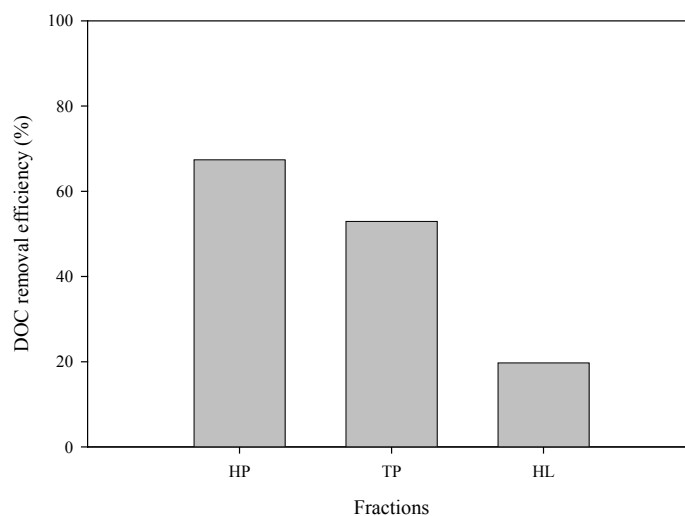


Figure 6.1 DOC removal of different fractions with UF performance (UF membrane used = NTR 7410; MWCO of 17,500 daltons, crossflow velocity = 0.5 m/s, transmembrane pressure = 300 kPa, Reynold's number.: 735.5, shear stress: 5.33 Pa)

6.3.2 Fouling of Different Fractions during UF Membrane at Constant Transmembrane Pressure

The performance of UF in treating different fractions of BTSE-S was studied in terms of normalized permeate flux (J/J_0) (Figure 6.2). Here, J_0 is pure water permeate flux. The flux decline with the HP fraction was very high compared with other fractions. The flux decline with the HL fraction was minimal. This phenomenon can be explained in terms of MW distribution and the interaction between organic matter and membrane surface. HL fraction included mainly the small MW compounds which were much smaller than the membrane pore size of 17500 daltons. Thus, these compounds would have passed through the membrane pores, even without an interaction of HL organic fraction and HP membrane. The high flux decline by the HP fraction is due to the pore blocking by the large MW present in the HP fraction. Further, there would have been a strong adsorption of HP compounds on the membrane surface. Thus, it can be concluded that HP fraction in BTSE-S is the main component which causes significant fouling. On the contrary, Lee et al. (2004) observed that the HL fraction resulted in significant flux decline. This may be due to the fact that this fraction contained a significant amount of colloidal and macromolecular organic matter with non-humic

properties. The shape and size of molecules and roughness of membrane are also important influential factors that affect flux decline.

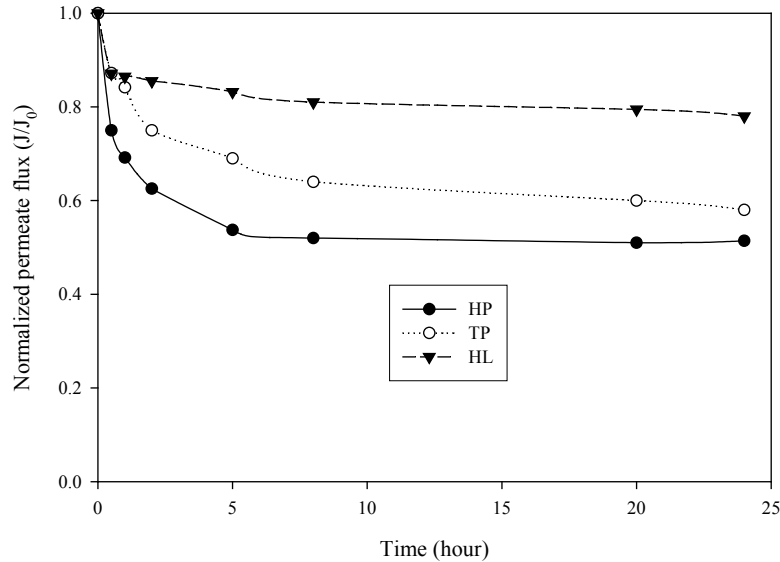


Figure 6.2 Temporal variation of filtration flux with different fractions ($J_0 = 3.01$ m/d (125.4 L/m²·h) at 300 kPa; crossflow velocity = 0.5 m/s)

6.3.3 Membrane Characterization of the Fouled Membrane Surface with Different Fractions

6.3.3.1 Foulant Concentration

The adsorbed organic foulants on the fouled surface of the UF membrane were analyzed after soaking the fouled membranes in a 0.1 N NaOH solution (Figure 6.3). The organic concentration on the fouled membrane surface was found to be in the following order: HP (0.075 mg DOC/cm² membrane) > BTSE-S alone (0.050 mg DOC/cm² membrane) > TP (0.040 mg DOC/cm² membrane) > HL (0.020 mg DOC/cm² membrane). The EfOM concentration of the HP fraction was 3.75 times as high as that of HL fraction. This result was similar to that of severe flux decline for the HP fraction.

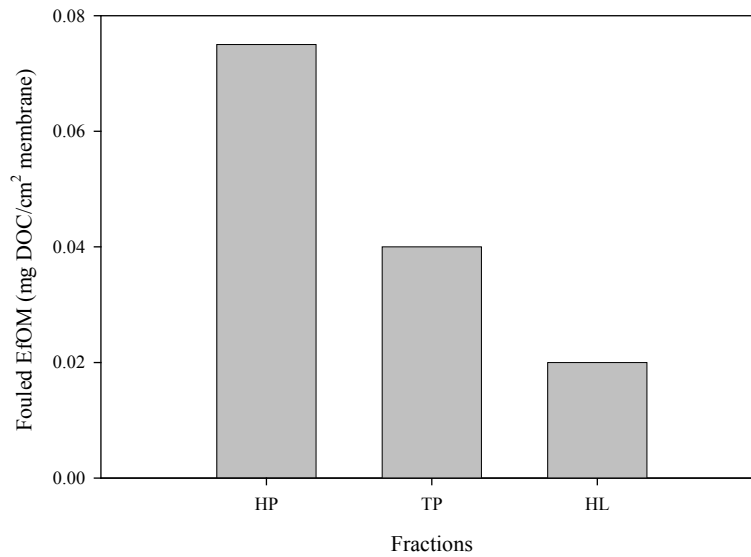


Figure 6.3 DOC concentration of adsorbed fractions on the fouled UF membrane surfaces

6.3.3.2 Contact Angle

The contact angle of the fouled membrane with different fractions was investigated (Figure 6.4). A higher contact angle indicates higher hydrophobicity of the membrane surface. Filtration of the HP and TP fractions increased the contact angle from 60° (clean) to 88° (HP) and 68° (TP), respectively, whilst the HL fraction slightly decreased the contact angle. Thus, the variation of contact angle also provides an additional conformation of the influence of the HP fraction in the fouling phenomena.

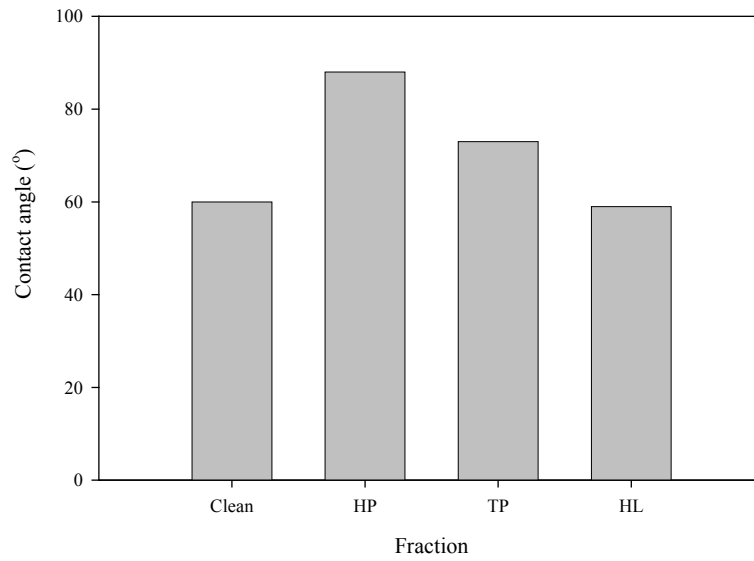


Figure 6.4 Contact angle on the fouled UF membrane surfaces

6.3.3.3 Zeta Potential

Figure 6.5 shows the values of zeta potential of the membrane after filtration of different fractions. The zeta potential of the clean membrane is strongly negative and the fouling did not change significantly this tendency. However, the absolute value of the zeta potential decreased with the TP fraction and increased with the HP fraction.

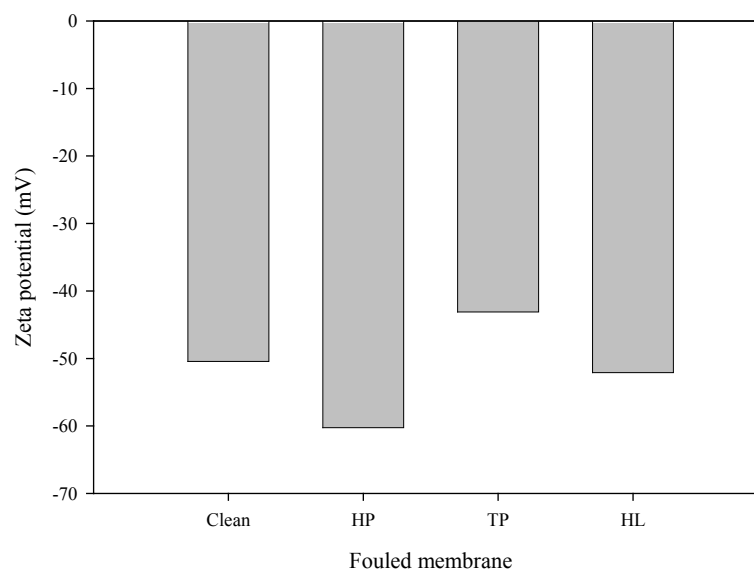


Figure 6.5 Zeta potential on the fouled UF membrane surfaces

6.3.3.4 ATR-FTIR Spectroscopy Results for Different Pretreatments

ATR-FTIR was employed to analyze the functional groups of the different fractions on the fouled membrane surface. The functional groups of the HP and TP fractions showed the same wavelength and those of HL and BTSE-S that had similar groups (Table 6.1). The main functional group of HP and TP fractions was the ketone groups (quinines) at 1643 cm^{-1} . Conversely, the functional groups of HL were similar to that of BTSE-S (Table 6.2). This confirms the predominant role of HL in BTSE-S. A major peak found in all the fractions was one at a wave number of 1650.5 cm^{-1} . This peak was from carboxylic acid group (COOH, C=O, range: $1670 - 1650\text{ cm}^{-1}$). Jarusutthirak et al. (2002) also studied the functional groups of different fractions in BTSE. In colloidal fraction, the peaks at wave numbers of 1540 and 1640 cm^{-1} (reflecting functional groups of primary and secondary amides), and a peak at wave number of 1040 cm^{-1} (indicating polysaccharides) are indicative of proteins and N-acetyl aminosugars. These compounds are present in a bacterial wall. In their study (Jarusutthirak et al., 2002), the HP and TP fractions included a peak of 1720 cm^{-1} , which was associated with carboxylic groups (humic and fulvic acids).

Table 6.1 FTIR functional group with different fractions

	1400 cm ⁻¹	1160 cm ⁻¹	1130 cm ⁻¹	880 cm ⁻¹	675 cm ⁻¹	615 cm ⁻¹
BTSE-S	High	High	Middle	High	High	High
HP	ND*	ND	ND	ND	ND	ND
TP	Middle	ND	ND	ND	ND	ND
HL	High	High	High	ND	High	High
Functional groups	Alcohols (R ₃ C-OH)	Alcohols (R ₃ C-OH) Esters (R-CO-O-R) Phosphorus, ((RR'R'')P=O) Ureas (R ₂ -N-CO-N-R ₂ , N-CN)	Alcohols (R ₃ C-OH, R ₃ C-OH) Silicons, Si-ph)	Carbo-acid, COOH, 960-875	Halogens (CF ₃ , C-F) Sulfur (C-SO ₂ -C, S-C)	Sulfur (C-SO ₂ -C, S-C)

* ND: not detectable, ** ph: phenol group

Table 6.2 FTIR functional group with the HL fraction

	1400 cm ⁻¹	1160 cm ⁻¹	1130 cm ⁻¹	880 cm ⁻¹	675 cm ⁻¹
Functional group of HL	Amides (CO-NH ₂ -, C-N)	Alcohols, Imides (CO-NH-CO-CN) Sulfur (C-SO ₂ -C, S-C) Ureas (R ₂ -N-CO-N-R ₂ , N-CN)	Esters, (CO-NH-CO-OH) Alkanes (CH ₃) ₂ , C-C) Amines (CH ₂ -NH-CH ₂ , C-N)	Alcohol (R ₃ C-OH) Alkenes (CH=CH) Cis, C-H)	Ureas (R ₂ -N-CO-NH ₂ , NH ₂ , NH ₂)

6.4 Effect of Pretreatment for Different Fractions of BTSE-S

6.4.1 Flocculation as Pretreatment for BTSE-S

Figure 6.6 shows the DOC removal efficiency from BTSE-S by flocculation with different FeCl₃ concentrations. Here, the conductivity of the BTSE-S fractions was adjusted to 15 mS/cm because the fractions consisted of the high salt concentration due to the use of HCl and NaOH during the isolation of fractions.

Figure 6.6 shows the DOC removal efficiencies of different fractions from BTSE-S. The removal efficiency of HP, TP and HL in terms of DOC at a FeCl_3 dose of 14 mg-Fe/L was 59%, 49% and 24%, respectively. This suggests that FeCl_3 flocculation can effectively remove HP compounds compared with the HL fraction. It may be due to the MW distribution present in HP which consists of large MW.

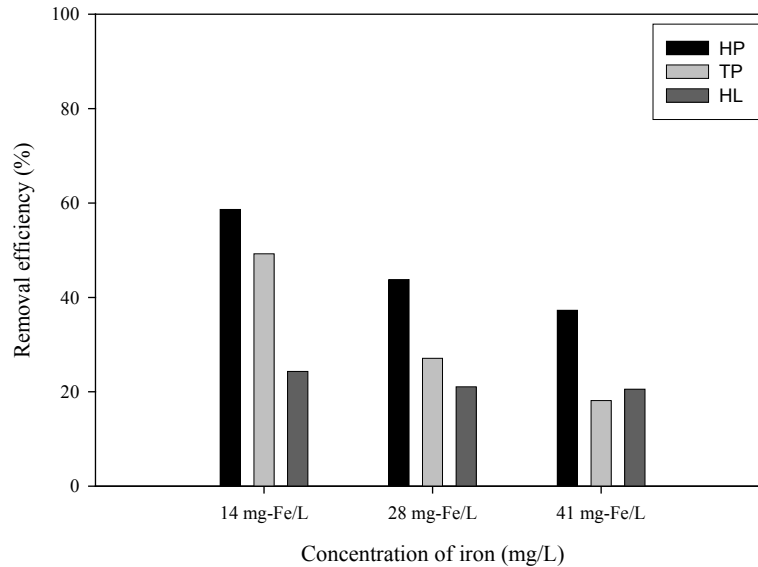


Figure 6.6 DOC removal efficiency of different fractions by FeCl_3 flocculation

6.4.2 Adsorption as Pretreatment for BTSE-S

The removal of different fractions of BTSE-S with different PAC doses is shown in Figure 6.7. A PAC concentration of 1 g/L led to a relatively high DOC removal of 79%.

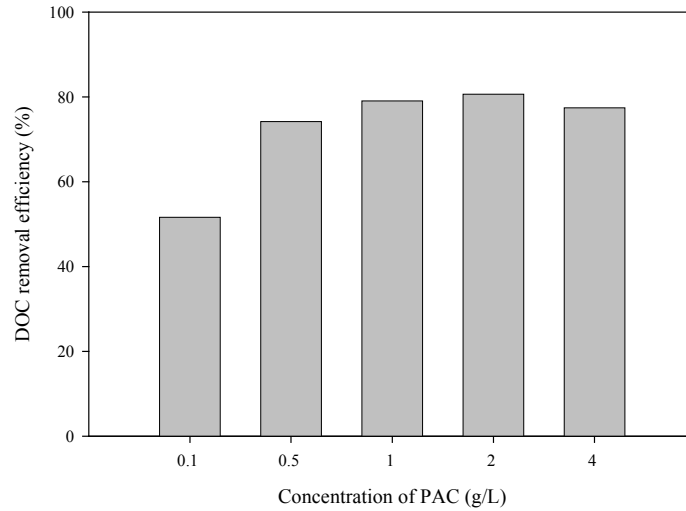


Figure 6.7 Effect of PAC dose in the DOC removal from BTSE-S (initial DOC = 6.5 mg/L; conductivity = 15 mS/cm)

The adsorption equilibrium of a multi-component adsorption system is influenced by many factors such as pH, temperature, and organic and inorganic contents. In this study, Freundlich, Sips, and Talu isotherms were used to predict the equilibrium (Figure 6.8). The isotherm parameters are presented in Table 6.3.

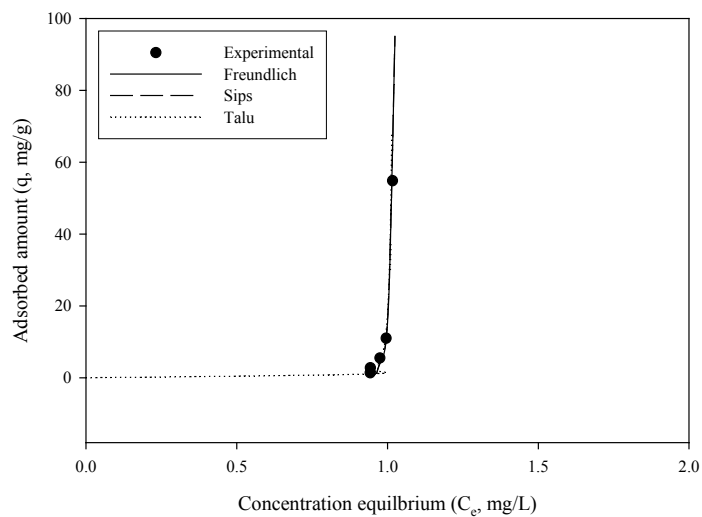


Figure 6.8 Adsorption isotherm results (BTSE-S with 15 mS/cm: 6.5 mg/L; Temp.: 25 °C)

Table 6.3 Isotherm parameter values (PAC with BTSE-S at initial concentration of 6.5 mg/L)

Freundlich constant	Values	Sips constant	Values	Talu constant	Values
K_F	1.66E+01	q_m	3.40E+10	q_m	1.239E+07
$1/n$	1.42E-02	K_S	4.89E-10	K	7.462E+01
		n	7.06E+01	H	7.672E+01

6.4.3 Adsorption Kinetics of BTSE-S

The study of PAC adsorption kinetics was then conducted with BTSE-S (Figure 6.9). It is important to design an adsorption system since it produces the necessary factors to estimate the mass transfer from the bulk solution to the adsorbent surface and to the interior of the adsorbent particle. In this study, Talu model and homogeneous surface diffusion model (HSDM) were used to investigate the intra particle diffusion mechanism and organic uptake rate. The model successfully predicted the batch adsorption kinetics experiments. The film mass transfer coefficient (k_f) and diffusion coefficient are shown in Table 6.4.

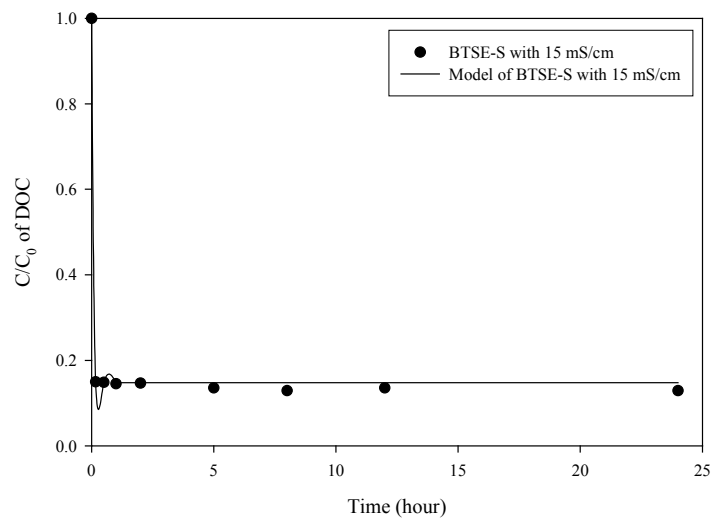


Figure 6.9 Adsorption kinetics of BTSE-S with 1 g/L PAC at 25 °C

Table 6.4 Film mass transfer coefficient (k_f) and diffusion coefficient (D_s) of batch experiments at initial PAC concentration of 1 g/L

BTSE-S with 15 mS/cm	
$k_f (\times 10^{-5} \text{ m/s})$	1.08E+00
$D_s (\times 10^{-11} \text{ m}^2/\text{s})$	2.01E+00

6.4.4 Adsorption as Pretreatment for Different Fractions of BTSE-S

DOC removal from different fractions by PAC adsorption (1 g/L) is presented in Figure 6.10. The organic removal from HP, TP and HL fractions by PAC was 57%, 55% and 16% respectively. The DOC removal from HP and TP was higher than that from HL and maybe due to the hydrophobic nature of PAC and EfOM.

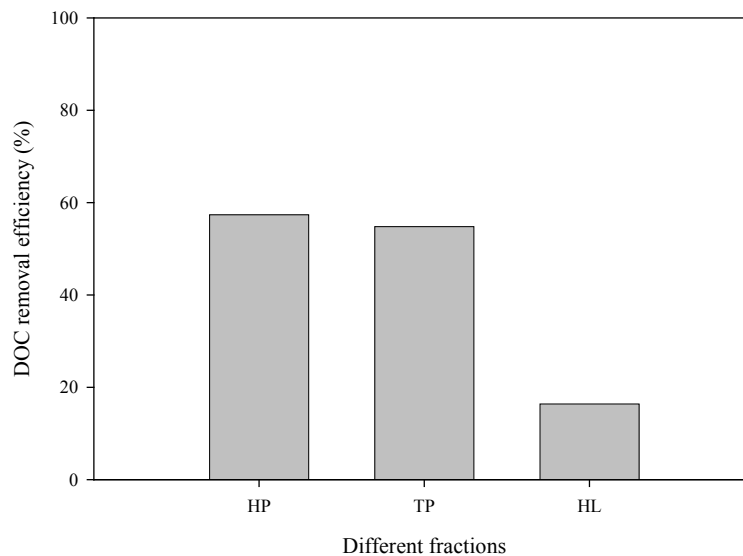
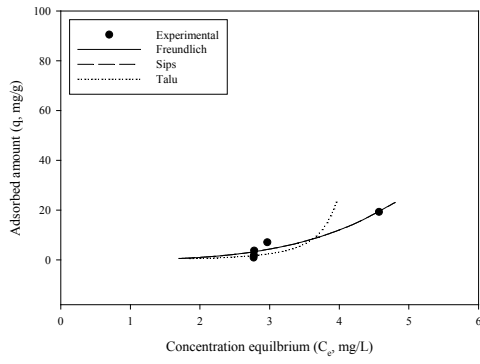


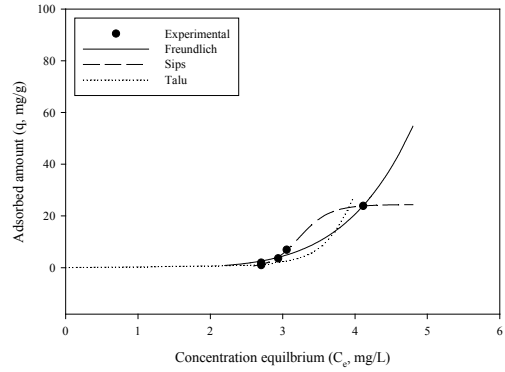
Figure 6.10 DOC removal of different BTSE-S fractions by PAC adsorption (PAC dose: 1 g/L; initial DOC concentration: 6.5 mg/L; mixing speed: 100 rpm; operation: 1 h; pH: 7)

The adsorption equilibrium results and isotherm predictions are given in Figure 6.11. The isotherm parameters are presented in Table 6.5. The average adsorption affinity (K_F) was more favorable with HP and TP fraction compared to the HL fraction.

a) For HP fraction



b) For TP fraction



c) For HL fraction

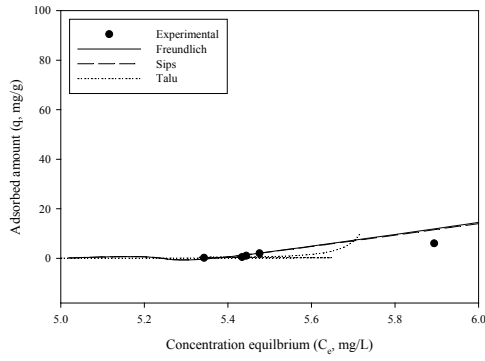


Figure 6.11 Adsorption isotherm plots (initial DOC concentration: 6.5 mg/L; Temp.: 25 °C)

Table 6.5 Isotherm parameter values for different fractions

	Freundlich constant	Values	Sips constant	Values	Talu constant	Values
HP	K_F	8.48E-02	q_m	1.55E+05	q_m	2.071E+05
	$1/n$	2.80E-01	K_S	5.46E-07	K	2.338E+00
			n	3.57E+00	H	1.059E+01
TP	K_F	1.25E-02	q_m	2.44E+01	q_m	5.471E+01
	$1/n$	1.87E-01	K_S	5.70E-09	K	4.777E+00
			n	1.61E+01	H	1.908E+01
HL	K_F	7.37E-17	q_m	3.14E+02	q_m	3.479E+06
	$1/n$	4.55E-02	K_S	1.70E-19	K	5.103E+02
			n	2.22E+01	H	2.958E+03

The Talu model and the HSDM were then used to investigate the intra particle diffusion mechanism and organic uptake rate by both of adsorbents (Figure 6.12). The results from batch kinetics experiments were simulated successfully. The film mass transfer coefficient (k_f) and diffusion coefficient of the adsorption kinetics are shown in Table 6.6.

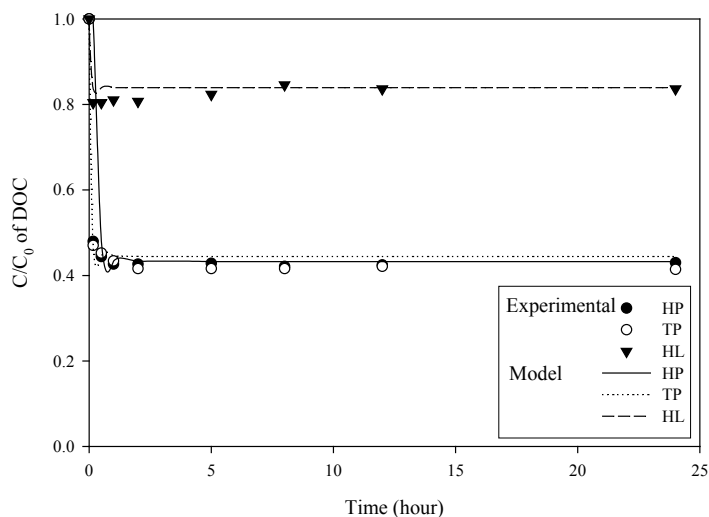


Figure 6.12 Adsorption kinetics result by PAC adsorption

Table 6.6 Film mass transfer coefficient (k_f) and diffusion coefficient (D_s) of fractions at initial PAC concentration of 1 g/L

	HP	TP	HL
$k_f (\times 10^{-5} \text{ m/s})$	3.69E-01	4.81E-01	2.96E+00
$D_s (\times 10^{-11} \text{ m}^2/\text{s})$	6.94E-01	9.05E-01	5.52E+00

6.5 MW Distribution

6.5.1 MW Distribution of Different Fractions

Following this global characterization of BTSE-S, the three fractions of BTSE-S separated were subjected to MW distribution analysis (Figure 6.13). The HP fraction showed peaks at 580, 865, and 43109 daltons; TP at 580 and 865 daltons; and HL at 263 to 580 daltons. These results are in agreement with the previous studies (Huber, 1998; Jarusutthirak, 2002).

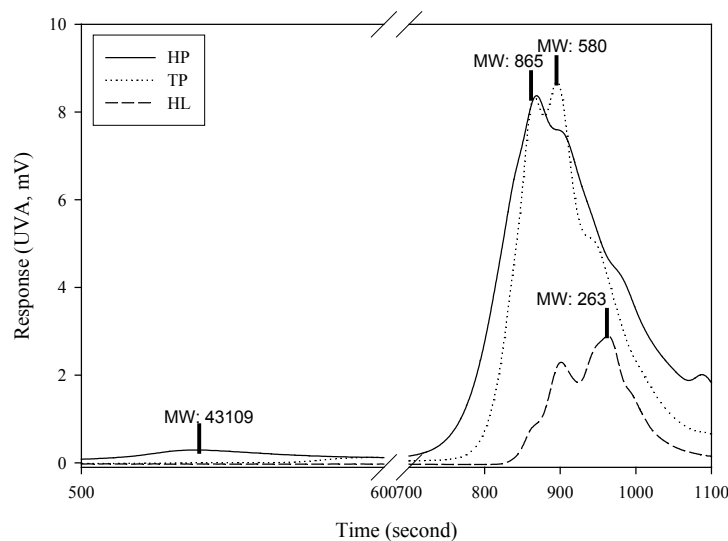


Figure 6.13 MW distribution of HP, TP, and HL fractions in terms of UV response and

6.5.2 After Flocculation of Different Fractions of BTSE-S

MW distribution of EfOM was investigated with different fractions after they underwent a flocculation pretreatment (Figure 6.14). The removal trend of organic molecules of different MWs in BTSE-S was different from that of different fractions extracted from BTSE-S. When the fractions were flocculated, the smallest MW (263 daltons) in the HP could not be removed by flocculation. The MW of 263 daltons and 865 were also difficult to be removed, whereas 580 daltons in the HL remained as the highest response. The mechanisms of HP removal by flocculation were similar to those of BTSE-S alone, suggesting that the mechanisms of flocculation could depend on the nature of HP.

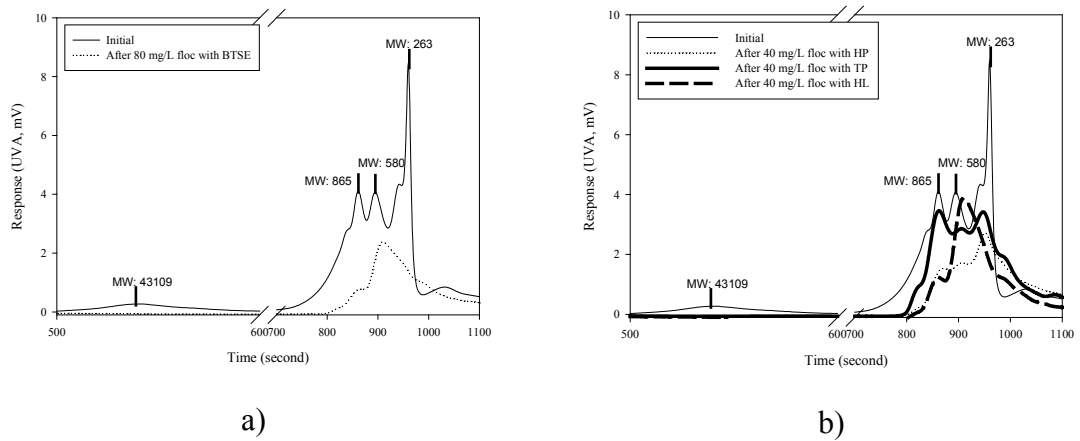


Figure 6.14 MW distribution of (a) BTSE-S and (b) different fractions after flocculation

6.5.3 After Adsorption of Different Fractions of BTSE-S

Figure 6.15 presents MW distribution of BTSE-S before and after PAC adsorption. It is evident from the results that the organic molecules in the MW of 260 and 870 daltons were adsorbed to a lesser extent than in that of 580 daltons.

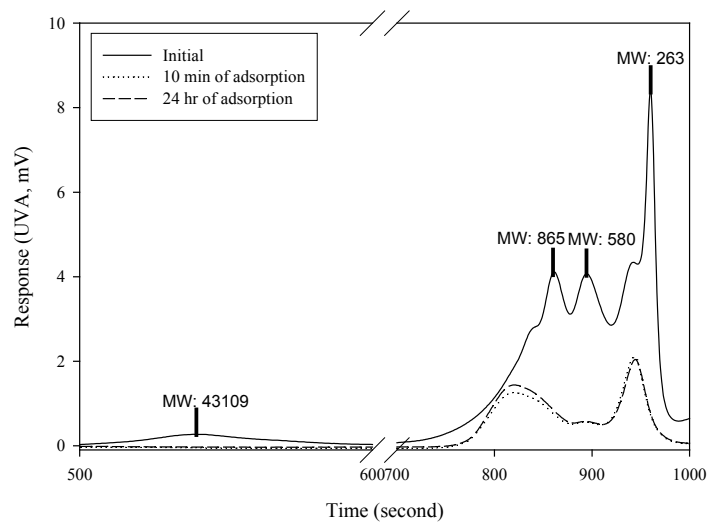


Figure 6.15 MW distribution of BTSE-S before and after PAC adsorption (PAC dose: 1 g/L)

6.5.4 MW Distribution with HP

Figure 6.16 (a) presents the MW distribution of the HP fraction after it has undergone adsorption with different doses of PAC. The adsorption time was 24 h. Figure 6.16 (b) presents the adsorption kinetics results after different adsorption times. MW distribution of the HP fraction included all the organic matter in terms of MW found in BTSE-S (263, 330, 580, 865, and 43109 daltons). When different concentrations of PAC were added, the OM removal in terms of MW distribution exhibited a similar pattern, i.e. that the affinity between PAC adsorption and EfOM is strong. The OM in the range of 865 daltons was least removed by PAC adsorption. MW distribution of effluent after adsorption for different durations at 2 h and 12 h (which indicated the adsorption was fast) showed similar trends.

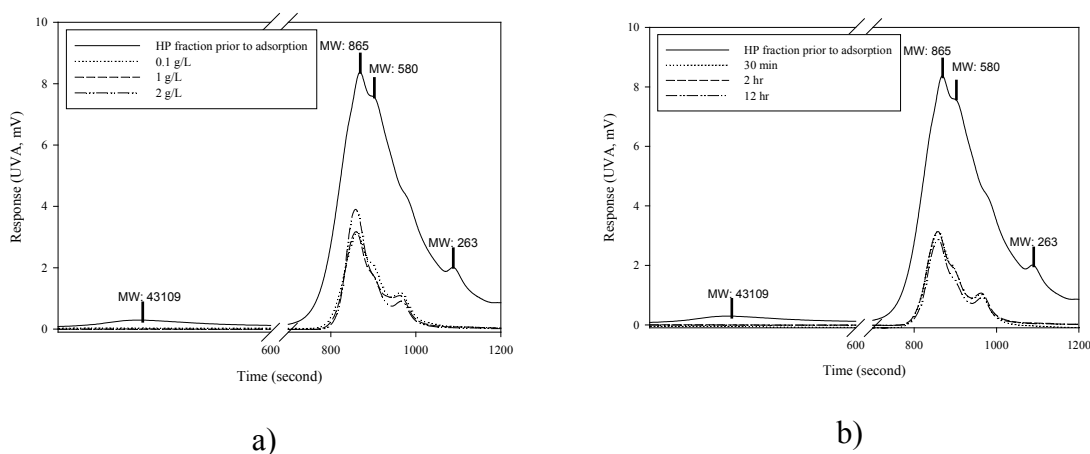
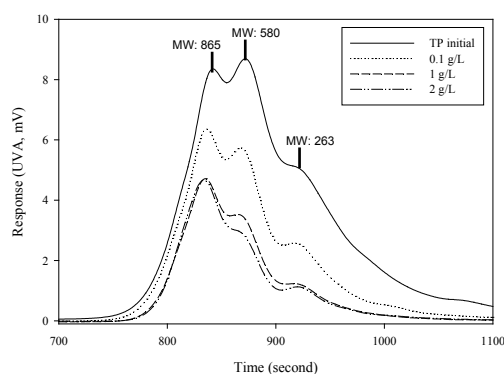


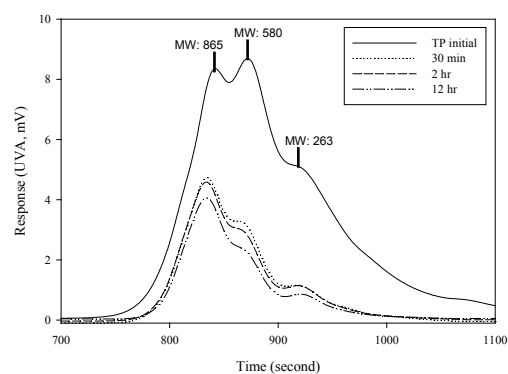
Figure 6.16 MW distribution of a) different PAC concentrations and b) batch kinetics

6.5.5 MW Distribution with TP

MW distribution of the isolated TP fraction with different PAC concentrations and batch kinetics was also conducted (Figure 6.17). The trend of MW distribution of the TP fraction was similar to that of the HP fraction except the largest MW of HP. TP did not have 43109 daltons. As the PAC concentration increased, MW distribution decreased with the same mechanisms of EfOM removal. The peak of 865 daltons remained like MW distribution of HP did.



a)

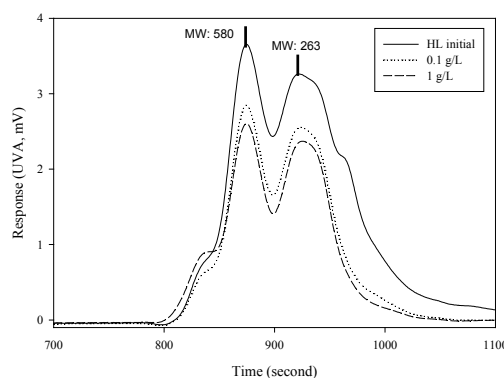


b)

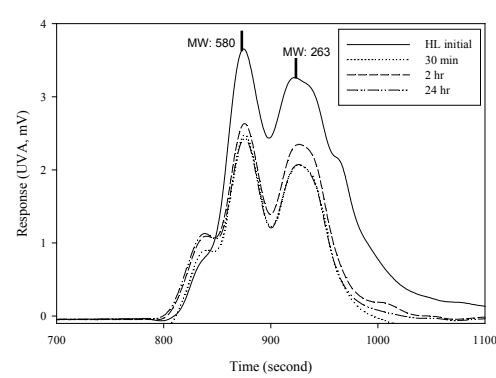
Figure 6.17 MW distribution of a) different PAC concentrations and b) batch kinetics

6.5.6 MW Distribution with HL

The MW distribution of the HL fraction with different PAC concentrations and batch kinetic are also shown in Figure 6.18. The MW distribution of the HL fraction included a majority of small MW such as 263, 330 and 580 daltons, which was not found in the large HP and TP fractions. The removal trend of MW distribution could not be identified in terms of different PAC concentrations and batch kinetics.



a)



b)

Figure 6.18 MW distribution of a) different PAC concentrations and b) batch kinetic

6.6 Concluding Remarks

In this chapter, a detailed characterization of pretreatment and membrane fouling with BTSE-S and its different fractions was made. The pretreatment of PAC adsorption with different fractions was also investigated in terms of adsorption equilibrium and kinetics. The results led to the following conclusions:

1. The organic removal efficiency by UF was higher for the HP fraction (67.4%) than for HL (19.7%) and BTSE-S (50.4%). As the membrane MWCO was 17500 daltons, the rejection of 50.4% suggests that the EfOM in the BTSE-S consists of about 50% larger MW than 17500 daltons.
2. The flux decline with the HP fraction was very high compared to the TP and HL fractions. The flux decline with the HL fraction was the minimum. Thus, it can be concluded that in the BTSE-S used in this study, HP fraction was the main component which caused severe fouling. This is also confirmed from the contact angle, EfOM and zeta potential values.
3. The main functional group of HP and TP indicated ketone groups (quinines). On the other hand, the functional groups of HL were similar to that of BTSE-S alone. This confirms the predominant role of HL in BTSE-S.
4. The removal efficiency of HP, TP, and HL at a FeCl_3 dose of 14 mg-Fe/L was 59%, 49%, and 24%, respectively, suggesting that FeCl_3 flocculation can effectively remove HP compounds compared to TP and HL fractions.
5. The removal of HP, TP and HL by 1 g/L of PAC adsorption was 57%, 55% and 16% respectively. The DOC removal of HP and TP was higher than that of HL and this may be due to the hydrophobic nature of PAC and EfOM.

6. When the fractions were flocculated, the smallest MW (263 daltons) in the HP could not be removed by flocculation. However, 580 daltons in the HL remained with the highest response.

7. When different PAC concentrations in the HP fraction were added, a peak of 865 daltons remained.

8. The trend of MW distribution of the TP fraction was similar to that of the HP fraction except the largest MW of HP. The peak of 865 daltons also remained like MW distribution of HP.

9. The MW distribution of the HL fraction included the majority of small MW such as 263, 330, and 580 daltons. The removal trend of MW distribution could not be identified.

CHAPTER 7



University of Technology, Sydney
Faculty of Engineering

PRODUCTIVITY ENHANCEMENT IN A CROSS-FLOW ULTRAFILTRATION MEMBRANE SYSTEM THROUGH AUTOMATED DE-CLOGGING OPERATIONS

7.1 Introduction

As a consequence of increasingly stringent standards for wastewater disposal and reuse, various new treatment technologies have emerged. Dependant upon the required effluent quality, membrane processes such as microfiltration (MF), ultrafiltration (UF), nanofiltration (NF) or reverse osmosis (RO) are used. However, problems associated with continued fouling during filtration operations prevent the wide application of membrane technology.

Pretreatment has been found to effectively reduce membrane fouling, however this produces additional sludge due to the addition of a coagulant or adsorbent. Alternatively, membrane fouling can be reduced by hydrodynamic cleaning, such as higher cross-flow and long-term relaxation modes.

Operating the system at higher rates of cross-flow and/or at reduced transmembrane pressures has been found to reduce membrane fouling (Chen et al., 1997). Increased shear created through cross-flow removes the foulant layer on the membrane surface. However, these techniques result in a decreased permeate flux leading to the requirement for larger membrane systems to treat any quantity of water or wastewater and this increases the capital costs since the membrane area required will be larger.

Resistance to the cross flow membrane system caused by concentration polarization and gel layer formation are considered to be reversible by applying clean water, while strong adsorption resistance is irreversible (Chen et al., 2003). In a study by Cho et al. (2000), flux was partially restored through the introduction of distillate water to the system followed by a period of relaxation. During this process, the absence of applied pressure to the membrane successfully reversed the resistance attributed to concentration polarization. The study also involved the increased rate of cross-flow of distillate water cross-flow and this was found to successfully reverse the resistance attributed to the gel layer formation.

While the results of these techniques are promising, the usage of distillate water and the single implementation of these cleaning techniques during the final stage of the filtration process minimize their potential usage in practical applications. In this study,

periodic relation and a periodic high rate of cross-flow were trialed both independently and in a combination.

In all experiments, the time allocated to the periodic cleaning procedure was fixed at 3.3% of the production interval, to minimize the operational losses of the system. The use of varied production intervals, varied ratios of periodic relaxation and the use of a periodic high rate cross-flow were investigated. The production loss in all experiments was also maintained at 3.3% during relation period due to the absence of permeate production.

The intermittent usage of the cleaning techniques leads to an increase in the operational life of the membrane system as it reduces the degree of fouling over time. In some cases, the utilization of these techniques actually leads to a decrease in net productivity of the system; due to losses attributed to the production being ceased while cleaning being greater than the gains in permeate flux resulting from the usage of the cleaning technique. When an optimal frequency, ratio and duration of the cleaning techniques are however used, it is possible to extend the membrane life while achieving a net increase in productivity.

7.2 Theoretical

7.2.1 Net Productivity

Equation 7.1 shows the net productivity of a cross-flow membrane system operating with a periodic cleaning technique to maximize the operational permeate flux by minimizing the resistance caused by concentration polarization and/or gel layer formation.

$$Flux_{net}(\%) = \frac{J \times T_P}{J_O(T_P + T_C)} \times 100 \quad (7.1)$$

where: $Flux_{net}$ = Productivity of the cross-flow membrane system operating with periodic cleaning

J	= Permeate flux at a given time of operation (varies with time)
J_0	= Pure water permeate flux
T_P	= Duration of permeate production cycle
T_C	= Duration of cleaning cycle

In order to maximize the net flux, three parameters are vital. These are the duration of the permeate production cycle, the duration of the cleaning cycle and the permeate flux. A nonlinear relationship exists between these parameters, so in this study a fixed ratio of the cleaning duration to the permeate production duration was maintained and the resultant permeate flux was continuously measured to evaluate the effectiveness of the cleaning techniques.

7.2.2 Membrane Resistance

A series of mathematical models has been developed to represent different membrane resistances (Cho et al., 2000). The flux decline can be related to various resistances as given in Figure 7.1 and equation 7.2:

$$J = \frac{\Delta P}{\mu(R_m + R_{cp} + R_g + R_{aw} + R_{as})} \quad (7.2)$$

where μ is the dynamic viscosity (kPa•sec), R_{cp} is the resistance due to concentration polarization (m^{-1}), R_g is the resistance due to the gel layer, R_{aw} is the resistance due to weak adsorption (m^{-1}) and R_{as} is the resistance due to strong adsorption (m^{-1}).

A simple example to determine this relationship is presented in Appendix B. The following details are the protocol that was used to investigate the resistances:

- i) Step 1: pure water is first filtered through the membrane until a constant flux is obtained,
- ii) Step 2: organic-containing water is introduced and the permeate rate is monitored with time,
- iii) Step 3: after the permeate rate reaches a constant value, pure water replaces the organic-containing water and the applied pressure is released to remove concentration polarization,

- iv) Step 4: the fouled membrane is then rinsed with pure water so that the gel layer (highly concentrated organic layer) is removed from the membrane surface and pure water filtration is again performed,
- v) Step 5: the membrane is soaked in a 0.1 M NaOH solution for overnight so that weakly adsorbed organic matter on the membrane surface is desorbed, then pure water is again filtered.

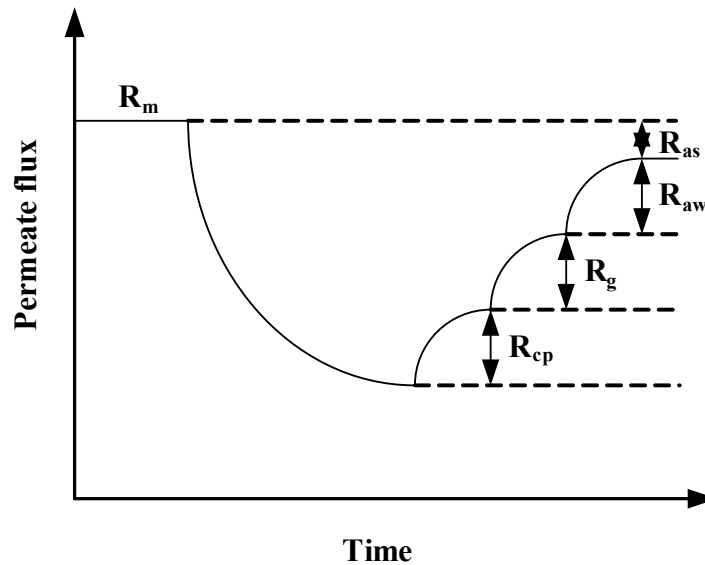


Figure 7.1 Schematic representations of resistances in series

7.2.3 Automated Operation

Figure 7.2 shows a block diagram of the control system used in this study. The SCADA interface was programmed so that the operator can simply enter the desired frequency of the cleaning technique, the cleaning type and its duration (Smith et al., 2005). The operator can also view the system statistics in real-time while the system is running. These include the operational mode, the current set points and also the exact duration of each of the automated cycles.

The programmable controller communicates directly with the SCADA interface and uses the times and modes set through the SCADA system in order to precisely generate the required control actions. The remaining times for each of the operational modes are also sent through the communications link to the SCADA system to inform the operator.

The flow rate of the system is calculated using an electronic balance and data logging software (Crown Scientific, Pty. Ltd., Australia). This gives a clear indication of the effectiveness of the cleaning techniques being investigated.

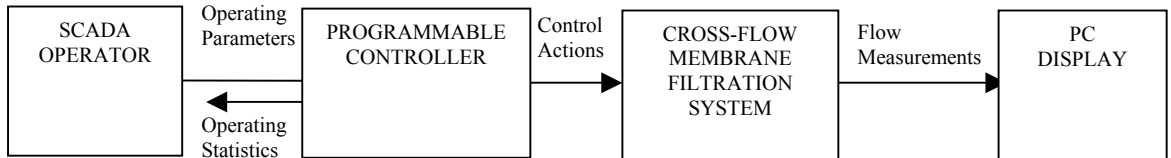


Figure 7.2 Block diagram for the control system used for periodic cleaning of the cross-flow membrane system

7.3 Experimental

7.3.1 Automation Set-up

The study was carried out with synthetic wastewater. Figure 7.3 presents the experimental schematic of the cross-flow unit (Nitto Denko, Corp.) used in this study. This system allows an investigation of the effect of periodic relaxation, a periodic high rate cross-flow and a combination of both membrane fouling and flux decline. Table 7.1 shows the status of the solenoid valves during each mode of operation.

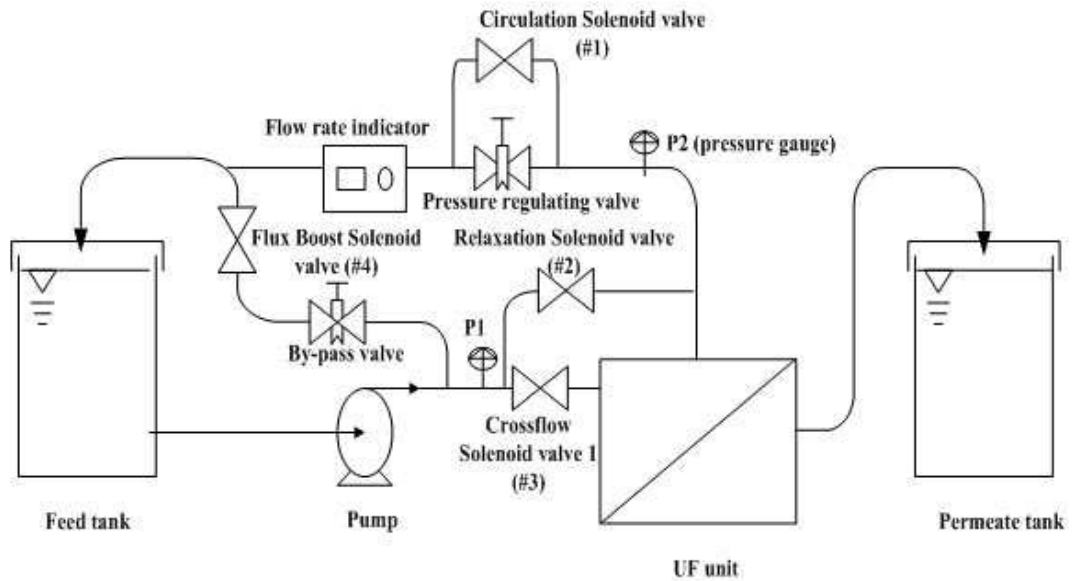


Figure 7.3 Experimental set-up of the cross-flow membrane system with the inclusion of 4 automated solenoid valves for control of the operating modes

Table 7.1 Status of solenoid valves during varied modes of operation.

Mode	Valve Position			
	Circulation (#1)	Relaxation (#2)	Cross-flow (#3)	Flux Boost (#4)
Production	Closed	Closed	Open	Open
Relaxation	Open	Open	Closed	Open
High rate Cross-flow	Open	Closed	Open	Closed

The automatic operations are selected through the operating mode popup screen in the SCADA system (Figure 7.4). The available operating selections include production only, periodic relaxation, periodic high rate cross-flow and a combination of the periodic relaxation followed by the periodic high rate cross-flow.

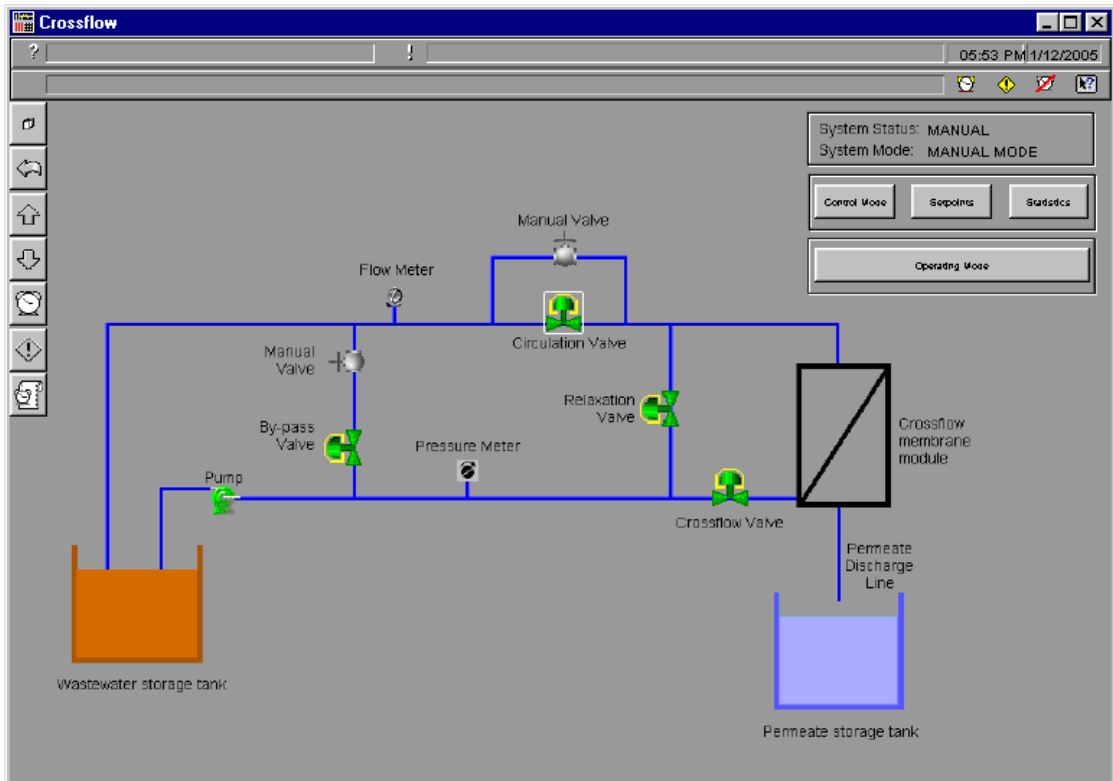


Figure 7.4 Operating mode popup screen in the SCADA system with Windows application

During the production only operating mode, the system operates indefinitely with no cleaning. During this mode of operation, the circulation (valve #1) and relaxation (valve #2) solenoid valves are closed and the cross-flow (valve #3) and flux boost (valve #4) solenoid valves are opened. This represents the traditional operating configuration for a cross-flow membrane system.

During the periodic relaxation operating mode, the system operates in a cycle alternating between production and relaxation modes. The valve operation during the production mode is the same as described in the production only operating mode, however periodic modes of relaxation intermittently operate on the membrane system.

During the relaxation mode of operation, the cross-flow (valve #3) solenoid valve is closed and the circulation (valve #1), relaxation (valve #2) and flux boost (valve #4) solenoid valves are opened. The frequency and duration of the periodic relaxation operating mode are set through the set-points popup display.

During the periodic high rate cross-flow operating mode, the system operates in a cycle alternating between production and high rate cross-flow modes. The valve operation during the production mode is the same as described in the production only operating mode, however periodic high rate cross-flow intermittently operate on the membrane system. During the high rate cross-flow mode of operation, the relaxation (valve #2) and flux boost (valve #4) solenoid valves are closed and the circulation (valve #1) and cross-flow (valve #3) are opened. The frequency and duration of the periodic high rate cross-flow mode are set through the set-points popup display.

The final system operating mode follows each production cycle with a periodic relaxation followed by a period of high rate cross-flow. The frequency and duration of the periodic relaxation and the periodic high rate cross-flow are set through the set-points popup display.

As a result of controlling these 4 valves, the cross-flow rate and the transmembrane pressure are altered. Table 7.2 shows the measured membrane cross-flow rates and the transmembrane pressures for each mode of operation. During the relaxation period, a small (50 kPa) transmembrane pressure results due to the application of the cleaning technique while the membrane is left in place.

Table 7.2 Membrane cross-flow rate and transmembrane pressure for each operating mode

MODE	Cross-flow rate (m/s)	Transmembrane Pressure (kPa)
Production	0.47	100, 300 or 500
Relaxation	0	50
High rate Cross-flow	1.61	65

A key feature of this system was the control of the circulation solenoid valve situated in parallel with the pressure regulating valve. Problems associated with increased rates of cross-flow that caused increased transmembrane pressures were alleviated, by opening the circulation (valve #1) and cross-flow (valve #3) during the high rate cross-flow as this allowed simultaneous increased rates of cross-flows at a decreased transmembrane pressures.

7.4 Results and Discussion

7.4.1 Effect of Different Pressures

Figure 7.5 shows the results of the flux decline when the system was operated at various transmembrane pressures (TMP) of 100 kPa, 300 kPa and 500 kPa without any cleaning. When the system was operated at 100 kPa, the fouling was minimal (less than 12%). When the system was operated at 300 kPa there was significant fouling and this increased to 38%. When the system was operated at 500 kPa, the fouling was severe and this increased to 56%. This suggests that as the pressure increases, the fouling significantly increases. Further experiments were then conducted at a transmembrane pressure of 300 kPa. This allowed the relative merits of various cleaning techniques to be evaluated.

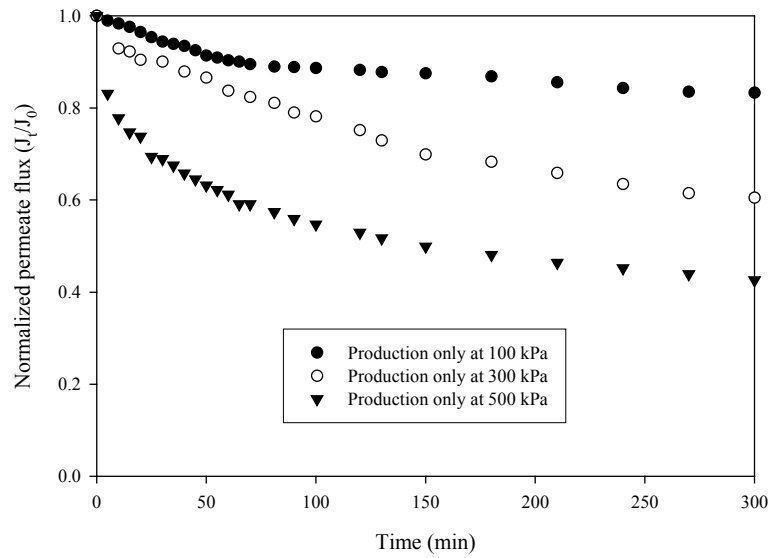


Figure 7.5 Results of the flux decline versus time for the three different values of transmembrane pressure (UF membrane used = NTR 7410; MWCO of 17,500 daltons, crossflow velocity = 0.5 m/s, transmembrane pressure = 100, 300 and 500 kPa, Reynold's number: 735.5, shear stress: 5.33 Pa)

Figure 7.6 presents different membrane resistances at pressures of 100, 300, and 500 kPa. The resistances of the concentration polarization and gel layer were relatively small compared with weak adsorption resistance (R_{aw}). As the transmembrane pressure increased, the resistance of weak adsorption significantly increased. The recovery of membrane flux from fouled membranes after the caustic chemical cleaning was 100% for all membranes. Therefore, the dominant fouling with synthetic wastewater was caused by the weak adsorption. This fouling could be reduced through applying caustic chemical cleaning. Cho et al. (2000) reported that when there is a higher portion of fouling by weak adsorption, caustic chemical cleaning is required.

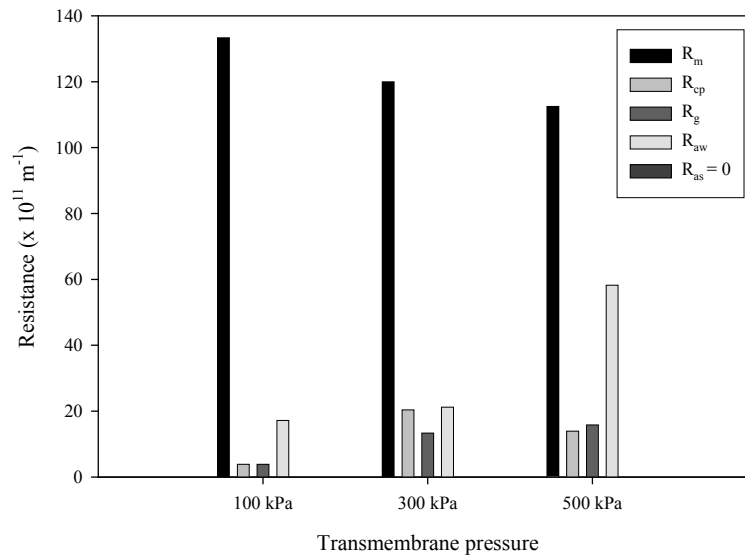


Figure 7.6 Different membrane resistances by fouling and flux decline at different pressures

7.4.2 Effect of Relaxation, Cross-flow and Relaxation and Cross-flow Cleanings

A series of experiments were then conducted to determine the effects of periodic relaxation, periodic high rate cross-flow and simultaneous periodic relaxation and periodic high rate cross-flow on the rate of flux decline. The four experiments are:

- i) Membrane filtration with no cleaning; in this study, it is referred to as production only.
- ii) Production cycles of 30 minutes followed by 1 minute of periodic relaxation.
- iii) Production cycles of 30 minutes followed by 1 minute of periodic high rate cross-flow.
- iv) Production cycles of 30 minutes followed by 30 seconds of periodic relaxation followed by 30 seconds of periodic high rate cross-flow.

The experiments were conducted with an operational loss of 3.2% due to production being stopped for 1 minute after every 30 minutes of production for the periodic cleaning (relaxation, high rate cross-flow or both).

Figure 7.7 shows the results of the flux decline with time for each of the cleaning methods adopted. Relaxation was found to be slightly more effective than the high rate cross-flow. This may be because there is a slightly higher TMP during the high rate cross-flow and also that there is a cross-flow continuously operating during production (although it is at a significantly lower flow rate and a higher TMP). A relaxation followed by a high rate cross-flow was found to give the best results, even though both durations were halved in order to maintain the operational losses at 3.2% for all cleaning techniques.

When operated individually, relaxation and the high rate cross-flow only provided an increase in flux of only approximately 2.5%. Considering the usage of these techniques incurs an operational loss of 3.2%, there is an actual loss in productivity resulting from their usage. However, the membrane life can be extended as the rate of flux decline is slightly less.

When both relaxation and the high rate cross-flow were used, there was an increase in flux of approximately 11%. This resulted in a net productivity improvement of 7.8%, after the operational losses were taken into account. Therefore, when operating under these conditions, there is both an extension to the life of the membrane and also an improvement in productivity of the system.

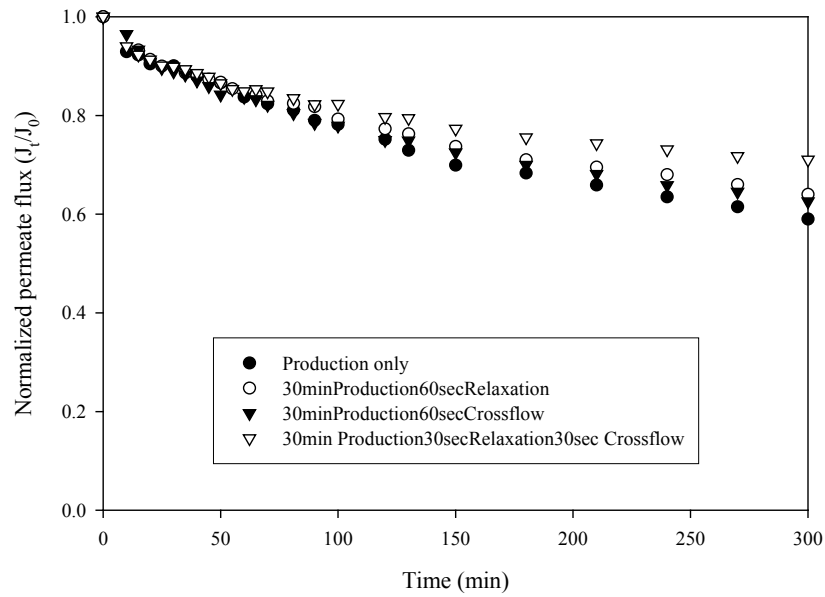


Figure 7.7 Results of the flux decline versus time for different cleaning techniques (UF membrane used = NTR 7410; MWCO of 17,500 daltons, crossflow velocity = 0.5 m/s, transmembrane pressure = 300 kPa, Reynold's number: 735.5, shear stress: 5.33 Pa)

Figure 7.8 shows the variation of different resistances for the relaxation and cross-flow modes. When the relaxation and cross-flow modes were applied, the resistances associated with the concentration polarization and the gel layer significantly decreased. However, the fouling caused by weak adsorption remained high. This indicates that these modes are most likely to improve the flux decline by the fouling of the concentration polarization and the gel layer and not weak and strong adsorption.

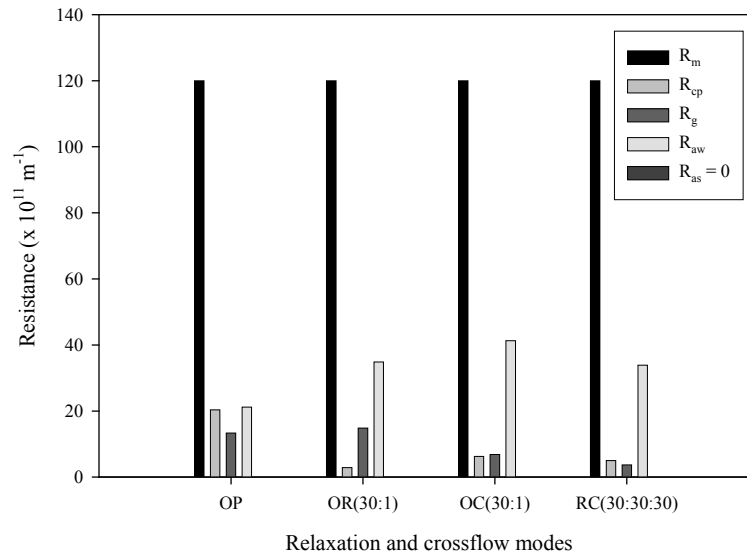


Figure 7.8 Different membrane resistances by fouling and flux decline at different cleaning techniques

7.4.3 Effect of Different Cleaning Intervals

The above experiments showed that the best results in terms of flux decline were obtained when relaxation was followed by the high rate cross-flow mode. Another set of experiments was conducted with increased production period. The relaxation and high rate cross-flow durations were modified accordingly. The operational losses were maintained at 3.2%. The five experiments are listed below:

- i) Production only
- ii) Production cycles of 15 minutes followed by 15 seconds of periodic relaxation followed by 15 seconds of periodic high rate cross-flow.
- iii) Production cycles of 30 minutes followed by 30 seconds of periodic relaxation followed by 30 seconds of periodic high rate cross-flow.
- iv) Production cycles of 60 minutes followed by 60 seconds of periodic relaxation followed by 60 seconds of periodic high rate cross-flow.
- v) Production cycles of 90 minutes followed by 90 seconds of periodic relaxation followed by 90 seconds of periodic high rate cross-flow.

Figure 7.9 shows the results of the flux decline with time for each of the experiments. Table 7.3 indicates that the effectiveness of the cleaning interval (relaxation and cross-flow) diminishes with increased durations past the 60 second relaxation and 60 second cross-flow point. This is indicated by an additional flux recovery of only 0.12% for the additional 1 minute of cleaning in the case of the 90 second relaxation and the 90 second cross-flow. Prior to this additional interval, the rate of flux recovery was approximately 1.2% for each 30 seconds of cleaning. Figure 7.10 also presents the resistance for different production periods. The fouling from only weak adsorption was significant when a 60 second relaxation and 60 second cross-flow cleaning was adopted.

In the case of the short-term experiments using the production periods of 15 and 30 minutes, the flux declined to approximately 2% and 4%, respectively (Figure 7.9). The flux decline continued after 90 minutes of production and it reached almost 5%, suggesting that the utilization of the cleaning method resulting in a 3.2% operational loss is eventually justified. It is therefore evident that a critical point exists where the application of a periodic cleaning technique is optimal.

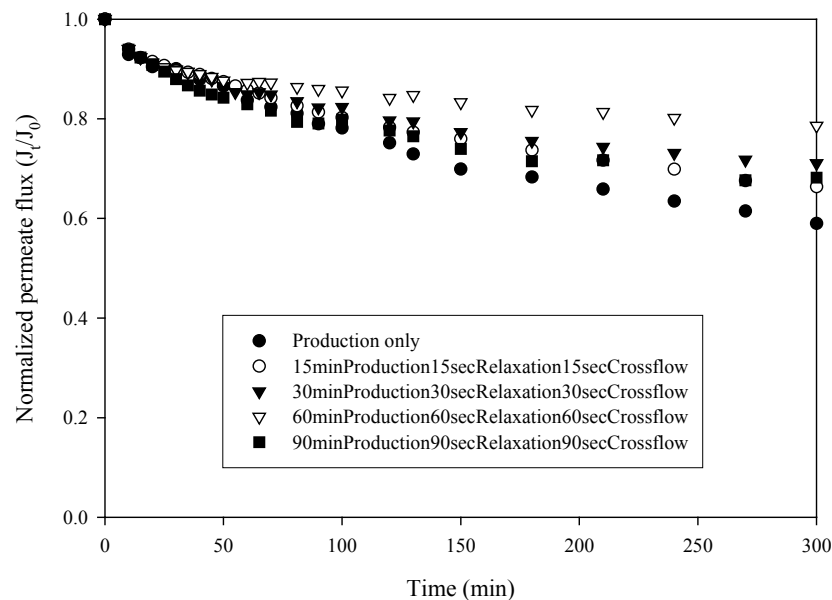


Figure 7.9 Results of the flux decline versus time for different production periods (UF membrane used = NTR 7410; MWCO of 17,500 daltons, crossflow velocity = 0.5 m/s, transmembrane pressure = 300 kPa, Reynold's number: 735.5, shear stress: 5.33 Pa)

Table 7.3 Flux recovered for each varied production interval

Experimental Condition	Total Flux recovered (%)
15minProd,15secRel,15secCross	0.625
30minProd,30secRel,30secCross	1.22
60minProd,60secRel,60secCross	2.88
90minProd,90secRel,90secCross	3

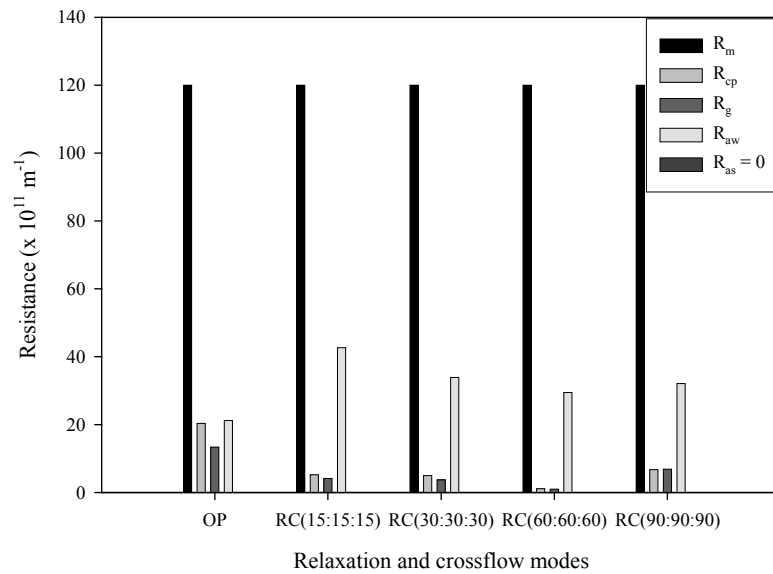


Figure 7.10 Different membrane resistances by fouling at different production periods

7.4.4 Modeling of Effective Flux Loss

Figure 7.11 shows the results of the variation of the recovered permeate flux with different cleaning intervals. It can be seen that the effectiveness of the cleaning interval (relaxation and cross-flow) diminishes with durations greater than 60 seconds relaxation and a 60 second cross-flow point. This is indicated by an additional flux recovery of only 0.12% for the additional 1 minute of cleaning in the case of the 90 seconds relaxation and the 90 second cross-flow. Prior to this additional interval, the rate of flux recovery was approximately 1.2% for each 30 seconds of cleaning.

Therefore, in this study it was found that the cleaning of the membrane for larger than 120 seconds was relatively unproductive.

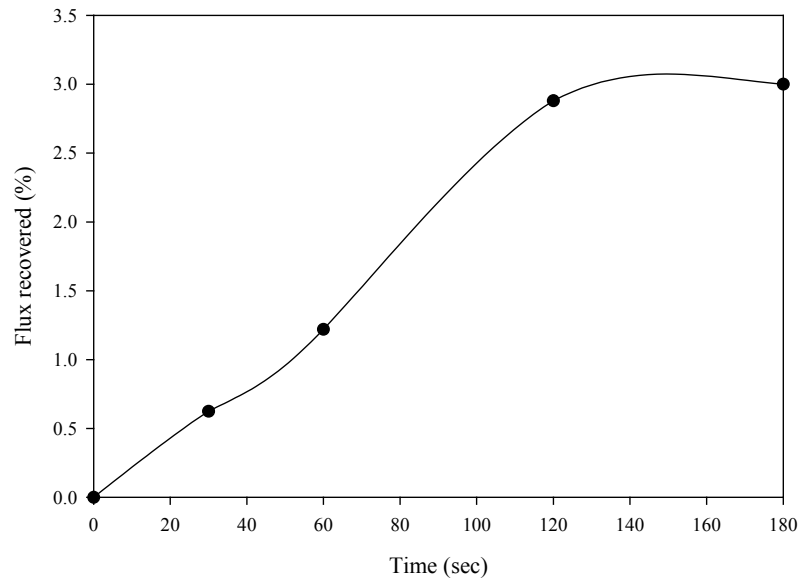


Figure 7.11 Results of the flux recovery versus cleaning time used with the relaxation and the high rate cross flow

Figure 7.12 shows the variation of the total flux loss with time. For the experimental conditions used in this study, the permeate flux decline was rapid during the first 30 minutes and then slowed down significantly.

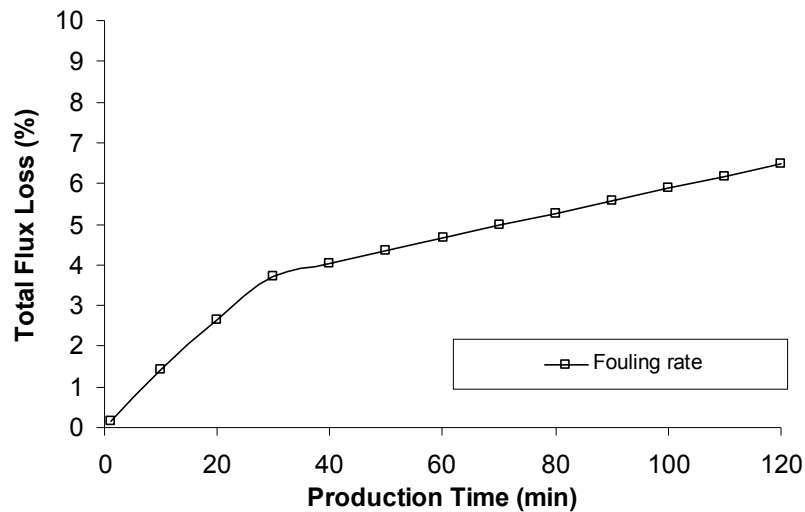


Figure 7.12 Results of the flux decline versus the production time used at a transmembrane pressure of 300 kPa

Using the results shown in Figures 7.11 and 7.12, the net permeate flux loss (%) was calculated to evaluate the effectiveness of different cleaning methods.

The net permeate flux loss shown in Figure 7.13 includes the operational loss due to the cleaning period used, the rate of flux decline of the membrane and also the flux recovered due to the cleaning operation for each of the cleaning intervals. For all of the cleaning intervals, there was a turning point as the production interval was extended. This occurs because the extended production intervals continually increased the ratio of production to cleaning, but eventually a minimum result was achieved where cleaning losses become less than the recovered flux. For all cleaning durations calculated however, there was no benefit realized if the periodic clean was utilized prior to approximately 50 minutes of production for the experimental conditions used in this study.

Equation 7.3 shows the net permeate flux loss formulae.

$$NetPermeateFluxLoss(\%) = Fouling_Rate(\%) + Operational_Loss(\%) - Flux_recovered(\%) \quad (7.3)$$

Figures 7.11 and 7.12 are used to calculate the fouling rate (%) and flux recovered (%) for the varied production intervals, with the operational loss calculated as shown in equation 7.4.

$$Operational_Loss(\%) = \frac{t_{cleaning_period}}{t_{cleaning_period} + t_{production_period}} \times 100 \quad (7.4)$$

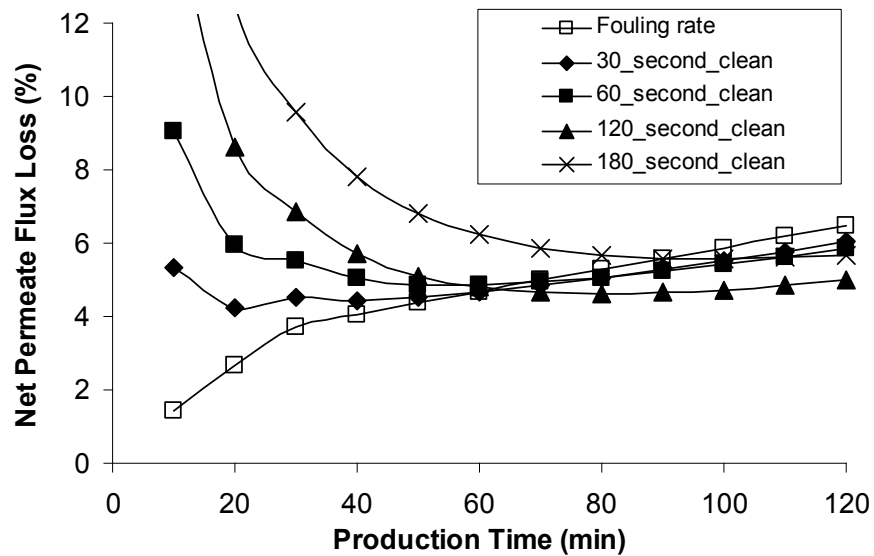


Figure 7.13 Results of the net flux loss versus the production time used

7.4.5 Effect of Cleaning Time Ratio

Figure 7.14 shows the experimental results obtained when the optimal production duration of 60 minutes was used with different ratios of relaxation and a relatively high rate cross flow velocity. The experimental conditions are listed below:

- i) Production only without any cleaning
- ii) Production cycles of 60 minutes followed by 20 seconds of periodic relaxation followed by 100 seconds of periodic high rate cross-flow.
- iii) Production cycles of 60 minutes followed by 60 seconds of periodic relaxation followed by 60 seconds of periodic high rate cross-flow.
- iv) Production cycles of 60 minutes followed by 100 seconds of periodic relaxation followed by 20 seconds of periodic high rate cross-flow.

Although the production and cleaning periods were maintained to keep the operational loss of 3.2%, it was found that the best results in terms of flux maximization occurred when there was an equal time allocated for the relaxation period and the high rate cross flow period. Interestingly, there was a higher rate of flux recovery when the period of relaxation was extended, however these gains were eroded quickly once production started with an increased rate of flux decline. Possibly, during the extended relaxation period, the foulant layer reduction that helped with the initial flux recovery did not have sufficient time to be completely removed due to the shortened cross flow duration. Thus, when production started again, there was the higher rate of flux decline. Figure 7.15 presents the resistances at different cleaning ratios.

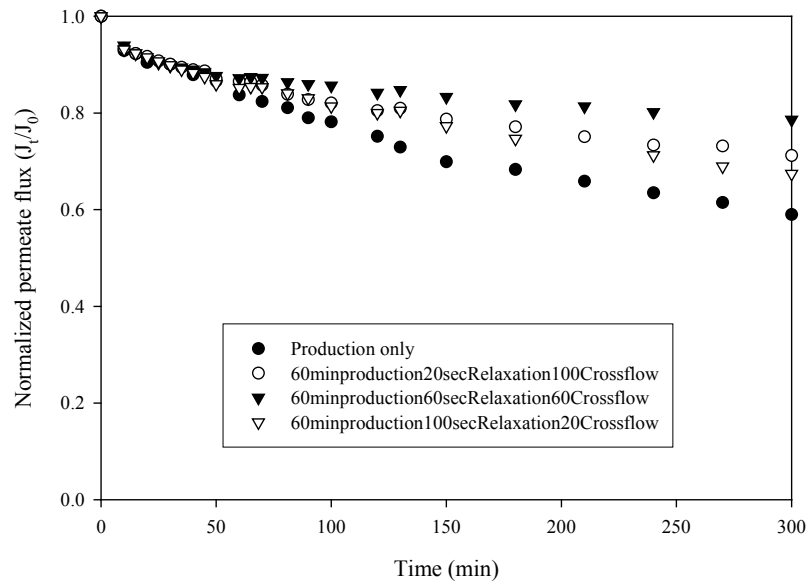


Figure 7.14 Results of the flux decline versus time for the 3 different cleaning ratios (UF membrane used = NTR 7410; MWCO of 17,500 daltons, crossflow velocity = 0.5 m/s, transmembrane pressure = 300 kPa, Reynold's number: 735.5, shear stress: 5.33 Pa)

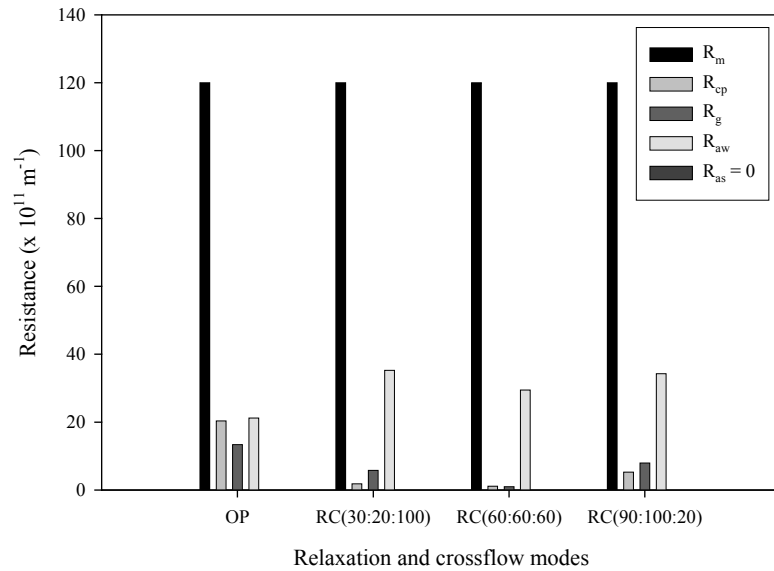


Figure 7.15 Different membrane resistances by fouling and flux decline at the 3 different cleaning ratios

7.4.6 Effect of Different Pressures with Optimum Cleaning Conditions

Figure 7.16 indicates that the periodic cleaning was less effective when the system was operated at 100 kPa and 500 kPa than when it was operated at 300 kPa. At 500 kPa, the cleaning resulted in a rapid flux improvement, but these gains were quickly lost when production was restarted. At 100 kPa, the cleaning resulted in an improvement in flux throughout the entire experiment; however these improvements were less than the operational losses encountered during cleaning. This was largely due to the fouling being quite low when the system is operated at a low pressure.

Therefore, the only benefit of cleaning at 100 kPa and 500 kPa would be to extend the membrane life.

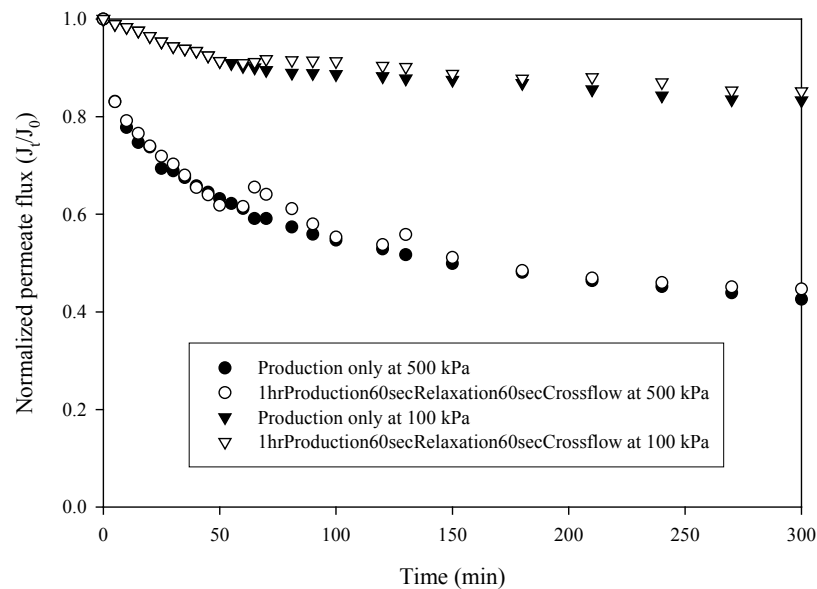


Figure 7.16 Results of the flux decline versus time for the optimal cleaning conditions (UF membrane used = NTR 7410; MWCO of 17,500 daltons, crossflow velocity = 0.5 m/s, transmembrane pressure = 100 and 500 kPa, Reynold's number: 735.5, shear stress: 5.33 Pa)

7.4.7 Effect of Flocculation with Optimum Cleaning Conditions

Figure 7.17 presents the effect of pretreatment of flocculation associated with the optimum cleaning conditions such as 1 hr production – 60 second relaxation – 60

second cross-flow. Here, the supernatant of flocculation underwent UF without any prefilters. The permeate flux after flocculation was not improved with the hydraulic cleaning method and may be due to the reduction of initial concentration and/or large MW of the feed. As the initial concentration and/or large MW of the feed after flocculation decreased, the cleaning roles of relaxation and cross-flow were marginal. This phenomenon can be considered in more detail in terms of the variation of resistances (Figure 7.18). All the resistances (R_{cp} , R_g and R_{aw}) after flocculation at 21 mg-Fe/L $FeCl_3$ were minimized. This suggests that there is not enough fouling to be removed by the cleaning of the relaxation and cross-flow.

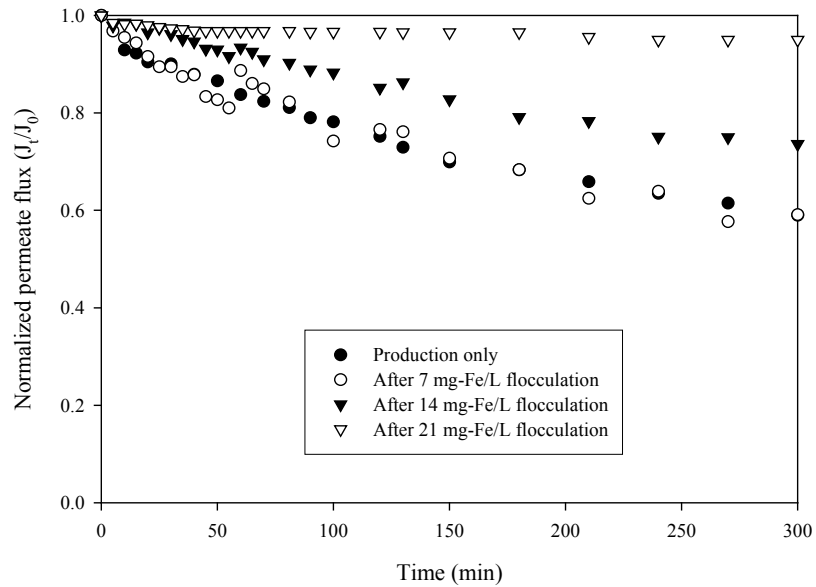


Figure 7.17 Results of the flux decline versus time after $FeCl_3$ flocculation for the optimal cleaning conditions (UF membrane used = NTR 7410; MWCO of 17,500 daltons, crossflow velocity = 0.5 m/s, transmembrane pressure = 300 kPa, Reynold's number: 735.5, shear stress: 5.33 Pa)

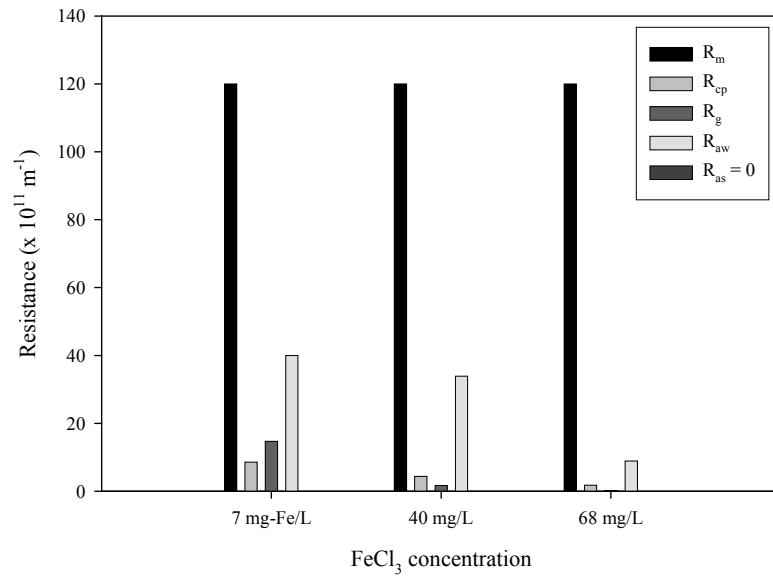


Figure 7.18 Different membrane resistances by fouling and flux decline at different FeCl₃ concentrations

7.4.8 Effect of Adsorption with Optimum Cleaning Conditions

Figure 7.19 shows the effect of pretreatment of PAC adsorption combined with the cleaning conditions. The supernatant after PAC adsorption was used for the UF experiments. Here, it should be noted that a small amount of PAC particle still remained in the pretreated water. The flux after PAC adsorption with the automated cleaning could not increase with 0.1 g/L and 1 g/L PAC adsorption and may be due to the coated PAC particle on the membrane surface. Thiruvengkatachari et al. (2005) reported that the coated membrane with PAC can effectively stop the fouling agents in the wastewater reaching the membrane pores and thereby limit membrane fouling. They also found that, without any pretreatment or addition of PAC in the tank, the PAC-coated membrane also had the ability to retain organic materials. The resistances after PAC adsorption are shown in Figure 7.20.

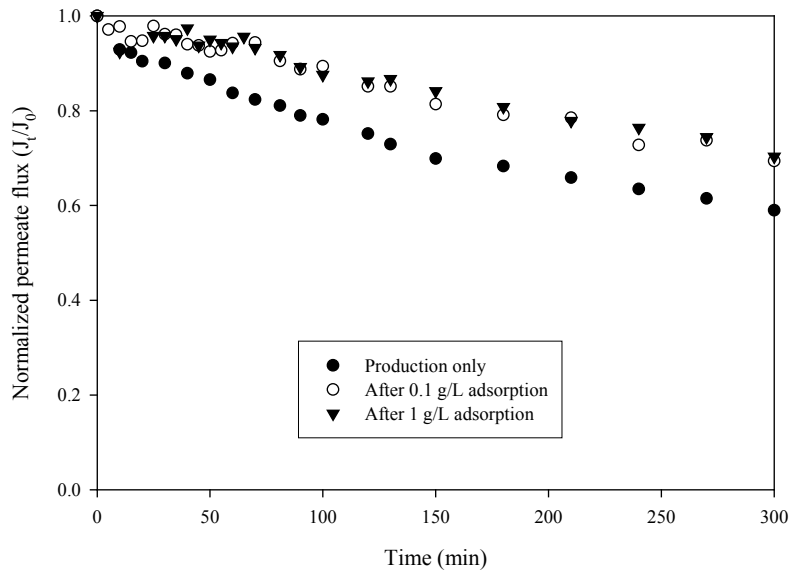


Figure 7.19 Results of the flux decline versus time after adsorption for the optimal cleaning conditions (UF membrane used = NTR 7410; MWCO of 17,500 daltons, crossflow velocity = 0.5 m/s, transmembrane pressure = 300 kPa, Reynold's number: 735.5, shear stress: 5.33 Pa)

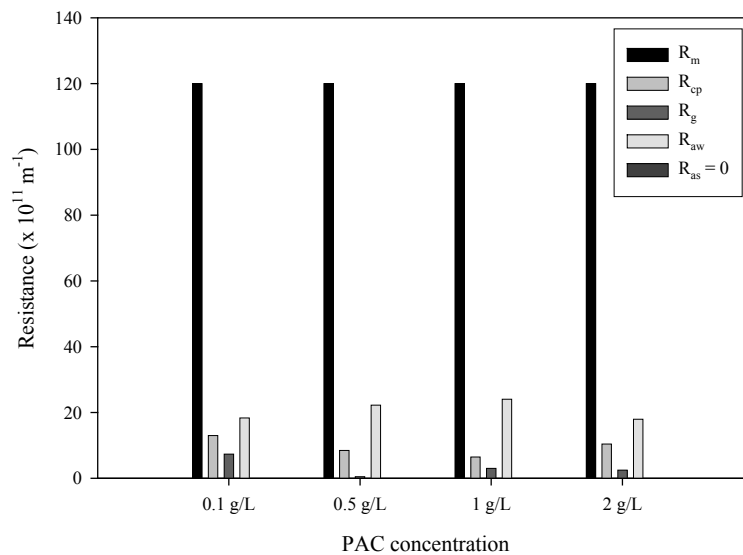


Figure 7.20 Different membrane resistances by fouling and flux decline at different PAC concentrations

7.5 Concluding Remarks

In this chapter, the effect of different hydraulic cleaning methods was investigated with the cross-flow UF unit. The cleaning methods in the SCADA system consisted of relaxation, high rate cross-flow and relaxation and high rate cross-flow. The results led to the following conclusions:

1. Membrane fouling in a cross flow ultrafiltration unit can be minimized by increasing the crossflow velocity or decreasing the operational transmembrane pressure. However, both of these techniques decrease the net productivity of the system and lead to larger sized membrane systems being required for treating a given quantity of wastewater.
2. Unlike backflushing, the use of periodic relaxation and a period high rate of cross flow at a decreased transmembrane pressure passively cleans the membrane, therefore requiring no permeate. However, during the cleaning operation, no permeate is produced.
3. A cleaning protocol utilizing a periodic relaxation step and/or a periodic increased cross flow rate at a decreased pressure can lead to productivity improvements and an increase in the operational lifetime of the membrane.
4. If the optimal frequency and duration of the cleaning step is used, a net productivity increase of 14.8% is achievable and a significant extension to the membrane's life results.
5. If the cleaning techniques used are non-optimal, the membranes operational lifetime is extended, however there is a net decrease in productivity due to the flux

improvements being unable to recover losses acquired while permeate production is stopped during the cleaning;

Utilizing the optimized periodic cleaning techniques developed in this study allows higher recovery rates for ultrafiltration to be achieved, without the problems of increased flux decline normally experienced when operating with high recovery rates.

CHAPTER 8



University of Technology, Sydney
Faculty of Engineering

MATHEMATICAL MODELING OF ULTRAFILTRATION ASSOCIATED WITH PRETREATMENT

8.1 Introduction

The application of membrane processes in wastewater treatment has increased since the appearance of synthetic asymmetric membranes in 1960 (Ridgway et al., 1996). A number of mathematical models have also been developed to describe membrane filtration. One approach has been to use transport modeling. The transport models developed have been classified into different groups: i) porous and nonporous membrane, ii) organic and inorganic and iii) different sizes of organic matter (OM).

The transport models developed for nonporous membranes (NF and RO) consist of three types: i) homogeneous membrane models (solution-diffusion, extended solution-diffusion and solution-diffusion-imperfection models), ii) pore-based models (preferential sorption-capillary flow, finely porous and surface force-pore flow models) and iii) irreversible thermodynamic models (Kedem-Katchalsky and Spiegler-Kedem models) (Bhattacharyya and Williams, 1992). The models of porous membranes (UF and MF) can be classified into: i) basic models based on Hagen-Poiseuille equation and Kozeny-Carman relationship), ii) Knudsen flow, iii) friction model and iv) concentration polarization (CP) model (resistance in series model, osmotic pressure model and mechanistic interpretation) (Mulder, 1996).

These models can be divided into four groups in terms of organic and inorganic characteristics of solutes (Lee et al., 2004).

- i) The non-charged colloids which follow mainly the CP relationship, convection and diffusion, Nernst-Plank equation, resistance in series and cake filtration theory.
- ii) The charged colloids which involve a relationship of convection and diffusion, Donnan exclusion, extended Nernst-Plank equation, resistance in series and cake filtration theory.
- iii) General organic matter which follows the CP relationship, thermodynamic model, diffusivity, resistance in series and adsorption layers.
- iv) Ions (anions) which obey Donnan exclusion and extended Nernst-Plank equation.

Few of these equations can be applied to ultrafiltration (UF) used in wastewater treatment because of organic fouling. The models can only be semi-empirical in wastewater conditions because it contains a mixture of different organic pollutants.

One of the simplest models in membrane filtration is one which relates the flux decline with time. As time proceeds, the permeate flux decreased with membrane fouling. A number of models have been developed to represent the flux decline. These models use the system parameters (such as viscosity, pore size, membrane thickness and pressure) and flow balance equations with specific boundary conditions (Cho, 1998). It is again difficult to use these models in practical applications.

Previous work has not attempted to quantify the membrane filtration with pretreatment of biologically treated sewage effluent (BTSE) and this is probably due to the following reasons:

- i) heterogeneous nature of organic matter (OM) in BTSE,
- ii) removal of some of the OM during pretreatment, thus the characteristics of the feed to the membrane change,
- iii) addition of inorganic salt. Inorganic salts added during the pretreatment of flocculation affect the transport phenomenon, and
- iv) the decreasing initial concentration after different pretreatments changes the initial conditions.

It is therefore difficult to predict the membrane filtration when it is combined with pretreatment. Thus, it is necessary to develop simple flux decline models for practical applications with the model coefficients calibrated with experimental flux decline for specific wastewater and operational conditions.

In this chapter, three different mathematical models relating the flux decline are investigated to quantify the effects of pretreatment. The models used are: i) empirical flux decline (EFD) model, ii) series resistance flux decline (SRFD) model and iii) modified series resistance flux decline (MSRFD) model. The coefficients of each model are calculated to establish a correlation between the coefficients and the type of pretreatment for a given water and membrane system.

8.2 Theoretical

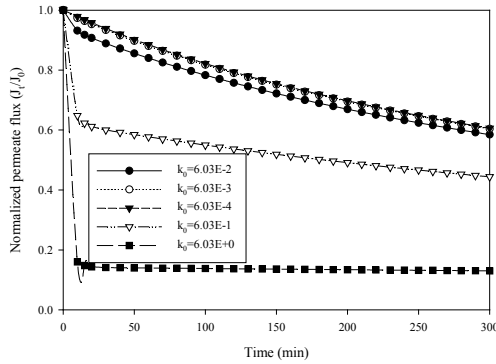
8.2.1 Empirical Flux Decline (EFD) Model

An empirical flux decline (EFD) model was introduced by Cho et al. (2002). The EFD model is one of the simple flux decline models (SFDMs) where EFD coefficients can be evaluated from experimental results using nonlinear regression. The equation consists of three flux-decline coefficients (k_0 , k_1 and d):

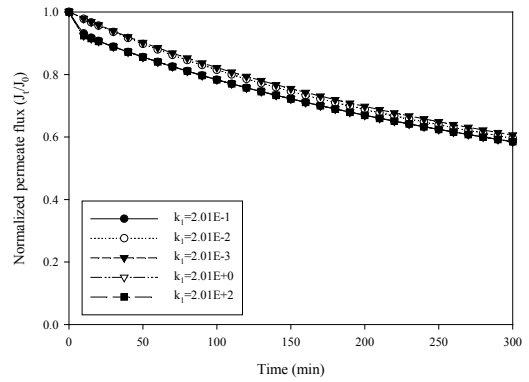
$$\frac{J_t}{J_0} = \frac{1}{1 + k_0(1 - e^{-k_1 t}) + dt} \quad (8.1)$$

where k_0 is the flux decline potential which is dimensionless, k_1 is the rate constant, and d is the flux decline kinetic constant. The unit of k_1 and d is 1/min.

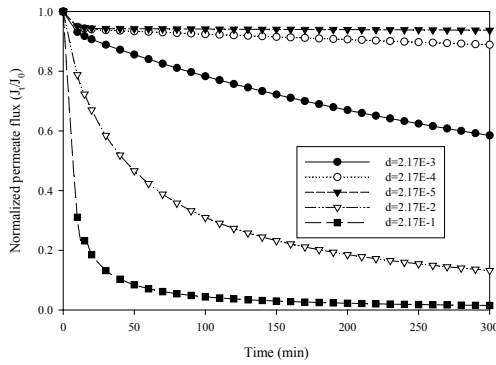
The values of k_0 , k_1 and d were calculated from the experimental flux decline curve (Figure 7.5, Chapter 7). The experimental values obtained for the UF at 300 kPa with no cleaning were used in the calculation. The values of k_0 , k_1 and d were estimated as 0.060, 0.201 and 0.002, respectively. In order to estimate the sensitivity of these three coefficients, the values of these coefficients were increased and decreased 10 and 100 times. Their effects on the flux decline were studied. The variations of k_0 , k_1 and d are shown in Figure 8.1. With changes in the k_0 , k_1 and d values, the pattern varied significantly.



a) effect of k_0 on normalized permeate flux ($k_1 = 0.201$ and $d = 0.002$)



b) effect of k_1 on normalized permeate flux ($k_0 = 0.060$ and $d = 0.002$)



c) effect of d on normalized permeate flux ($k_0 = 0.060$ and $k_1 = 0.201$)

Figure 8.1 Effect of k_0 , k_1 and d values on flux decline (UF membrane used = NTR 7410; MWCO of 17,500 daltons; crossflow velocity = 0.5 m/s; transmembrane pressure = 300 kPa ($J_0 = 1.84$ m/d); Reynold's number: 735.5; shear stress: 5.33 Pa)

To study the sensitivity of the model coefficients, the fit value was calculated using the equation 8.2:

$$Fit_Value = \sum_{all_time_points} \left(\frac{C_{coefficient}^{baseline} - C_{coefficient}^{simulated}}{C_{coefficient}^{baseline}} \right)^2 \quad (8.2)$$

here $C_{coefficient}^{baseline}$ is the experimental value of the flux decline. In this case, it is the flux values of UF conducted at 300 kPa with no cleaning. $C_{coefficient}^{simulated}$ is the simulated flux values for different model coefficients.

Hozalski and Bouwer (2000) reported that the fit value provides a quantitative comparison of the agreement between the simulation and the experimental data or the relative agreement between two different simulations. As the fit value increases, the level of agreement between the two simulations decreases. When the adjustment of an input coefficient significantly increases the fit value, the model is sensitive to that coefficient. Therefore, in this study, the sensitivity of each coefficient in the model was investigated.

Tables 8.1, 8.2 and 8.3 show the sensitivity of the k_0 , k_1 and d values using EFD coefficients. When k_0 and d were increased, the fit value increased significantly as compared to variation of k_1 . Thus, the model output in the EFD simulation is sensitive to the coefficients, k_0 and d . The k_1 value which had lower sensitivity was fixed.

Table 8.1 Effect of the k_0 value for EFD model ($k_1 = 0.201$ and $d = 0.002$)

k_0 coefficient	Fit value
0.0006	0.066
0.006	0.054
0.602	2.498
6.028	20.409

Table 8.2 Effect of the k_1 value for EFD model ($k_0 = 0.060$ and $d = 0.002$)

k_1 coefficient	Fit value
0.0002	0.0666
0.002	0.0419
2.009	0.0001
20.086	0.0001

Table 8.3 Effect of the d value for EFD model ($k_0 = 0.060$ and $k_1 = 0.201$)

d coefficient	Fit value
0.00002	3.836
0.0002	2.922
0.022	12.481
0.217	26.910

8.2.2 Series Resistance Flux Decline (SRFD) Model

In the series resistance flux decline (SRFD) model used in this study, it was assumed that concentration, pore blocking and gel layer resistances were negligible compared with adsorption resistance because the dominant fouling with synthetic wastewater was caused by weak adsorption (Figure 7.6, Chapter 7), i.e., only the resistances due to membrane and adsorption were considered (Eq. 8.3). Membrane resistance is constant whereas adsorption resistance varies with time. Adsorption can be represented by Freundlich isotherm equation (Eq. 8.4).

$$J = \frac{\Delta P}{\mu(R_m + R_a)} \quad (8.3)$$

$$R_a(t) = K_F' \times t^{\frac{1}{n'}} \quad (\text{Freundlich form}) \quad (8.4)$$

where K_F' and $1/n'$ are SRFD constants with Freundlich equation and t is filtration time (min).

Figure 8.2 presents the effect of K_F' and $1/n'$ on flux variation. The experimental results obtained with UF at 300 kPa were used to first evaluate the K_F' and $1/n'$ values. Tables 8.4 and 8.5 clearly show that the K_F' value is more sensitive than $1/n'$.

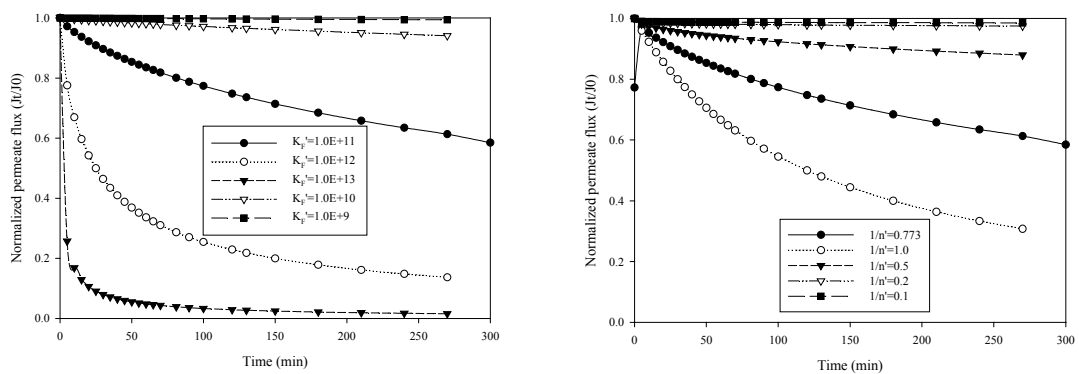


Figure 8.2 Effect of K_F' and $1/n'$ on flux decline

Table 8.4 Sensitivity of K_F' ($1/n' = 0.773$)

K_F' coefficient	Fit value
1.0E+09	2.074
1.0E+10	1.587
1.0E+12	8.588
1.0E+13	20.690

Table 8.5 Sensitivity of $1/n'$ ($K_F' = 1.0E+11$)

$1/n'$ coefficient	Fit value
0.1	2.012
0.2	1.890
0.5	1.047
1.0	1.827

8.2.3 Modified Series Resistance Flux Decline (MSRFD) Model

The modified series resistance flux decline (MSRFD) model considers the interfacial concentration (C_m) at the membrane surface in the adsorption term (Cho, 1998). The MSRFD model also takes into account the adsorption resistance only. OM accumulated on the membrane surface is considered as adsorption material. The adsorption resistances (R_a) can be measured using the interfacial concentration at the membrane surface by the concentration of the bulk and permeate. The interfacial membrane concentration (C_m) is calculated using adsorption isotherm equations.

$$J = \frac{\Delta P}{\mu(R_m + R_a)} \quad (8.5)$$

$$R_a(t) = K_F' \times C_m^{1/n'} \text{ (Freundlich form)} \quad (8.6)$$

$$R_a(t) = \frac{a'' C_m}{1 + b'' C_m} \text{ (Langmuir form)} \quad (8.7)$$

$$R_a(t) = \frac{q_m'' C_m^{\frac{1}{n''}}}{1 + K_s'' C_m^{\frac{1}{n''}}} \text{ (Sips form)} \quad (8.8)$$

The relationship between the permeate concentration (C_p) and the bulk concentration (C_b) can be given by Eq. 8.9, which is based on a film theory.

$$C_m = C_p + (C_b - C_p) \exp\left(\frac{J}{k}\right) \quad (8.9)$$

$$k = 1.62 \left(\frac{UD^2}{d_h L} \right)^{0.33} \quad (8.10)$$

where K_F'' and $1/n''$ are MSRFD constants with Freundlich isotherm constant, a'' and b'' are MSRFD constants with Langmuir, q_m'' is sorption capacity with Sips, $1/n''$ and K_s'' are with Sips, C_m is the interfacial membrane concentration (mg/L), U is the average velocity of the feed fluid (m/s), D is the diffusion coefficient of OM (m^2/s), d_h is the equivalent hydraulic diameter (m), and L is channel length (m). The diffusion coefficient was evaluated using a diffusion cell experiment.

8.2.4 Model Application

The flux declines obtained for different pressures and pretreatments was fitted using EFD, SRFD and MSRFD models. The coefficients which had lower sensitivity were fixed to a constant value. The models were solved by nonlinear regression and Nelder-Mead methods.

8.3 Results and Discussion

8.3.1 EFD Model Prediction of Experimental Results with Different Pressures

The experimental results with different pressures were compared with the corresponding simulated curves using EFD model (Figure 8.3). The detailed experimental conditions of different pressures used in this study are described in Chapter 7. The simulated curves fitted well with the experimental profiles. The flux-decline coefficients are presented in Table 8.6. As pressures increased, the flux significantly decreases with time. The k_0 and d values at 500 kPa were found to be 7 and 6 times higher compared to those at 100 kPa. The k_0 and d values (which had higher sensitivity) were found to increase with pressure.

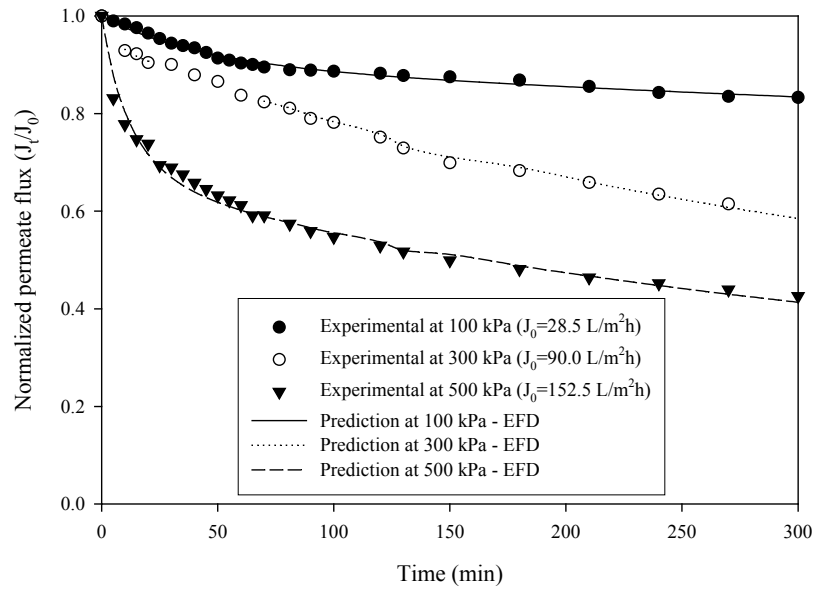


Figure 8.3 Experimental and predicted flux decline profiles with different pressures

Table 8.6 EFD model coefficients obtained from experimental data with different pressures ($k_1 = 2.15E-02$)

Pressure	k_0	d
Production only at 100 kPa	1.11E-01	2.97E-04
Production only at 300 kPa	1.83E-01	1.53E-03
Production only at 500 kPa	7.87E-01	1.76E-03

8.3.2 EFD Model Prediction of UF Experimental Results with Different Pretreatments

Figures 8.4 (a) and (b) present the results of the experimental and predicted flux profiles of UF after a pretreatment of flocculation with different doses of $FeCl_3$ and adsorption with different doses of PAC. The simulated curves fitted well with the experimental results. The flux-decline coefficients are presented in Table 8.7. The values of model coefficients are lower for UF with pretreatment. The improvement on the reduction in flux decline was observed in UF when it underwent a pretreatment of 21 mg-Fe/L flocculation. This resulted in a reduction of k_0 and d values (Table 8.7 and Figure 8.5). These values can also be used to compare the efficiency of different

pretreatments. For example, the coefficients of k_0 and d after a pretreatment of 14 mg-Fe/L flocculation were similar to those after a pretreatment with 0.1 g/L PAC adsorption (Figure 8.5). This indicates that the EFD coefficient values can be used as an index to compare and recommend the suitable pretreatment.

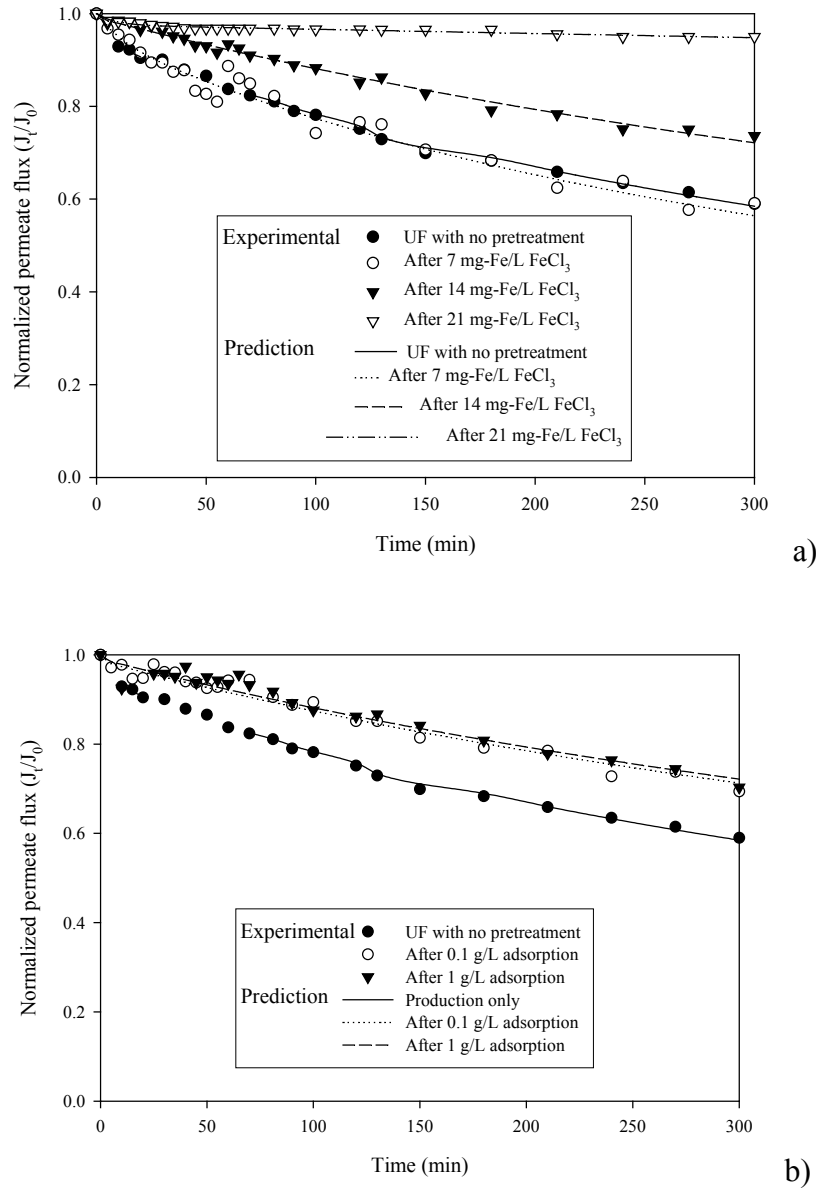


Figure 8.4 Experimental and predicted flux decline in UF after a pretreatment (UF membrane of MWCO 17,500 daltons; pressure = 300 kPa)

Table 8.7 Flux decline coefficients of EFD model with pretreatment ($k_1 = 2.15E-02$)

Pretreatment	k_0	d
UF operation at 300 kPa	1.83E-01	1.53E-03
After 7 mg-Fe/L flocculation	8.46E-02	2.26E-03
After 14 mg-Fe /L flocculation	2.42E-02	1.19E-03
After 21 mg-Fe /L flocculation	3.60E-02	5.47E-05
After 0.1 g/L adsorption	1.24E-02	1.31E-03

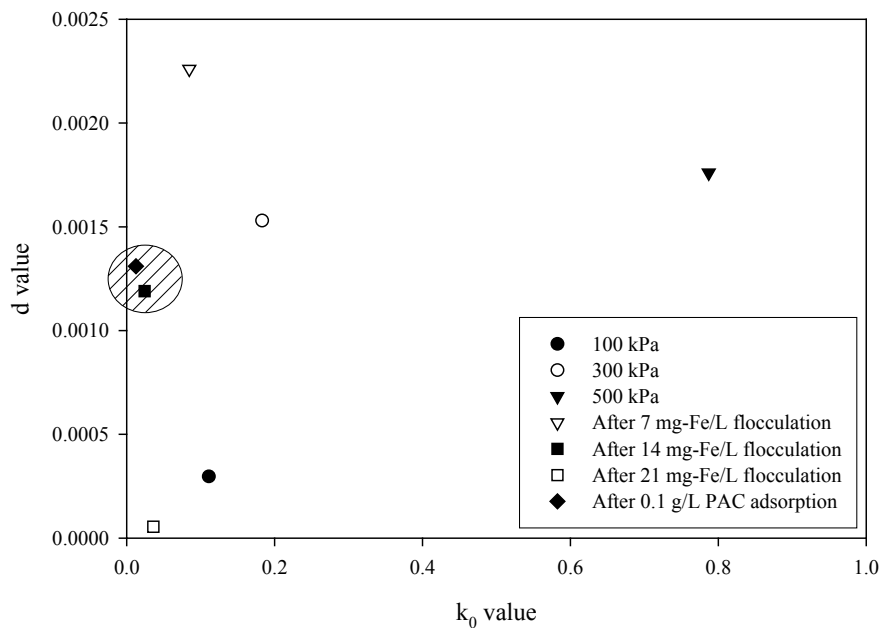


Figure 8.5 Comparison of flux-decline coefficients of EFD model

8.3.3 SRFD Model Prediction of Experimental Results

The experimental results with different pressures were compared with the simulated curves using SRFD model (Figure 8.6). Tables 8.8 and 8.9 present the SRFD model coefficients obtained for UF experiments with different pressures and pretreatments. The fit value of K_F' was more sensitive than that of $1/n'$. As pressure was increased, the coefficient of K_F' at 500 kPa increased significantly. On the other hand, as membrane fouling decreased with the pretreatment of flocculant, the value of K_F' decreased (Figure 8.6). The pretreatments of 14 mg-Fe/L flocculation ($5.12E+10$) and 0.1 g/L PAC adsorption ($5.33E+10$) also showed a similar trend. This suggests that the SRFD

coefficient values can also be used as an index to compare and suggest a suitable pretreatment.

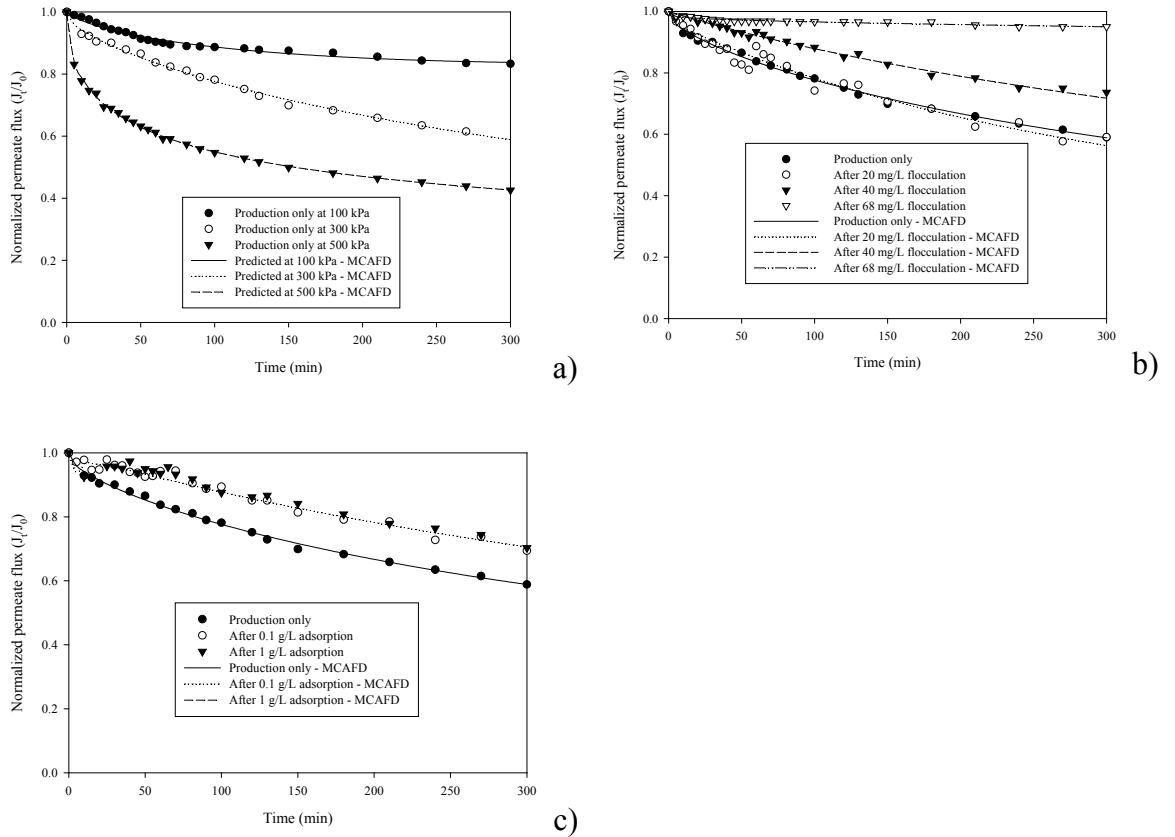


Figure 8.6 Experimental and predicted flux decline in UF after a) different pressures, b) flocculation and c) PAC adsorption (UF membrane of MWCO 17,500 daltons; pressure = 300 kPa)

Table 8.8 Flux decline coefficients of SRFD model (Freundlich) at different pressures with no pretreatment ($1/n' = 7.75E-01$)

Pressure	K_F'
100 kPa	3.96E+10
300 kPa	9.91E+10
500 kPa	2.23E+12

Table 8.9 Flux decline coefficients of SRFD model (Freundlich) with pretreatment ($1/n' = 7.75E-01$)

Pretreatment	K_F'
After 7 mg-Fe/L flocculation	1.03E+11
After 14 mg-Fe /L flocculation	5.12E+10
After 21 mg-Fe /L flocculation	1.01E+10
After 0.1 g/L PAC adsorption	5.33E+10

8.3.4 MSRFD Model Coefficients Calculated for UF with Different Pretreatments

Table 8.10 presents the variation of the bulk (C_b), permeate (C_p) and membrane (C_m) concentrations with UF filtration for a range of pressures and with pretreatments. The adsorption resistance is also shown. When the pressure was increased from 100 kPa to 500 kPa, the bulk concentration increased from 12.7 mg/L to 19.1 mg/L. However, the membrane concentration increased from 17.6 mg/L to 55.4 mg/L (more than 3 times). This caused a significant increase in adsorption resistance (up to 5.7 times when the pressure was increased from 100 kPa to 500 kPa). On the other hand, when a pretreatment of flocculation with 21 mg-Fe/L $FeCl_3$ was provided, the values of the C_b , C_m and R_a significantly decreased by 4.4, 3.1 and 12.9 times, respectively. After 0.1 g/L adsorption as a pretreatment, the values decreased by 2.2, 2.0 and 1.8 times, respectively. This suggests that pretreatment can significantly decrease membrane fouling.

Table 8.10 Concentration of organic matter and adsorption resistance

	C_b (mg/L)	C_p (mg/L)	C_m (mg/L)	R_a (m^{-1})
100 kPa	12.7	1.9	17.6	2.67E+12
300 kPa	17.0	2	38.4	8.38E+12
500 kPa	19.1	2.1	55.4	1.52E+13
21 mg-Fe/L flocculation	3.86	1.1	12.5	6.48E+11
0.1 g/L adsorption	7.59	1.5	19.6	4.62E+12

The concentration on the interfacial membrane surface (C_m) versus adsorption resistance (R_a) was calculated from the UF experimental results conducted at three different pressures (100, 200 and 300 kPa). The graphs between R_a and C_m are presented in Figure 8.7. Of the three adsorption isotherms used to calculate adsorption resistance, the Sips isotherm of the membrane fouling fitted better with the experimental results.

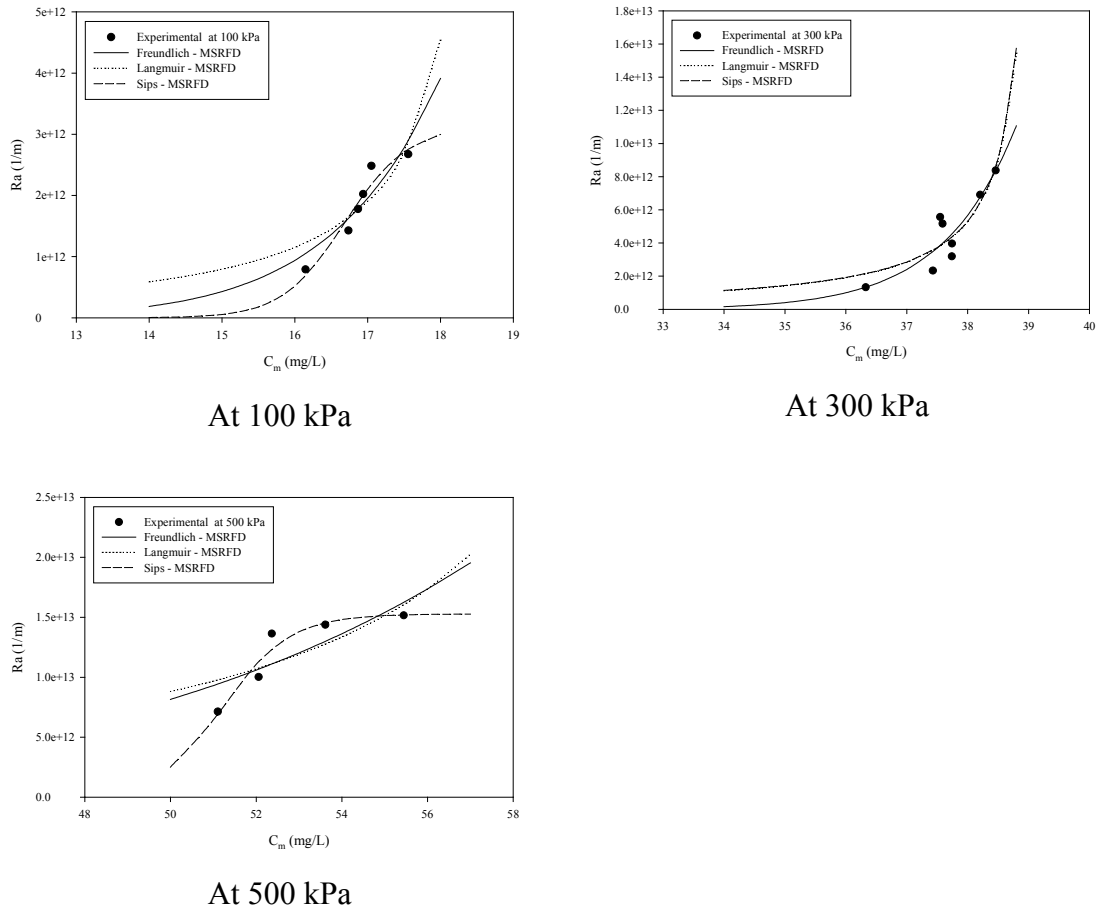


Figure 8.7 Comparison of experimental and predicted adsorption resistance values calculated from MSRFD model

8.3.5 MSRFD Model Coefficients Calculated For UF operated at Different Pressures

Table 8.11 presents the MSRFD model coefficients. An Freundlich isotherm was used with the MSRFD model. As the membrane fouling decreased, the values of K_F' and $1/n'$ significantly increased (Table 8.11 and Figure 8.8).

Table 8.11 Flux decline coefficients of MSRFD model (Freundlich) with different pressures

Cleaning	K_F''	$1/n''$
Production only at 100 kPa	1.78E+00	7.98E-02
Production only at 300 kPa	3.71E+00	7.98E-02
Production only at 500 kPa	4.80E+00	7.98E-02

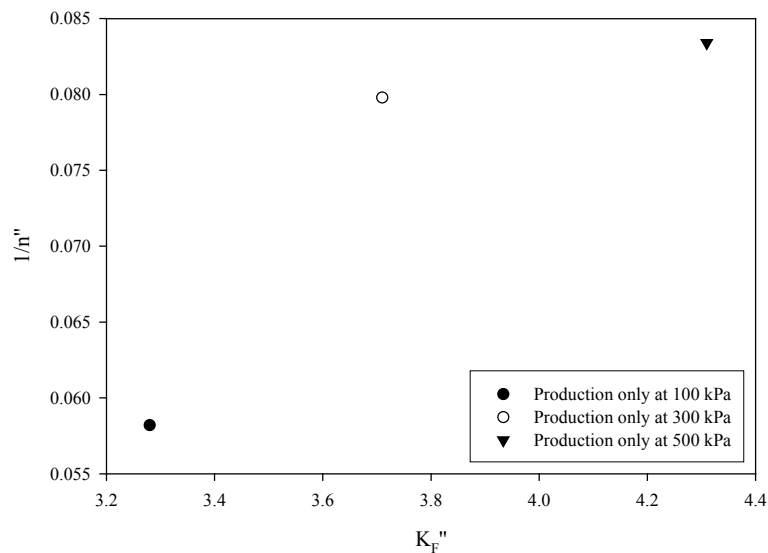


Figure 8.8 Comparison of flux-decline coefficients of MSRFD model

8.4 Concluding Remarks

In this chapter, three different semi-empirical mathematical models were investigated to semi-quantify the effects of different pressures and pretreatments on the flux decline. The three different models used were i) empirical flux decline (EFD) model, ii) series resistance flux decline (SRFD) model and iii) modified series resistance flux decline (MSRFD) model. The coefficients of each model were evaluated from experimental

results with different conditions to study the correlation of different pretreatment methods. The findings are as follows:

In the EFD model, the coefficients of k_0 and d were sensitive. This model fitted well with experimental flux decline curves. As pressure increased, the flux significantly decreased with time. The k_0 and d values at 500 kPa were found to be 7 and 6 times higher compared to those at 100 kPa. The k_0 and d values (which had higher sensitivity) were found to increase with increase in pressure. When the flux improved after the pretreatment of 21 mg-Fe/L flocculation, the k_0 and d values decreased significantly. These values can thus be used to compare the efficiency of different pretreatments. For example, the coefficients of k_0 and d after 14 mg-Fe/L flocculation were similar to those after 0.1 g/L PAC adsorption. This implies that the flux decline coefficient values by the EFD model can be used as an index to suggest flux decline and to compare the benefits of different operating conditions and pretreatments.

In the SRFD model, adsorption resistance varied with time. The K_F' was more sensitive than $1/n'$. As the pressure was increased, the coefficient also increased. On the other hand, as membrane fouling decreased with different doses of flocculant, the value of K_F' decreased. The pretreatments of 14 mg-Fe/L flocculation and 0.1 g/L PAC adsorption also showed a similar K_F' trend. This suggests that the SRFD coefficient values can also be used as an index to compare and decide on a suitable pretreatment.

In the MSRFD model, when the pressure was increased from 100 kPa to 500 kPa, the bulk concentration increased from 12.7 mg/L to 19.1 mg/L. The concentration near the membrane surface increased from 17.6 mg/L to 55.4 mg/L (more than 3 times). This caused a significant increase in adsorption resistance (up to 5.7 times). When flocculation of 21 mg-Fe/L was used as a pretreatment at a pressure of 300 kPa, the values of the C_b , C_m and R_a significantly decreased by 4.4, 3.1 and 12.9 times, respectively. After 0.1 g/L adsorption as a pretreatment, the values decreased 2.2, 2.0 and 1.8 times, respectively. These trends clearly indicate that the pretreatment can significantly decrease membrane fouling.

CHAPTER 9



**University of Technology, Sydney
Faculty of Engineering**

PHOTOCATALYSIS HYBRID SYSTEM IN THE REMOVAL OF ORGANIC MATTER FOR WASTEWATER REUSE

9.1 Introduction

Water requirements in the world are increasing with population growth and with industrialization. The reuse of wastewater after treatment will help to maintain environmental quality and relieve the unrelenting pressure on conventional natural freshwater sources. Although the effluent from the secondary and tertiary wastewater treatment can be discharged into waterways, it cannot be used for reuse purposes without further treatment. Thus, an advanced treatment technology is required to remove various organic matters, pathogenic microorganisms and persistent organic pollutants (POPs) in wastewater.

Advanced oxidation processes (AOPs), especially, photocatalysis are attractive to degrade POPs from biologically treated sewage effluent (BTSE). Photocatalytic reactions allow a complete degradation of organic pollutants into very small and harmless species without use of any chemicals. This avoids sludge production and the need for its disposal (Molinari et al., 2002; Sagawe et al., 2003). Titanium dioxide (TiO₂) catalyzed photocatalysis is used because of its capability of removing a wide range of pollutants. The photochemical stability, low toxicity and low cost are its other advantages (Arana et al., 2002; Blount et al., 2001). This process is based on the electronic excitation of a molecule or solid caused by light absorption e.g. UV light that drastically alters its ability to lose or gain electrons and promote decomposition of pollutants to harmless by-products (Molinari et al., 2002). Photo-induced electrons (e⁻) and positive holes (h⁺) are produced from TiO₂ with UV light (Eq. 9.1). These charged species can further generate free radicals (Eq. 9.2 and 9.3). The highly oxidizing positive hole h⁺ has been considered to be the dominant oxidizing species contributing to the mineralization process resulting from the TiO₂ photocatalysis (Chu and Wong, 2004).



Photocatalysis efficiency can be improved by using different chemical couplings in the solution to the surface of TiO₂. It is well known that the following effects affect the increase of organic removal in photocatalysis; i) photo-Fenton reactions ii) Cl-based

chemical flocculants, iii) acidic conditions, iv) ferric, ferrous and aluminum salts and v) PAC additions (Sarria et al., 2003; Gogate and Pandit, 2003; Lee et al., 2003; Arana et al., 2002).

9.1.1 Photo-Fenton Reaction

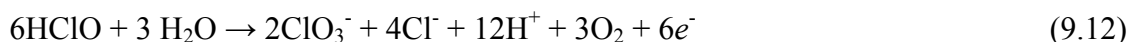
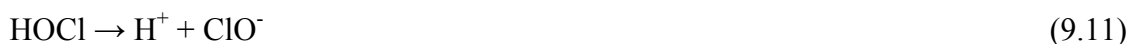
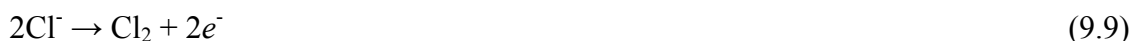
The photo-Fenton reaction produces the hydroxyl radical with a metal to ligand charge transfer. Many studies have found that photo-Fenton's systems are useful in treating a variety of contaminants including aromatic and aliphatic organic compounds (Lu et al., 1994; Doong et al., 2000; Arana et al., 2001). In the photo-Fenton process with ferric (Fe^{3+}) ions under the UV radiation, the super-oxide change and pH effect the organic activation, followed by super-oxide addition in the degradation of organic matter with ferric ions. The degradation rate of organic compounds such as phenol and nitrobenzene in the reactor with added Fe^{3+} follows first-order kinetics (Rodriguez et al., 2002). The detailed reactions related to photo-Fenton are:



9.1.2 Chloride-Based Flocculant

The chloride-based flocculants such as supporting electrolyte and a source of chloride reactant result in a superior organic and color removal (Kim et al., 2003). Chemical oxygen demand (COD) removal rates through the use of chloride-based chemical flocculants are about 10 – 17 times (70% removal) faster than those adopting sulphate-based flocculants in textile wastewater. The color removal was also high (with the highest removal up to 80% - 90%). After the flocculation with 3.25 mM FeCl_3 , the chloride concentration remained up to 14.96 mM, which means that the majority of chlorides are still present in the pretreated wastewater after flocculation. Vlyssides et al. (1999) reported that by adding 2 ml HCl (36%) as a supporting electrolyte, 86% of COD was removed

after 18 minutes of the oxidation process. The general role of the chloride reactions involved in oxidation processes are:



9.1.3 pH Effect

Organic degradation is much greater under acidic conditions (both at high and lower temperature) than normal basic conditions (Al-Rasheed and Cardin, 2003). For charged substrates of organic pollutants, the pH value has a significant effect on the photocatalytic degradation. The degradation rate constants decrease when the initial pH value exceeds 6 (An et al., 2003).

9.1.4 PAC Addition

Photocatalysis efficiency can also be improved by collecting the pollutant in the solution onto the surface of TiO_2 . Adsorbents such as PAC, silica, and zeolite are used to promote the adsorption. It is well known that PAC can be very efficient when it is mixed with TiO_2 in photocatalytic processes (Arana et al., 2002; Arana et al., 2003a; Arana et al., 2003b). Arana et al. (2002) observed that i) the combination of PAC and TiO_2 results in fast decantability in comparison with that of TiO_2 alone, ii) a TiO_2 particle distribution on the PAC surface yields in a homogeneous particle size distribution and iii) the rate of organic removal by the PAC and TiO_2 was six times higher than that with TiO_2 alone.

None of the previous studies dealt with the synergistic effect of PAC adsorption and TiO_2 photocatalysis in removing EfOM from BTSE. Most specifically, no study discussed the

organic degradation in terms of MW distribution of organic matter. In order to investigate the synergetic effect in detail, it is necessary to study the removal of organic matter of different MW ranges. Hence, this study experimentally evaluated the advantages of the chemical coupling of photocatalytic reaction with PAC adsorption. The synergy effects of photooxidation and flocculation were also studied using i) chloride-based flocculants (poly aluminum chloride and ferric chloride) and ii) sulphate-based flocculants (ferrous sulphate and aluminum sulphate). Finally, the application of a photocatalysis hybrid system in real wastewater was evaluated.

9.2 Comparison of Nanofiltration with Flocculation-Microfiltration-Photocatalysis Hybrid System

This first part deals with comparison of effluent quality of nanofiltration (NF) with that of a photocatalysis hybrid system.

9.2.1 Flocculation-Microfiltration-Photocatalysis Hybrid System

9.2.1.1 DOC Removal

The effect of photocatalysis (with TiO_2 as catalyst) was investigated after a pretreatment of ferric chloride flocculation and microfiltration as prefilter. The experiments were conducted with synthetic wastewater. As can be seen in Figure 9.1, the DOC removal of photocatalysis alone was 37% (up to 6 hours) and 60% (after 17 hours). The pretreatment of flocculation followed by microfiltration led to a higher DOC removal efficiencies (up to 96.6%). Similar trends were observed by Gogate and Pandit (2004). They reported that sensitizers or catalysts such as ferrous, silver, and manganese ions, can also be used to improve the treatment efficiency of the photocatalytic oxidation process.

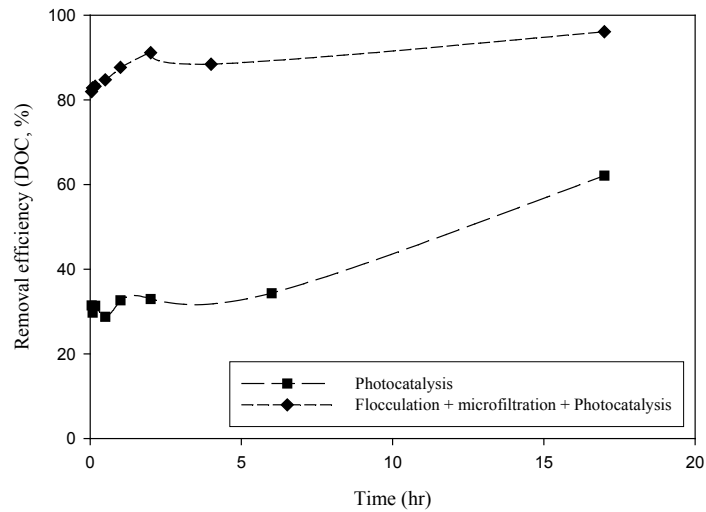


Figure 9.1 DOC removal by photocatalysis with and without pretreatment ($T = 25\text{ }^{\circ}\text{C}$; Air = 1.5 VVM; $\text{TiO}_2 = 1\text{ g/L}$ without pretreatment; UV lamp intensity = 8 W; C_0 and C = influent and effluent DOC concentration)

9.2.1.2 Molecular Weight Distribution

The MW distribution of the influent and effluent of the photocatalysis was determined (Figure 9.2) and the large MW organics were removed by TiO_2 adsorption. The slight decrease of the small MW occurred over time (up to 30 minutes). The UV response of the small MW organics increased after 30 minutes to 6 hours of an experimental run. After that, the intensity of the small MW organics decreased gradually. These experimental results imply that at an initial state, the photocatalysis breaks the large MW organics and then with time, the small MW organics are further oxidized during photocatalysis process.

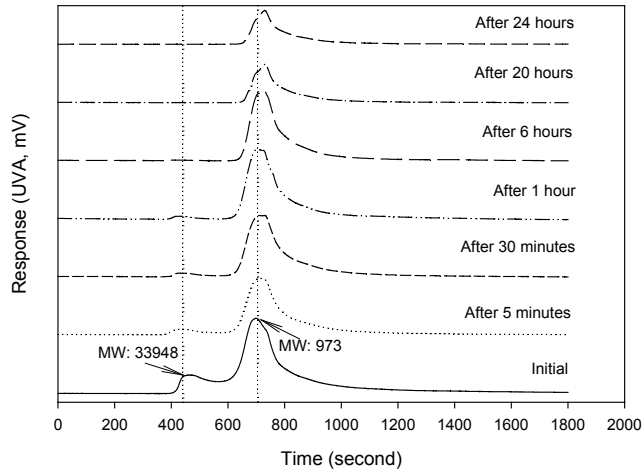


Figure 9.2 MW size distributions of synthetic wastewater with photocatalysis at different times ($T = 25\text{ }^{\circ}\text{C}$; air = 1.5 VVM; $\text{TiO}_2 = 1\text{ g/L}$ without pretreatment; UV lamp intensity = 8 W)

Figure 9.3 shows the response versus elapsed time graph of the effect of photocatalysis after pretreatments of flocculation and MF. As can be seen in Figure 9.3, practically all the organic matters (both small and large MW organics) were removed by employing flocculation and MF prior to photocatalysis. An additional mechanism for superior organic removal by the hybrid system could be due to the photo-Fenton process ($h\nu/\text{Fe}^{3+}/\text{H}_2\text{O}_2$ or O_2) (Sarria et al., 2003).

It is possible to represent the synthetic organic matter (SOM) degradation by a simplified schematic as shown in Figure 9.4. A reduction-oxidation cycle of Fe^{3+} - Fe^{2+} and the photocatalysis of Fe^{3+} aqueous complexes [SOM-Fe^{3+}] seems to be a possible way to represent the photo-Fenton degradation of SOM.

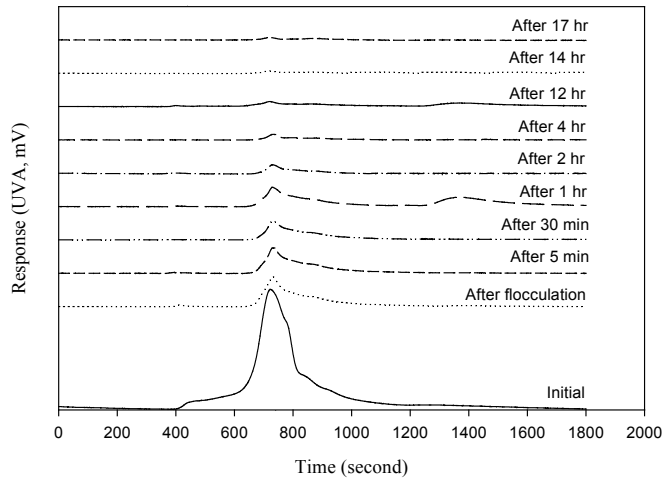


Figure 9.3 Molecular size distributions of SOM (after the treatment of flocculation and microfiltration (T = 25 °C; Air = 1.5 VVM; TiO₂ = 0.5 g/L with pretreatment, UV lamp intensity = 8 W)

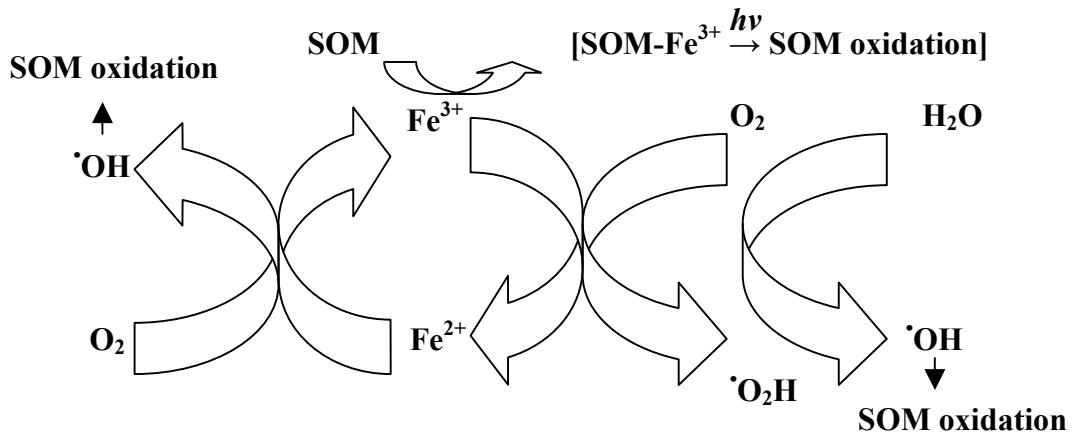


Figure 9.4 Schematic of Photo-Fenton degradation of SOM (adapted from Sarria et al., 2003)

9.2.1.3 Nanofiltration for SOM Removal

The synthetic wastewater was filtered through a NF unit (NTR 729HF: MWCO 700 daltons). The DOC removal by the NF unit is shown in Figure 9.5 (where C and C₀ are the effluent and influent DOC values). The NF alone gave rise to 92.4% DOC removal. Figure 9.5 also shows that there was minimal flux decline during the 20 hours experiment. The NF was also successful in removing practically all the organics from 970 daltons to 33,950 (Figure 9.6). In terms of DOC removal and the range MW of organics, the hybrid

system with flocculation-microfiltration-photocatalysis could be an alternative technology in treating organic matter.

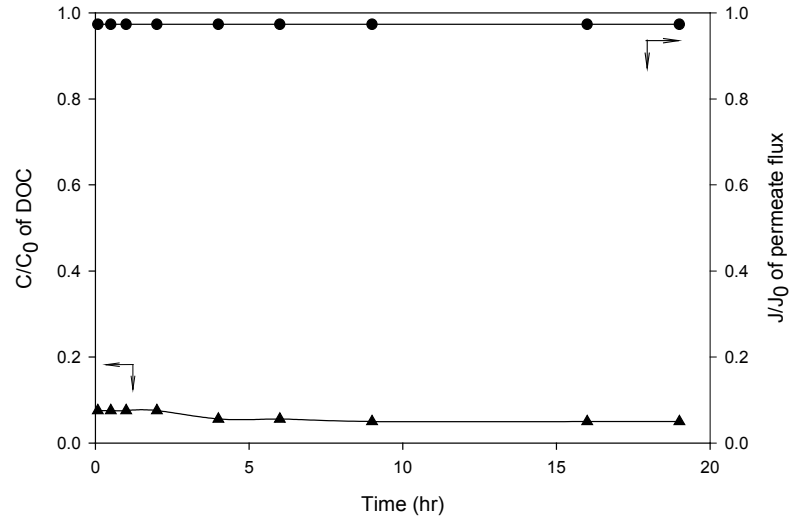


Figure 9.5 DOC removal and permeate flux with NF unit (NTR 729HF nanofiltration membrane, Nitto Denko Corp., operating pressure 300 kPa, flow rate = 0.5 m/s, T = 30 °C)

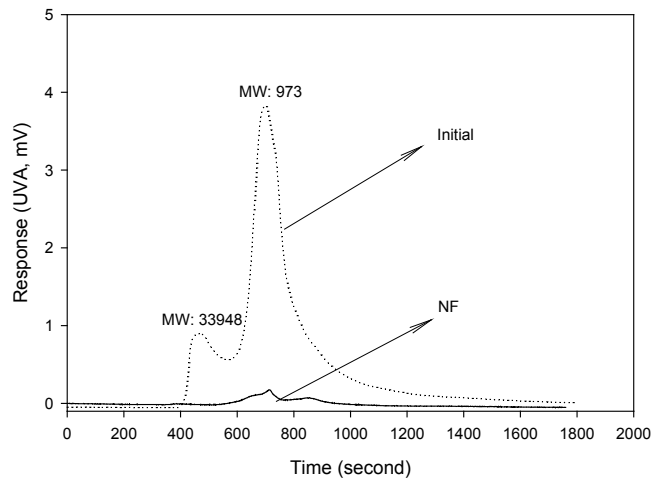


Figure 9.6 MW size distribution of nanofiltration effluent with synthetic wastewater (NTR 729HF nanofiltration membrane, Nitto Denko Corp., operating pressure 300 kPa, flow rate = 0.5 m/s, T = 30 °C, Reynold's no. = 735.5 (laminar flow) and shear stress = 5.33 Pa)

9.2.2 Chemical Coupling of Photocatalysis with Flocculation and Adsorption in the Removal of Organic Matter

The second part of the experimental study was to investigate the usefulness of chemical coupling, such as flocculation and adsorption, with the photocatalysis hybrid system in treating organic matter. Synthetic wastewater was also used as a feed in this study.

9.2.2.1 Effect of the Surface Area of UV Lamp on Photocatalytic Reaction

The effect of the surface area of UV lamp was first studied in terms of DOC removal (Figure 9.7). One, two and three lamps were used in three different experiments. The surface areas of exposure of the 1, 2 and 3 lamps were 179 cm², 358 cm² and 537 cm², respectively. The total volume of the solution used in each experiment was 1.5 L. The DOC removal profile (in terms of $C/C_0 = \text{DOC}/\text{DOC}_0$) is shown in Figure 9.7 (a). Here C and C_0 are the effluent and influent DOC concentrations, respectively. As can be seen in Figure 9.7 (a), a reverse reaction was observed during the first two hours of operation (i.e., the effluent organic concentration in terms of DOC increased with time, up to first two hours). Only the forward photocatalytic reaction was observed by a number of researchers when they used a single compound (Chu and Wong, 2004; Lu et al., 1994; Konstantinou et al., 2001]. Figures 9.7 (b) and (c) show the rate of change of C/C_0 during the reverse and forward reactions. The pseudo first order equation was used to determine the rate constant (k) (Eq. 9.17).

$$\ln\left(\frac{C_0}{C}\right) = kt \quad (9.17)$$

where t = the illumination (operation) time (h) and k = the apparent photodegradation rate constant (1/h).

The overall rate is presented in Figure 9.7 (d). The overall rate constant (k) with the 3 lamps was 6.9 times higher than with one lamp. The reverse rate constant of the 3 lamps was 27.6 times higher than that of one lamp during the first two hours of experiments. This implies that as the lamp surface increases, the rate constant of the reverse and forward reactions also increases.

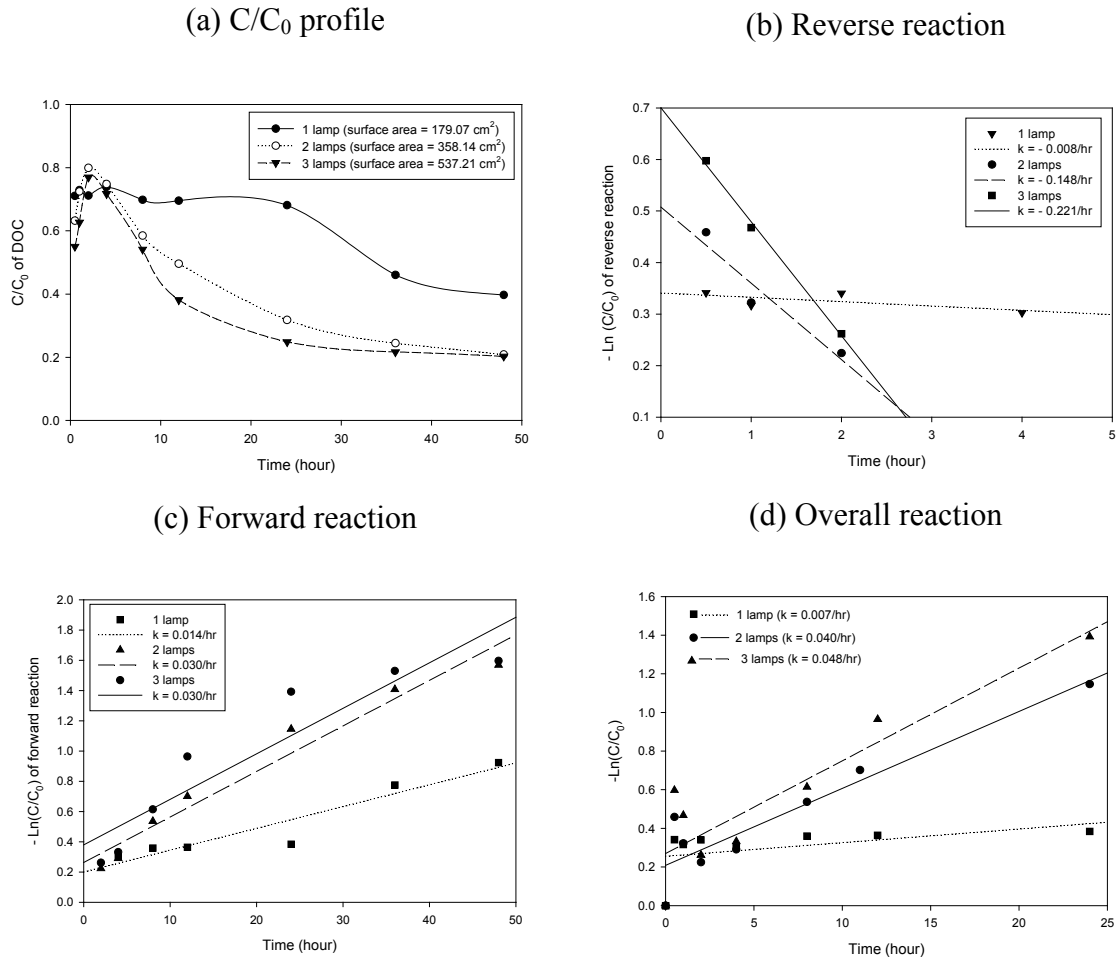


Figure 9.7 Effect of surface area of UV lamp on photocatalysis ($\text{TiO}_2 = 1 \text{ g/L}$; initial DOC of the wastewater = 11.46 mg/L; $T = 25 \text{ }^\circ\text{C}$; Air = 3.3 VVM; intensity = 8 W UV-C)

9.2.2.2 Effect of TiO_2 Concentration on Photocatalytic Reaction

Figure 9.8 shows the effect of different TiO_2 concentrations on the photocatalytic reaction. The TiO_2 concentration was varied from 0.1 to 10 g/L where both reverse and forward reactions were observed. However, at a very low concentration of TiO_2 only the forward reaction was observed. This may be due to either very low concentration of TiO_2 or the minimal adsorption of OM on TiO_2 , which led to the forward reaction from the beginning. Both reverse and forward reactions occurred when higher TiO_2 amounts were used. The k value was higher for larger TiO_2 concentration (Figures 9.8 (b) and (c)). This was evident up to a TiO_2 concentration of 2 g/L. There was no significant degradation when the TiO_2 dose was increased beyond 2 g/L. Thus, the TiO_2 concentration of 2 g/L was selected as an optimum concentration in subsequent experiments. Al-Rasheed and Cardin (2003) also

found that the decomposition was faster with the increase in TiO_2 concentration. They found the optimum concentration of TiO_2 as 2.5 g/L.

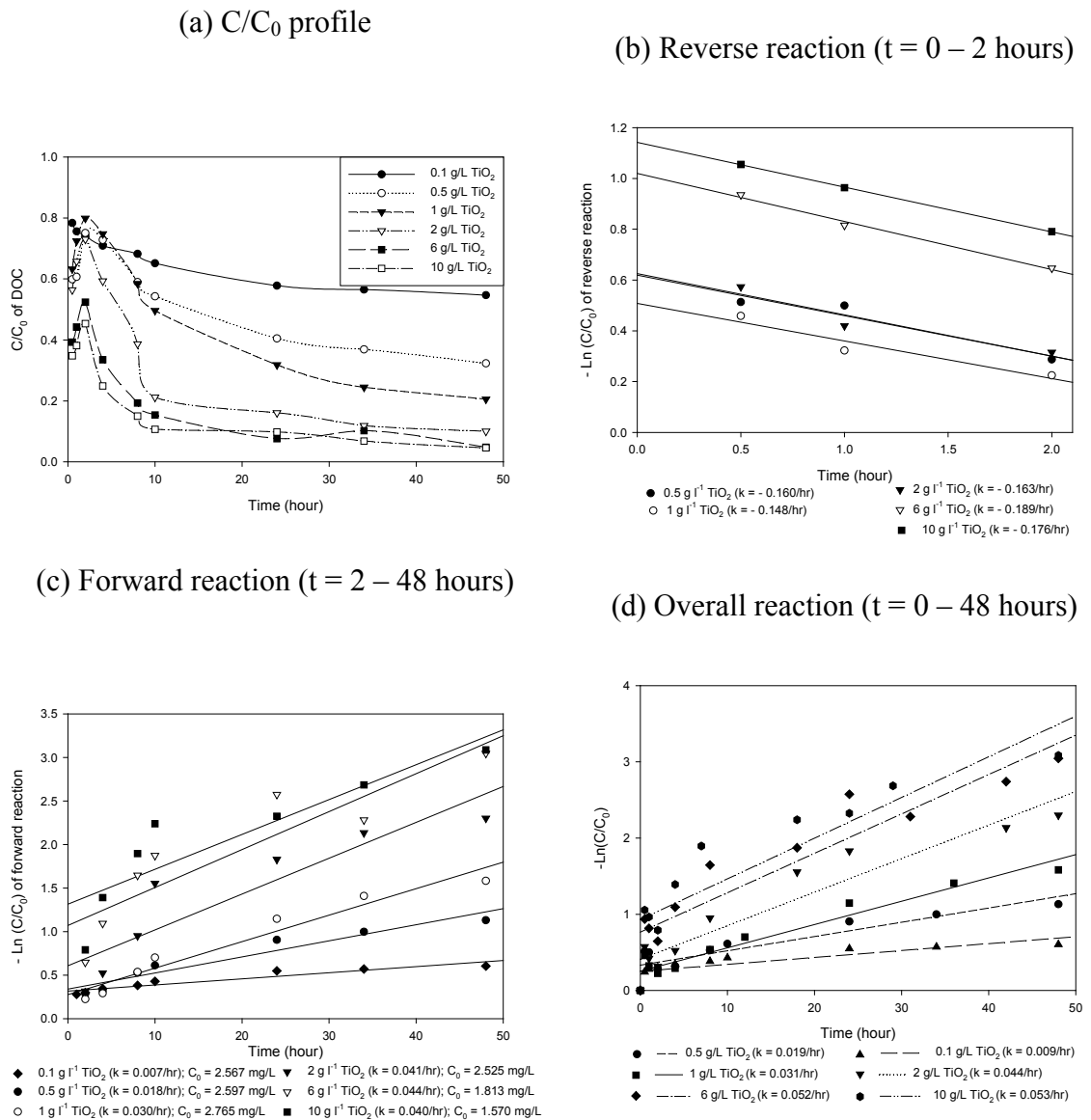


Figure 9.8 Effect of TiO_2 concentration on photocatalysis (initial concentration (C_0) = 11.46 mg/L (in terms of DOC); $T = 25^\circ\text{C}$; Air = 3.3 VVM; intensity = 8 W with the 3 lamps)

9.2.2.3 Effect of PAC Adsorption as a Pretreatment to TiO₂ Photocatalysis

The effect of PAC adsorption as a pretreatment to TiO₂ photocatalysis was investigated (Figure 9.9). This pretreatment was proposed to assess its effect on the improvement of reaction rate and on elimination/reduction of small MW of OM from the wastewater at the initial period of the experiment by PAC adsorption (in order to eliminate the reverse reaction). After a pretreatment of adsorption with different doses of PAC, photocatalysis experiments with the 2 g/L TiO₂ dose were performed. The results show that PAC adsorption followed by photocatalysis was not effective in alleviating reverse reaction (Figure 9.9). Although, the overall DOC removal was higher in the presence of pretreatment (Figure 9.9) compared with Figure 9.7 (b), the reverse reaction was still significant during the first two hours of the experiment. Although the PAC removed the small MW OM in the wastewater, the small OM produced by the degradation of TiO₂ during the post treatment caused the reverse reaction. The contribution to DOC concentration by the small MW organic matter may be more than that of large MW. Higher doses of PAC were found to reduce the extent of the reverse reaction.

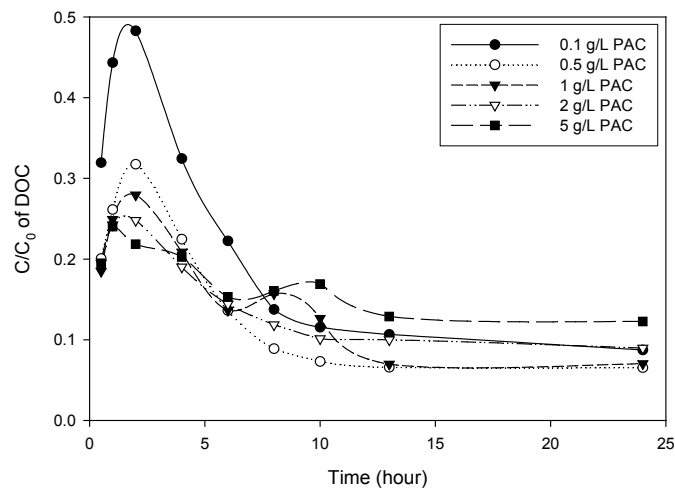


Figure 9.9 Effect of PAC adsorption followed by photocatalysis (wastewater concentration (DOC) = 11.46 mg/L; TiO₂ = 2 g/L; T = 25 °C; Air = 3.3 VVM; intensity = 8 W with the 3 lamps)

9.2.2.4 Performance of Simultaneous Addition of PAC and TiO₂ in the Photocatalytic System

Experiments with simultaneous PAC and TiO₂ additions were then conducted to verify whether the reverse reaction could be eliminated (Figure 9.10). The OM removal during photocatalysis was improved by simultaneous PAC addition. This may be due to: i) adsorption of pollutant in the solution onto PAC, ii) better rate constant and iii) fast decantability with PAC (Arana et al., 2002; Kaneko and Okura, 2002). It was observed that simultaneous PAC adsorption and photocatalysis led also to a superior DOC removal compared with PAC adsorption followed by photocatalysis.

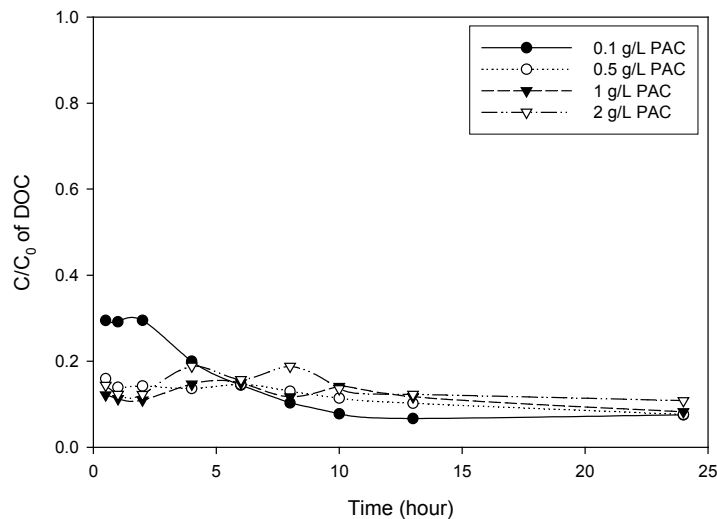


Figure 9.10 Performance of coupling of PAC adsorption with TiO₂ photocatalysis system (wastewater concentration (DOC) = 11.46 mg/L; TiO₂ = 2 g/L; T = 25 °C; Air = 3.3 VVM; intensity = 8 W with the 3 lamps)

9.2.2.5 Effect of FeCl₃ Flocculation as a Pretreatment to TiO₂ Photocatalysis

The effect of flocculation with FeCl₃ as pretreatment to TiO₂ photocatalysis was also investigated (Figure 9.11). Past studies have shown that the presence of ferrous ions, silver ions, manganese ions, etc., can be used to improve the treatment efficiency of photocatalytic oxidation process (Sarria et al., 2003; Gogate and Pandit, 2003). When a FeCl₃ of 17 to 23 mg-Fe/L was used, the organic removal efficiency was improved and it

eliminated the initial reverse reaction. It should be noted that 23 mg-Fe/L FeCl₃ was found to be the optimum flocculant dose from a Jar test flocculation experiment. Inadequate FeCl₃ doses (less than 10 mg-Fe/L) resulted in initial reverse reaction and inferior DOC removal. In any case, the results were better than with no flocculant addition. An overdose of FeCl₃ (41 mg-Fe/L) resulted in slightly less DOC removal.

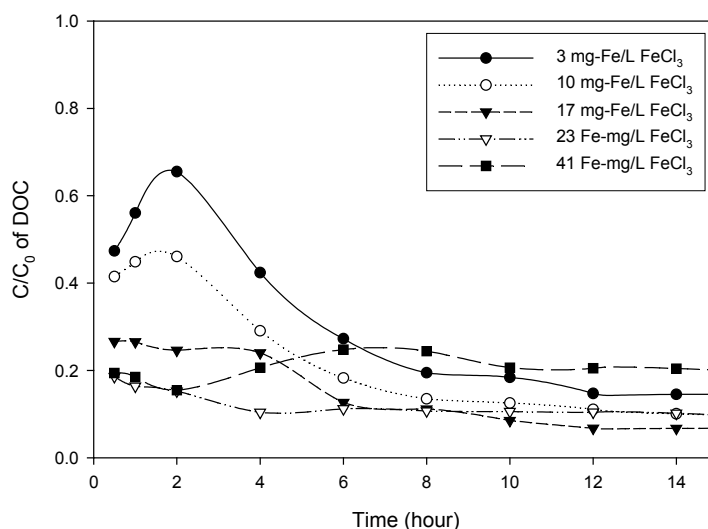
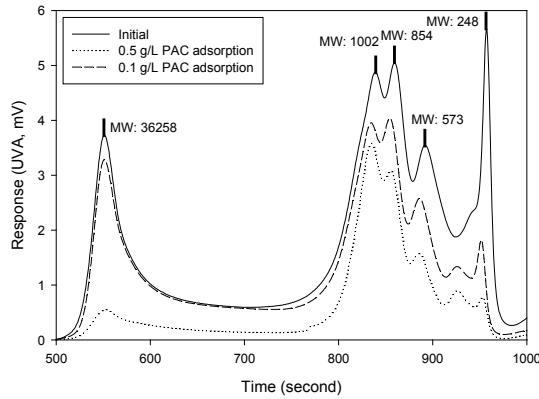


Figure 9.11 Effect of FeCl₃ flocculation followed by photocatalysis (wastewater concentration (DOC) = 11.46 mg/L; TiO₂ = 2 g/L; T = 25 °C; Air = 3.3 VVM; intensity = 8 W with the 3 UV lamps)

9.2.2.6 Molecular Weight Distribution

Figure 9.12 presents the MW distribution of OM of the wastewater effluent after the wastewater had undergone adsorption and flocculation with different PAC and FeCl₃ doses, respectively. Flocculation as pretreatment removed the large MW organic matter (in the range of 850 to 36260 daltons) from the wastewater (Figure 9.12 (b)). Thus, the photocatalysis employed after flocculation showed the forward reaction from the beginning. FeCl₃ flocculation also removed some of the small MW organic compounds. Flocculation with an insufficient dose of FeCl₃ (10 mg-Fe/L or less) did not remove the majority of large MW organic matter. This is why the reverse reaction was observed after photocatalysis when an insufficient FeCl₃ dose was used.

(a) after PAC adsorption



(b) after FeCl₃ flocculation

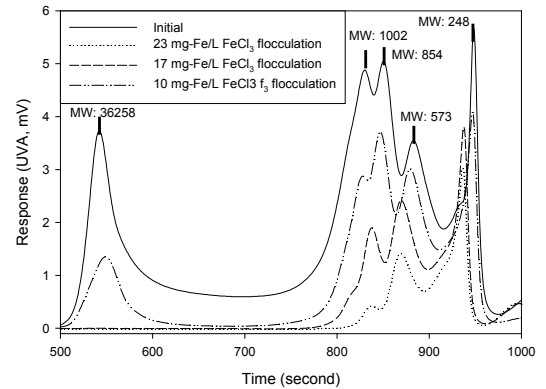


Figure 9.12 MW distribution after FeCl₃ flocculation (mixing speed: 1 min at 100 rpm and 20 min at 30 rpm) and PAC adsorption (mixing speed: 100 rpm; contact time: 1 h)

The MW distribution of organic matter after PAC adsorption followed by photocatalysis is presented in Figure 9.13. The concentration of small MW organic matter increased with up to 2 hours of the photocatalysis process. This may be why the reverse reaction was observed up to 2 hours. After 2 hours of photocatalysis, the amount of small MW compounds started to decrease with time.

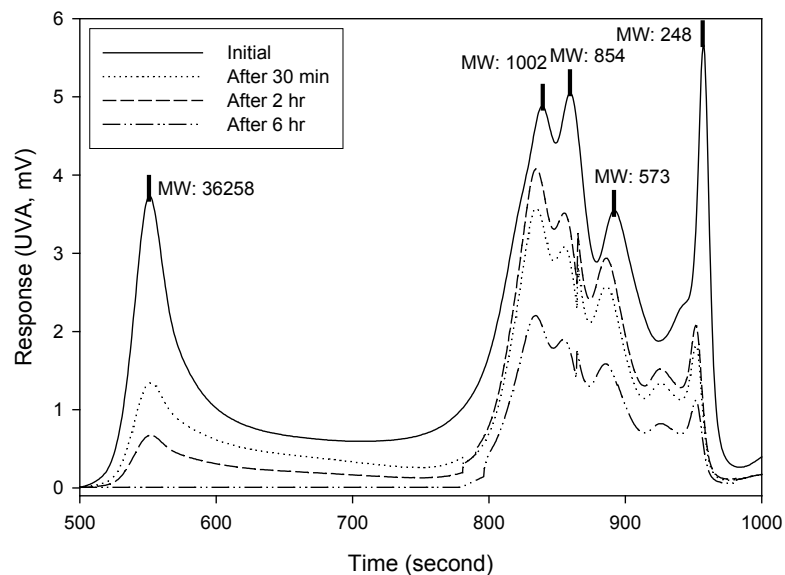


Figure 9.13 MW distribution of PAC adsorption followed by photocatalysis (wastewater concentration (DOC) = 11.46 mg/L; T = 25 °C; Air = 3.3 VVM; each 3 UV lamps intensity = 8 W; TiO₂ concentration = 2 g/L)

Following the pretreatment of FeCl_3 flocculation, the photocatalysis removed the majority of organics of different MWs (Figure 9.14). When photocatalysis was conducted without a pretreatment of flocculation, the majority of organics of large MW were present and they acted as the rate-limiting factor for the photocatalytic reaction. Thus, the reverse reaction occurred. However, when the pretreatment of flocculation treatment removed most of the large MW organic compounds, the remaining small MW could easily be removed. The photocatalytic reaction removed the organic compounds of large MW initially and then the smaller MW over time (854 daltons > 573 > 248). This suggests that photocatalysis degrades the large MW organic matter into small MW organic compounds and then mineralizes the small MW organic compounds into CO_2 and H_2O .

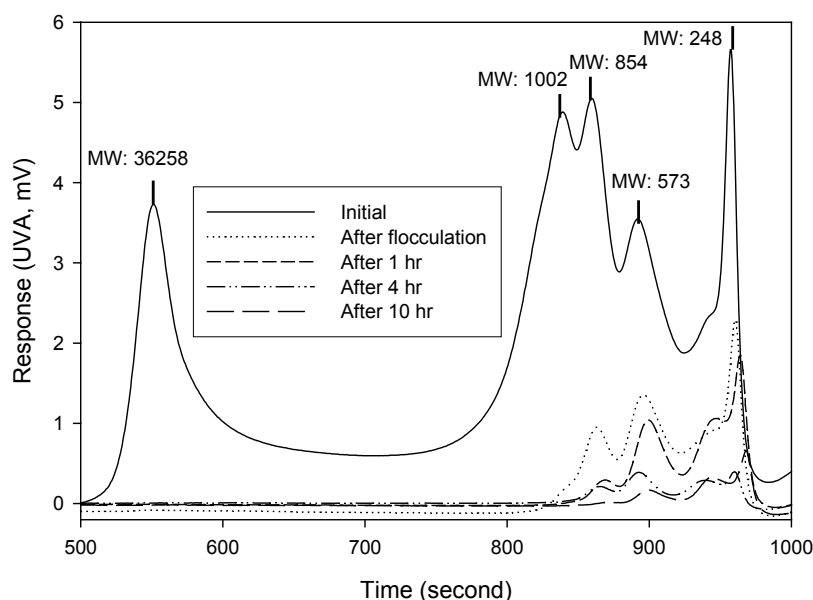


Figure 9.14 MW distribution after FeCl_3 flocculation followed by TiO_2 photocatalysis (wastewater concentration (DOC) = 11.46 mg/L; FeCl_3 dose = 23 mg-Fe/L; $T = 25^\circ\text{C}$; Air = 3.3 VVM; three lamps with an intensity of each lamp = 8 W; TiO_2 concentration = 2 g/L)

9.2.2.7 Synergistic Effect of FeCl_3 Flocculation to Photocatalysis

The above results show that flocculation followed by photocatalysis resulted in a relating high rate of removal of organic matter. The reasons for this may be the occurrence of photo-Fenton reaction and/or the removal of the large MW of organic matter by flocculation. The above reasoning was verified through simple experiments.

Results of photocatalysis in the presence of photo-Fenton reaction and chloride-based salts were presented.

Figure 9.15 presents the DOC removal efficiency by i) TiO_2 adsorption, ii) photocatalysis at the optimum pH and iii) photocatalysis with different flocculants (FeCl_3 , $\text{Al}_2(\text{SO}_4)_3 \cdot 18\text{H}_2\text{O}$, and $\text{FeSO}_4 \cdot 7\text{H}_2\text{O}$). The DOC removal by TiO_2 adsorption alone, flocculation alone with FeCl_3 , $\text{Al}_2(\text{SO}_4)_3 \cdot 18\text{H}_2\text{O}$, and $\text{FeSO}_4 \cdot 7\text{H}_2\text{O}$, flocculation followed by TiO_2 adsorption, photocatalysis alone at pH 4 and flocculation followed by photocatalysis at pH 4 was 60%, 72%, 80%, 85%, and 92%, respectively. The DOC removal with flocculation followed by photocatalysis was the highest. The DOC removal was almost the same even when different flocculants (iron and non-iron salts) were employed. It was noticed that there is only a slight improvement in performance if preflocculation (for the particular synthetic wastewater used) is applied.

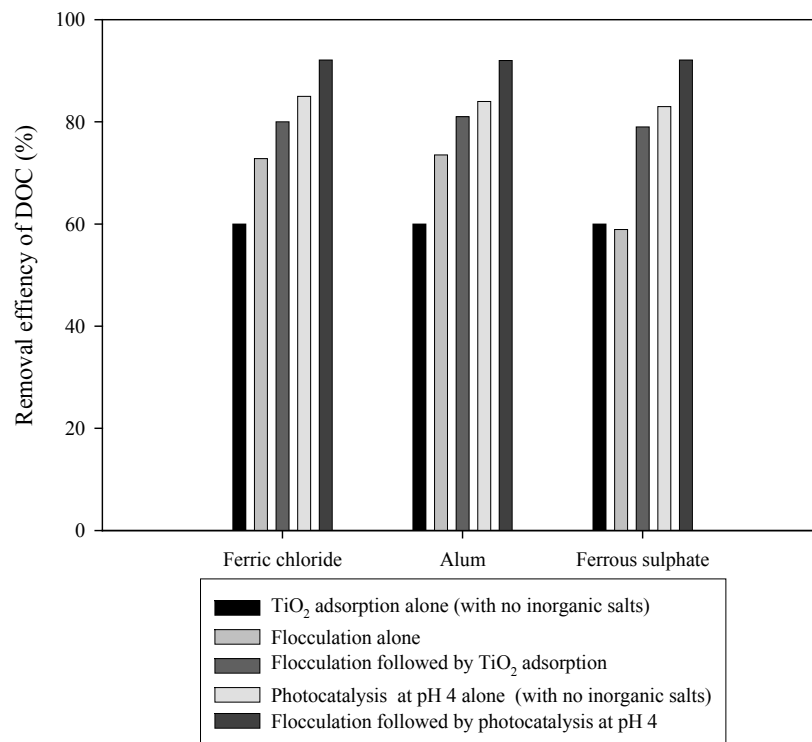


Figure 9.15 DOC removal by i) TiO_2 adsorption alone, ii) flocculation alone, iii) flocculation followed by TiO_2 adsorption, iv) photocatalysis at pH 4 alone and flocculation followed by photocatalysis at pH 4

An experiment was conducted to investigate the effect of the initial DOC concentration of wastewater on the removal of DOC by photocatalysis (Figure 9.16). When the DOC initial concentration was approximately 2.3 mg/L (which was the similar concentration after the pretreatment of flocculation), the effluent DOC concentration was 0.48 mg/L (which was the same DOC value with flocculation followed by photocatalysis for a wastewater containing an initial DOC of 10.6 mg/L). Thus, superior DOC removal of the hybrid system with flocculation followed by photocatalysis is probably due to the effect of initial organic loading in this study. Even when the initial DOC concentration was high, the final DOC concentration was 1.5 mg/L after 3 h of photooxidation. After the photooxidation of wastewater, the initial DOC concentration was 2.4 mg/L as a similar DOC value. The only difference was that the photooxidation rate was higher with the wastewater of higher DOC concentration (Figure 9.16 (b)).

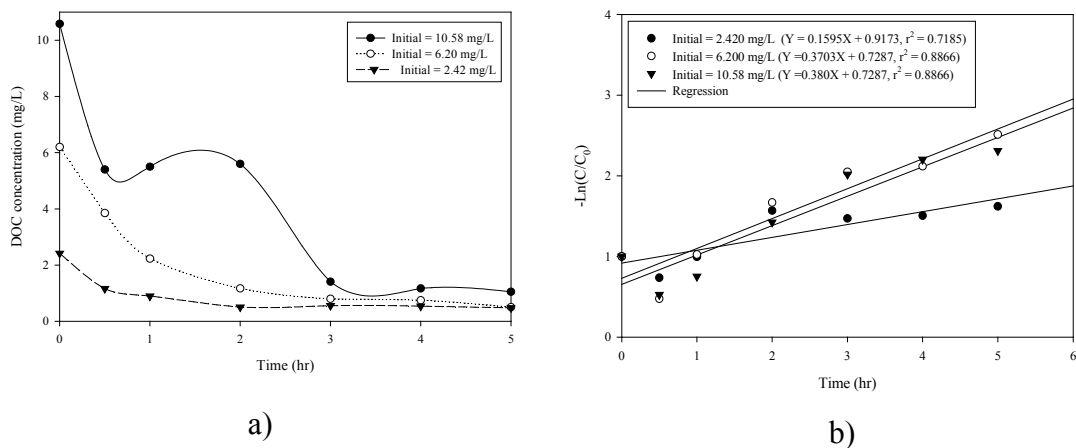


Figure 9.16 (a) DOC variations and (b) reaction rates of different initial concentrations in photocatalysis ($T = 30\text{ }^{\circ}\text{C}$; Air = 0.1 VVM; intensity = 8 W with the 3 lamps)

9.2.3 Application of Photocatalysis Hybrid System to Biologically Treated Sewage Effluent (BTSE)

9.2.3.1 Effect of UV Light Intensity on Photodegradation

A detailed study was undertaken with photocatalysis with BTSE from the Gwanju wastewater treatment plant, Korea. The effect of UV lamp intensity was studied by using 8 W UV-C (approximately 253 nm), 15 W UV-C (approximately 235 nm) and 15 W UV-A (approximately 315 – 400 nm) (Figure 9.17). The DOC removal was 70% after

3-hour operation when 15 W UV-C was used. However, use of 15 W UV-A and 8 W UV-C resulted in only 40% removal. This may have been due to the fact that the wavelength of 315 – 400 nm was not appropriate in the degradation of the EfOM. As expected, the 15 W UV-C gave rise to a better removal than the 8 W UV-C. The higher the light intensity, the higher is the DOC removal. In the subsequent experiments, the UV-C lamp with 15 W was used.

Figure 9.18 presents the MW distribution of EfOM. The photooxidation with UV-C 15W lamp and 2 g/L of TiO₂ removed the majority of MW (263 daltons, 580, 865, and 43109) within the first 30 minutes of operation.

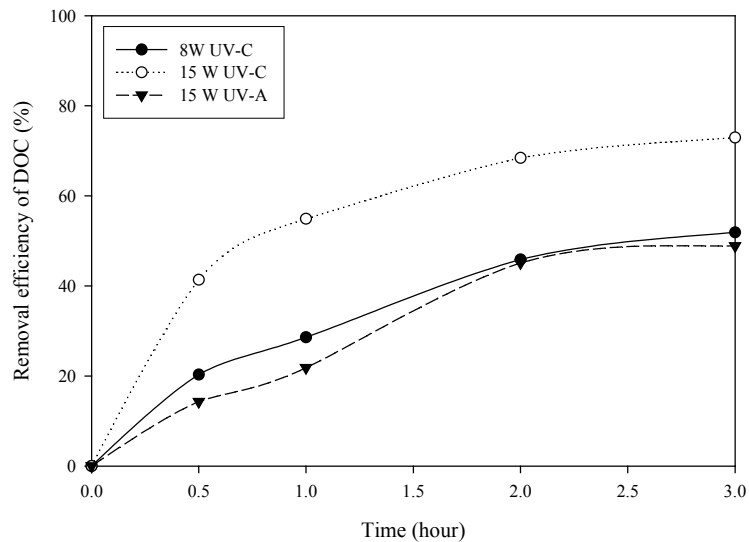


Figure 9.17 C/C_0 variation at different UV intensities (initial DOC concentration = 6.5 mg/L; TiO₂ concentration = 2 g/L; air = 25 L/min)

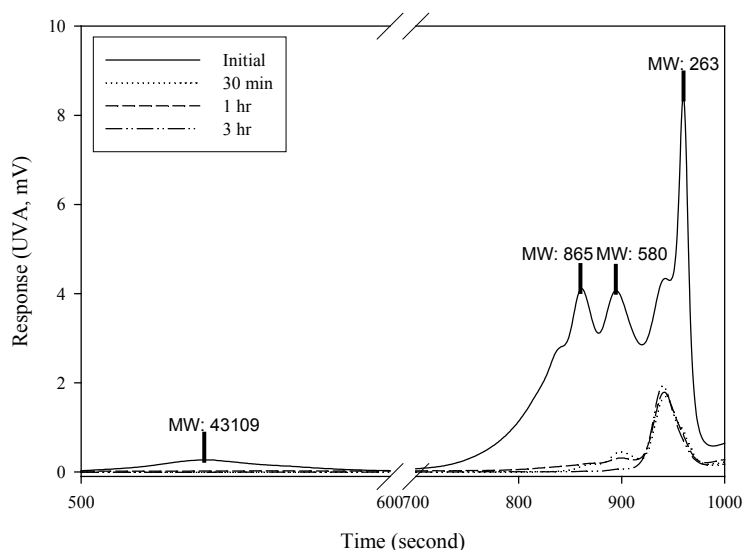


Figure 9.18 MW distribution of EfOM at different UV intensities (initial DOC concentration = 6.5 mg/L; TiO₂ concentration = 2 g/L; air = 25 L/min)

9.2.3.2 Effect of Fractions in Photodegradation

The hydrophobic (HP), transphilic (TP) and hydrophilic (HL) compounds were isolated from BTSE to investigate the effect of EfOM removal from each fraction during the photocatalytic reaction (Figure 9.19). DOC removal was high (80%) for HP and TP components. DOC removal from HL fraction was however minimum, suggesting that the HL fraction may be the rate limiting fraction in photocatalytic degradation. Wiszniowski et al. (2004) also indicated that DOC removal from humic acid (HA) (which represents HP and TP fractions) was 88% after 6 h of photooxidation. They used a TiO₂ loading of 1.0 g/L.

Figures 9.19 (b), (c) and (d) present the MW distribution of HP, TP and HL fractions before and after these fractions had undergone photocatalysis. MW distribution of the HP fraction included all the MWs as shown in Figure 9.18 for BTSE (260 daltons, 330, 580, 870, and 43110). Photocatalytic degradation with the HP fraction removed the majority of large MW (43110 daltons) within 30 minutes. The OM corresponding to MW of 865 daltons was removed after this HP fraction underwent a photooxidation of 1 hour. The OM of wide range of MW in the TP fraction was also removed during the photocatalysis (Figure 19 (c)). However, the HL fraction indicated a poor removal

(Figure 9.19 (d)), especially, the smallest MW (260 daltons) seemed to be a rate limiting MW in the HL fraction.

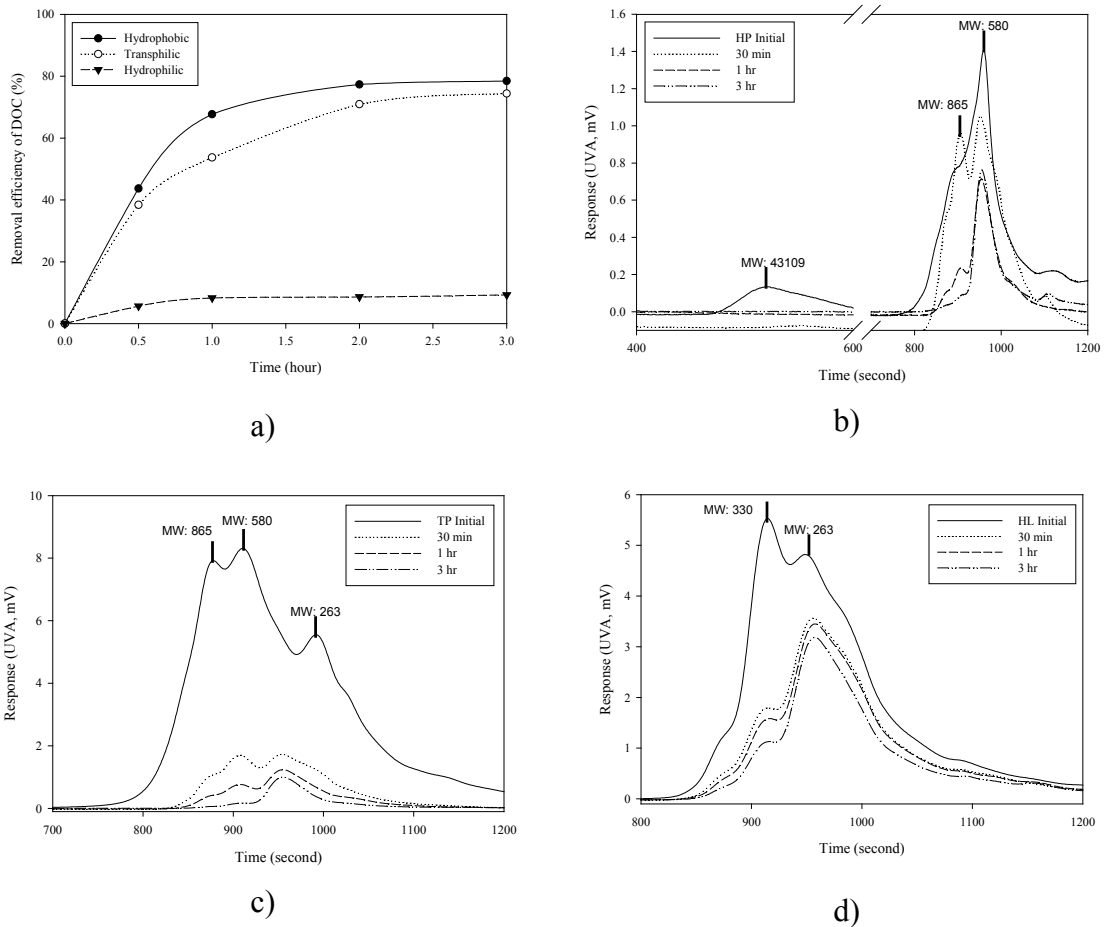


Figure 9.19 (a) C/C_0 profile and MW distribution of different fractions of EfOM by photocatalysis with (b) HP, (c) TP, and (d) HL fractions (initial concentration = 6.5 mg/L; TiO_2 concentration = 2 g/L; air = 5 VVM; UV intensity = UV-C 15W)

9.2.3.3 Effect of Simultaneous FeCl_3 and TiO_2 Addition in Photocatalysis

The effect of simultaneous FeCl_3 and TiO_2 additions in photocatalytic degradation of EfOM was studied to investigate the synergistic effect (Figure 9.20). The combined addition of TiO_2 and FeCl_3 removed the EfOM by up to 90%. Figure 9.20 (b) presents the MW distribution of EfOM. The OM of MW of 330 daltons was removed to a least amount.

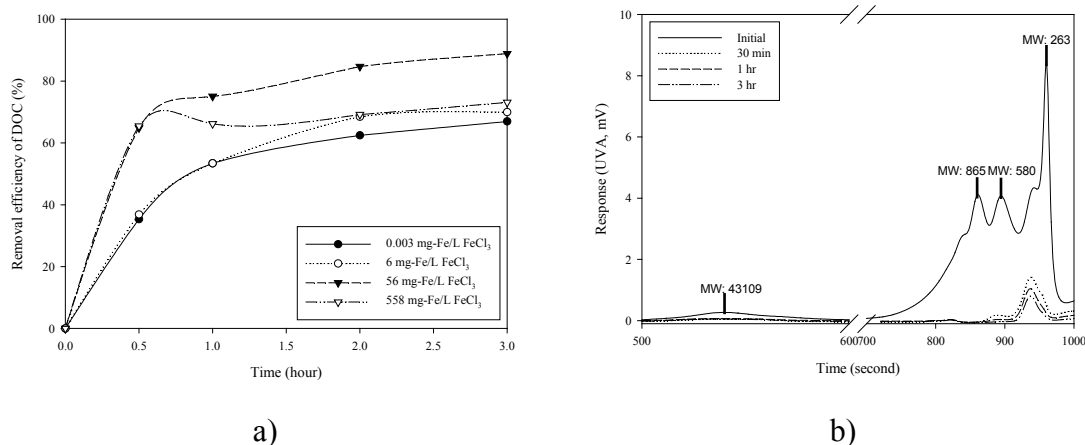


Figure 9.20 (a) C/C_0 profile and (b) MW distribution after simultaneous FeCl_3 and TiO_2 additions in photocatalysis (initial concentration = 6.5 mg/L; TiO_2 concentration = 2 g/L; air = 5 VVM; UV intensity = UV-C 15W; Figure (b) corresponds to 56 mg-Fe/L addition)

9.2.3.4 Effect of FeCl_3 Flocculation Followed by Photocatalysis

The effect of FeCl_3 flocculation followed by photocatalytic degradation was investigated in terms of DOC removal (Figure 9.21 (a)). When the BTSE was flocculated with 69 mg-Fe/L of FeCl_3 , the DOC removal was up to 55%. The hybrid process with FeCl_3 flocculation (69 mg-Fe/L) followed by photocatalysis indicated the highest DOC removal by up to 92.1%. This removal was similar to that with NF (Figure 4.7, Chapter 4). The flocculation-photocatalysis hybrid system could therefore be an alternative way to remove EfOM from BTSE.

The MW distribution curve (Figure 9.21 (b)) shows minimum removal of the MW fraction of 330 daltons. The flocculation followed by photocatalysis showed high removal for other MW ranges of EfOM. This trend of MW distribution was similar with those observed in NF membrane effluents (Figure 4.7, Chapter 4).

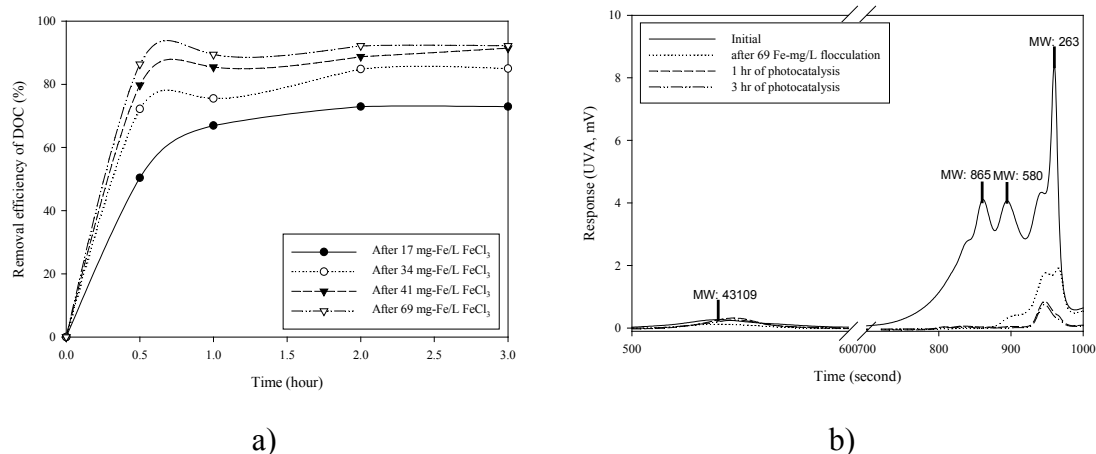


Figure 9.21 (a) C/C_0 variation and (b) MW distribution with FeCl₃ flocculation (69 mg-Fe/L) followed by photocatalysis (initial DOC concentration = 6.5 mg/L; TiO₂ concentration = 2 g/L; air = 5 VVM)

9.2.3.5 Effect of PAC Adsorption as a Pretreatment to TiO₂ Photocatalysis

The effect of (i) PAC adsorption as a pretreatment to TiO₂ photocatalysis and (ii) simultaneous addition of PAC with TiO₂ in the photocatalysis was investigated (Figure 9.22). The EfOM removal was increased from 52% with photocatalysis alone to 77.5% with TiO₂ photocatalysis with simultaneous PAC addition at 0.5 g/L (Figure 9.22 (a)). This increase of DOC removal is probably due to the adsorption of small MW organics by PAC. The non-porous TiO₂ adsorb the large MW and PAC removes the small MW. As the photocatalytic reaction proceeded, the large MW compounds were photodegraded into small MW compounds which were then adsorbed by PAC. However, when PAC was added at high concentration, the DOC removal was decreased and this maybe due to the interference of the passage of UV light through the BTSE solution. Figure 9.22 (b) represents the effect of pretreatment of PAC adsorption on photocatalysis. The results suggest that PAC adsorption followed by photocatalysis is also effective in improving the DOC removal.

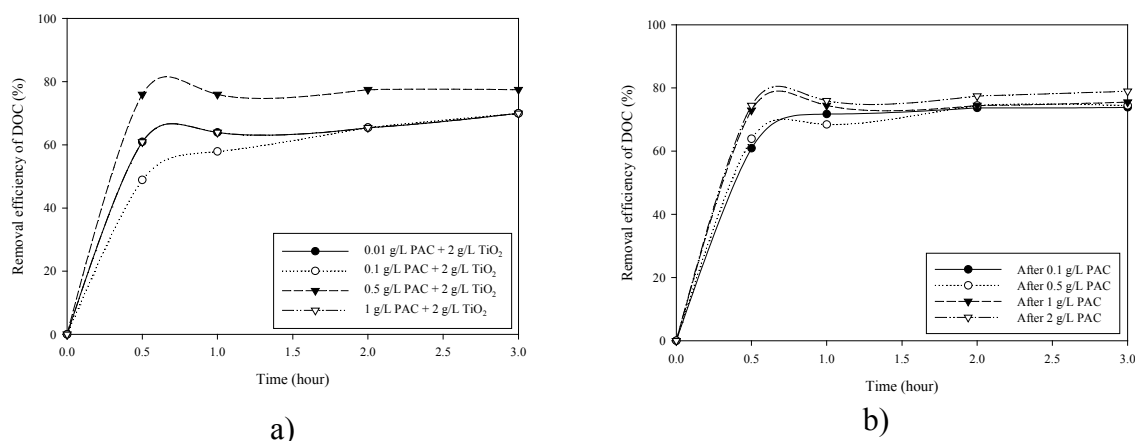


Figure 9.22 C/C_0 variation of (a) simultaneous PAC addition and (b) PAC adsorption followed by photocatalysis (initial concentration = 6.5 mg/L; TiO₂ concentration = 2 g/L; air = 5 VVM)

Figure 9.23 presents the MW distribution of the effluent obtained from the process of PAC adsorption followed by photocatalysis. 1 g/L of PAC adsorption followed by photocatalysis removed practically all ranges of MW of EfOM in BTSE. The removal response of compounds in the range of 300 to 900 daltons was in the order of 530 daltons < 870 daltons < 330 daltons (Figure 9.23). The same trend of MW distribution was also observed with effluent from NF (Figure 4.7, Chapter 4).

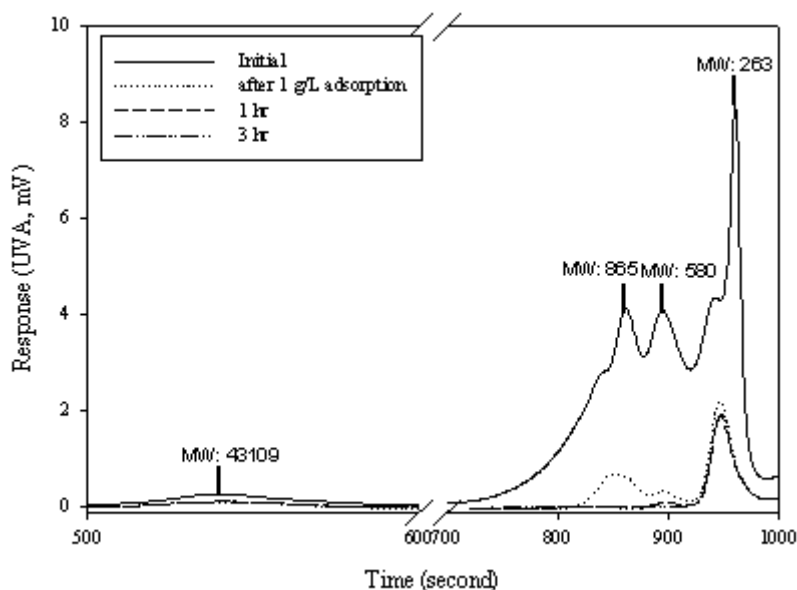


Figure 9.23 MW distribution of EfOM with PAC adsorption followed by photocatalysis (initial concentration = 6.5 mg/L; TiO₂ concentration = 2 g/L; 5 VVM)

9.3 Concluding Remarks

In this chapter, a photocatalysis hybrid system was experimentally studied to evaluate the advantages of the chemical coupling of photocatalytic reaction with PAC adsorption and FeCl_3 flocculation.

With synthetic wastewater:

1. The photocatalytic reaction showed both forward and reverse reactions with TiO_2 doses of more than 0.1 g/L concentrations. At a very low TiO_2 concentration (less than 0.1 g/L of TiO_2), only the forward reaction was observed. This may be due to very low concentrations of TiO_2 and the adsorption of OM on TiO_2 was minimal. The rate constant (k) was higher for larger TiO_2 concentrations. There was no significant improvement in OM degradation when the TiO_2 dose was increased beyond 2 g/L.
2. The amount of small MW organics increased with the photocatalysis (after 30 minutes up to 6 hours of detention time). After that, the amount of the small MW organics reduced gradually. This implies that up to 6 hours, the photocatalysis break down the large MW organics into smaller MW components and then the smaller MW is removed during photoreactor process. The majority of very large MW organics (> 30,000 daltons) were removed by adsorption on TiO_2 .
3. The flocculation as a pretreatment with an optimum dose of FeCl_3 (23 mg-Fe/L) gave rise to high levels of OM removal. This included removal of small MW organics. The small MW organics remaining after the pretreatment was removed by photocatalysis. These results suggest that flocculation and microfiltration followed by photocatalysis could be a suitable hybrid system to remove organic matter.
4. Flocculation and microfiltration followed by photocatalysis led to very high DOC removal of 96.6%. The nanofiltration alone (MWCO: 700 daltons) led to a DOC removal of 92.4%.

5. When flocculation was used as a pretreatment to photocatalysis, the organic removal efficiency was enhanced. Further, it also reduced/eliminated the initial reverse reaction, however, inadequate FeCl₃ doses (less than 10 mg-Fe/L) resulted in initial reverse reaction and inferior DOC removal. Flocculation, used as a pretreatment removed the large MW organic matter (in the range of 854 to 36258 daltons) from the synthetic wastewater. Thus, the photocatalysis after flocculation showed the forward reaction from the beginning. Flocculation with an insufficient dose of FeCl₃ (10 mg-Fe/L or less) did not remove the majority of large MW organic matter. This is the reason why the reverse reaction was observed after the photocatalysis (as post treatment) when an insufficient FeCl₃ dose was applied.

6. The photocatalysis system with a pretreatment of adsorption was not effective in alleviating reverse reaction. The PAC adsorption followed by photocatalysis caused reverse reaction because the large MW OM remained in the solution after the PAC adsorption was adsorbed onto the TiO₂ surface and was broken down into the small MW OM, thus increasing the organic concentration. When PAC and TiO₂ were added simultaneously, the reverse reaction was eliminated. The OM removal by photocatalysis was also improved by simultaneous PAC addition. PAC adsorption removed the majority of small MW organic matter degraded by TiO₂ photocatalysis in the range of 570 and 250 daltons.

With biologically treated sewage effluent (BTSE):

7. The EfOM removal from the BTSE-S was increased from 52% with photocatalysis alone to 77.5% with photocatalysis by simultaneous PAC addition at a dose of 0.5 g/L.

8. The amount of EfOM remaining was in order of 530 daltons < 865 daltons < 330 daltons with PAC adsorption followed by photocatalysis. This suggests that after PAC adsorption, the photocatalytic reaction is more favorable to remove 530 daltons more than large MW.

9. The HP and TP compounds isolated from BTSE-S were removed by up to 80% of DOC during the photocatalysis, however, the HL removal was low, suggesting that HL may be the rate limiting compounds within BTSE.

10. Both hybrid systems ((i) with simultaneous PAC adsorption and TiO_2 photocatalysis and (ii) FeCl_3 flocculation followed by TiO_2 photocatalysis) removed the EfOM by up to 90%. The MW of organic matter of 330 daltons was low.

Thus, the photocatalysis with the FeCl_3 flocculation and PAC adsorption hybrid system can be a possible option in the removal of DOC in wastewater reuse.

CHAPTER 10



University of Technology, Sydney
Faculty of Engineering

CONCLUSIONS AND RECOMMENDATIONS

10.1 Conclusions

As the problem of water shortage increases, wastewater reuse is becoming more important. The biologically treated sewage effluent (BTSE) discharged into waterways, cannot be reused for domestic or industrial purposes without additional treatment. Further treatment is therefore important if water is to be reused. Membrane technology is the most widely used process in water reuse, however, the operating costs associated with this technology are high and membrane fouling is often severe. A pretreatment to membrane filtration can significantly decrease membrane fouling and in this study, different pretreatments to UF and NF membranes were investigated in detail. Effluent organic matter (EfOM) and membranes were also characterized. The filtration flux of ultrafiltration (UF) (with and without pretreatment) was predicted using simple flux decline models.

10.1.1 Characteristics of Wastewater and Membrane

Three wastewaters were used in this study namely synthetic wastewater, BTSE collected during summer (BTSE-S) and BTSE collected during winter (BTSE-W). The synthetic wastewater consisted of tannic acid, sodium lignin sulfonate, sodium lauryl sulfate, peptone, arabic acid (with the large molecular weight (MW) organic matter), peptone, beef extract and humic acid (with the small MW organic matter). The MW of the mixed synthetic wastewater ranged from 290 to about 34100 daltons with the highest fraction at 940 – 1200 daltons. The weight-averaged MW of the wastewater was approximately 29500 daltons. The BTSE-S and BTSE-W were drawn from Gwangju wastewater treatment plant in Korea. The MW distribution of the BTSE-S comprised of small (260, 580 and 870 daltons) and large (43110 daltons) MW. The peaks having 260 daltons indicated the highest response in BTSE-S. On the other hand, the MW of the EfOM in BTSE-W ranged from 300 daltons to about 98940 with the highest fraction between 300 and 5000 daltons. In BTSE-S, the fraction percentages of hydrophobic (HP), transphilic (TP) and hydrophilic (HL) compounds were 25.3%, 15.9% and 58.8%, respectively. In BTSE-W, the fraction percentages of HP, TP and HL were 50.6%, 17.1% and 32.4%, respectively. This suggests that fractions of BTSE vary from season to season. The HP fraction in BTSE-S included 580, 865 and 43109

daltons; TP (580 and 865 daltons) and HL (from 263 to 580 daltons). The EfOM of protein-like substances in BTSE-S included high responses at 44944 and 235 daltons. However, the MW of 376 and 748 daltons indicates low intensity, suggesting that these peaks may be due to humic substances including humic and fulvic acids. The majority of the protein-like substances were found at 235, 23440 and 44944 daltons in HP, 235 and 44944 daltons in TP and 235 daltons in HL.

The membranes used in this study were NTR 7410 (UF, 17500 MWCO), NTR 729HF (NF, 700 MWCO), LES 90 (NF, 250 MWCO) and LF 10 (NF, 200 MWCO). The isoelectro points of NTR 7410, NTR 729HF, LES 90 and LF 10 were pH 2.6, pH 3.3, pH 3.4 and pH 3.4, respectively. The higher negative zeta potential values of NTR 7410 and NTR 729HF are probably due to its larger pore sizes compared to other membranes. The majority of membranes have a hydrophobic character except the NTR 729HF membrane. The average roughness ranged from 85.9 nm (LES 90) > 75.2 nm (NTR 729HF) > 64.7 nm (LF 10) > 10.1 nm (NTR 7410).

10.1.2 Flocculation as Pretreatment

Dissolved organic carbon (DOC) removal by flocculation was 57.6% from BTSE-S and 78% from synthetic wastewater. Flocculation removed the organic colloidal portion in BTSE-W by up to 65%. Flocculation removed HP (68.5%) and HL (61.8%) fractions from BTSE-W and HP (39.3%) and HL (59.7%) fractions from BTSE-S. This suggests that removal of different fractions by flocculation depended on a negative ion effect. Flocculation significantly removed large MW EfOM and also partially removed small MW organics. The mechanism of small MW organic matter removal by flocculation with FeCl_3 is mainly through complexation of Fe. Flocculation could not remove the majority of small MW (260 daltons, 330 and 580) in BTSE-S.

The UF after the pretreatment by flocculation gave rise to an additional 12% of DOC removal from BTSE-S. This pretreatment increased the permeate flux by up to 60% compared with that without pretreatment. The contact angle was 69° without pretreatment and 30° with flocculation as pretreatment. The zeta potential decreased from -98 mV up to -18 mV after the pretreatment of flocculation and this may be due to the adsorption of ferric ion on the membrane surface. The thickness of fouling layer

measured by the SEM image of the membrane cross-section decreased from 4.3 μm without pretreatment to 0.13 μm with pretreatment of flocculation. The adsorbed EfOM concentration of the fouled membrane was decreased from 0.011 mg EfOM/cm² membrane surface without pretreatment to 0.005 mg EfOM/cm² membrane surface with pretreatment of flocculation. The weight-averaged MW of foulants shifted from 675 daltons (without pretreatment) down to 415 daltons (with flocculation).

The adequateness of flocculation with reduced doses of ferric chloride (FeCl_3) as a pretreatment to UF was investigated for synthetic wastewater in terms of the decline of performance flux and the removal of organic matter of different molecular weights. Pretreatment of flocculation with FeCl_3 dose of 23 mg-Fe/L removed 75% of DOC, which led to only an additional 9.6% of DOC removal by the UF as a post treatment. On the other hand, a partial FeCl_3 dose of 7 mg-Fe/L removed only 34% of DOC and the UF removed another 48%. The flux decline (after 6 hours of operation) with no pretreatment was 32%. The UF with the pre-flocculation with the optimum dose of 23 mg-Fe/L FeCl_3 did not experience any flux decline during the operation of 6 hours. The pre-flocculation with sub-optimal doses of FeCl_3 of 7 – 10 mg-Fe/L led to a significant flux decline, whereas a dose of 14 – 17 mg-Fe/L of FeCl_3 showed only minimum flux decline. The peaks corresponding to larger MW (36260 daltons) were not observed in the flocculated effluent with a FeCl_3 dose of 17 mg-Fe/L and more. The effluent after flocculation with FeCl_3 of less than 14 mg-Fe/L showed peaks corresponding to large MW, indicating the dose of less than 14 mg-Fe/L was not adequate.

10.1.3 Adsorption as Pretreatment

DOC removal by adsorption was 65.4% from BTSE-S and 55% from synthetic wastewater. The PAC adsorption removed significant but less amount of organic colloids (less than 30%). Adsorption removed HP (71.4%) and HL (57.4%) fractions from BTSE-W and HP (72.0%) and HL (67.1%) fractions from BTSE-S. PAC adsorption removed the large amount of the HP compounds during both seasons. This may be due to the HP characteristics of PAC adsorption which is favorable to the removal of HP. As expected, PAC mainly removed the majority of small MW organics and partially removed large MW organics from BTSE-W. The removal of large MW organics

by PAC can be explained as the adsorption onto the larger pores of PAC. In addition, some of the larger MW organics may have been retained on the outer surface of PAC. Adsorption could remove 330 daltons, 870 and 43110 from BTSE-S. Protein-like substance (MW of 44940 daltons) was not removed by PAC adsorption.

The UF after pretreatment by PAC adsorption gave an additional 8% of additional DOC removal from BTSE-S. This pretreatment increased the permeate flux by 36% compared to that without pretreatment. The contact angle of the fouled UF membrane was 69° without pretreatment and 50° with adsorption as pretreatment. The zeta potential decreased from -98 mV up to -52 mV after pretreatment of adsorption. The functional group after adsorption as pretreatment on the UF fouled membrane surface was ether (C-O-C). The SEM image revealed that the thickness of the cross-section fouling layer of the membrane decreased from 4.3 µm without pretreatment to 0.26 µm with pretreatment of adsorption. The adsorbed EfOM concentration of the fouled membrane was decreased from 0.011 mg EfOM/cm² membrane surface without pretreatment and 0.007 mg EfOM/cm² membrane surface with pretreatment. The weight-averaged MW of foulants shifted from 675 daltons (without pretreatment) down to 399 daltons (with adsorption).

10.1.4 Flocculation Followed by Adsorption as Pretreatment

DOC removal by flocculation followed by adsorption (Floc-Ads) was 89% and 92% for BTSE-S and synthetic wastewater, respectively. A significant amount of HP and HL fractions of organic matter could also be removed by incorporating the pretreatment of Floc-Ads. Floc-Ads removed HP (82.9%) and HL (81.8%) fractions from BTSE-W and HP (82.8%) and HL (85.7%) fractions from BTSE-S. In principle, the flocculation and adsorption are used mainly to remove HP portions of large and small MW organics, respectively. The removal of the HL portion of organics by flocculation may be due to the large dose of FeCl₃ used (through sweep flocculation mechanism). The removal of the HL portion of organics by adsorption could be attributed to the physical affinity between hydrophilic organic molecules and PAC (through van der Waals, electro static forces and chemisorption). The pretreatment by Floc-Ads led to a high removal of both small and

large organic matter, for example, all of MW from 5000 to 98940 could be removed. Floc-Ads also significantly removed all the protein-like substances.

The pretreatment of Floc-Ads led to practically no filtration flux decline and superior DOC removal. The pretreatment of Floc-Ads resulted in the highest flux improvement. The highest EfOM concentration on the fouled membranes was observed to be 0.011 mg EfOM/cm² membrane surface on the UF membrane in BTSE-S. However, the pretreatment with flocculation followed by adsorption led to the lowest fouling concentration (0.005 mg EfOM/cm² membrane surface). That was similar to that for the clean membrane.

For the NF, the concentration of organic matter on the membranes decreased to 5.671×10^{-3} (NTR 729HF) and 4.940×10^{-3} (LF 10) mg EfOM/cm² of membrane from 6.372×10^{-3} (NTR 729HF) and 4.979×10^{-3} (LF 10) mg EfOM/cm² of membrane with the pretreatment. NF alone and Floc-Ads had nearly the same efficiency in terms of DOC removal. Floc-Ads as pretreatment resulted in an increase of the initial permeate flux from 32.9 L/m²·h without pretreatment to 108.4 L/m²·h. In the NF experiments the direct application of NF without any pretreatment showed a similar filtration flux compared to that with pretreatment. The flux ratio (J/J_0) was only marginally higher with pretreatment. The removal efficiency was also similar with and without pretreatment. From this result it can be concluded that NF membranes may be operated for polishing BTSE without any pretreatment.

To investigate the adequateness of flocculation and adsorption (with reduced chemical doses) as pretreatment, semi flocculation followed by semi adsorption to UF was investigated for synthetic wastewater. PAC adsorption removed the majority of smaller MW organic matter of 850, 570 and 250 daltons from the pre-flocculated water with FeCl₃ dose of 17 mg-Fe/L or more. The weight-averaged MW values of the compounds in the effluent after flocculation with more than 17 mg-Fe/L FeCl₃ was much lower (less than 700 daltons) when compared with the one with less than 14 mg-Fe/L FeCl₃ (around 29000 daltons which is in the similar range of the influent). A 17 mg-Fe/L of FeCl₃ and 0.5 g/L of PAC removed a majority of DOC (88%), thus reducing the organic loading to UF used as post treatment. Although flocculation with lower doses of FeCl₃ (3 mg-Fe/L) followed by PAC adsorption of 0.5 g/L and UF removed the same amount of

organic matter, the majority of the DOC removal was achieved by the post treatment of UF rather than by pretreatment. This resulted in significant flux decline in UF. When the FeCl_3 concentration was decreased from 17 mg-Fe/L to 14 mg-Fe/L, the increase of weight-averaged MW (M_w) was significant. The same trend was observed with the PAC adsorption of the flocculated effluent (with FeCl_3 dose of 3 to 14 mg-Fe/L). This phenomenon could be due to following two reasons: i) the FeCl_3 dose of 14 mg-Fe/L or less was not sufficient to remove the large MW SOM, and ii) the PAC adsorbed only smaller MW organic matter. The flux decline was proportional to the large M_w . This suggests that flocculation as pretreatment is more important than adsorption to increase a permeate flux because flocculation removes the majority of large MW.

10.1.5 Biofiltration as Pretreatment

The GAC biofilter with a shallow GAC filter depth led to a DOC removal of 69% from BTSE-S even after 45 days of operation. It removed HP (23.5%) and HL (61.1%) fractions from BTSE-S. This suggests that GAC biofilter is better at removing HL organic fraction. During the operation of GAC biofiltration for 45 days, significant removal of the small MW occurred at the initial period of first 2 days, suggesting that the adsorption is the initial mechanism. However, as time proceeds, the small molecule could not be removed and some large MW organics (35000 daltons) remained. They are probably extracellular polymer substances (EPS) produced by microorganisms in the biofilter.

The UF after pretreatment by biofiltration gave an additional 13% of DOC removal (with BTSE-S). This pretreatment increased the permeate flux by up to 32% compared to that without pretreatment. Even though the DOC removal by GAC was better than that with PAC adsorption and flocculation, the flux decline of GAC biofilter was higher than that of PAC adsorption. The large molecules may have been responsible for the permeate flux decline in the UF observed after biofiltration. The flux increased in the following order: Floc-Ads > FeCl_3 flocculation > PAC adsorption > GAC biofiltration > without pretreatment. The contact angle was 69° without pretreatment and 54° with biofiltration as pretreatment. The contact angle of the UF surface followed the same order as the flux increase. The zeta potential decreased after the pretreatment. The

functional group after adsorption as pretreatment on the UF fouled membrane surface was urea (R-NH-CO-NH-R). The thickness of fouling layer (measured by SEM image) decreased from 4.3 μm to 0.52 μm with pretreatment of biofiltration. The adsorbed EfOM concentration of the fouled membrane decreased from 0.011 mg EfOM/cm² membrane surface without pretreatment to 0.008 mg EfOM/cm² membrane surface with pretreatment of biofiltration. The weight-averaged MW of foulants shifted from 675 daltons (without pretreatment) down to 387 daltons (with biofiltration).

10.1.6 Photocatalysis Membrane Hybrid System

Flocculation and microfiltration followed by photocatalysis led to similar DOC removal of 96.6% as that of NF alone (92.4%) with synthetic wastewater. The majority of very large MW organics (> 30,000 daltons) were removed by adsorption on TiO₂. The flocculation as a pretreatment with an optimum dose of FeCl₃ (23 mg-Fe/L) gave rise to higher removal of SOM. This included removal of small MW organics. The small MW organics remaining after the pretreatment was removed by photocatalysis. These results suggest that flocculation and microfiltration followed by photocatalysis could be a suitable hybrid system to remove the synthetic organic matter (SOM).

Photocatalytic reaction showed both forward and reverse reactions with TiO₂ doses of more than 0.1 g/L concentrations. When PAC and TiO₂ were added simultaneously, the reverse reaction was eliminated. The SOM removal was also improved by simultaneous PAC addition. This study experimentally evaluated the advantages of the chemical coupling of photocatalytic reaction with PAC adsorption and FeCl₃ flocculation. PAC adsorption removed the majority of small MW organic matter degraded by TiO₂ photocatalysis in the range of 570 and 250 daltons. When flocculation was used as pretreatment to photocatalysis, the organic removal efficiency was enhanced. Further, it also reduced/eliminated the initial reverse reaction. However, inadequate FeCl₃ doses (less than 10 mg-Fe/L) resulted in initial reverse reaction and inferior DOC removal. Flocculation, used as a pretreatment removed the large MW organic matter (in the range of 850 to 36260 daltons) from the synthetic wastewater. Flocculation with an insufficient dose of FeCl₃ (10 mg-Fe/L or less) did not remove the majority of large

MW organic matter. This is the reason why the reverse reaction was observed after the photocatalysis (as post treatment) when insufficient FeCl_3 dose was used.

Real wastewater (BTSE-S) was evaluated with the photocatalysis hybrid system. The EfOM removal was increased from 52% with photocatalysis alone to 77.5% with photocatalysis by simultaneous PAC addition at a dose of 0.5 g/L. The removal of HP and TP fractions isolated from BTSE was more than 80% (in terms of DOC) by photocatalytic reaction. However, the HL fraction could not be removed. Both hybrid systems ((i) simultaneous PAC adsorption and TiO_2 photocatalysis and (ii) FeCl_3 flocculation followed by TiO_2 photocatalysis) removed the EfOM by up to 90%. The photocatalysis with the FeCl_3 flocculation and PAC adsorption hybrid system can therefore be an alternative way to remove DOC in wastewater reuse processes.

10.1.7 Automated Declogging in Crossflow Ultrafiltration

The utilization of two automated cleaning techniques was investigated in order to reduce the fouling problems encountered in the cross flow membrane systems when operated with high permeate flux rates. The two cleaning techniques studied were the (i) periodic membrane relaxation and (ii) periodic high rate cross-flow. An optimized usage of these two de-clogging techniques was obtained, with a 1 hour production period followed by a 1 minute relaxation period and then a 1 minute high cross-flow rate period and this resulted in a net productivity increase of 14.8%. Utilizing the optimized periodic cleaning techniques developed in this study allows higher recovery rates for UF to be achieved, without the problems of increased flux decline normally experienced when operating at high recovery rates.

In this study, the dominant fouling of membranes was caused by the weak adsorption. When the relaxation and cross-flow modes were applied, the resistances associated with the concentration polarization and the gel layer significantly decreased. However, the fouling caused by weak adsorption remained high. This indicates that the cleaning adopted in this study improves the flux decline caused by fouling of the concentration polarization and the gel layer and not by the weak and strong adsorption.

10.1.8 Pretreatment of Different Fractions in BTSE

In order to optimize the performance of the membrane filtration of BTSE, it is essential to identify the membrane fouling caused by different fractions of BTSE. A detailed characterization of membrane fouled with different fractions revealed the following. The organic removal efficiency by UF was higher for the HP fraction (67.4%) than for HL (19.7%). As the membrane MWCO was 17500 daltons, the rejection of 50.4% suggests that the EfOM in the BTSE-S consists of about 50% large MW than 17500 daltons. The flux decline with the HP fraction was very high compared with the TP and HL fractions due to the interaction between HP fraction and HP membrane nature and MW range present in the HP fraction. The flux decline with the HL fraction was minimal. Thus, it can be concluded that in the BTSE-S used in this study, the HP fraction was the main component which caused severe fouling. This was also confirmed from the contact angle, concentration of EfOM foulant on the membrane surface and zeta potential results. The main functional group of HP and TP indicated ketone groups (quinines).

As the foulants on the UF and NF membrane surfaces have been found to be in the range of 183-513 daltons, this fouling may be assumed to be due to adsorption of recalcitrant matter, carbohydrates, amino acids and fatty acids. Although the MWCO of UF is large (17500 MWCO), the foulants are small in size (386 daltons). This may be due to interaction between EfOM and membrane pores. The foulant MW (d_p) to membrane MWCO (d_m) corresponds to a ratio of only 4.3 (where d_p : particle diameter and d_m : membrane pore diameter) because a 17500 MWCO of UF corresponds to a pore size of about 1.3 nm and 386 daltons MW corresponds to 0.3 nm. With such a ratio, strong interaction with the walls of the pores can be expected. Further, in this study, the samples were filtered by 0.45 μm membranes before DOC measurement, whereas previous studies claiming that the main foulants during UF and NF are humic and fulvic acids (4700 – 30400 daltons) did not use prefiltration with 0.45 μm membranes.

10.1.9 Flux Decline Model with Pretreatment

Three different semi-empirical mathematical models were investigated to semi quantify the effects of different pressures and pretreatments. The three different models used were i) empirical flux decline (EFD) model, series resistance flux decline (SRFD) model and iii) modified series resistance flux decline (MSRFD) model. The coefficients of each model were evaluated from the experimental results to identify the correlation with different pretreatment methods. In the EFD model, the coefficients of k_0 and d exhibited high sensitivity. These values can also be used to compare the efficiency of different pretreatments. For example, the coefficients of k_0 and d after 14 mg-Fe/L flocculation were similar to those after 0.1 g/L PAC adsorption. This suggests that the flux decline coefficient values by the EFD model can be used as an index to process flux decline and to compare different operating conditions and pretreatments.

In the SRFD model, adsorption resistance varied with time. The fit value of K_F' was more sensitive than that of $1/n'$. The pretreatments of 14 mg-Fe/L flocculation and 0.1 g/L PAC adsorption also showed a similar K_F' value. This suggests that the SRFD coefficient values can also be used as an index to compare and decide on a suitable pretreatment. In the MSRFD model, when the pressure was increased from 100 kPa to 500 kPa, the bulk concentration (C_b) increased from 12.7 mg/L to 19.1 mg/L. The concentration near membrane surface (C_m) increased from 17.6 mg/L to 55.4 mg/L (more than 3 times). This caused a significant increase in adsorption resistance (up to 5.7 times). When flocculation of 21 mg-Fe/L was used as a pretreatment at a pressure of 300 kPa, the values of the C_b , C_m and R_a significantly decreased by 4.4, 3.1 and 12.9 times, respectively. After 1 g/L PAC adsorption as a pretreatment, the values decreased 2.2, 2.0 and 1.8 times, respectively. Thus, pretreatment can significantly decrease membrane fouling.

10.2 Recommendations

Although pretreatment reduces the flux decline caused by membrane fouling, it cannot completely prevent membrane fouling. With time, membrane fouling by organic matter

is converted into biofouling. Biofouling caused by extracellular enzyme produced by various microorganisms and bacteria themselves will dominate. Biofouling cannot be handled by pretreatment. Also, the increased concentration of the retentate will constantly accelerate membrane fouling; hence, it is important to deal with biofouling and the increased concentration of the retentate.

An integrated photocatalysis membrane hybrid system would lead to a near-zero fouling system. Photocatalytic reaction results in a complete degradation of organic pollutants into very small and harmless species without the need for any chemicals. This avoids sludge production and its disposal. This decreases the frequency of membrane cleanings and/or replaces membrane cleaning methods which are another source of contamination to environment. For example, cleaning chemicals such as acids, alkali, detergents, enzymes, complexing agents and disinfectants are needed to be treated again after their usage. The integrated photocatalysis membrane hybrid system would be an attractive process as an alternative way of cleaning.

The integrated photocatalysis membrane hybrid system also prevents biofouling on membrane surface. Ultraviolet (UV) technology itself can be used to disinfect water without the presence of a semiconductor. Photocatalysis with UV light removes waste compound via oxidative (electrophilic) attack of HO• and leads to a complete mineralization to yield innocuous CO₂ and mineral acids, taking advantage of the extremely high redox potential (2.8 V) of the HO•. This strong oxidant radical attacks proteins, lipids and DNA of microorganisms and breaks down large organic matter to smaller sizes. Thus, the integrated photocatalysis membrane hybrid system results in the decrease of the retentate concentration and biofouling.

10.2.1 Near-Zero Fouling System I

Figure 10.1 shows a proposed schematic of a near-zero fouling system I. Membrane can be prepared by coating it with TiO₂ nanoparticles. The coating takes place H-bonding interaction with the COOH functional group of aromatic polyamide thin-film layer of the membrane (Kim et al., 2003). UV light is directly provided to the membrane surface as shown in Figure 10.1. Near-zero fouling system I can

significantly prevent biofouling. Further, the modification of foulant occurring on the membrane surface by photocatalytic reaction would result in the decrease of flux decline. For example, the foulant consisting of aromatic organics (coiled and compacted configuration) can be converted into aliphatic compounds (stretched and linear configuration) by photocatalytic reaction, which reduces membrane fouling. Also, the UV light increases the temperature on the membrane surfaces and the permeate flux would therefore be improved. However, it should be noted that some membranes are weakened by direct UV light (Ollis, 2003).

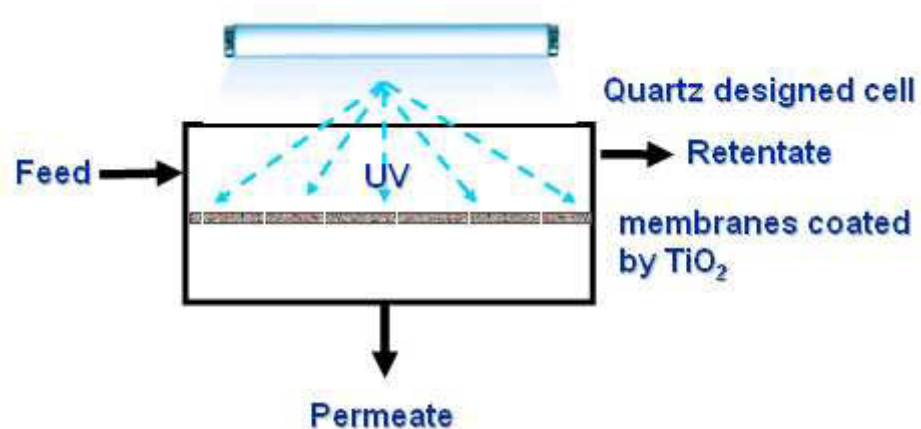


Figure 10.1 Schematic of near-zero fouling system I

10.2.2 Near-Zero Fouling System II

Figure 10.2 presents another proposed schematic of a near-zero fouling system. The system can be coated with TiO₂ nanoparticles. This system is devised as in-line absorption system with TiO₂. The suspended TiO₂ particles are recirculated in the retentate. The particles adsorb a number of foulants and lead to photocatalytic reaction with UV light. TiO₂ nanoparticles which induce photocatalytic reaction with visible light are currently being developed, however, it should be noted that the suspended TiO₂ particles would lead to the formation of dense cake layers and result in a greater flux decline (Lee et al., 2001).

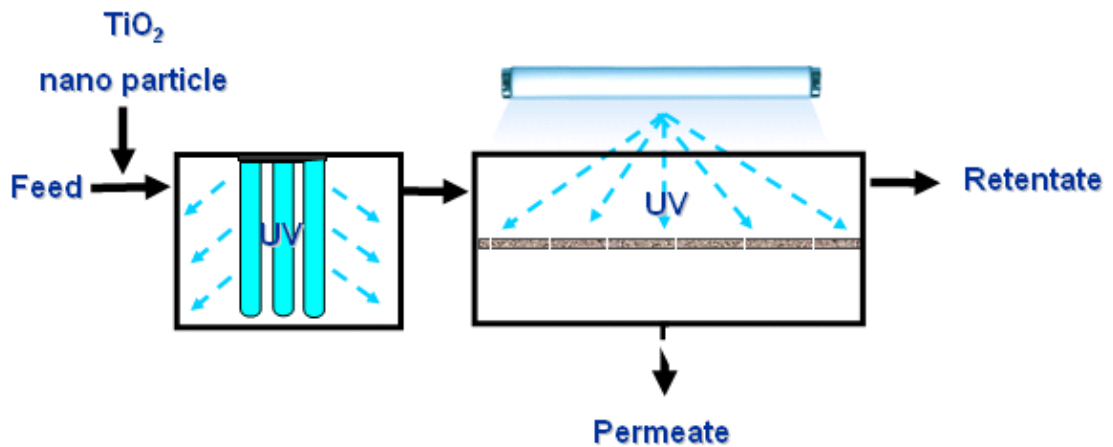


Figure 10.2 Schematic of near-zero fouling system II

10.2.3 Near-Zero Fouling System III

Figure 10.3 illustrates a schematic of another proposed near-zero fouling system. This system is devised to maximize the synergistic effect of photocatalytic reaction and flocculation. FeCl₃ flocculation as pretreatment leads to photo-Fenton reaction and removes large organic matter. Titanium tetrachloride (TiCl₄) and zirconium sulfate flocculation followed by UV and membrane hybrid system will accelerate the photocatalysis process which is one of the bottlenecks of photocatalysis. The flocculation with titanium tetrachloride and zirconium sulfate would also solve the sludge problem after flocculation. The settled flocs produced by these flocculants can be recycled as TiO₂ particles after a recovery (heating) process. Also, the suspended TiO₂ aqueous materials would improve the photocatalytic reaction with UV light.

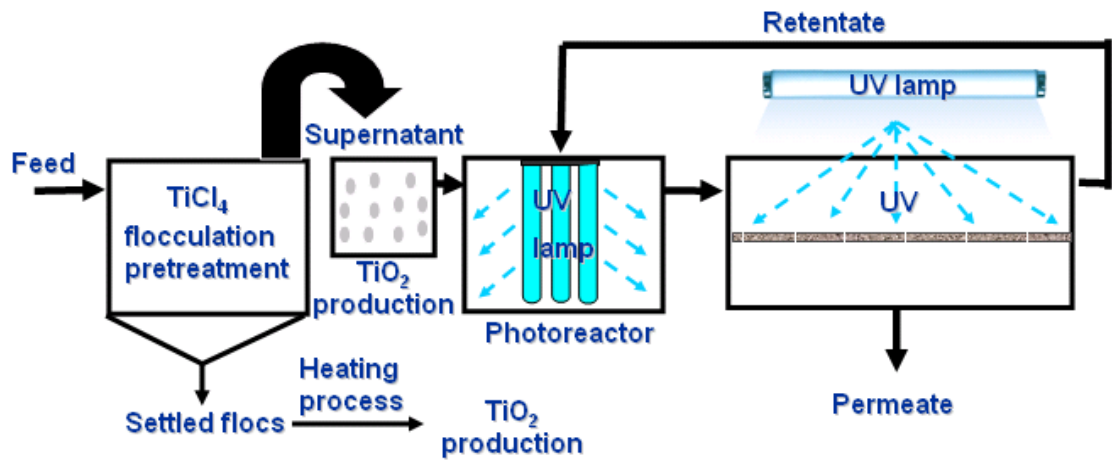


Figure 10.3 Schematic of near-zero fouling system III

REFERENCES

- Abdessemed D, Nezzal G. (2002) Treatment of primary effluent by coagulation-adsorption-ultrafiltration for reuse. *Desalination* 152 (1-3), 367-373.
- Abdessemed D., Nezzal G., and Ben Aim R. (2000) Coagulation-adsorption-ultrafiltration for wastewater treatment and reuse. *Desalination* 131, 307-314.
- Adams C., Wang Y., Loftin K., and Meyer M. (2002) Removal of antibiotics from surface and distilled water in conventional water treatment processes. *Journal of Environmental Engineering* 123, 253-260.
- Adin A., Soffer Y. and Ben Aim R. (1998) Effluent pre-treatment by iron coagulation applying various dose-pH combinations for optimum particle separation. *Water Science and Technology* 38 (5), 27-34.
- Aguayo S., Muñoz M. J., Torre A. de la, Roset J., Peña E. de la and Carballo M. (2004) Identification of organic compounds and ecotoxicological assessment of sewage treatment plants (STP) effluents. *Science of The Total Environment* 38 (1-3), 69-81.
- Aguiar A, Lefebvre E, Rahni M, Beguebe B. (1996) Relationship between raw water TOC and the optimum coagulant dose (iron III chloride). *Environmental Technology* 17 (1-3), 381-389.
- Ahn K.H. and Song K.G. (1999) Treatment of domestic wastewater using microfiltration for reuse of wastewater. *Desalination* 126 (1-3), 7-14.
- Al-Asheh S., Banat F., Al-Omari R. and Duvnjak Z. (2000) Predictions of binary sorption isotherms for the sorption of heavy metals by pine bark using single isotherm data. *Chemosphere* 41, 659-665.
- Al-Bastaki, N.M. (2003) Performance of advanced methods for treatment of wastewater: UV/TiO₂, RO and UF. *Chemical Engineering and Processing*, 43 (7), 935-940.
- Al-Malack M.H. and Anderson G.K. (1996) Coagulation-crossflow microfiltration of domestic wastewater. *Journal of Membrane Science* 121 (1), 59-65.
- Alonso E., Santos A., Solis G.J. and Riesco P. (2001) On the feasibility of urban wastewater tertiary treatment by membranes: a comparative assessment. *Desalination* 141 (1), 39-51.
- Al-Rasheed R. and Cardin D.J. (2003a) Photocatalytic degradation of humic acid in saline waters part 2. Effect of various photocatalytic materials. *Applied Catalysis A: General* 246 (1), 39-48.
- Al-Rasheed R. and Cardin D.J. (2003b) Photocatalytic degradation of humic acid in saline waters. Part 1. Artificial seawater: influence of TiO₂, temperature, pH, and air-flow. *Chemosphere* 51, 925-933.
- Amirtharajah A. and Mills K.J. (1982) Rapid mix design for mechanisms of alum coagulation. *AWWA* 74 (4), 210.
- Amirtharajah A. and O'Melia C.R. (1990) Coagulation processes: destabilization, mixing and flocculation. In: *Water quality and treatment*, Chapter 6.
- Amy G. and Cho J. (1999) Interactions between Natural Organic Matter (NOM) and Membranes : Rejection and Fouling. *Water Science and Technology* 40 (9), 131-139.
- An T., Gu H., Xiong Y., Chen W., Zhu X., Sheng G. and Fu J. (2003) Decolourization and COD removal from reactive dye-containing wastewater using sonophotocatalytic technology. *Journal of chemical technology and biotechnology* 78, 1141-1148.

- APHA, (1995) Standard methods for the examination of water and waste water (18), American Public Health Association (APHA), Washington, DC.
- Apostolidis N. (2004) Implementing integrated water management in major regional schemes. Enviro 04 Convention & Exhibition, Sydney, 28 March – 1 April.
- Aquino S.F. and Stuckey D.C. (2004) Soluble microbial products formation in anaerobic chemostats in the presence of toxic compounds. *Water Research* 38 (2), 255-266
- Arana J., Dona-Rodriguez J.M., Tello Rendon E., Garriga I Cabo C., Gonzalez-Diaz O., Herrera-Melian J.A., Perez-Pena J., Colon G., and Navio J.A. (2003a) TiO₂ activation by using activated carbon as a support Part I. surface characterization and decantability study. *Applied Catalysis B: Environmental* 44 (2), 161-172.
- Arana J., Dona-Rodriguez J.M., Tello Rendon E., Garriga I Cabo C., Gonzalez-Diaz O., Herrera-Melian J.A., Perez-Pena J., Colon G., and Navio, J.A. (2003b) TiO₂ activation by using activated carbon as a support Part II. Photoreactivity and FTIR study. *Applied Catalysis B: Environmental* 44 (2), 153-160.
- Arana J., Melian J.A.H., Rodriguez J.M.D., Diaz O.G., Viera A., Pena J.P., Sosa P.M.M., Jimenez V.E. (2002) TiO₂-photocatalysis as a tertiary treatment of naturally treated wastewater. *Catalysis Today* 76 (2-4), 279-289.
- AWWA. (2004) Magnetic ion exchange resin exceeds EPA disinfection byproduct (DBP) standards. *Filtration & Separation* 41 (4), 28-30.
- Baker A. (2001) Fluorescence excitation-emission matrix characterization of some sewage-impacted rivers. *Environmental Science & Technology* 35 (5), 948-953.
- Banin E. (1992) Effects of aluminium complexes on neuronal function. Ph. D. Dissertation, The Hebrew University of Jerusalem.
- Barceló D. (2003) Emerging pollutants in water analysis. *TrAC Trends in Analytical Chemistry* 22 (10), xiv-xvi.
- Barker D.J. and Stuckey D.C. (2001) Modeling of soluble microbial products in anaerobic digestion: the effect of feed strength and composition. *Water Environ Res* 73 (2), 173–184.
- Bellamy L.J. (1975) The infra-red spectra of complex molecules. Chapman and Hall, London.
- Benefield L.D., Judkins J.F. and Weand B.L. Process chemistry for water and wastewater treatment. Prentice-Hall, Englewood Cliffs, N.J. 1982.
- Beri R.G., Hacche L.S. and Martin C.F. HPLC: practical and industrial applications. CRC press, 2nd Ed., Washington D.C., Ch. 6, 2001.
- Bhattacharyya D. and Williams M.E. Reverse osmosis In Chapter 22. Winston Ho, W.S. and Sirkar, K.K. Membrane handbook. 1992.
- Blount M.C., Kim D.H. and Falconer J.L. (2001) Transparent thin-film TiO₂ photocatalysis with high activity. *Environmental Science and Technology* 35 (14), 2988-2994.
- Bolto B., Dixon D. and Eldridge R. (2004) Ion exchange for the removal of natural organic matter Reactive and Functional Polymers. *Reactive and Functional Polymers* 60, 171-182.
- Bourke M, Slunjski M, O Leary B, Smith P, (1999) Scale-Up of the MIEX DOC Process for Full Scale Water Treatment Plants, 18th Federal Convention AWWA Proceedings 99, Adelaide.
- Brattebo H, Odegaard H, Halle O, (1987) Ion Exchange for the Removal of Humic Acids in Water Treatment. *Water Research* 21 (9), 1045-1052.

- Bruggen B.V., Vandecasteele C., Gestel T.V., Doyen, W., and Leysen R. (2003) A review of pressure-driven membrane process in wastewater treatment and drinking water production. *Environmental Progress* 22, 46-56.
- Bruvold W.H. (1985) Obtaining public support for reuse water, *Journal of American Water Works Association (AWWA)*, 77 (7), 72-77.
- Bruvold W.H. (1988) Public opinion on water reuse options, *Journal of Water Pollution Control Federation*, 60 (1), 45-49.
- Carrol T., King S., Gray S.R., Bolto B.A., and Booker N.A. (2000) The fouling of microfiltration membranes by NOM after coagulation treatment. *Water Research* 34 (11), 2861-2868.
- Casey T.J. *Unit Treatment Processes in Water and Wastewater Engineering*, John Wiley & Sons, 1997, Chichester, England.
- Causserand C., Rouaix S., Akbari A., and Aimar P. (2004) Improvement of a method for the characterization of ultrafiltration membranes by measurements of tracers retention. *Journal of Membrane Science* 238, 177-190.
- Chapman H., Vigneswaran S., Ngo H.H., Dyer S., and Ben Aim R. (2002) Pre-flocculation of secondary treated wastewater in enhancing the performance of microfiltration. *Desalination* 146, 367-372.
- Chaudhary D.S. (2003) Adsorption – Filtration Hybrid System in Wastewater Treatment and Reuse, Doctoral thesis of philosophy, University of Technology, Sydney.
- Chaudhary D.S., Vigneswaran S., Ngo H. H., Shim W.G. and Moon H. (2003) Biofilter in water and wastewater treatment: Feature review paper, *Korean Journal of Chemical Engineers* 20 (6), 1054-105.
- Chellam S. and Taylor J.S. (2001) Simplified analysis of contaminant rejection during ground- and surface water nanofiltration under the information collection rule. *Water Research* 35 (10), 2460-2474.
- Chen J., Kim S. and Ting Y. (2003) Optimisation of membrane physical and chemical cleaning by a statistically designed approach. *Journal of Membrane Science* 219, 27-45.
- Chen V., Fane A.G., Madaeni S. and Wenten I.G. (1997) Particle deposition during membrane filtration of colloids: transition between concentration polarization and cake formation. *Journal of Membrane Science* 125, 109-122.
- Chin Y., Aiken G. and O'Loughlin E. (1994) Molecular weight, polydispersity, and spectroscopic properties of aquatic humic substances. *Environmental Science and Technology* 28, 1853-1858.
- Cho J. (2005) membrane selection guide. http://env1.kjist.ac.kr/cgi-bin/kimsboard/kimsboard.cgi?db=nom_news&action=view&file=2425961.cgi&re=0&no=31&p=3.
- Cho J. *Membrane engineering*. Dong Wa Publication, Seoul, Korea, 2003, 169-182.
- Cho J., Amy G. and Pellegrino J. (2000) Membrane filtration of natural organic matter: factors and mechanisms affecting rejection and flux decline with charged ultrafiltration (UF) membrane. *Journal of Membrane Science* 164 (1-2), 89-110.
- Cho J., Amy G., Pelligrino J. and Yoon Y. (1998) Characterization of clean and natural organic matter (NOM) fouled NF and UF membranes, and the foulants characterization. *Desalination* 118, 101-108.
- Cho, J. Natural organic matter (NOM) rejection by, and flux-decline of , nanofiltration (NF) and ultrafiltration (UF) membranes. Ph.D. dissertation, Department of Civil,

- Environmental, and Architectural engineering, University of Colorado at Boulder, 1998.
- Choo K.H. and Kang S.K. (2003) Removal of residual organic matter from secondary effluent by iron oxides adsorption. *Desalination* 154 (2), 139-146.
- Chronakis I.S. (2001) Gelation of edible blue-green algae protein isolate (*Spirulina platensis* Strain Pacifica): thermal transitions, rheological properties, and molecular forces involved. *J. Agric. Food Chem.* 49, 888–898.
- Chu W. and Wong C.C. (2004) The photocatalytic degradation of dicamba in TiO₂ suspensions with the help of hydrogen peroxide by different near UV irradiations. *Water Research* 38 (4), 1037-1043.
- Chun M.S., Cho H.I., and Song I.K. (2002) Electrokinetic behavior of membrane zeta potential during the filtration of colloidal suspensions. *Desalination* 148, 363-367.
- Clark M.M. and Heneghan K.S. (1991) Ultrafiltration of lake water for potable water production. *Desalination* 80 (2-3), 243-249.
- Clark M.M., Baudin I. and Anselme C. Membrane-powdered activated carbon reactors. In: *Water Treatment Membrane Processes*, ed. J. Mallevalle, McGraw-Hill, New York, NY, USA, 1996.
- Coax S. (2004) Use of alternative water sources: issues for the water industry. *Enviro 04 Convention & Exhibition, Sydney, 28 March – 1 April.*
- Coble P.G., Green S.A., Blough N.V. and Gagosian R.B. (1990) Characterization of dissolved organic matter in the Black Sea by fluorescence spectroscopy. *Nature* 348 (6300), 432-435.
- Combe C., Molis E., Lucas P., Riley R. and Clark M. (1999) The effect of CA membrane properties on adsorptive fouling by humic acid. *Journal of Membrane Science* 154 (1999), 73–87.
- Cooper A.R. Determination of molecular weight, Wiley, New York, NY. 1989.
- Craig G. and Griffiths P. (2003) Seven years experience reusing sewage using microfiltration on a 1640 MW power station. *Proceedings of the AWWA membrane conference, Atlanta, Georgia.*
- Cuperus F.P. and Smolders C.A. (1991) Characterization of UF membranes (membrane characteristics and characterization technique). *Journal of Membrane Science* 34, 135-173.
- Daughton C.G. and Ternes T.A. (1999) Pharmaceuticals and personal care products in the environment: Agents of subtle change? *Environmental Health Perspectives* 107 (6), 907-938.
- del Rio J.C., McKinney D.E., Knicker H., Nanny M.A., Minard R.D. and Hatcher P.G. (1998) Structural characterization of bio- and geo-macromolecules by off-line thermochemolysis with tetramethylammonium hydroxide. *Journal of Chromatography A* 823 (1-2), 433-448.
- Dempsey B. A., Ganho R. N., and O'Melia, C. R. (1984) Coagulation of humic substances by means of aluminum salts. *Journal of American Water Works Association* 74, 141-150.
- DeWolfe J., Dempsey B., Taylor M. and Potter J.W. (2003) *Guidance manual for coagulant changeover.* AWWA Research foundation, Denver.
- DiGiano F.A., Braghetta A., Nilson J. and Utne B. (1994) Fouling of nanofiltration membranes by natural organic matter. *National Conference on Environmental Engineering, American Society of Civil Engineers*, 320-328.

- Dignac M.F., Ginestet P., Ryback D., Bruchet A., Urbain V. and Scribe P. (2000) Fate of wastewater organic pollution during activated carbon sludge treatment: nature of residual organic matter. *Water Research* 37, 4185-4194.
- Dillon P. and Ellis D. (2004) Australian water conservation and reuse research program. *Enviro 04 Convention & Exhibition, Sydney, 28 March – 1 April.*
- Dolan J.W. (1990) Problems in size exclusion chromatography. *LC-GC* 8, 290.
- Dolan J.W. and Snyder L.R., (1989) *Troubleshooting LC systems: a comprehensive approach to troubleshooting LC equipment and separations*, Humana, Clifton, NJ, 412-414.
- Doong R.A., Maithreepala R.A. and Chang S.M. (2000) Heterogeneous and homogeneous photocatalytic degradation of chlorophenols in aqueous titanium dioxide and ferrous ion. *Water Science and Technology* 42 (7-8), 253-260.
- Drewes J. and Fox P. (1999) Fate of Natural Organic Matter (NOM) during Groundwater Recharge using Reclaimed Water. *Water Science and Technology*, 40 (9), 241–248.
- Dubois M., Gilles K.A., Hamilton J.K., Rebers P.A. and Smith F. (1956) Colorimetric method for determination of sugars and related substances. *Anal Chem* 28 (3), 350–356.
- Duin O., Wessels P., van der Roest H., Uijterlinde C. and Schoonewille H. (2000) Direct nanofiltration or ultrafiltration of WWTP effluent? *Desalination* 132 (1-3), 65-72.
- Edzwald J.K., Becker W.C., Wattier K.L. (1985) Surrogate parameters for monitoring organic matter and THM precursors. *JAWWA* 77 (4), 122-132.
- Ellis T.G. (2004) Chemistry of wastewater. *Encyclopedia of Life Support System (EOLSS)*, Developed under the Auspices of the UNESCO, Eolss Publishers, Oxford, UK, <http://www.eolss.net>.
- Ernst M., Sachse A., Steinberg C.E.W. and Jekel M. (2000) Characterization of the DOC in nanofiltration permeates of a tertiary effluent. *Water Research* 34 (11), 2879-2886.
- Escobar I. and Randall A. (1999) Influence of nanofiltration on distribution system biostability. *J. Am. Water Works Assoc.* 91 (6), 76–89.
- Escobar I.C. and Randall A.A. (2001) Assimilable organic carbon (AOC) and biodegradable dissolved organic carbon (BDOC): complementary measurements. *Water Research* 35 (18), 4444-4454.
- Ettre L.S. and Zlatkis A. (1979) *75 years of chromatography. A historical dialogue*, Elsevier, Amsterdam.
- Fan L., Harris J., Roddick F. and Booker N. (2001) Influence of the characteristics of natural organic matter on the fouling of microfiltration membranes. *Water Research* 35 (18), 4455–4463.
- Fane A.G. (1996) Membrane for water production and wastewater reuse. *Desalination* 106, 1-9.
- Fearing D.A., Banks J., Guyetand S., Eroles C.M., Jefferson B., Wilson D., Hillis P., Campbell A.T. and Parsons S.A. (2004) Combination of ferric and MIEX[®] for the treatment of a humic rich water. *Water Research* 38 (10), 2551-2558.
- Fox A., Morgan S.L. and Gilbert J. (1989) Preparation of alditol acetates and their analysis by gas chromatography GC and mass spectrometry. In: Bierman, C.J. and MacGinnis, G.D., Editors, 1989. *Analysis of Carbohydrates by GLC and MS*, CRC Press, 87–117.
- Frederick K, (1997) A Look at Uniform Ion-Exchange Resins *Ultrapure Water, Sep 1997*, 66-67

- Gander M., Jefferson B. and Judd S. (2000) Aerobic MBRs for domestic wastewater treatment: a review with cost considerations. *Separation and Purification Technology* 18 (2), 119-130.
- GCHERI (Gwangju City Health & Environment Research Institute (2005) <http://hevi.gjcity.net/index.html>.
- Gehrke C.W., Wixom R.L. and Bayer E. (2001) *Chromatography – A century of discovery 1900 – 2000. The Bridge to the Sciences/Technology*, Elsevier, Amsterdam.
- Gibson H.E. and Apostolidis N. (2001) Demonstration, the solution to successful community acceptance of water recycling. *Water Science and Technology* 43 (10), 259-266.
- Goel S., Hozalski R. M., and Bouwer E. J. (1995) Biodegradation of NOM: effect of NOM source and ozone dose, *Journal of American Water Works Association* 87 (1), 90.
- Gogate P.R. and Pandit A.B. (2003) A review of imperative technologies for wastewater treatment I: oxidation technologies at ambient conditions. *Advances in Environmental Research* 8 (3-4), 501-551.
- Gottlieb M. (1996) The Reversible Removal of Naturally Occuring Organics Using Resins Regenerated with Sodium Chloride, *Ultrapure Water* Nov 1996, 53-58.
- Gray S.R. and Bolto B.A. (2003) Predicting NOM fouling rates of low pressure membranes. *International membrane science and technology (IMSTEC) proceedings*, Sydney, Australia.
- Guo W.S., Chapman H., Vigneswaran S. and Ngo H.H. (2004) Experimental investigation of adsorption-flocculation-microfiltration hybrid system in wastewater reuse. *Journal of Membrane Science* 242 (1-2), 27-35.
- Gusses A. M., Allgeier S. C., Speth T. F. and Summers R. S. (1997) Evaluation of surface water pretreatment processes using rapid bench-scale membrane test. *Proceedings, AWWA Membrane Technology Conference*, New Orleans, 765-782.
- Hansen, J. (2004) Use of alternative water sources: Sydney water's experience. *Enviro 04 Convention & Exhibition*, Sydney, 28 March – 1 April.
- Her N.G., Amy G., Foss D., Cho J., Yoon Y. and Kosenka P. (2002) Optimization of method for detecting and characterizing NOM by HPLC-size exclusion chromatography (SEC) with UV and on-line DOC detection, *Environmental Science and Technology* 36, 1069-1076.
- Her, N.G. Identification and characterization of foulants and scalants on NF membrane. Ph.D. dissertation, Department of Civil, Environmental, and Architectural engineering, University of Colorado at Boulder, 2002.
- Hoang T.T.L., Shon H.K., Chaudhary D.S., Vigneswaran S. and Ngo H. H. (2004) Granular activated carbon (GAC) biofilter for low strength wastewater treatment. *Fluid/Particle Separation Journal* 16 (2), 185-191.
- Hong S. and Elimelech M. (1997) Chemical and physical aspects of natural organic matter (NOM) fouling of nanofiltration membranes. *Journal of Membrane Science*, 132, 159-181.
- Hongve D., Baann J., Becher G. and Beckmann O.-A. (1999) Experiences from Operation and Regeneration of an Anionic Exchanger for Natural Organic Matter (NOM) Removal *Water Science and Technology* 40 (9), 215-221
- Howe K., Clark M.M. (2002) Fouling of microfiltration and ultrafiltration membranes by natural waters. *Environ. Sci. Technol.* 36 (16), 3571-3576.

- Hozalski R.M. and Bouwer E.J. (2000) Non-steady state simulation of BOM removal in drinking water biofilters: model development. *Water Research* 35 (1), 198-210.
- Huang C.H. and Sedlak D.L. (2001) Analysis of estrogenic hormones in municipal wastewater effluent and surface water using ELISA and GC/MS/MS. *Environmental Toxicology and Chemistry* 20, 133-139.
- Huber S.A. (1998) Evidence for membrane fouling by specific TOC constituents. *Desalination* 119 (1-3), 229-234.
- Huck P. M. (1990) Measurement of Biodegradable Organic Matter and Bacterial Growth Potential in Drinking Water, *Journal of American Water Works Association* 82 (7), 78-86.
- Imai A., Fukushima T., Matsushige K., Kim Y.H. and Choi K. (2002) Characterization of dissolved organic matter in effluents from wastewater treatment plants. *Water Research* 36, 859-870.
- Issaq H.J. (2001) *A century of separation science*, Dekker, New York, NY.
- Ito K., Jian W. Nishijima W., Baes A.U., Shoto E. and Okada M. (1998) Comparison of ozonation and AOPs combined with biodegradation for removal of THM precursors in treated sewage effluents. *Water Science and Technology* 38 (7), 179-186.
- Jarusutthirak C. (2002) Fouling and flux decline of reverse osmosis (RO), nanofiltration (NF) and ultrafiltration (UF) membranes associated with effluent organic matter (EfOM) during wastewater reclamation/reuse. Ph. D. Dissertation, University of Colorado at Boulder.
- Jarusutthirak C. and Amy G. (2001) Membrane filtration of wastewater effluents for reuse: effluent organic matter rejection and fouling. *Water Science and Technology* 43 (10), 225-232.
- Jarusutthirak C., Amy G. and Croué J.-P. (2002) Fouling characteristics of wastewater effluent organic matter (EfOM) isolates on NF and UF membranes. *Desalination* 145 (1-3), 247-255.
- Johnson J.F. (1998) Chromatography, in polymers: polymer characterization and analysis, *Encyclopedia Reprint Series*, Kroschwitz, J.I., John Wiley & Sons, New York, 78-118.
- Jones K. and O'Melia C. (2000) Protein and humic acid adsorption onto hydrophilic membrane surface effects of pH and ionic strength. *Journal of Membrane Science* 165, 31-46.
- Jucker C. and Clark M.M. (1994) Adsorption of aquatic humic substances on hydrophobic ultrafiltration membranes. *Journal of Membrane Science* 97 (27), 37-52.
- Kahn S. (2004) Identifying impediments to municipal water recycling in Australia. *Enviro 04 Convention & Exhibition*, Sydney, 28 March – 1 April.
- Kameya T., Murayama T., Kitano M. and Urano, K. (1995) Testing and classification methods for the biodegradabilities of organic compounds under anaerobic conditions. *The Science of the Total Environment* 170, 31-41.
- Kaneko M. and Okura I. (2002) *Photocatalysis: science and technology*. Springer and Kodansha, 158-180.
- Khan S.J., Wintgens T., Sherman P., Zaricky J. and Schafer A.I. (2003) Removal of hormones and pharmaceuticals in the “Advanced Water Recycling Demonstration Plant” in Queensland, Australia in proceedings of Ecohazard IWA conference, Aachen, Germany.
- Kim D.H. (2004) Electrostatic interactions between ions/NOM acids and membranes. PhD thesis. Gwanju Institute of Science and Technology, 155-165.

- Kim S.H., Kwak S.-Y., Sohn, B.-H. and Park T.H. (2003) Design of TiO₂ nanoparticle self-assembled aromatic polyamide thin-film-composite (TFC) membrane as an approach to solve biofouling problem. *Journal of Membrane Science*, 211, 157-165.
- Kim S.L., Chen J.P. and Ting Y.P. (2002) Study on feed pre-treatment for membrane filtration of secondary effluent. *Separation and Purification Technology* 29, 171-179.
- Kim T.H., Park C., Shin E.B., and Kirm S. (2003) Effects of Cl⁻-based chemical coagulants on electrochemical oxidation of textile wastewater. *Desalination* 155 (1), 59-65.
- Kim, K.J. and Fane A.G. (1994) Low voltage scanning electron microscopy in membrane research. *J. Membrane Sci.* 88, 103-114.
- Kishino H., Ishida H., Iwabu H. and Nakano I. (1996) Nakano Domestic wastewater reuse using a submerged membrane bioreactor. *Desalination* 106 (1-3), 115-119.
- Kleine J., Peinemann K.V., Schuster C. and Warnecke H.J. (2002) Multifunctional system for treatment of wastewaters from adhesive-producing industries: separation of solids and oxidation of dissolved pollutants using coated microfiltration membranes. *Chemical Engineering Science* 57 (9), 1661-1664.
- Konstantinou I.K., Sakellariades T.M., Sakkas V.A. and Albanis T.A. (2001) Photocatalytic degradation of selected s-triazine herbicides and organophosphorus insecticides over aqueous TiO₂ suspensions. *Environmental Science and Technology* 35 (2), 398-405.
- Kumar V., Wati L., Nigam P., Banat I.M., Yadav B.S., and Singh D. (1998) Decolorization and biodegradation of anaerobically digested sugarcane molasses spent ash effluent from biomethanation plants by white rot fungi. *Process Bio. Cycle* 39, 64-72.
- Kwon B., Lee S., Cho J., Ahn H., Lee D. and Shin H.S. (2005) Biodegradability, DBP formation, and membrane fouling potential of natural organic matter: characterization and controllability. *Environmental Science and Technology* 39 (3), 732-739.
- Lahoussine-Turcaud V., Wiesner M.R. and Bottero J.-Y. (1990) Fouling in tangential-flow ultrafiltration: The effect of colloid size and coagulation pretreatment. *Journal of Membrane Science* 52 (2), 173-190.
- Lainé J., Hagstrom J.P., Clark M. and Mallevalle J. (1989) Effects of ultrafiltration membrane composition. *Journal of American Water Works Association* 11 (6), 61-67.
- Lawrence (1993) A telephone survey of Orange County Voters within the Orange County Water District, unpublished report prepared for Adler Public Affairs, Oct.-Nov.
- Lee H., Amy G., Cho J., Yoon Y., Moon S.H. and Kim I.S. (2001) Cleaning strategies for flux recovery of an UF membrane fouled by Natural Organic Matter. *Water Research* 35 (14), 3301-3308.
- Lee S. (2004) Transport characteristics and sorption correlation of natural organic matter in nanofiltration and ultrafiltration membranes. Doctoral thesis of philosophy, Gwangju Institute of Science and Technology, 44-70.
- Lee S. and Cho J. (2004) Elimelech, M. Influence of colloidal fouling and water recovery on salt rejection in RO and NF membrane separations. *Desalination* 160, 1-12.
- Lee S., Cho Y.G., Song Y., Kim I.S. and Cho J. (2003a) Transport characteristics of wastewater effluent organic matter in nanofiltration and ultrafiltration membranes. *Journal of Water Supply* 52 (2), 129-139.
- Lee S., Park G., Amy G., Hong S.K., Moon S.H., Lee D.H. and Cho J. (2002a) Determination of membrane pore size distribution using the fractional rejection of nonionic and charged macromolecules. *J. Membrane Sci.* 201 (1-2), 191-201.
- Lee S., Shim Y. and Cho J. (2002b) Determination of mass transport characteristics for NOM in UF and NF membranes. *Water Science and Technology* 2, 151-160.

- Lee S.A., Choo K.H., Lee C.H., Lee H.I., Hyeon T., Choi W. and Kwon H.H. (2001) Use of ultrafiltration membranes for the separation of TiO₂ photocatalysts in drinking water treatment. *Ind. Eng. Chem. Res.* 40, 1712-1719.
- Lee, H.S., Hur T., Kim S., Kim J.H. and Lee H.I. (2003b) Effects of pH and surface modification of TiO₂ with SiO_x on the photocatalytic degradation of a pyrimidine derivative. *Catalysis Today* 84 (3-4), 173-180
- Leenheer J.A., Croue J.P., Benjamin M., Korshin G.V., Hwang C.J., Bruchet A. and Aiken G.R. (2000) Comprehensive isolation of natural organic matter from water for spectral characterizations and reactivity testing. In: Barrett S.E., Krasner S.W. and Amy G.L. (Eds.), *ACS symposium series* 761.
- Levine A.D., Tchobanoglous G. and Asano T. (1985) Characterization of the size distribution of contaminants in wastewater: treatment and reuse implications, *Journal WPCF* 57 (7), 805-816.
- Li F., Yuasa A., Ebie K., Azuma Y., Hagishita T. and Matsui, Y. (2002) Factors affecting the adsorption capacity of dissolved organic matter onto activated carbon: modified isotherm analysis. *Water research* 36, 4592-4604.
- Licsko I. (2003) Coagulation mechanisms – nano- and microprocesses. *Nano and micro particles in water and wastewater treatment, Conference proceeding* 207-216.
- Lin C.F., Huang Y.J. and Hao O.J. (1999) Ultrafiltration processes for removing humic substances: effect of molecular weight fractions and PAC treatment. *Wat. Res.* 33 (5), 1252-1264.
- Lin C.F., Lin T.Y. and Hao O.J. (2000) Effects of humic substance characteristics on UF performance. *Water Res.* 34 (4), 1097–1106.
- Listowski A. and MacCormick T. (2004) Sustainable water management in urban areas: does it make cents? *Enviro 04 Convention & Exhibition, Sydney, 28 March – 1 April.*
- Liu C., Caothien S., Hayes J., Caothuy T., Otoyoto T. and Ogawa T. (2005) *Membrane Chemical Cleaning: From Art to Science.* Scientific and Laboratory Services, Pall Corporation, Industrial Membrane Systems, Asahi Chemical Industry Co., Ltd. Industry report.
- López-Ramírez J.A., Sahuquillo S., Sales D. and Quiroga J.M.(2003) Pre-treatment optimisation studies for secondary effluent reclamation with reverse osmosis. *Water Research* 37 (5), 1177-1184.
- Lu M.C., Roam G.D., Chen J.N., and Huang C.P. (1994) Photocatalytic oxidation of dichlorvos in the presence of hydrogen peroxide and ferrous ion. *Water Science and Technology* 30 (9), 29-38.
- Malcolm R.L. (1985) *Geochemistry of stream fulvic and humic substances.* Aiken et al., *Humic substances in soil, sediments and water.* John Wiley and Sons, 181-209.
- Mameri N., Abdessemed D., Belhocine D., Lounici H. (1996) Treatment of fishery washing water by ultrafiltration. *AIChE Journal* 67, 169-175.
- Marks J. (2004) Back to the future: reviewing the findings on acceptance of reclaimed water. *Enviro 04 Convention & Exhibition, Sydney, 28 March – 1 April.*
- Matijevic E. (1973) Colloid stability and complex chemistry', *Journal of Colloid and Interface Science* 43 (2), 239-247.
- Matsui Y., Colas F. and Yuasa A. (2001) Removal of a synthetic organic chemical by PAC-UF systems –II: Model application. *Water Research* 35 (2), 464-470.

- McCarthy A.A., Gilboy P., Walsh P.K. and Foley G. (1999) Characterisation of cake compressibility in dead-end microfiltration of microbial suspensions. *Chem. Eng. Comm.* 173, 79-90.
- Metcalf and Eddy Inc., *Wastewater Engineering: Treatment, Disposal and Reuse*, 3rd edition, Revised by Tchobanoglous, G. and Burton, F., McGraw-Hill, Inc., Singapore, 1991.
- Meyers P., (1995) Operating Experiences with a New Organic Trap Resin, *International Water Conference Proceedings 1995*,
- Molinari R., Borgese M., Drioli E., Palmisano L. and Schiavello M. (2002) Hybrid processes coupling photocatalysis and membranes for degradation of organic pollutants in water. *Catalysis Today* 75 (1-4), 77-85.
- Molinari R., Grande C., Drioli E., Palmisano L. and Schiavello M. (2001) Photocatalytic membrane reactors for degradation of organic pollutants in water. *Catalysis Today* 69, 273-279.
- Montgomery J.M. (1985) *Water treatment principles and design*. John Wiley & Sons, New York.
- Mulder M. *Basic principles of membrane technology* (2nd edition). Boston: Kluwer Academic Publishers, 1996.
- Murk A.J., Legler J., Van Lipzig M.M.H., Meerman J.H.N., Belfroid A.C., Spenklink A., Van der Burg B., Rijs G.B.J. and Vethaak D. (2002) Detection of estrogenic potency in wastewater and surface water with three in vitro bioassays. *Environ Toxicol Chem* 21 (1), 16-23.
- Murry P. (1995) *Water treatment, principles and practices of water supply operations*. American water works association, 2 eds, Denver, 375-378,
- Najm I.N., Snoeyink V.L., Suidan M. T., Lee C.H. and Richard Y. (1990) Effect of particle size and background natural organics on the adsorption efficiency of PAC. *Journal of American Water Works Association* 82 (1), 65-72.
- Namkung E. and Rittmann B.E. (1986) Soluble microbial products (SMP) formation kinetics by biofilms. *Water Research* 20 (6), 795-806.
- Nasu M., Goto M., Kato H., Oshima Y. and Tanaka H. (2001) Study on endocrine disrupting chemicals in wastewater treatment plants. *Water Sci Technol* 43 (2), 101-108.
- Noguera D.R., Araki N. and Rittmann B.E. (1994) Soluble microbial products (SMP) in anaerobic chemostats. *Biotechnol Bioeng* 44, 1040-1047.
- Nollet L.M.L. (2000) *Handbook of water analysis*. Marcel Dekker, Inc., New York, 390-398.
- Ødegaard H. (1989) Appropriate technology for wastewater treatment in coastal tourist areas. *Water Sci. Technol.* 21 (1), 1-17.
- Ollis D.F. (2003) Integrating photocatalysis and membrane technologies for water treatment. *Ann. N.Y. Acad. Sci.*, 984, 65-84.
- Owen D.M., Amy G.L., Chowdhury Z.K. (1993) Characterisation of natural organic matter and its relationship to treatability. AWWARF and AWWA conference proceedings, Denver, CO.
- Packham C (1971) State of the art of coagulation: mechanisms and stoichiometry. *AWWA*, 63 (2), 99.
- Painter H.A. (1973) Organic compounds in solution in sewage effluents. *Chem. Ind.* September, 818-822.

- Parkin G.F. and McCarty P.L. (1981) Production of soluble organic nitrogen during activated sludge treatment. *J. WPCF* 53 (1), 99-112.
- Pawar N.J., Pondhe G.M. and Patil S.F. (1998) Groundwater pollution due to sugar-mill effluent, at Sonai, Maharashtra. India. *Environ. Geol.* 34, 151–160.
- Peeters J.M.M., Mulder M.H.V. and Strathmann H. (1999) Streaming potential measurements as a characterization method for nanofiltration membranes. *Colloids and Surfaces A Physicochemical and Engineering Aspects* 150, 247-259.
- Pempkowiak J. and Obarska-Pempkowiak H. (2002) Long-term changes in sewage sludge stored in a reed bed. *The Science of the Total Environment* 297, 59-65.
- Perminova I.V., Frimmel F.H., Kudryavtsev A.V., Abbt-Braun G., Hesse S. and Petrosyan V.S. (2003) Molecular weight characteristics of humic substances from different environments as determined by size exclusion chromatography and their statistical evaluation. *Environ. Sci. Technol.* 37 (11), 2477-2485.
- Petrović M., Gonzalez S. and Barceló D. (2003) Analysis and removal of emerging contaminants in wastewater and drinking water. *TrAC Trends in Analytical Chemistry* 22 (10), 685-696.
- Peuravuori J. and Pihlaja K. (1999) Structural characterization of humic substances. In: Keskkitalo, J. and Eloranta, P. (eds) *Limnology of humic waters*. Backhuys, Leiden, 22-34.
- Peuravuori J., Lehtonen T. and Pihlaja K. (2002) Sorption of aquatic humic matter by DAX-8 and XAD-8 resins: Comparative study using pyrolysis gas chromatography. *Analytica Chimica Acta* 471 (2), 219-226.
- Pirbazari M., Badriyha B.N. and Ravindran V. (1992) MF-PAC for treating waters contaminated with natural and synthetic organics. *Journal of American Water Works Association* 84 (12), 95-103.
- Pirkanniemi K. and Sillanpää M. (2002) Heterogeneous water phase catalysis as an environmental application: a review. *Chemosphere* 48 (10) 1047-1060.
- Poole, C.F. (2003) *The essence of chromatography*, Elsevier Science B.V. Netherland.
- Potts D.E., Ahlert R.C., and Wang S.S. (1981) A critical review of fouling of reverse osmosis membranes. *Desalination* 36, 235-264.
- Rachwal A.J., Bauer M.J., Chipps M.J., Colbourne J. S. and Foster D. M. Comparisons between slow sand and high rate biofiltration. In: *advances in slow sand and alternative biological filtration*. Edited by Graham, N. and Collins, R., John Wiley & Sons Ltd., Chichester, England, 1996.
- Radcliffe J.C. (2003), An overview of water recycling in Australia – results from the recent ATSE study. CD-ROM, *Water Recycling Australia*, 2nd National Conference 1-3 September, 2003 Brisbane. Australian Water Association, Sydney.
- Radcliffe J.C. (2003a) Water, second/third time around. In “Water – the Australian Dilemma”, ATSE 2003 Symposium, Melbourne, Nov. 17-18 2003. Australian Academy of Technological Sciences and Engineering, Melbourne.
- Rand G.M. (1995) *Fundamental of Aquatic Toxicology: effects, environmental fate and risk assessment*, 2nd edition. , Taylor & Francis, London.
- Rathjen D. (2003) *Recycling water for our cities report to prime minister’s science, engineering and innovation council*, 28 November 2003.
- Rebhun M. Meir S. and Laor Y. (1998) Using dissolved humic acid to remove hydrophobic contaminants from water by complexation-flocculation process. *Environmental Science and Technology* 32, 981-986.

- Redondo J.A. and Lomax I. (2001) Y2K generation FILMTEC RO membranes combined with new pretreatment techniques to treat raw water with high fouling potential: summary of experience. *Desalination* 136, 287-306.
- Réveill  V., Mansuy L., Jard  E., and Garnier-Sillam   (2003) Characterisation of sewage sludge-derived organic matter: lipids and humic acids. *Organic Geochemistry* 34 (4), 615-627.
- Ridgway H.F., Flemming H.C. and Mallevalle J. Water treatment: membrane processes, American Water Works Association, Lyonnaise des Eaux and Water Research Commission of South Africa, New York, 1996, 6.2-6.20.
- Rittmann B.E. and McCarty P.L. (2001) Environmental biotechnology: principles and applications. , McGraw-Hill International Editions, London, UK.
- Rittmann B.E., Bae W., Namkung E. and Lu C.J. (1987) A critical evaluation of microbial product formation in biological processes. *Water Sci Technol* 19, 517-528.
- Rodriguez M., Adberrazik N.B., Contreras S., Chamarro E., Gimenez J. and Esplugas S. (2002) Iron (III) photooxidation of organic compounds in aqueous solutions. *Appl Catal B* 37, 131-137.
- Roila T., Kortelainen P., David M.B. and Makinen I. (1994) Acid-base characteristics of DOC in Finnish lakes. In: Senesi, N., Miano, T.M. (eds) Humic substances in the global environment and implications for human health. Elsevier, Amsterdam, 863-868.
- Sacher F., Haist-Gulde B., Brauch H.-J., Preub G., Wilme U., Zullei-Seibert N., Meisenheimer M., Welsch H. and Ternes T.A. (2000) Behavior of selected pharmaceuticals during drinking water treatment. 219th ACS National Meeting, San Francisco, CA, 116-118.
- Sagawe G., Brandi R.J., Bahnemann D. and Cassano A.E. (2003) Photocatalytic reactors for treating water pollution with solar illumination. I: a simplified analysis for batch reactors. *Chemical Engineering Science* 58 (12), 2587-2599.
- Sarria V., Kenfack S., Guillod O. and Pulgarin C. (2003) An innovative coupled solar-biological system at field pilot scale for the treatment of biorecalcitrant pollutants. *Journal of Photochemistry and Photobiology A: Chemistry* 159 (1), 89-99.
- Schafer A.I. (2001) Natural organics removal using membranes: principles, performance, and cost. Technomic Publishing Company, Inc., Pennsylvania, USA
- Semerjian L. and Ayoub G.M. (2003) High-pH-magnesium coagulation-flocculation in wastewater treatment . *Advances in Environmental Research* 7 (2), 389-403.
- Seo G.T. (1997) Ohgaki S, Suzuki Y. Sorption characteristics of biological powdered activated carbon in BPAC-MF (biological activated carbon-microfiltration) system for refractory organic removal. *Wat. Sci. Technol.* 35(7), 163-170.
- Servais P., Billen G. and Hascoet M.C. (1987) Determination of the biodegradable fraction of dissolved organic matter in waters. *Water Research* 21, 445-450.
- Shim W.G., Chaudhary D.S., Vigneswaran S., Ngo H.H., Lee J.W. and Moon H. (2004) Mathematical modeling of granular activated carbon (GAC) biofiltration system, *Korean J. Chem. Eng.* 21, 212-220.
- Shiozawa T., Tada A., Nukaya H., Watanabe T., Takahashi Y., Asanoma M., Ohe T., Sawanishi H., Katsuhara T., Sugimura T., Wakabayashi K. and Terao, Y. (2000) Isolation and identification of a new 2-phenylbenzotriazole-type mutagen (PTBA-3) in the Nikko River in Aichi, Japan. *Chem Res Toxicol* 13 (7), 535-540.

- Shon H.K., Guo W. S., Vigneswaran S., Ngo H.H. and Kim In S. (2004a) Effect of flocculation in membrane-flocculation hybrid system in water reuse. *Separation Science and Technology*, 39 (8), 1871-1883.
- Shon H.K., Nathaporn A., Vigneswaran S., Ngo H.H. and Kim J.-H. (2005b) Photocatalysis hybrid system in the removal of effluent organic matter (EfOM). *International Conference on Advances in Industrial Wastewater Treatment*, 9 – 11 February, Chennai, India.
- Shon H.K., Vigneswaran S. and Ngo H.H. (2005a) Effect of partial flocculation and adsorption as pretreatment to ultrafiltration in treating wastewater. *American Institute of Chemical Engineers (AIChE Journal)*, In press.
- Shon H.K., Vigneswaran S., Ben Aim R., Ngo H. H., Kim In S. and Cho J. (2005b) Influence of flocculation and adsorption as pretreatment on the fouling of ultrafiltration and nanofiltration membranes: application with biologically treated sewage effluent. *Environmental Science & Technology*, 39 (10), 3864-3871.
- Shon H.K., Vigneswaran S., Kim I.S., Cho J. and Ngo H.H. (2004b) The effect of pretreatment to ultrafiltration of biologically treated sewage effluent: a detailed effluent organic matter (EfOM) characterization. *Wat. Res.* 38 (7), 1933-1939.
- Shon H.K., Vigneswaran S., Kim In S., Cho J., and Ngo H.H. (2004c) Effect of pretreatment on the fouling of membranes: application in biologically treated sewage effluent. *Journal of Membrane Sci.*, 234 (1-2), 111-120.
- Shon H.K., Vigneswaran S., Kim J.H., Ngo H.H. and Park N.E. (2004d) Comparison of nanofiltration with flocculation-microfiltration-photocatalysis hybrid system in dissolved organic matter removal. *9th World Filtration Congress*, New Orleans, Louisiana, USA, on April 18- 22.
- Shon H.K., Vigneswaran S., Ngo H. H. and Ben Aim R. (2005c) Is semi-flocculation effective as pretreatment to ultrafiltration in wastewater treatment? *Water Research* 39 (1), 147-153.
- Shon H.K., Vigneswaran S., Ngo H.H. and Kim I.S. (2003a) Effect of pre-treatment on nonofiltration used in wastewater reuse, *Asian Waterqual2003-IWA Asia-Pacific Regional conference proceedings*. Bangkok, Thailand.
- Shon H.K., Vigneswaran S., Ngo H.H. and Kim J.-H. (2005d) Chemical coupling of photocatalysis with flocculation and adsorption in the removal of organic matter. *Water Research*, 39 (12), 2549-2558.
- Shon H.K., Vigneswaran S., Ngo H.H., Kim D.H., Park N.E., Jang N.J. and Kim I.S. (2003b) Characterization of effluent organic matter (EfOM) of fouled nanofilter (NF) membranes, *International membrane science and technology (IMSTEC) proceedings*, Sydney, Australia.
- Shon H.K., Vigneswaran S., Ngo H.H., Kim In S. and Ben Aim R. (2005e) Foulant characterization of the NF membranes with and without pretreatment of biologically treated wastewater. *Water Science & Technology*, 51 (6-7), 277-284.
- Skoog D.A. and Leary J.J. (1992) *Principles of instrumental analysis*. 4th edition, Saunders College Publishing, Fort Worth.
- Skoog D.A., Holler F.J. and Nieman T.A. (1998) *Principles of instrumental analysis*, 5thed., Harcourt Brace College Publishers, PA, USA.
- Slunjski M., Bourke M., Nguyen H., Morran J. and Bursill D. (1999) MIEX® DOC Process – A New Ion Exchange. *18th Federal Convention, Australian Water & Wastewater Association, Proceedings* 11-14 April 1999, Adelaide Australia.

<http://www.orica.com/Business/CHE/CHLORALKALI/WCHE00017.nsf/0/699ce37915caf471ca256cd000226362/>

- Smith P.J., Vigneswaran S., Ngo H.H., Ben-Aim R. and Nguyen H. (2005) Design of a generic control system for optimising back flush durations in a submerged membrane hybrid reactor. *Journal of Membrane Science* 255 (1-2), 99-106.
- Snoeyink V.L., Campos C. and Marinas B.J. (2000) Design and performance of powdered activated carbon/ultrafiltration systems. *Water Science and Technology* 42 (12), 1-10.
- Snyder L.R. and Kirkland J.J. (1985) Introduction to modern liquid chromatography. 2nd Ed., John Wiley & Sons, New York, Chap. 12.
- Snyder S. and Westerhoff P. (2005) Conventional and advanced water treatment processes to remove EDCs and PPCPs. Presentation from Southern Nevada Water Authority. <http://www.snwa.com/html/index.html>.
- Snyder S., Vanderford B., Pearson R., Quiñones and Yoon Y. (2003a) Analytical method used to measure endocrine disrupting compound in water. *Practice Periodical of Hazardous, Toxic, and Radioactive waste management* 7(4), 224-234.
- Snyder S.A., Westerhoff P., Yoon Y. and Sedlak D.C. (2003b) Pharmaceuticals, personal care products and endocrine disrupters in water: implications for water treating. *Environmental Engineering Science* 20(5), 449-469.
- Soffer Y., Gilron J. and Adin A., (2002) Steaming potential and SEM-EDX study of UF membranes fouled by colloidal iron. *Desal.* 146, 115-121.
- Soria V., Campos A., Garcia R. and Parets M.J. (1990) Solution properties of polyelectrolytes. VI. Secondary effects in aqueous size-exclusion chromatography. *J. Liq. Chromatogr.* 13, 1785.
- Speth T.F., Summers S.R. and Gusses A.M. (1998) Nanofiltration foulants from a treated surface water. *Environmental Science and Technology* 32 (22), 3612-3617.
- Stainfield G. and Jago P.H. (1987) The development and use of a method for measuring the concentration of assimilable organic carbon in water. WRC Environment Report, RU 1628-M, Manheim, UK.
- Steinberg C.E.W. (2003) Ecology of humic substances in freshwaters. Springer.
- Stull J.K., Swift D.J.P. and Niedoroda A.W. (1996) Contaminant dispersal on the Palos Verdes continental margin: I. sediments and biota near a major California wastewater discharge. *The Science of the Total Environment* 179, 73-90.
- Summers R.S. and Roberts P.V. (1984) Simulation of DOC removal in activated carbon beds, *Journal of Environmental Engineering* 110 (2) 73-92.
- Sundstorm D.W. and Klei H.E. (1980) Sundstorm and Klei Wastewater Treatment, Prentice Hall, Englewood Cliffs, NJ.
- Symons J., Fu P., Kim P. (1995) Sorption and Desorption Behaviour of Natural Organic Matter onto Strong-Base Anion Exchanger, Ch 4 in *Ion Exchange Technology* edited by Sengupta A., Technomic Publishing Co. Inc., Lancaster, PA, USA
- Talu O. and Meunier F. (1996) Adsorption of associating molecules in micropores and application to water on carbon. *American Institute of Chemical Engineers Journal* 42 (3), 809-819.
- Tanaka H., Yakou Y., Takahashi A., Higashitani T. and Komori K. (2001) Comparison between estrogenicities estimated from DNA recombinant assay and from chemical analyses of endocrine disruptors during sewage treatment. *Water Sci Technol* 43 (2), 125-132.

- Tandanier C.J., Berry D.F. and Knocke W.R. (2000) Dissolved organic matter apparent molecular distribution and number-average apparent molecular weight by batch ultrafiltration. *Environ. Sci. Technol.* 34 (11), 2348-2353.
- Tang C. (2003) Membrane coupled photocatalytic treatment of textile effluent. Ph.D. dissertation. The University of New South Wales, School of Chemical Engineering and Industrial Chemistry, Australia.
- Tang C. and Chen V. (2002) Nanofiltration of textile wastewater for water reuse, *Desalination* 143 (1), 11-20.
- Tanninen J., Kamppinen L. and Nyström M. (2003) Nanofiltration – principles and applications, Chapter 10, pretreatment/hybrid process. Elsevier Advanced Technology Publisher, London.
- Tchobanoglous G. and Burton F.L. (1991) Wastewater engineering: treatment, disposal, and reuse. 3rd Eds., McGraw-Hill, Inc. New York.
- Tchobanoglous G., Darby J., Bourgeois K., McArdle J., Genest P. and Tylla M. (1998) Ultrafiltration as an advanced tertiary treatment process for municipal wastewater. *Desalination* 119 (1-3), 315-321.
- Ternes T.A. (1998) Occurrence of drugs in German sewage treatment plants and rivers. *Water Research* 32, 3245-3260.
- Ternes T.A., Kreckel P. and Mueller J. (1999) Behaviour and occurrence of estrogens in municipal sewage treatment plants – II. Aerobic batch experiments with activated sludge. *Science and the Total Environment* 225, 91-99.
- Thanuttamavong M., Yamamoto K, Oh J.I., Choo K.H. and Choi S.J. (2002) Rejection characteristics of organic and inorganic pollutants by ultra low-pressure nanofiltration of surface water for drinking water treatment. *Desalination* 145, 257-264.
- Thanuttamavong, M. Ultra low pressure nanofiltration of river water for drinking water treatment, Ph.D. dissertation, Department of Urban Engineering, University of Tokyo, 2002, 70-80.
- Thiruvengkatachari R., Shim W.G., Lee J.W. and Moon H. (2005) Powdered Activated Carbon Coated Hollow Fiber Membrane: Preliminary Studies on its Ability to Limit Membrane Fouling and to Remove Organic Materials. *Korean Journal of Chemical Engineering* 22 (2), 250-255.
- Thurman E.M. (1985) Organic geochemistry of natural waters. Martinus Nijhoff/Dr. W. Junk Publishers. The Netherlands
- Tiehm A. and Neis U. (2005) Ultrasonic dehalogenation and toxicity reduction of trichlorophenol. *Ultrasonics Sonochemistry* 12(1-2), 121-125.
- Tixier C., Singer H.P., Oellers S. and Müller S.R. (2003) Occurrence and fate of carbamazepine, clofibric acid, diclofenac, ibuprofen, ketoprofen, and naproxen in surface waters. *Environmental Science and Technology* 37 (6), 1061-1068.
- Tonkes M., Pols H., Warmer H., Bakker V. (1998) Whole-effluent assessment. RIZA Report 98.034. Institute for Inland Water Management and Waste Water Treatment, Lelystad, The Netherlands.
- Urfer D., Huck P.M., Booth S.D.J. and Coffey B.M. (1997) Biological filtration for BOM and particle removal: a critical review, *Journal of American Water Works Association* 89 (12), 83-98.
- Vanderford B.J., Pearson R.A., Rexing D.J., and Snyder, S.A. (2003) Analysis of endocrine disruptors, pharmaceuticals, and personal care products in water using

- liquid chromatography/tandem mass spectrometry. *Analytical Chemistry* 75(22), 6265-6274.
- Verwey E.J.W. and Overbeek J.T.G. *Theory of the stability of lyophobic colloids*. Amsterdam. Elsevier Scientific Publishing, 1948.
- Vigneswaran S. and Visvanathan C. (1995) *Water treatment processes: simple options*. CRC press, Florida, USA.
- Vigneswaran S., Chaudhary D.S., Ngo H.H., Shim W.G. and Moon H. (2003) Application of a PAC-membrane hybrid system for removal of organics from secondary sewage effluent: Experiment and modeling. *Separation Science and Technology* 38 (10), 2183-2199.
- Vigneswaran S., Shon H.K., Boothanon S., Ngo H.H. and Ben Aim R. (2004) Membrane-flocculation-adsorption hybrid system in wastewater treatment: micro and nano size organic matter removal. *Water Science & Technology*. 50 (12), 265-271.
- Vilge-Ritter A., Rose J., Masion A., Bottero J.Y. and Laine J.M. (1999) Chemistry and structure of aggregates formed with Fe-salts and natural organic matter. *Colloids and Surfaces* 147 (3), 297-308.
- Vlyssides A.G., Loizidou M., Karlis P.K., Zorpas A.A. and Papaioannou D. (1999) *J. Hazard. Mat. B* 70, 41-52.
- Volk, C., Renne, C., Rober, C. and Jore, J.C. (1994) Comparison of two techniques for measuring biodegradable dissolved organic carbon in water. *Environ. Technol.* 15, 545-556.
- Wang G.S., Chen H.W. and Kang S.F. (2001) Catalyzed UV oxidation of organic pollutants in biologically treated wastewater effluents. *The Science of the Total Environment* 277, 87-94.
- Water Directorate (2000) *Survey of NSW local government effluent and biosolids reuse 2000*, prepared for NSW Local Government Water Industry Directorate. NSW Department of Public Works and Services, Sydney, NSW.
- Weber Jr W.J. (1972) *Physical processes for water quality control*, ed. Wiley Interscience, New York.
- Weis A., Bird M.R. and Nystrom M. (2003) The chemical cleaning of polymeric UF membranes fouled with spent sulphite liquor over multiple operational cycles. *J. Membrane Sci.* 216, 67-79.
- Wetzel R.G. (1975) *Limnology*, W.B. Saunders Company, Philadelphia.
- Wetzel R.G., Hatcher, P.G., and Bianchi, T.S. (1995) Natural photolysis by ultraviolet irradiance of recalcitrant dissolved organic matter to simple substrates for rapid bacterial metabolism. *Limnology and Oceanography* 40, 1369-1380.
- Wiesner M.R., Clark M.M. and Mallevalle J. (1989) Membrane filtration of coagulated suspensions. *Journal of Environmental Engineering*, 115 (1), 20-40.
- Wiesner M.R., Hackney J., Sethi S., Jacangelo J.G. and Laine J.M. (1994) Cost estimates for membrane filtration and conventional treatment. *Journal of American Water Works Association* 86 (12), 33-41.
- Wingender J., Neu T.R. and Flemming H.-C. (1999) What are bacterial extracellular polymeric substances?. In: Wingender, J., Neu, T.R., and Flemming, H.-C. Editors, *Microbial extracellular polymeric substances: characterization, structure and function*, Springer, Berlin.
- Wiszniewski J., Robert D., Surmacz-Gorska J., Miksch K. and Weber J.V. (2004) Photocatalytic decomposition of humic acids on TiO₂ Part I: Discussion of adsorption

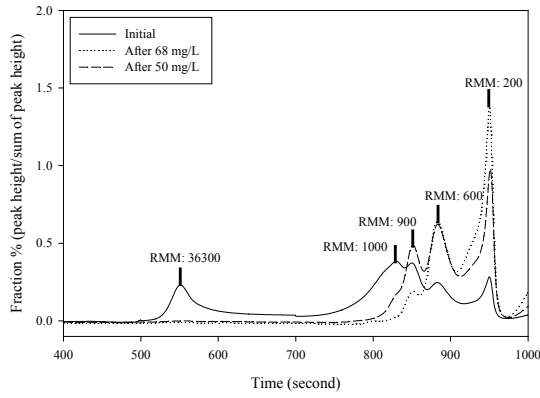
- and mechanism. *Journal of Photochemistry and photobiology A: Chemistry*. 152 (1-3), 267-273.
- Wu C.S. (1999) *Column handbook for size-exclusion chromatography*, Academic Press, San Diego, CA.
- Yates III L.M. and Von Wandruszka R. (1999) Decontamination of Polluted Water by Treatment with a Crude Humic Acid Blend. *Environ. Sci. Technol.* 33, 2076-2080.
- Yau W.W., Ginnard C.R. and Kirkland J.J. (1978) Broad-range linear calibration in high-performance size-exclusion chromatography using column packings with bimodal pores. *J. Chromatogr.* 149, 465.
- Yau W.W., Kirkland J.J. and Bly D.D. (1979) *Modern size-exclusion liquid chromatography*, Wiley, New York, NY.
- Yuan and Zydney, 1999 W. Yuan and A. Zydney, Humic acid fouling during microfiltration, *J. Membr. Sci.* 157 (1999), pp. 1–12.
- Yuan W. and Zydney A.L. (2000a) Humic acid fouling during microfiltration. *Journal of Membrane Science* 157, 1-12.
- Yuan, W. and Zydney A.L. (2000b) Humic acid fouling during ultrafiltration. *Environ. Sci. Technol.* 34, 5043-5050.
- Zhang G. and Liu Z. (2003) Membrane fouling and cleaning in ultrafiltration of wastewater from bank note printing works, *J. Membrane Sci.* 211, 235-249.
- Zhang M. and Song L. (2000) Mechanisms and parameters affecting flux decline in cross-flow microfiltration and ultrafiltration of colloids. *Environ. Sci. Technol.* 34 (17), 3767-3773.
- Zhang M., Li C., Benjamin M.M. and Chang Y. (2003) Fouling and natural organic matter removal in adsorbent/membrane systems for drinking water treatment. *Environ. Sci. Technol.* 37, 1663-1669.
- Zhang R., Vigneswaran S., Ngo H.H. and Nguyen H. (2005) Magnetic ion exchanger (MIEX®) as a pre-treatment to a submerged membrane system in the treatment of biologically treated wastewater. *Desalination*, In press.
- Zhang X., Bishop P. and Kinkle B. (1999) Comparison of extraction methods for quantifying extracellular polymers in biofilms. *Wat Sci Tech* 39, 211–218.
- Zhu X. and Elimelech M. (1997) Colloidal fouling of reverse osmosis membranes: measurements and fouling mechanism. *Environ. Sci. Technol.* 31, 3654-62.

Appendix A

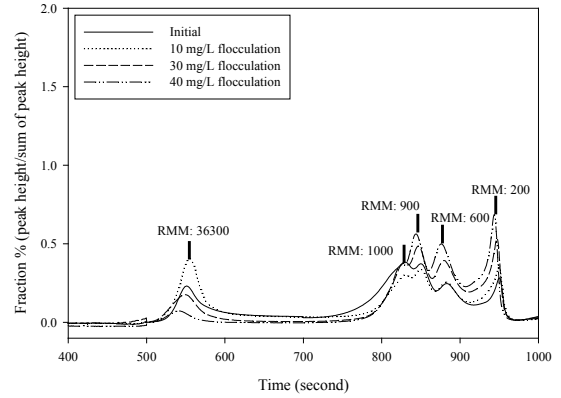
Appendix A.1 MW distribution after (a) flocculation with the large doses of FeCl₃, (b) flocculation with the small doses of FeCl₃, (c) adsorption with the large doses of PAC, and (d) adsorption with the small doses of PAC

Appendix A.2 MW distribution of organic matter after flocculation followed by PAC adsorption

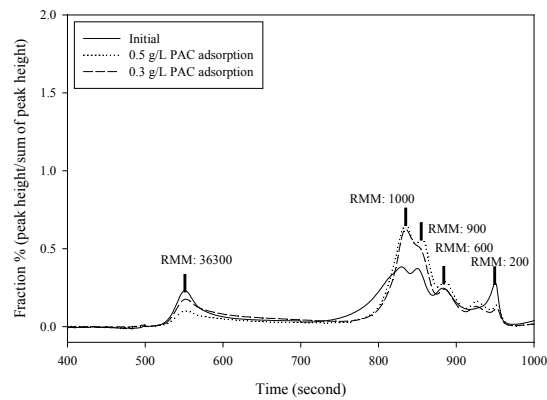
Appendix A.3 MW distribution after flocculation and adsorption as pretreatment and UF as post treatment ($J_0 = 1.84$ m/d at 300 kPa; crossflow velocity = 0.5 m/s; MWCO of 17,500 daltons; Reynold's number: 735.5; shear stress: 5.33 Pa)



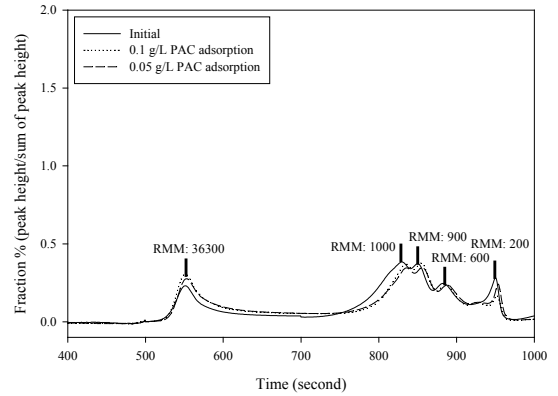
(a)



(b)

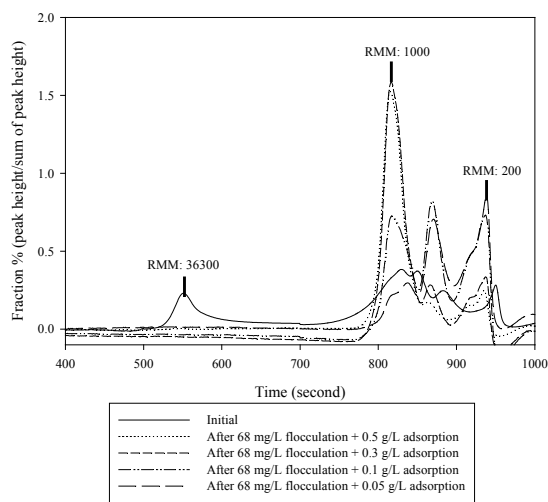


(c)

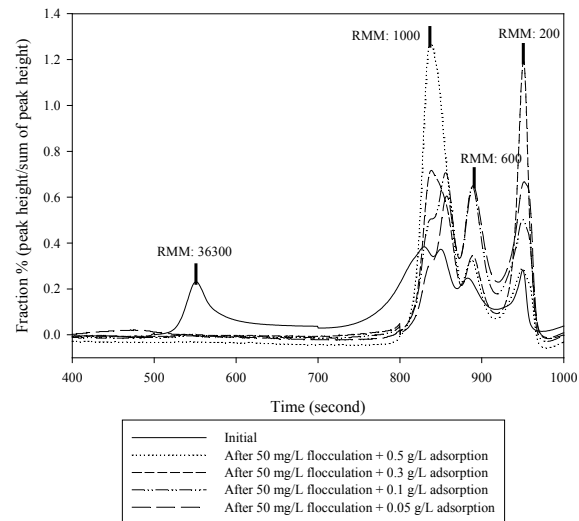


(d)

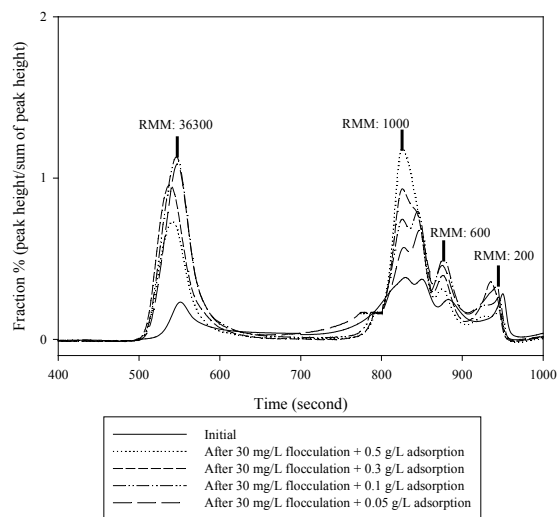
Appendix A.1 MW distribution after (a) flocculation with the large doses of FeCl_3 , (b) flocculation with the small doses of FeCl_3 , (c) adsorption with the large doses of PAC, and (d) adsorption with the small doses of PAC



(i)

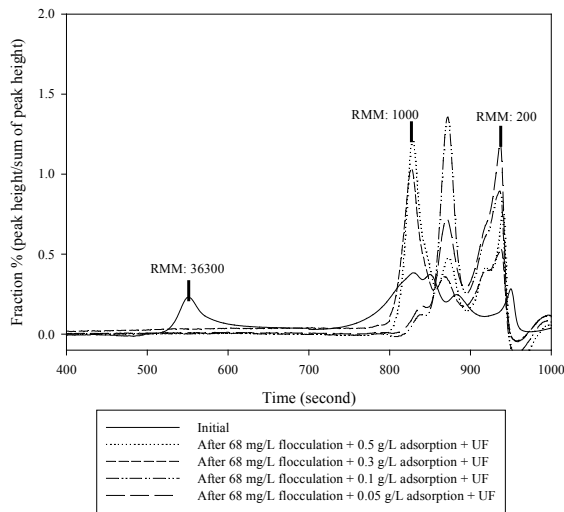


(ii)

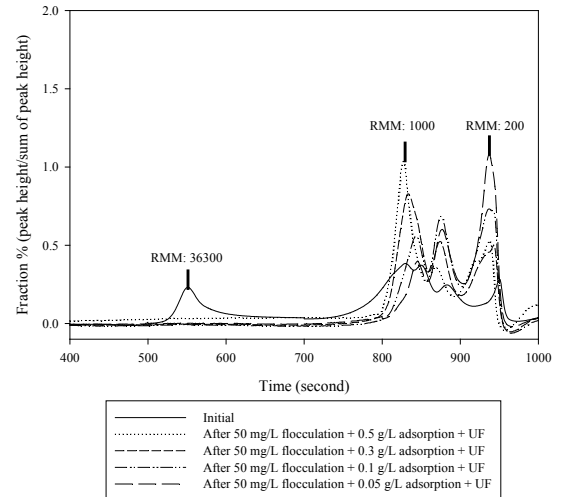


(iii)

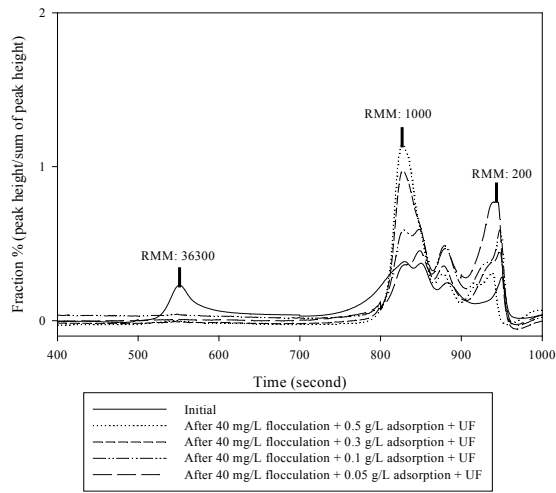
Appendix A.2 MW distribution of organic matter after flocculation followed by PAC adsorption



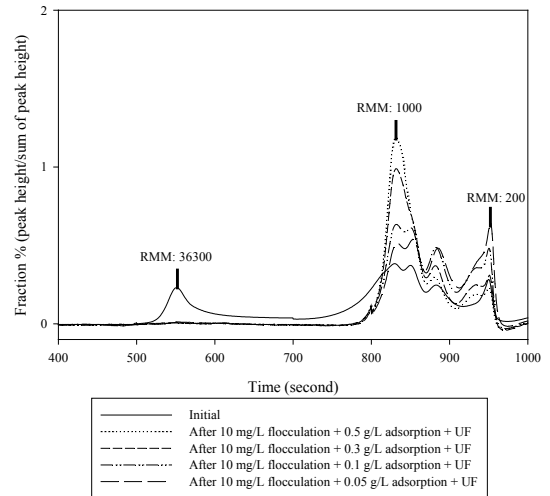
(i)



(ii)



(iii)



(iv)

Appendix A.3 MW distribution after flocculation and adsorption as pretreatment and UF as post treatment ($J_0 = 1.84$ m/d at 300 kPa; crossflow velocity = 0.5 m/s; MWCO of 17,500 daltons; Reynold's number: 735.5; shear stress: 5.33 Pa)

Appendix B

Step 1: pure water is first filtered through the membrane until a constant flux is obtained,

$$R_m = \frac{\Delta P}{\mu J} = \frac{300kPa}{1} \times \frac{m^2}{10^{-3} NS} \times \frac{\min}{9ml} = 1.2 \times 10^{13} m^{-1}$$

Step 2: after the permeate rate reaches a constant value, pure water replaces the organic-containing water and the applied pressure is released to remove concentration polarization,

$$R_{cp} = \frac{\Delta P}{\mu J} - R_m = \left(\frac{300kPa}{1} \times \frac{m^2}{10^{-3} NS} \times \frac{\min}{7.695ml} \right) - (1.2 \times 10^{13} m^{-1}) = 2.035 \times 10^{12} m^{-1}$$

Step 3: the fouled membrane is then rinsed with pure water so that the gel layer (highly concentrated organic layer) is removed from the membrane surface and pure water filtration is again performed,

$$R_g = \frac{\Delta P}{\mu J} - R_m = \left(\frac{300kPa}{1} \times \frac{m^2}{10^{-3} NS} \times \frac{\min}{8.1ml} \right) - (1.2 \times 10^{13} m^{-1}) = 1.333 \times 10^{12} m^{-1}$$

Step 4: the membrane is soaked in a 0.1 M NaOH solution for overnight so that weakly adsorbed organic matter on the membrane surface is desorbed, then pure water is again filtered.

$$R_{aw} = \frac{\Delta P}{\mu J} - R_m = \left(\frac{300kPa}{1} \times \frac{m^2}{10^{-3} NS} \times \frac{\min}{7.65ml} \right) - (1.2 \times 10^{13} m^{-1}) = 2.118 \times 10^{12} m^{-1}$$

Finally, the resistance by strong adsorption can be calculated:

Permeate flux with initial pure water - no recovered permeate flux after above cleaning

$$R_{as} = \frac{\Delta P}{\mu J} - R_m = \left(\frac{300kPa}{1} \times \frac{m^2}{10^{-3} NS} \times \frac{\min}{9ml} \right) - (1.2 \times 10^{13} m^{-1}) = 0 m^{-1}$$

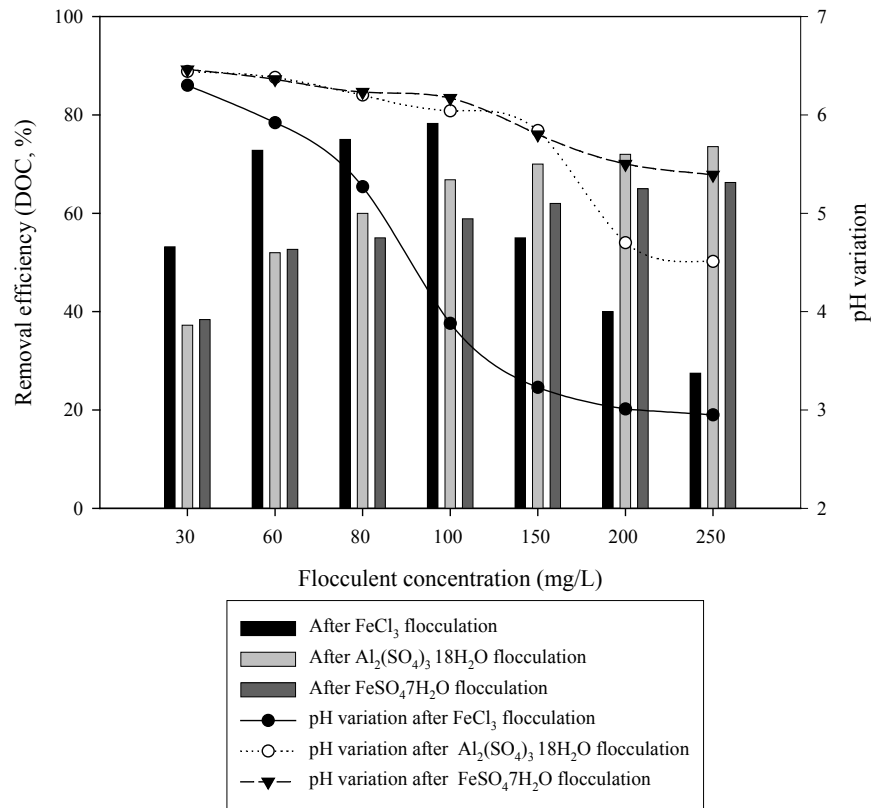
Appendix C

Synergistic Effect of FeCl₃ Flocculation to Photocatalysis

Preflocculation with Different Flocculants

It is essential to first investigate the optimal doses of different flocculants and the ranges of pH in terms of DOC removal. Appendix C.1 shows the removal of DOC with different flocculants (FeCl₃, Al₂(SO₄)₃•18H₂O, and FeSO₄•7H₂O) were used. The concentrations of the flocculants were varied from 30 to 250 mg/L to compare the equivalent concentration of the ferric, aluminum, and ferrous salts. Here, ferric chloride of 68 mg/L (20 Fe-mg/L), alum of 250 mg/L (20 Al-mg/L), and ferrous sulphate of 100 mg/L (20 Fe-mg/L) are equivalent to the metal salts (ferric, aluminum, and ferrous compounds) of 20 mg/L. When FeCl₃ flocculation was used, DOC removal increased until the flocculant concentration of 100mg/L. Then, it rapidly decreased. With Al₂(SO₄)₃•18H₂O and FeSO₄•7H₂O flocculation, DOC removal increased with increasing concentration of flocculants. The similar equivalent concentration of approximately 20 Fe/Al-mg/L with different salts resulted in highest DOC removal. Thus, the optimal concentrations of FeCl₃, Al₂(SO₄)₃•18H₂O, and FeSO₄•7H₂O were decided to 60 mg/L, 250 mg/L, and 100 mg/L, respectively.

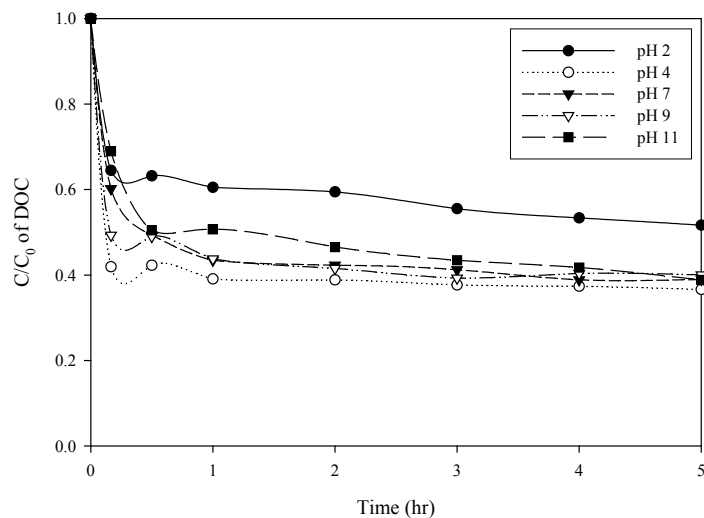
Appendix C.1 also shows pH variations with different flocculants. The solution of pH significantly decreased with increasing FeCl₃ concentrations up to pH 3. The doses by alum and ferrous sulphate slightly decreased the pH up to pH 4.3 and 5.4 at 250 mg/L, respectively. This suggests that ferric hydrolysis by FeCl₃ flocculation releases hydrogen ions and they deplete the limited alkalinity of the system. Thus, the pH decreased significantly.



Appendix C.1 DOC removal and pH variation during flocculation with different flocculants (initial pH = 7.3)

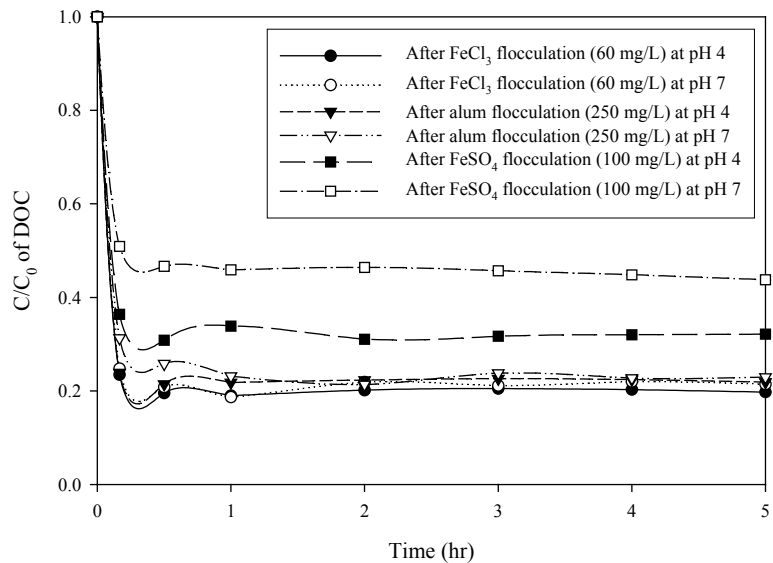
Effect of TiO₂ Adsorption

Appendix C.2 shows the adsorption kinetics by P25 TiO₂ particles. This experiment was conducted using pH values of 2, 4, 7, 9, and 11 to identify the relationship between pH change and DOC removal. This removal ratio of DOC decreased with increasing operational time. Finally, the highest DOC removal resulted from using pH 4. However, DOC removal except for using pH 2 resulted in similar results using pH 4 at 5 hours. This can be concluded that DOC removal with different pH between TiO₂ particle and organic matter showed the ranges of pH 4 – 7. These ranges were determined as an optimal pH to identify pH effect after different flocculants.



Appendix C.2 Adsorption kinetics by P25 TiO₂

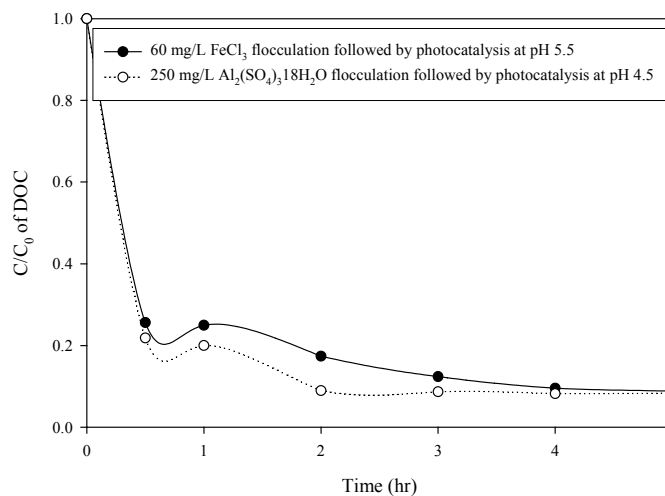
Appendix C.3 shows the adsorption kinetics on TiO₂ particles after flocculation by different flocculants. Flocculation experiments showed that the concentrations of FeCl₃ (60 mg/L), Al₂(SO₄)₃•18H₂O (250 mg/L), and FeSO₄•7H₂O (100 mg/L) resulted in the same equivalent concentration of different salts which represented the highest DOC removal after flocculation. Therefore, in this study the doses were added during flocculation. The best DOC removal of about 0.2 ratio was at a dose of FeCl₃ (60 mg/L) at pH 4. Here, it should be noted that the trend of DOC removal by TiO₂ adsorption alone (60%), flocculation alone (72%), and flocculation followed by TiO₂ adsorption (80%) indicated different results. It may be due to overlapping of different MW removals between flocculation and TiO₂ adsorption. Thus, the removal of DOC with TiO₂ adsorption slightly increased 10% after flocculation.



Appendix C.3 Adsorption kinetics on TiO₂ after different flocculations at pH 4 and 7

Effect of Photo-Fenton Reaction

Appendix C.4 presents the effect of photo-Fenton reaction with flocculation followed by photocatalysis without pH adjustment. Ferric and aluminum salts were selected to investigate the occurring photo-Fenton reaction ($h\nu/\text{Fe}^{3+}/\text{O}_2$) (Sarria et al., 2003). These amounts used were 20 mg/L of ferric and aluminum salts and then, the pH was 5.5 after FeCl₃ and 4.5 after alum flocculation. The DOC was removed up to 92% with both salts after 5-hour run. This suggests that the photo-Fenton reaction related to the photocatalysis hybrid system is marginal in this study.



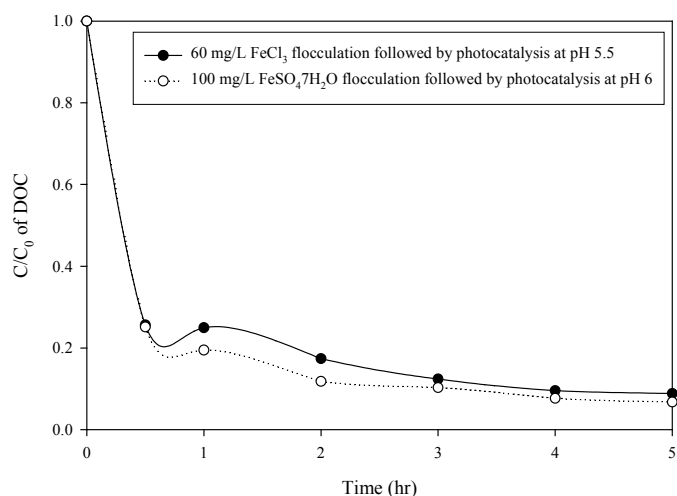
Appendix C.4 Effect of different flocculation followed by photocatalysis (wastewater concentration (DOC) = 10.58 mg/L; T = 30 °C; Air = 0.1 VVM; intensity = 8 W with the 3 lamps)

Effects of Chloride-based Salts and Ferric and Ferrous Salts

Appendix C.5 presents the effect of chloride-based salts with flocculation followed by photocatalysis without pH adjustment. Ferric chloride and ferrous sulphate were used to identify the influence of chloride-based salts. Here, it was assumed that the effect of photo-Fenton reaction was the same as both ferric and ferrous salts. These amounts used were also 20 mg/L of ferric and ferrous salts and then, the pH was 5.5 after ferric chloride and 6 after ferrous sulphate. The DOC was similar to both treatments up to 92%. This suggests that the effect of the chloride-based salt is also unobserved in this study. On the contrary, Kim et al. (2003) reported that COD removal rates of adopting chloride-based chemical flocculants were about 10 – 17 times (70% removal) faster than those of adopting sulphate-based flocculants in textile wastewater.

Appendix C.5 also shows the effect of ferric and ferrous salts without pH adjustment. As discussed above, DOC removal of the alum was similar to those of ferric and ferrous flocculation. It can be assumed that there are no effects of ferric and ferrous salts as well. Finally, it can be concluded that different flocculants with flocculation followed by

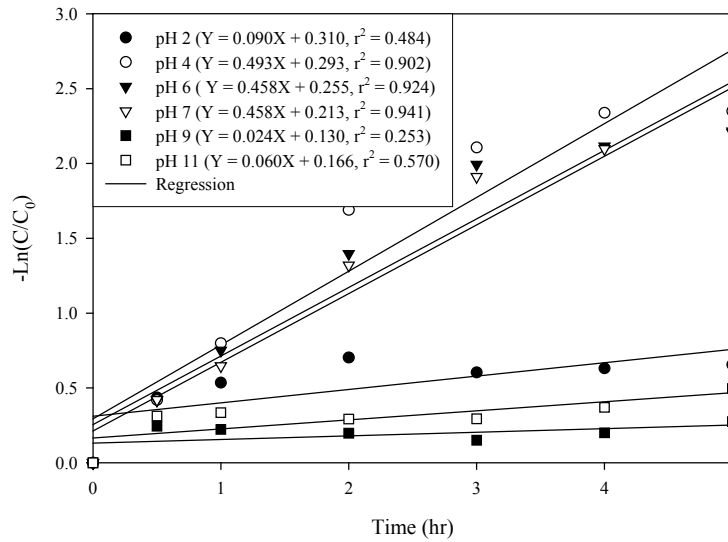
photocatalysis could not affect an improvement based on different salts, i.e., i) photo-Fenton reaction, ii) chloride-based salts, and iii) ferric and ferrous salts in treating organic matter used in this study.



Appendix C.5 Effect of different flocculation followed by photocatalysis (wastewater concentration (DOC) = 10.58 mg/L; T = 30 °C; Air = 0.1 VVM; intensity = 8 W with the 3 lamps)

Effect of pH

Appendix C.6 shows the effects of pH on photocatalysis in terms of reaction rate. This experiment was conducted using various pH values at pH 2, 4, 6, 7, 9, and 11. The DOC removal using pH 4, 6, and 7 on photocatalysis decreased with increased operational time. The DOC removal reached up to 85%. On the other hand, DOC removal observed with the pH 2, 9, and 11 solutions after photocatalysis indicated lower values. The reaction rates with the optimal pH were 20 times faster than those of others, suggesting that the photocatalytic reaction is favorable to acidic conditions. This result is an agreement with previous researches (Lee et al., 2003; Al-Rasheed and Cardin, 2003; An et al., 2003). Lee et al. (2003) reported that the surface hydroxyl of TiO₂ exists as forms of TiOH₂⁺ and TiO⁻ in strong acidic and basic conditions, respectively. Thus, the negative charged organic matter under the acidic pH could be well adsorbed on the TiO₂ particles with the decrease of repulsion.



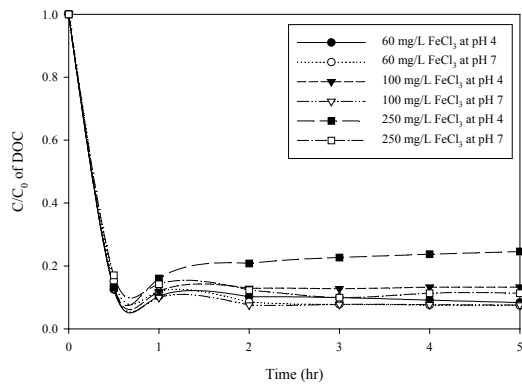
Appendix C.6 (a) DOC removal and (b) reaction rate of pH in photocatalysis (wastewater concentration (DOC) = 10.58 mg/L; T = 30 °C; Air = 0.1 VVM; intensity = 8 W with the 3 lamps)

Appendix C.7 presents a detailed influence of pH with flocculation followed by photocatalysis. As discussed above, flocculation decreased pH from pH 4.5 to pH 6 and the optimal pH in removing organic matter was the ranges of pH 4 to pH 7. Thus, pH from 4 to 7 was set to compare the effect of pH with flocculation and the concentrations of different flocculants were equivalent to 20 mg/L.

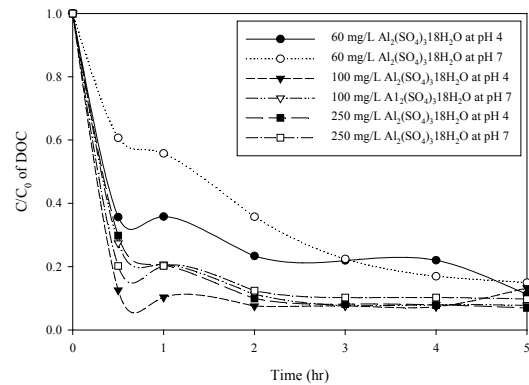
Appendix C.7 (a) shows the effect of FeCl_3 flocculation followed by photocatalysis with pH adjustment. The pH with the concentrations of 60 mg/L, 100 mg/L, and 250 mg/L of FeCl_3 was pH 5.92, pH 3.88, and pH 2.80, respectively. The pH was adjusted to pH 4 and pH 7 with different concentrations. The majority of DOC removals with different concentrations and pHs were similar with more or less 90%.

Appendix C.7 (b) illustrates the effect of $\text{Al}_2(\text{SO}_4)_3 \cdot 18\text{H}_2\text{O}$ flocculation followed by photocatalysis with pH adjustments of pH 4 and pH 7. Every DOC removal at pH 4 was superior to those at pH 7 and the best DOC removal was at a dose of $\text{Al}_2(\text{SO}_4)_3 \cdot 18\text{H}_2\text{O}$ (100 mg/L) at pH 4.

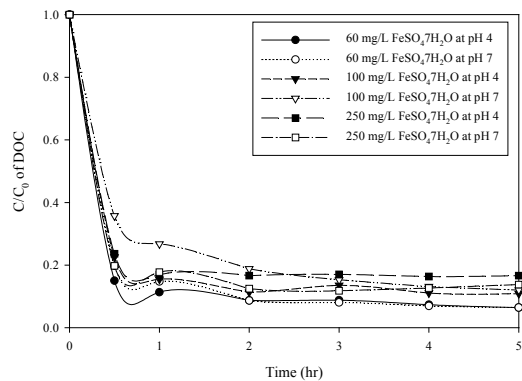
Appendix C.7 (c) describes the effect of $\text{FeSO}_4 \cdot 7\text{H}_2\text{O}$. The best DOC removal occurred at a dose of $\text{FeSO}_4 \cdot 7\text{H}_2\text{O}$ (60mg/L), whose addition was the same as the optimal FeCl_3 removal. These trends of DOC variations with ferric chloride flocculation followed by photocatalysis were related to those of alum and ferrous sulphate followed by photocatalysis. This suggests that pH could not affect DOC removal with different flocculants.



a)



b)



c)

Appendix C.7 (a) Effect of FeCl_3 flocculation followed by photocatalysis, (b) $\text{Al}_2(\text{SO}_4)_3 \cdot 18\text{H}_2\text{O}$ flocculation followed by photocatalysis, and $\text{FeSO}_4 \cdot 7\text{H}_2\text{O}$ flocculation followed by photocatalysis at pH 4 and pH 7 (wastewater concentration (DOC) = 10.58 mg/L; $T = 30^\circ\text{C}$; Air = 0.1 VVM; intensity = 8 W with three lamps)

Appendix D

Peer reviewed journal paper

1. **H.K. Shon**, S. Vigneswaran, In S. Kim, J. Cho, and H. H. Ngo (2004) The effect of pretreatment to ultrafiltration of biologically treated sewage effluent: a detailed effluent organic matter (EfOM) characterization. *Water Research*, 38 (7), 1933-1939. (IF: 2.304, JCR Category; water resource: 1/55)
2. **H.K. Shon**, S. Vigneswaran, In S. Kim, J. Cho, and H. H. Ngo (2004) Effect of pretreatment on the fouling of membranes: application in biologically treated sewage effluent. *Journal of Membrane Science*, 234 (1-2), 111-120. (IF: 2.108, JCR Category; polymer science: 28/72)
3. T. T. L. Hoang, **H.K. Shon**, Chaudhary, D. S., Vigneswaran, S. and Ngo, H. H. (2004) Granular activated carbon (GAC) biofilter for low strength wastewater treatment. *Fluid/Particle Separation Journal*, 16 (2), 185-191.
4. **H. K. Shon**, W. S. Guo, S. Vigneswaran, H. H. Ngo, and In S. Kim (2004) Effect of flocculation in membrane-flocculation hybrid system in water reuse. *Separation Science and Technology*, 39 (8), 1871-1883. (IF: 0.896, JCR Category; chemistry, multidisciplinary: 114/123)
5. S. Vigneswaran, **H.K. Shon**, S. Boothanon, H.H. Ngo and R. Ben Aim (2004) Membrane-flocculation-adsorption hybrid system in wastewater treatment: micro and nano size organic matter removal. *Water Science & Technology*. 50 (12), 265-271. (IF: 0.586, JCR Category; engineering, environmental: 13/35)
6. **H.K. Shon**, S. Vigneswaran, H. H. Ngo, and R. Ben Aim (2005) Is semi-flocculation effective as pretreatment to ultrafiltration in wastewater treatment? *Water Research*, 39 (1), 147-153. (IF: 2.304, JCR Category; water resource: 1/55)
7. **H.K. Shon**, S. Vigneswaran, J.-H. Kim, H. H. Ngo, and N.E. Park (2005) Comparison of nanofiltration with flocculation – microfiltration – photocatalysis hybrid system in dissolved organic matter removal. *Filtration Journal*, 5 (3), 215-221.

8. **H.K. Shon**, S. Vigneswaran, H. H. Ngo, In S. Kim and R. Ben Aim (2005) Fouling characterization of the NF membranes with and without pretreatment of biologically treated wastewater. *Water Science & Technology*, 51 (6-7), 277-284. (IF: 0.586, JCR Category; engineering, environmental: 13/35)
9. **H.K. Shon**, S. Vigneswaran, R. Ben Aim, H. H. Ngo, In S. Kim, and J. Cho (2005) Influence of flocculation and adsorption as pretreatment on the fouling of ultrafiltration and nanofiltration membranes: application with biologically treated sewage effluent. *Environmental Science & Technology*, 39 (10), 3864-3871. (IF: 3.557 JCR Category; environmental sciences: 1/131)
10. **H.K. Shon**, S. Vigneswaran, H. H. Ngo, and J.-H. Kim (2005) Chemical coupling of photocatalysis with flocculation and adsorption in the removal of organic matter. *Water Research*, 39 (12), 2549-2558. (IF: 2.304, JCR Category; water resource: 1/55)
11. **H.K. Shon**, S. Vigneswaran, and H. H. Ngo (2005) Effect of partial flocculation and adsorption as pretreatment to ultrafiltration in treating wastewater. *American Institute of Chemical Engineers (AIChE Journal)*, In press. (IF: 1.761, JCR Category; engineering, chemical: 9/119)
12. P.J. Smith, **H.K. Shon**, S. Vigneswaran, H.H. Ngo, R. Ben Aim, and H. Nguyen (2005) A novel automated approach to improving permeability, productivity and the life cycle of a Cross-flow Membrane System. *Journal of Membrane Science*, submitted. (IF: 2.108, JCR Category; polymer science: 28/72)
13. **H.K. Shon**, S. Vigneswaran, In S. Kim, J. Cho and H.H. Ngo (2005) The effect of fractions on UF membrane fouling by effluent organic matter: a detailed characterization. *Journal of Membrane Science*, submitted. (IF: 2.108, JCR Category; polymer science: 28/72)
14. J.-H. Kim, **H.K. Shon**, G. Seo, B.C. Choi, J.B. Kim, S.J. Song and S. Vigneswaran (2005) Disinfection of swimming pool and tap water by photocatalytic reactor. *Water Journal*, submitted.
15. **H.K. Shon** and S. Vigneswaran. (2005) Effluent organic matter (EfOM) in wastewater: constituents, effects and treatment. *Critical Reviews in Environmental*

Science and Technology, submitted. (IF: 1.684, JCR Category; Environmental sciences: 25/134)

Peer reviewed conference paper

1. **H.K. Shon**, N.E. Park, D.H. Kim, S. Vigneswaran, In. S. Kim, S.H. Moon and H.H. Ngo (2003) Organic characterization of flocculation and adsorption pretreatment for the increase of membrane flux at Water Purification and Reuse conference in Postdam, Germany, June 8-13.
2. **H.K. Shon**, S. Vigneswaran, H. H. Ngo, and In S. Kim (2003) Effect of high rate pretreatment on nanofiltration system in wastewater reuse, oral presentation at ASIA-Waterqual in Bangkok, IWA.
3. W.S. Guo, S. Vigneswaran, H. H. Ngo, **H.K. Shon** and S. Shimohoki (2003) Improving the performance of a crossflow microfiltration in tertiary wastewater treatment and reuse by specific pretreatment processes oral presentation at ASIA-Waterqual 2003 in Bangkok, IWA.
4. S. Vigneswaran, **H.K. Shon**, S. Boothanon, H.H. Ngo and R. Ben Aim (2003) Membrane-flocculation-adsorption hybrid system in wastewater treatment: micro and nanosize organic matter removal, Nano and micro particle in water and wastewater treatment, Zurich, Switzerland, IWA.
5. **H. K. Shon**, S. Vigneswaran, H. H. Ngo, D. H. Kim, N. E. Park, N. J. Jang, and In S. Kim (2003) Characterization of effluent organic matter (EfOM) of fouled nanofilter (NF) membranes at International Membrane Science and Technology (IMSTEC), University of New South Wales (UNSW), Sydney, Australia.
6. Do Hee Kim, **H. K. Shon**, S. Vigneswaran, and Jaeweon Cho (2003) Evaluating interactions between NOM molecules and various membranes with flow field-flow fractionation at International Membrane Science and Technology (IMSTEC), University of New South Wales (UNSW), Sydney, Australia, Nov..
7. **H. K. Shon**, S. Vigneswaran, H. H. Ngo, and Ben Aim R. (2003) Low pressure nanofiltration with adsorption as a pretreatment in tertiary wastewater treatment

for reuse. International Membrane Science and Technology (IMSTEC), University of New South Wales (UNSW), Sydney, Australia.

8. Ahn, Y., **H.K. Shon**, Vigneswaran, S., Kim, In S. (2003) Microbial analyses of granulated activated carbon biofilter for the treatment of secondary effluent at Korean Society on Water Quality, Korea.
9. **H.K. Shon**, Saravanamuthu, Vigneswaran, In S., Kim, Jaeweon, Cho and Huu Hao, Ngo (2004) Characterization Of Different Treatments With Biologically Treated Sewage Effluent and synthetic wastewater, Enviro04, Sydney, Australia.
10. **H. K. Shon**, S. Vigneswaran, J. H. Kim, H. H. Ngo, and N.E. Park (2004) Comparison of nanofiltration with flocculation-microfiltration-photocatalysis hybrid system in dissolved organic matter removal. 9th World Filtration Congress, New Orleans, Louisiana, USA.
11. **H. K. Shon**, S. Vigneswaran, and R. Ben Aim (2004) Pre- and post-membrane treatment. World Filtration Congress Workshop, New Orleans, Louisiana, USA.
12. **H. K. Shon**, S. Vigneswaran, H. H. Ngo, and A. Johnston (2004) Photocatalysis hybrid system in wastewater reuse. *Showcase 2004*, University of Technology, Sydney. 25th May.
13. Hoang, T. T. L., **H. K. Shon**., Chaudhary, D. S., Vigneswaran, S. and Ngo, H. H. (2004) Granular activated carbon (GAC) biofilter for low strength wastewater treatment. American Filtration and Separation Society, Maryland, USA.
14. **H. K. Shon**, S. Vigneswaran, H. H. Ngo, In S. Kim, and R. Ben Aim (2004) Foulant Characterization of the NF Membranes with and without Pretreatment of Biologically Treated wastewater, Water Environment Membrane Technology, Seoul Korea, IWA.
15. **H.K. Shon**, A. Nathaporn, S. Vigneswaran, H. H. Ngo, and J.-H. Kim (2005) Photocatalysis hybrid system in the removal of effluent organic matter (EfOM). International Conference on Advances in Industrial Wastewater Treatment, 9 – 11 February, Chennai, India.
16. S. Vigneswaran, Chaudhary, D.S., Guo, W., **H.K. Shon**, Ngo, H.H. and Ben Aim, R. (2005) Effect of pre-treatment on organic removal from biologically treated sewage effluent by membrane hybrid system. AWA Membrane & Desalination

Specialty Conference (Harvesting water using alternative technologies) 23 – 25 February, Adelaide, SA, Australia.

17. A. Nathaporn, **H. K. Shon**, S. Vigneswaran and H. H. Ngo (2005) Photocatalytic hybrid system in degradation of herbicide (metsulfuron-methy), IWA-Asia Pacific Regional Group (ASPIRE) Conference and Exhibition, July 10-15, 2005, IWA, Singapore.
18. **H.K. Shon**, S. Vigneswaran, H.H. Ngo, In S. Kim, and J. Cho (2005) The effect of pretreatment on UF membrane fouling by effluent organic matter: a detailed characterization. International Congress on Membranes and Membrane Processes 2005 (ICOM2005), August 21-26 2005, Seoul, Korea.